Supporting Information

Tethering chiral Rh diene complexes inside mesoporous solids: experimental and theoretical study of substituent, pore and linker effects on asymmetric catalysis

Manuel Kirchhof,[a] Katrin Gugeler,[b] Ann-Katrin Beurer,[c,+] Felix Richard Fischer,[d,+] Derman Batman,[a] Soeren Bauch,[b] Sofia Kolin,[b] Elliot Nicholas,[a] Roland Schoch,[e] Charlotte Vogler,[f] Shravan R. Kousik,[g] Anna Zens,[a] Bernd Plietker,[d] Petia Atanasova,[g] Stefan Naumann,[f] Matthias Bauer,[e] Johanna R. Bruckner,[h] Yvonne Traa,[c] Johannes Kästner,[b] and Sabine Laschat*[a]

[a] Institute of Organic Chemistry, University of Stuttgart, Pfaffenwaldring 55, 70569 Stuttgart, Germany. E-mail: sabine.laschat@oc.uni-stuttgart.de

[b] Institute for Theoretical Chemistry, University of Stuttgart, Pfaffenwaldring 55, 70569 Stuttgart, Germany.

[c] Institute of Technical Chemistry, University of Stuttgart, Pfaffenwaldring 55, 70569 Stuttgart, Germany.

[d] Chair of Organic Chemistry I, Technical University of Dresden, 01069 Dresden, Germany.

[e] Department Chemistry and Center for Sustainable Systems Design (CSSD), University of Paderborn, 33098 Paderborn.

[f] Institute of Polymer Chemistry, University of Stuttgart, Pfaffenwaldring 55, 70569 Stuttgart, Germany.

[g] Institute for Materials Science, University of Stuttgart, Heisenbergstr. 3, 70569 Stuttgart, Germany.

[h] Institute of Physical Chemistry, University of Stuttgart, Pfaffenwaldring 55, 70569 Stuttgart, Germany.

+ These coauthors contributed equally to this work.

Table of contents

1 Experimental procedures for the synthesis of chiral dienes S3
1.1 General experimental S3
1.2 Synthesis of the naphthyl-substituted norbornadienes S4
1.3 Synthesis of the phenyl-substituted norbornadienes S11
1.4 Synthesis of alcohols, alkynes, alkynones and triazoles S20
1.5 Rh-catalyzed 1,2-additions S35
2 NMR spectra S37
2.1 Synthesis of the naphthyl-substituted norbornadienes S37
2.2 Synthesis of the phenyl-substituted norbornadienes S49
2.3 Synthesis of alcohols, alkynes, alkynones and triazoles S65
2.4 Rh-catalyzed 1,2-additions S90
3 Synthesis of the supports and immobilization of ligands S91
3.1 Synthesis of the mesoporous materials S91
3.2 Selective functionalization of the materials S93
3.3 Immobilization of alkynes and alkynones S94
4 Characterization of the supports S95
4.1 FTIR spectra S99
4.2 ICP-OES Measurements S99
5 Data for the immobilization on OMS S102
6 Additional Experiments S103
6.1 Hot filtration test S103
6.2 Stability tests S104
6.3 Recycling and leaching test S108
6.4 Catalyst loading experiments S111
7 Computational Studies S112
8 XAS measurements S113
8.1 Experimental details S113
8.2 Data analysis S113
8.3 XANES analysis details S114
8.4 EXAFS analysis details S115
9 HPLC Chromatograms S117
10 References S118

1 Experimental procedures for the synthesis of chiral dienes

1.1 General experimental

Chemicals and solvents were used as received from the supplier unless stated otherwise. Anhydrous solvents were obtained by distillation under a nitrogen atmosphere using suitable drying agents. Ethyl acetate and hexanes were distilled prior to their use as eluents in column chromatography. Solvents for catalysis and the 3.1 M KOH solution were degassed by bubbling nitrogen through them. All NMR spectra were recorded on a Bruker *Avance 300* (^{1}H, 300 MHz; ^{13}C, 75 MHz), *Avance 500* (^{1}H, 500 MHz; ^{13}C, 126 MHz) or a *Avance 700* (^{1}H, 700 MHz; ^{13}C, 176 MHz) spectrometer at room temperature. The NMR spectra were referenced to tetramethylsilane (δ = 0.00 ppm) and calibrated on the respective residual solvent peaks. Infrared spectra were recorded on a *Bruker Vektor22* spectrometer equipped with an *MKII golden gate single reflection diamant ATR* system. All mass spectra were recorded with a Bruker *Daltonics micro-TOF-Q* using electrospray ionization (ESI) with nitrogen as carrier gas. The melting points of the synthesized compounds were determined with a Stuart *SMP10* melting-point apparatus. Specific rotation values $[\alpha]_D^{20}$ were determined with a Perkin Elmer *Polarimeter 241* at 20 °C using the sodium D-line (λ = 589 nm). All HPLC chromatograms were recorded on a Shimadzu *LC-20AT* setup consisting of a *LC-20A* pump, a *DGU-20A5* degasser, a *SIL-20A* autosampler and an *SPD-20A* UV-Vis detector operating at λ = 235 nm. For the mobile phase *n*-hexane/isopropanol mixtures were used. The stationary phase was a chiral Chiralcel® OD-H column. The chromatograms were evaluated with the program *LCsolution v.1.21* from *LabSolutions*.

1.2 Synthesis of the naphthyl-substituted norbornadienes

The naphthyl derivatives were synthesized similar to a procedure that was established in our previous publication (Scheme S1).[1] The synthetic procedures can be found in the general procedures GP1 – GP6.

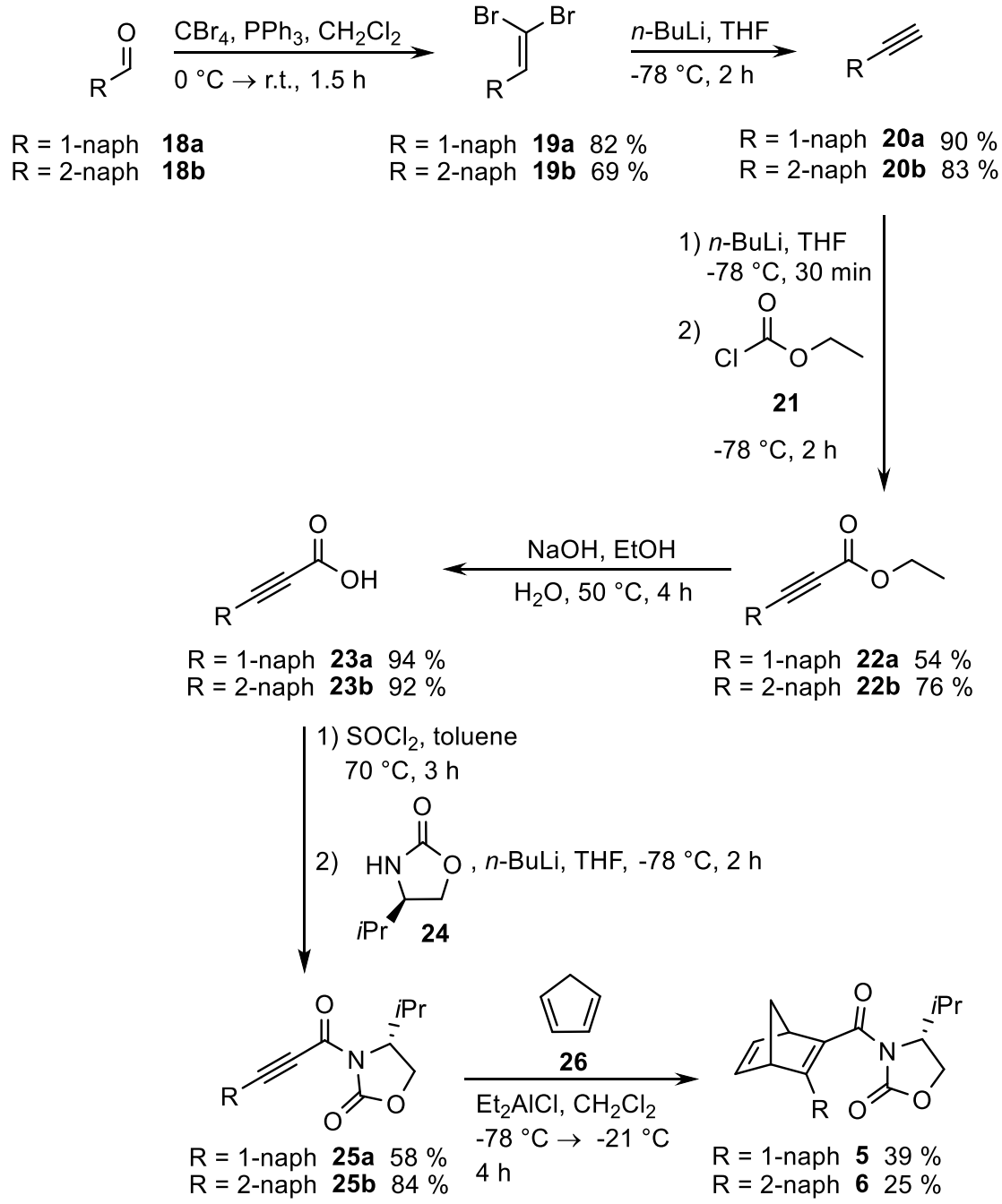

Scheme S1

General procedure for the synthesis of the dibromoalkenes (19a,b) [GP 1]

According to ref.,[2] under a nitrogen atmosphere PPh_3 (40.3 g, 0.15 mol) was added to a solution of CBr_4 (25.5 g, 76.8 mmol) in abs. CH_2Cl_2 (120 mL) and stirred for 30 min at 0 °C. The respective naphthaldehyde **18a**,**b** (10.0 g, 64.0 mmol) was slowly added, and the reaction mixture was stirred for 1.5 h at room temperature. The reaction mixture was filtered through Celite®, the solvent was removed under reduced pressure and the crude product was purified by column chromatography on silica.

General procedure for the synthesis of the alkynes (20a,b) [GP 2]

According to ref.,[3] under a nitrogen atmosphere *n*BuLi (51.3 mL, 35.5 g, 0.13 mol, 2.5 M in hexanes) was added to a solution of the respective dibromoalkene **19a**,**b** (10.0 g, 32.1 mmol) in abs. THF (100 mL) at -78 °C and the reaction mixture was stirred for 2 h at -78 °C. A saturated aqueous NH_4Cl solution (80 mL) was added and the aqueous phase was extracted with EtOAc (2 × 70 mL). The combined organic layers were dried over $MgSO_4$ and the solvent was removed under reduced pressure. The crude product was purified by column chromatography on silica.

General procedure for the synthesis of the propargylic esters (22a,b) [GP 3]

According to ref.,[4] under a nitrogen atmosphere *n*BuLi (12.4 mL, 8.59 g, 31.0 mmol, 2.5 M in hexanes) was added to a solution of the respective alkyne **20a**,**b** (4.37 g, 28.7 mmol) in abs. THF (80 mL) at -78 °C and the reaction mixture was stirred for 30 min at -78 °C. Ethyl chloroformate **21** (3.4 mL, 3.84 g, 35.4 mmol) was added and the reaction mixture was stirred for 2 h at -78 °C. A saturated aqueous NH_4Cl solution (100 mL) was added and the aqueous phase was extracted with EtOAc (3 × 70 mL). The combined organic layers were dried over $MgSO_4$, the solvent was removed under reduced pressure and the crude product was purified by column chromatography on silica.

General procedure for the synthesis of the propargylic acid derivatives (23a,b) [GP 4]

According to ref.,[5] the respective propargylic ester **22a**,**b** (4.53 g, 20.2 mmol) was dissolved in EtOH (100 mL) and a NaOH solution (230 mL, 14 wt% in H_2O) was added. The reaction mixture was stirred for 4 h at 50 °C. After cooling to room temperature 1 M HCl (350 mL) was added and the aqueous layer was extracted with CH_2Cl_2 (2 × 70 mL). The combined organic layers were dried over $MgSO_4$ and the solvent was removed under reduced pressure. The product was obtained without further purification.

General procedure for the synthesis of the imides (25a,b) [GP 5]

Under a nitrogen atmosphere thionyl chloride (0.27 mL, 0.44 g, 3.67 mmol) was added to a solution of the respective propargylic acid derivative **23a**,**b** (0.60 g, 3.06 mmol) in toluene (40 mL) and the reaction mixture was stirred for 3 h at 70 °C. The solvent was removed under reduced pressure and the acyl chloride was obtained without further purification. In a second Schlenk flask the oxazolidinone **24** (0.44 g, 2.78 mmol) was dissolved in abs. THF (5 mL) under a nitrogen atmosphere and *n*BuLi (1.1 mL, 0.76 g, 11.9 mmol, 2.5 M in hexanes) was added dropwise at -78 °C. The reaction mixture was stirred for 2 h at -78 °C. A solution of the respective acyl chloride in abs. THF (5 mL) was added dropwise, the reaction mixture was stirred for 2 h at -78 °C and a saturated aqueous NH_4Cl solution (70 mL) was added. The aqueous layer was extracted with EtOAc (3 × 50 mL), the combined organic layers were dried over $MgSO_4$ and the solvent was removed under reduced pressure. The crude product was purified by column chromatography on silica.

General procedure for the synthesis of the norbornadienes (5, 6) [GP 6]

According to ref.,[1] under a nitrogen atmosphere Et_2AlCl (3.3 mL, 3.20 g, 3.18 mmol, 1 M in hexanes) and freshly distilled cyclopentadiene **26** (0.71 mL, 0.57 g, 8.62 mmol) were added to a solution of the respective imide **25a**,**b** (0.63 g, 1.87 mmol) in abs. CH_2Cl_2 (20 mL) at -78 °C. The reaction mixture was stirred for 4 h at -20 °C and 1 M HCl (8 mL) was added dropwise. The aqueous layer was extracted with CH_2Cl_2 (2 × 50 mL), the combined organic layers were dried over $MgSO_4$ and the solvent was removed under reduced pressure. The crude product was purified by column chromatography on silica.

2-(2,2-Dibromovinyl)naphthalene (19a)

Synthesis according to GP 1; orange solid (82 %); column chromatography on silica (hexanes / EtOAc = 10 : 1); R_f = 0.92 (hexanes/EtOAc = 10 : 1, UV); m.p.: 51 °C; ^{1}H NMR (700 MHz, $CDCl_3$): δ = 7.92–7.86 (m, 4H, 2-H, 4'-H, 5'-H, 8'-H), 7.62 (d, J = 7.1 Hz, 1H, 2'-H), 7.58–7.49 (m, 3H, 3'-H, 6'-H, 7'-H) ppm; ^{13}C NMR (176 MHz, $CDCl_3$): δ = 136.0 (C-2), 133.6 (1'-C_{Ar}), 133.3 (4a'-C_{Ar}), 130.8 (8a'-C_{Ar}), 129.0 (4'-C_{Ar}), 128.7 (5'-C_{Ar}), 126.9 (2'-C_{Ar}), 126.7 (7'-C_{Ar}), 126.4 (6'-C_{Ar}), 125.4 (3'-C_{Ar}), 124.3 (8'-C_{Ar}), 93.1 (C-1) ppm. The spectroscopic data are in accordance with literature.[2]

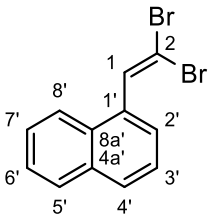

$C_{12}H_8Br_2$
312.00 g/mol

19a

2-(2,2-Dibromovinyl)naphthalene (19b)

Synthesis according to GP 1; colorless solid (69 %); column chromatography on silica (hexanes / EtOAc = 10 : 1); R_f = 0.83 (hexanes / EtOAc = 10 : 1, UV); m.p.: 101 °C; ^{1}H NMR (700 MHz, $CDCl_3$): δ = 8.02 (s, 1H, 1'-H), 7.87–7.82 (m, 3H, 4'-H, 5'-H, 8'-H), 7.68–7.62 (m, 2H, 1-H, 3'-H), 7.55–7.49 (m, 2H, 6'-H, 7'-H) ppm; ^{13}C NMR (176 MHz, $CDCl_3$): δ = 137.1 (C-2), 133.1 (2'-C_{Ar}), 133.1 (8a'-C_{Ar}), 132.9 (4a'-C_{Ar}), 128.4, 128.3, 128.1, 127.8, 126.9, 126.6 (6 × C_{Ar}), 125.8 (8'-C_{Ar}), 90.0 (C-1) ppm. The spectroscopic data are in accordance with literature.[2]

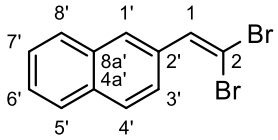

$C_{12}H_8Br_2$
312.00 g/mol

19b

1-Ethynylnaphthalene (20a)

Synthesis according to GP 2; red oil (90 %); column chromatography on silica (hexanes); R_f = 0.39 (hexanes, UV); ^{1}H NMR (400 MHz, $CDCl_3$): δ = 8.40 (d, J = 8.0 Hz, 1H, 8'-H), 7.89–7.86 (m, 2H, 2'-H, 5'-H), 7.77 (d, J = 7.1, 1H, 4'-H), 7.61 (t, J = 7.5 Hz, 1H, 7'-H), 7.55 (t, J = 7.5 Hz ,1H, 6'-H), 7.45 (t, J = 7.5 Hz, 1H, 3'-H), 3.50 (s, 1H, 2-H) ppm; ^{13}C NMR (101 MHz, $CDCl_3$): δ = 133.7 (8a'-C_{Ar}), 133.2 (4a'-C_{Ar}), 131.4 (2'-C_{Ar}), 129.4 (4'-C_{Ar}), 128.4 (5'-C_{Ar}), 127.1 (7'-C_{Ar}), 126.6 (6'-C_{Ar}), 126.2 (3'-C_{Ar}), 125.2 (8'-C_{Ar}), 119.9 (1'-C_{Ar}), 82.1 (C-1), 81.9 (C-2) ppm. The spectroscopic data are in accordance with literature.[6]

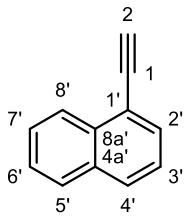

$C_{12}H_8$
152.20 g/mol

20a

2-Ethinylnaphthalin (20b)

Synthesis according to GP 2; colorless solid (83 %); column chromatography on silica (hexanes); R_f = 0.65 (hexanes, UV); m.p.: 35 °C; ^{1}H NMR (300 MHz, $CDCl_3$): δ = 8.04 (s, 1H, 1‘-H), 7.84–7.78 (m, 3H, 4‘-H, 5‘-H, 8‘-H), 7.55–7.48 (m, 3H, 3‘-H, 6‘-H, 7‘-H), 3.15 (s, 1H, 2-H), ppm; ^{13}C NMR (75 MHz, $CDCl_3$): δ = 133.2 (4a‘-C_{Ar}), 133.0 (8a‘-C_{Ar}), 132.4 (1‘-C_{Ar}), 128.7, 128.2, 127.92, 127.91, 127.0, (5 × C_{Ar}), 126.8 (8‘-C_{Ar}), 119.5 (2‘-C_{Ar}), 84.1 (C-1), 77.5 (C-2) ppm. The spectroscopic data are in accordance with literature.[7]

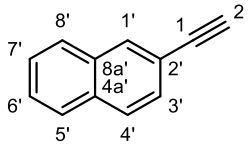

$C_{12}H_8$
152.20 g/mol

20b

Ethyl-3-(naphthalen-1-yl)propiolate (22a)

Synthesis according to GP 3; yellow oil (54 %); column chromatography on silica (hexanes / EtOAc = 40 : 1); R_f = 0.40 (hexanes / EtOAc = 40 : 1, UV); ^{1}H NMR (400 MHz, $CDCl_3$): δ = 8.35 (d, J = 7.1 Hz, 1H, 8‘-H), 7.95 (d, J = 7.1 Hz, 1H, 4‘-H), 7.87 (t, J = 7.5 Hz, 2H, 2‘-H, 5‘-H), 7.63 (t, J = 7.5, 1H, 7‘-H), 7.56 (t, J = 7.5, 1H, 6‘-H), 7.47 (t, J = 7.5 Hz, 1H, 3‘-H), 4.36 (q, J = 7.1 Hz, 2H, CH_2CH$_3$), 1.41 (t, J = 7.2 Hz, 3H, CH$_2$CH_3) ppm; ^{13}C NMR (101 MHz, $CDCl_3$): δ = 154.3 (C-1), 133.8 (8a‘-C_{Ar}), 133.2 (4a‘-C_{Ar}), 133.1 (2‘-C_{Ar}), 131.4 (4‘-C_{Ar}), 128.6 (5‘-C_{Ar}), 127.8 (7‘-C_{Ar}), 127.0 (6‘-C_{Ar}), 125.9 (8‘-C_{Ar}), 125.2 (3‘-C_{Ar}), 117.4 (1‘-C_{Ar}), 85.5 (C-2), 84.5 (C-3), 62.3 (CH_2CH$_3$), 14.3 (CH$_2$CH_3) ppm. The spectroscopic data are in accordance with literature.[8]

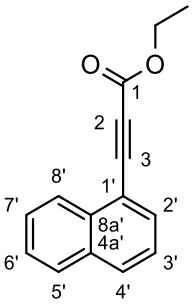

$C_{15}H_{12}O_2$
224.26 g/mol

22a

Ethyl-3-(naphthalen-2-yl)propiolate (22b)

Synthesis according to GP 3; colorless solid (76 %); column chromatography on silica (hexanes / EtOAc = 40 : 1); R_f = 0.29 (hexanes / EtOAc = 40 : 1, UV); m.p.: 54 °C; ^{1}H NMR (300 MHz, $CDCl_3$): δ = 8.16 (s, 1H, 1‘-H), 7.90–7.77 (m, 3H, 4‘-H, 5‘-H, 8‘-H), 7.50–7.61 (m, 3H, 3‘-H, 6‘-H, 7‘-H), 4.33 (q, J = 7.1 Hz, 2H, CH_2CH$_3$), 1.38 (t, J = 7.2 Hz, 3H, CH$_2$CH_3) ppm; ^{13}C NMR (75 MHz, $CDCl_3$): δ = 154.3 (C-1), 134.4 (1‘-C_{Ar}), 134.0 (4a‘-C_{Ar}), 132.7 (8a‘-C_{Ar}), 128.5, 128,4, 128.3, 128.0, 128.0, 127.1 (6 x C_{Ar}), 117.0 (2‘-C_{Ar}), 86.7 (C-3), 81.1 (C-2), 62.3 (CH_2CH$_3$), 14.3 (CH$_2$CH_3) ppm. The spectroscopic data are in accordance with literature.[9]

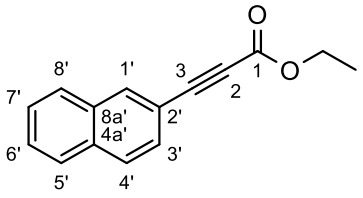

$C_{15}H_{12}O_2$
224.26 g/mol

22b

3-(Naphthalen-1-yl)propiolic acid (23a)

Synthesis according to GP 4; colorless solid (94 %); washing with hot hexanes; m.p.: 134 °C; ^{1}H NMR (500 MHz, CD_3OD): δ = 8.14 (d, J = 7.1 Hz, 1H, 8‘-H), 7.86 (d, J = 7.1 Hz, 1H, 2‘-H), 7.78 (d, J = 7.1 Hz, 1H, 5‘-H), 7.69 (d, J = 7.1 Hz, 1H, 4‘-H), 7.49 (t, J = 7.5 Hz, 1H, 7‘-H), 7.42 (t, J = 7.5 Hz, 1H, 6‘-H), 7.35 (t, J = 7.5 Hz, 1H, 3‘-H) ppm; ^{13}C NMR (126 MHz, $CDCl_3$): δ = 156.9 (C-1), 135.0 (8a‘-C_{Ar}), 134.7 (4a‘-C_{Ar}), 134.1(4‘-C_{Ar}), 132.6 (2‘-C_{Ar}), 130.0 (5‘-C_{Ar}), 128.9 (7‘-C_{Ar}), 128.2 (6‘-C_{Ar}), 126.5 (3‘-C_{Ar}), 126.5 (8‘-C_{Ar}), 118.4 (1‘-C_{Ar}), 86.9 (C-2), 84.8 (C-3) ppm. The spectroscopic data are in accordance with literature.[10]

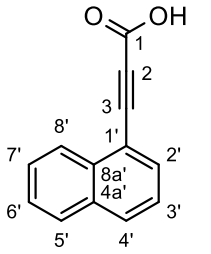

$C_{13}H_8O_2$
196.21 g/mol

23a

3-(Naphthalen-2-yl)propiolic acid (23b)

Synthesis according to GP 4; colorless solid (92 %); obtained without further purification; m.p.: 142 °C; ^{1}H NMR (700 MHz, CD_3OD): δ = 7.98 (m, 1H, 1‘-H), 7.72–7.69 (m, 3H, 4‘-H, 5‘-H, 8‘-H), 7.42–7.35 (m, 3H, 3‘-H, 6‘-H, 7‘-H), ppm; ^{13}C NMR (176 MHz, $CDCl_3$): δ = 156.9 (C-1), 135.4 (4a‘-C_{Ar}), 135.1 (1‘-C_{Ar}), 134.3 (8a‘-C_{Ar}), 129.8, 129.3, 129.2, 129.2, 129.1, 128.3 (6 x C_{Ar}), 118.3 (2‘-C_{Ar}), 87.1 (C-3), 82.3 (C-2) ppm. The spectroscopic data are in accordance with literature.[11]

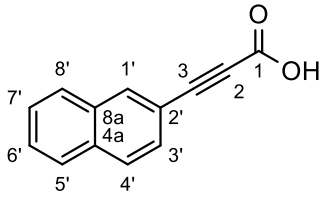

$C_{13}H_8O_2$
196.21 g/mol

23b

(*R*)-4-Isopropyl-3-(3-(naphthalen-1-yl)propioloyl)oxazolidin-2-one (25a)

Synthesis according to GP 5; orange solid (58 %); recrystallization from hexanes / EtOAc; m.p.: 104 °C; $[\alpha]_D^{20}$ = –55.6° [c = 10 mg/mL, CH_2Cl_2]; ^{1}H NMR (700 MHz, $CDCl_3$): δ = 8.64 (d, J = 7.1 Hz, 1H, 8‘-H), 7.99–7.94 (m, 2H, 2‘-H, 4‘-H), 7.87 (d, J = 7.1 Hz, 1H, 5‘-H), 7.66 (t, J = 7.5 Hz, 1H, 7‘-H), 7.56 (t, J = 7.5 Hz, 1H, 6‘-H), 7.48 (t, J = 7.5 Hz, 1H, 3‘-H), 4.56–4.51 (m, 1H, 2‘‘-H), 4.35 (t, J = 8.4 Hz, 1H, 3‘‘-H), 4.28 (dd, J = 3.0 Hz, 9.0 Hz, 1H, 2‘‘-H), 2.53–2.47 (m, 1H, 4‘‘-H), 0.98 (d, J = 6.9 Hz, 3H, 5‘‘-H), 0.96 (d, J = 6.9 Hz, 3H, 5‘‘-H) ppm; ^{13}C NMR (176 MHz, $CDCl_3$): δ = 152.9, 151.0 (2 × *C*=O), 134.3 (2‘-C_{Ar}), 134.2 (8a‘-C_{Ar}), 133.1 (4a‘-C_{Ar}), 132.0 (4‘-C_{Ar}), 128.4 (5‘-C_{Ar}), 128.0 (7‘-C_{Ar}), 127.1 (6‘-C_{Ar}), 126.4 (8‘-C_{Ar}), 125.2 (3‘-C_{Ar}), 117.6 (1‘-C_{Ar}), 93.5 (C-2), 85.8 (C-3), 63.2 (C-3‘‘), 58.8 (C-2‘‘), 28.6 (C-5‘‘), 18.1 (C-4‘‘), 14.9 (C-5‘‘) ppm; FTIR (ATR): $\tilde{\nu}$ = 3060 (w), 2964 (w), 2876 (w), 2204 (s), 1785 (vs), 1653 (s), 1586 (w),

1508 (w), 1486 (w), 1463 (w), 1386 (m), 1365 (s), 1323 (s), 1270 (m), 1236 (m), 1203 (s), 1145 (w), 1120 (w), 1091 (m), 1059 (m), 1049 (w), 1016 (w), 993.6 (m), 970 (w), 913 (w), 865 (w), 805 (m), 773 (s), 728 (m), 703 (m), 669 (w), 612 (w), 567 (w), 535 (w), 492 (w), 444 (w) cm^{-1}; LRMS (ESI): *m*/*z* = 308.1 $[M + H]^+$, 330.1 $[M + Na]^+$; HRMS (ESI): calcd. for $[C_{19}H_{18}NO_3]^+$ 308.1281, found 308.1281.

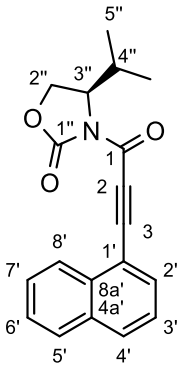

$C_{19}H_{17}NO_3$
307.35 g/mol

25a

(*R*)-4-Isopropyl-3-(3-(naphthalen-2-yl)propioloyl)oxazolidin-2-one (25b)

Synthesis according to GP 5; colorless solid (84 %); column chromatography on silica (hexanes / EtOAc = 10 : 1); R_f = 0.24 (hexanes / EtOAc = 10 : 1, UV); m.p.: 104 °C; $[\alpha]_D^{20}$ = –51.2° [c = 10 mg/mL, CH_2Cl_2]; ^{1}H NMR (500 MHz, $CDCl_3$): δ = 8.25 (s, 1H, 1‘-H), 7.88–7.81 (m, 3H, 4‘-H, 5‘-H, 8‘-H), 7.68–7.64 (m, 1H, 3‘-H), 7.58–7.51 (m, 2H, 6‘-H, 7‘-H), 4.53–4.50 (m, 1H, 2‘‘-H), 4.35–4.31 (m, 1H, 3‘‘-H), 4.28–4.25 (m, 1H, 2‘‘-H), 2.51–2.45 (m, 1H, 4‘‘-H), 0.97 (d, *J* = 6.9 Hz, 3H, 5‘‘-H), 0.95 (d, *J* = 6.9 Hz, 3H, 5‘‘-H) ppm; ^{13}C NMR (126 MHz, $CDCl_3$): δ = 152.8, 151.0 (2 × *C*=O), 135.0 (1‘-C_{Ar}), 134.2 (4a‘-C_{Ar}), 132.7 (8a‘-C_{Ar}), 128.6 (6‘-C_{Ar}), 128.5 (3‘-C_{Ar}), 128.5 (7‘-C_{Ar}), 128.2 (5‘-C_{Ar}), 128.0 (4‘-C_{Ar}), 127.1 (8‘-C_{Ar}), 117.1 (2‘-C_{Ar}), 95.2 (C-2), 81.5 (C-3), 63.5 (C-3‘‘), 58.8 (C-2‘‘), 28.7 (C-5‘‘), 18.1 (C-4‘‘), 14.9 (C-5‘‘) ppm; FTIR (ATR): $\tilde{\nu}$ = 3059 (w), 2964 (w), 2875 (w), 2207 (s), 1784 (s), 1653 (s), 1626 (w), 1595 (w), 1501 (w), 1485 (w), 1466 (w), 1385 (m), 1365 (s), 1348 (m), 1316 (vs), 1271 (m), 1257 (m), 1200 (s), 1143 (m), 1104 (m), 1056 (m), 1025 (m), 1008 (m), 975 (w), 952 (w), 902 (w), 862 (m), 818 (m), 771 (w), 750 (m), 729 (m), 700 (s), 663 (w), 645 (w), 572 (w), 530 (w), 498 (w), 475 (m) cm^{-1}; LRMS (ESI): *m*/*z* = 308.1 $[M + H]^+$, 330.1 $[M + Na]^+$; HRMS (ESI): calcd. for $[C_{19}H_{18}NO_3]^+$ 308.1281, found 308.1282.

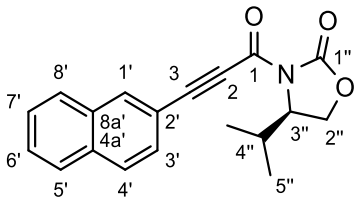

$C_{19}H_{17}NO_3$
307.35 g/mol

25b

(*R*)-4-Isopropyl-3-((1*R*,4*S*)-3-(naphthalen-1-yl)bicyclo[2.2.1]hepta-2,5-diene-2-carbonyl)oxazolidin-2-one (5)

Synthesis according to GP 6; colorless oil (39 %); column chromatography on silica (hexanes / EtOAc = 10 : 1) followed by preparative HPLC on an Orbit 100 Sil column (250 × 20 mm, 5 µm, hexanes / *i*PrOH 99 : 1, flow rate: 19 mL/min, λ = 245 nm, R_t = 15.29 min); R_f = 0.13 (hexanes / EtOAc = 10 : 1, UV); $[\alpha]_D^{20}$ = –16.1° [c = 10 mg/mL, CH_2Cl_2]; ^{1}H NMR (700 MHz, $CDCl_3$): δ = 7.86–7.71 (m, 3H, 4‘-H, 5‘-H, 8‘-H), 7.49–7.38 (m, 3H, 3‘-H, 6‘-H, 7‘-H), 7.33–7.19 (m, 1H, 2‘-H), 7.17 (dd, *J* = 3.0, 4.8 Hz, 1H, 6-H), 6.94 (dd, *J* = 3.0, 4.8 Hz, 1H, 5-H), 4.24–4.18 (m, 1H, 3‘‘-H), 3.98–3.94 (m, 1H, 4-H), 3.94–3.87 (m, 3H, 1-H,

2‘‘-H), 2.80 (dt, *J* = 1.7 Hz, 6.3 Hz 1H, 7-H), 2.22 (dt, *J* = 1.7 Hz, 6.3 Hz, 1H, 7-H), 2.06–1.97 (m, 1H, 4‘‘-H), 0.70 (d, *J* = 6.9 Hz, 3H, 5‘‘-H), 0.44–0.34 (m, 3H, 5‘‘-H) ppm; ^{13}C NMR (176 MHz, $CDCl_3$): δ = 167.5 (C-6‘‘), 161.3 (C-3), 153.3 (C-1‘‘), 144.6 (C-2), 144.1 (C-6), 141.0 (C-5), 135.0, 133.7, 130.9, 128.4, 128.3, 126.4, 126.1, 125.9, 125.4 (9 × C_{Ar}), 124.4 (1’-C_{Ar}), 71.7 (C-7), 63.2 (C-2‘‘), 58.9 (C-1), 58.5 (3‘‘-H), 54.6 (C-4), 28.5 (C-4‘‘), 18.0 (C-5‘‘), 14.4 (C-5‘‘) ppm; FTIR (ATR): $\tilde{\nu}$ = 3059 (w), 2965 (w), 2936 (w), 2873 (w), 2206 (w), 1780 (vs), 1667 (s), 1588 (w), 1558 (w), 1507 (w), 1485 (w), 1463 (w), 1386 (m), 1364 (m), 1324 (m), 1297 (s), 1273 (m), 1255 (m), 1203 (s), 1142 (w), 1119 (w), 1094 (m), 1073 (w), 1052 (w), 1015 (w), 994 (w), 947 (w), 911 (w), 882 (w), 862 (w), 802 (m), 776 (s), 730 (m), 711 (m), 683 (w), 646 (w), 567 (w), 491 (w), 439 (w) cm^{-1}; LRMS (ESI): *m*/*z* = 245.1 $[C_{18}H_{13}O]^+$, 374.2 $[M + H]^+$, 396.2 $[M + Na]^+$; HRMS (ESI): calcd. for $[C_{24}H_{24}NO_3]^+$ 374.1751, found $[M + H]^+$ 374.1753.

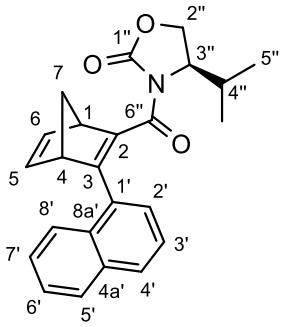

$C_{24}H_{23}NO_3$
373.45 g/mol

5

(*R*)-4-Isopropyl-3-((1*R*,4*S*)-3-(naphthalin-2-yl)bicyclo[2.2.1]hepta-2,5-dien-2-carbonyl)-oxazolidin-2-on (6)

Synthesis according to GP 6; colorless solid (25 %); column chromatography on silica (hexanes / EtOAc = 10 : 1); R_f = 0.18 (hexanes / EtOAc = 10 : 1, UV); m.p.: 124 °C; $[\alpha]_D^{20}$ = –55.6° [c = 10 mg/mL, CH_2Cl_2]; ^{1}H NMR (700 MHz, $CDCl_3$): δ = 7.80–7.74 (m, 4H, 1‘-H, 4‘-H, 5‘-H, 6‘-H), 7.48–7.43 (m, 2H, 6‘-H, 7‘-H), 7.42–7.37 (m, 1H, 3‘-H), 7.04 (dd, *J* = 3.0, 4.8 Hz, 1H, 6-H), 6.96 (dd, *J* = 3.0, 4.8 Hz, 1H, 5-H), 4.49–4.44 (m, 1H, 3‘‘-H), 4.22–4.13 (m, 2H, 2‘‘-H), 4.08–4.04 (m, 1H, 4-H), 3.87–3.84 (m, 1H, 1-H), 2.62 (dt, *J* = 1.7, 6.3 Hz, 1H, 7-H), 2.51–2.42 (m, 1H, 4‘‘-H), 2.16 (dt, *J* = 1.7 Hz, 6.3 Hz, 1H, 7-H), 0.92 (d, *J* = 6.9 Hz, 3H, 5‘‘-H), 0.87 (d, *J* = 6.9 Hz, 1H, 5‘‘-H), ppm; ^{13}C NMR (176 MHz, $CDCl_3$): δ = 168.2 (C-6‘‘), 160.1 (C-3), 153.3 (C-1‘‘), 143.7 (C-6), 142.2 (C-2), 140.9 (C-5), 133.3, 133.2, 133.2, 128.3, 128.0, 127.8, 124.4, 126.4 (8 × C_{Ar}), 125.6 (1‘-C_{Ar}), 124.9 (C_{Ar}), 71.3 (C-7), 63.5 (C-2‘‘), 58.9 (C-3‘‘), 56.2 (C-4), 55.6 (C-1), 28.6 (C-4‘‘), 18.2 (C-5‘‘), 14.9 (C-5‘‘) ppm; FTIR (ATR): $\tilde{\nu}$ = 3058 (w), 2964 (w), 2873 (w), 2252 (w), 1778 (vs), 1666 (s), 1625 (w), 1595 (w), 1557 (w), 1504 (w), 1485 (w), 1464 (w), 1385 (m), 1362 (s), 1322 (s), 1296 (s), 1270 (s), 1201 (s), 1142 (m), 1119 (m), 1096 (m), 1077 (m), 1053 (m), 1015 (m), 981 (w), 909 (m), 881 (w), 858 (m), 817 (m), 783 (m), 750 (m), 729 (s), 712 (vs), 683 (w), 658 (w), 626 (w), 574 (w), 528 (w), 501 (w), 476 (m), 438 (w) cm^{-1}; LRMS (ESI): *m*/*z* = 245.1 $[C_{18}H_{13}O]^+$, 374.2 $[M + H]^+$, 396.2 $[M + Na]^+$; HRMS (ESI): calcd. for $[C_{24}H_{24}NO_3]^+$ 374.1751, found $[M +H]^+$ 374.1754.

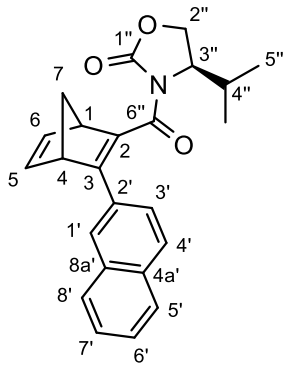

$C_{24}H_{23}NO_3$
373.45 g/mol

6

1.3 Synthesis of the phenyl-substituted norbornadienes

General remark about the synthesis of the norbornadiene (2c)

The chiral norbornadiene **2c** was synthesized according to a literature protocol from our previous publication.[1] The analytical data was in good agreement with our previous results.

General procedure for the substitution of norbornadiene acid (27) with oxazolidinones and lactams (2a,b, 14a–d) [GP 7]

Under a nitrogen atmosphere thionyl chloride (0.22 mL, 0.37 g, 3.09 mmol) was added to a solution of the norbornadiene acid **27** (0.16 g, 0.77 mmol) in abs. CH_2Cl_2 (15 mL) and the reaction mixture was refluxed for 4 h. The solvent was removed under reduced pressure and the acyl chloride was taken up in abs. THF (15 mL). In a second Schlenk flask the respective oxazolidinone **28a,b** or lactam **13a–d** (0.70 mmol) was dissolved in abs. THF (15 mL) under a nitrogen atmosphere and *n*-BuLi (0.28 mL, 0.19 g, 0.70 mmol, 2.5 M in hexanes) was added dropwise at -78 °C. The reaction mixture was stirred for 30 min at -78 °C and the solution of the acyl chloride in abs. THF was added dropwise. The reaction mixture was stirred for 3-5 h until full conversion was observed via thin-layer chromatography (TLC). A saturated aqueous NH_4Cl solution (20 mL) was added and the aqueous layer was extracted with EtOAc (3 × 30 mL). The combined organic layers were dried over $MgSO_4$, the solvent was removed under reduced pressure and the crude product was either purified by column chromatography on silica or recrystallization from hexanes / EtOAc.

General procedure for the substitution of norbornadiene acid (28) with imidazolidinones (12, Ph(ImC$_1$)) [GP 8]

Under a nitrogen atmosphere thionyl chloride (0.27 mL, 0.45 g, 3.77 mmol) was added to a solution of the norbornadiene acid **27** (0.20 g, 0.94 mmol) in abs. CH_2Cl_2 (50 mL) and the reaction mixture was refluxed for 4 h. The solvent was removed under reduced pressure and the acyl chloride was taken up in abs. THF (30 mL). In a second Schlenk flask the respective imidazolidinone **10** or **11** (0.94 mmol) was dissolved in abs. THF (30 mL) under a nitrogen atmosphere and NaH (34.0 mg, 1.41 mmol, 60 wt% in mineral oil) was added at 0 °C. The reaction mixture was stirred for 30 min at 0 °C and the solution of the acyl chloride in abs. THF was added dropwise. The reaction mixture was stirred for 3 h until full conversion was observed via TLC. A saturated aqueous NH_4Cl solution (30 mL) was added and the aqueous layer was extracted with EtOAc (3 × 30 mL). The combined organic layers were dried over $MgSO_4$, the solvent was removed under reduced pressure and the crude product was either purified by column chromatography on silica or recrystallization.

(1*R*,4*S*)-3-Phenylbicyclo[2.2.1]hepta-2,5-dien-2-carboxylic acid (27)

According to ref.,[12] the chiral norbornadiene **2c** (0.70 g, 2.16 mmol) was dissolved in a mixture of THF (45 mL) and H_2O (9 mL) and H_2O_2 (0.44 mL, 0.49 g, 4.31 mmol, 30 wt% in H_2O) and LiOH · H_2O (0.18 g, 4.31 mmol) were added at 0 °C. The reaction mixture was stirred for 3 h at room temperature, acidified with 1 M HCl (50 mL) and the aqueous phase was extracted with EtOAc (3 × 40 mL). The combined organic layers were dried over $MgSO_4$, the solvent was removed under reduced pressure and the crude product was purified by column chromatography (hexanes/EtOAc = 5 : 1). The carboxylic acid **27** was obtained as a colorless solid (0.37 g, 1.74 mmol, 81 %).

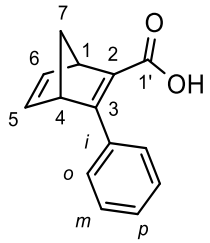

$C_{14}H_{12}O_2$
212.24 g/mol

27

R_f = 0.33 (hexanes / EtOAc = 5 : 1, UV); m.p.: 88 °C; ^{1}H NMR (400 MHz, $CDCl_3$): δ = 7.59–7.48 (m, 2H, o-Ar*H*), 7.42–7.29 (m, 3H, *m*-Ar*H, p*-Ar*H*), 7.00 (dd, *J* = 3.0, 4.9 Hz, 1H, 6-H), 6.92 (dd, *J* = 3.0, 4.9 Hz, 1H, 5-H), 4.15–4.04 (m, 1H, 1-H), 3.93–3.83 (m, 1H, 4-H), 2.28 (dt, *J* = 1.4, 6.3 Hz, 1H, 7-H), 2.08 (dt, *J* = 1.4, 6.3 Hz, 1H, 7-H) ppm; ^{13}C NMR (101 MHz, $CDCl_3$): δ = 170.8 (C-1‘), 170.0 (C-3), 144.0 (C-6), 140.7 (C-5), 138.5 (*i*-C_{Ar}), 135.5 (C-2), 128.9 (*p*-C_{Ar}), 128.1 (*m*-C_{Ar}), 127.9 (*o*-C_{Ar}), 70.7 (C-7), 59.2 (C-4), 53.0 (C-1) ppm. The spectroscopic data were in accordance with literature.[13]

3-((1*R*,4*S*)-3-Phenylbicyclo[2.2.1]hepta-2,5-diene-2-yl)proxazolidin-2-one (2a)

Synthesis according to GP 7; white solid (86 %); filtration over silica (hexane / EtOAc = 2 : 1) followed by recrystallization from hexanes / EtOAc; m.p.: 75 °C; $[\alpha]_D^{20}$ = −4.3 ° [c = 10 mg/mL, CH_2Cl_2]; ^{1}H NMR (500 MHz, $CDCl_3$): δ = 7.36–7.26 (m, 5H, *o*-Ar*H, m*-Ar*H*, *p*-Ar*H*), 6.99 (dd, *J* = 3.0, 4.9 Hz, 1H, 6-H), 6.92 (dd, *J* = 3.0, 4.9 Hz, 1H, 5-H), 4.39–4.24 (m, 2H, 3‘-H), 4.02 (t, *J* = 7.9 Hz, 2H, 2‘-H), 3.96–3.92 (m, 1H, 1-H), 3.90–3.86 (m, 1H, 4-H), 2.62 (dt, *J* = 1.4, 6.3 Hz, 1H, 7-H), 2.13 (dt, *J* = 1.4, 6.3 Hz, 1H, 7-H), ppm; ^{13}C NMR (126 MHz, $CDCl_3$): δ = 168.1 (C-4‘), 161.6 (C-3), 152.6 (C-1‘), 143.6 (C-6), 141.4 (C-5), 141.1 (C-2), 135.5 (*i*-C_{Ar}), 128.5 (*o*-C_{Ar}), 128.4 (*p*-C_{Ar}), 126.7 (*m*-C_{Ar}), 71.6 (C-7), 62.3 (C-3’), 56.4 (C-1), 55.3 (C-4), 43.0 (C-2’), ppm; FTIR (ATR): $\tilde{\nu}$ = 3064 (w), 2989 (w), 2940 (w), 2871 (w), 1780 (vs), 1667 (m), 1619 (w), 1558 (w), 1492 (w), 1478 (w), 1444 (w), 1384 (m), 1334 (m), 1298 (m), 1274 (m), 1221 (m), 1122 (w), 1100 (w), 1075 (w), 1037 (m), 1010 (w), 979 (w), 952 (w), 903 (w), 882 (w), 853 (w), 802 (w), 760 (m), 721 (w), 706 (m), 635 (w), 549 (w), 495 (w), 441 (w) cm^{-1}; LRMS (ESI): *m*/*z* = 195.1 $[C_{14}H_{11}O]^+$, 282.1 $[M + H]^+$, 304.1 $[M + Na]^+$; HRMS (ESI): calcd. for $[C_{17}H_{15}NO_3Na]^+$ 304.0944, found $[M + Na]^+$ 304.0944.

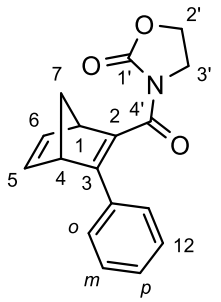

$C_{17}H_{15}NO_3$
281.12 g/mol

2a

(*R*)-4-Benzyl-3-((1*R*,4*S*)-3-phenylbicyclo[2.2.1]hepta-2,5-diene-2-carbonyl)oxazolidin-2-one (2b)

Synthesis according to GP 7; colorless oil (45 %); column chromatography on silica (hexanes / EtOAc = 5 : 1); R_f = 0.36 (hexanes / EtOAc = 5 : 1, UV); $[\alpha]_D^{20}$ = –69.0 [c = 10 mg/mL, CH_2Cl_2]; ^{1}H NMR (500 MHz, $CDCl_3$): δ = 7.37–7.23 (m, 8H, *o*-Ar*H*, *m*-Ar*H*, *m*'-Ar*H*, *p*-Ar*H*, *p*'-Ar*H*), 7.22–7.17 (m, 2H, *o*'-Ar*H*), 7.01 (dd, *J* = 3.0 Hz, 4.9 Hz, 1H, 6-H), 6.89 (dd, *J* = 3.0 Hz, 4.9 Hz, 1H, 5-H), 4.67–4.58 (m, 1H, 3'-H), 4.11–4.02 (m, 2H, 2'-H), 3.96–3.91 (m, 1H, 1-H), 3.84–3.79 (m, 1H, 4-H), 3.46 (dd, *J* = 3.8, 13.6 Hz, 1H, 4'-H), 2.69 (dd, *J* = 3.8, 13.6 Hz, 1H, 4'-H), 2.57 (dt, *J* = 1.4 Hz, 6.3 Hz, 1H, 7-H), 2.11 (dt, *J* = 1.4 Hz, 6.3 Hz, 1H, 7-H) ppm; ^{13}C NMR (126 MHz, $CDCl_3$): δ = 168.0 (C-6'), 161.6 (C-3), 152.6 (C-1'), 143.7 (C-6), 141.6 (C-2), 141.0 (C-5), 135.7 (*i*'-C_{Ar}), 135.5 (*i*-C_{Ar}), 129.5 (*o*'-C_{Ar}), 129.1 (*m*'-C_{Ar}), 128.53 (*p*-C_{Ar}), 128.45 (*o*-C_{Ar}), 127.4 (*p*'-C_{Ar}), 126.8 (*m*-C_{Ar}), 71.4 (C-7), 66.6 (C-2'), 56.5 (C-1), 55.8 (C-3'), 55.2 (C-4), 37.9 (C-4') ppm; FTIR (ATR): $\tilde{\nu}$ = 3063 (w), 3028 (w), 2986 (w), 2938 (w), 2870 (w), 1779 (s), 1664 (m), 1604 (w), 1559 (w), 1493 (w), 1454 (w), 1386 (m), 1348 (s), 1329 (m), 1296 (m), 1265 (s), 1210 (s), 1196 (s), 1098 (m), 1075 (m), 1044 (w), 1031 (m), 1011 (m), 977 (w), 960 (w), 909 (m), 835 (w), 800 (w), 760 (s), 729 (s), 697 (vs), 646 (w), 600 (w), 569 (w), 549 (w), 526 (w), 504 (w), 446 (w) cm^{-1}; LRMS (ESI): *m*/*z* = 195.1 $[C_{14}H_{11}O]^+$, 372.2 $[M + H]^+$, 394.1 $[M + Na]^+$; HRMS (ESI): calcd. for $[C_{24}H_{21}NO_3Na]^+$ 394.1414, found $[M + Na]^+$ 394.1405.

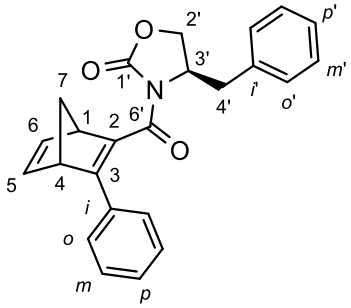

$C_{24}H_{21}NO_3$
371.44 g/mol

2b

1-((1*R*,4*S*)-3-Phenylbicyclo[2.2.1]hepta-2,5-diene-2-carbonyl)pyrrolidin-2-one (14a)

Synthesis according to GP 7; white solid (46 %); recrystallization from hexanes / EtOAc; m.p.: 151 °C; $[\alpha]_D^{20}$ = –45.6 [c = 10 mg/mL, CH_2Cl_2]; ^{1}H NMR (500 MHz, $CDCl_3$): δ = 7.33–7.27 (m, 2H, *o*-Ar*H*), 7.26–7.18 (m, 3H, *m*-Ar*H*, *p*-Ar*H*), 6.97 (dd, *J* = 3.0, 4.9 Hz, 1H, 6-H), 6.91 (dd, *J* = 3.0, 4.9 Hz, 1H, 5-H), 3.94–3.89 (m, 1H, 1-H), 3.85–3.73 (m, 3H, 4-H, 2'-H), 2.61 (dt, *J* = 1.4, 9.8 Hz, 1H, 7-H), 2.42–2.29 (m, 2H, 4'-H), 2.12 (dt, *J* = 1.4, 9.8 Hz, 1H, 7-H), 1.88–2.03 (m, 2H, 3'-H) ppm; ^{13}C NMR (126 MHz, $CDCl_3$): δ = 174.2 (C-1'), 168.7 (C-5'), 159.4 (C-3), 143.6 (C-6), 142.7 (C-2), 141.4 (C-5), 128.3 (*o*-C_{Ar}), 135.8 (*i*-C_{Ar}), 128.1 (*p*-C_{Ar}), 126.6 (*m*-C_{Ar}), 71.4 (C-7), 56.0 (C-1), 55.2 (C-4), 45.7 (C-2'), 33.0 (C-4'), 17.7 (C-3') ppm; FTIR (ATR): $\tilde{\nu}$ = 3062 (w), 2984 (w), 2937 (w), 2894 (w), 2870 (w), 1738 (s), 1657 (s), 1618 (m), 1558 (w), 1492

(w), 1458 (w), 1444 (w), 1419 (w), 1359 (m), 1325 (s), 1297 (s), 1285 (s), 1264 (vs), 1246 (s), 1225 (s), 1190 (m), 1117 (w), 1081 (w), 1021 (w), 994 (w), 935 (w), 879 (w), 829 (w), 812 (w), 795 (w), 764 (m), 718 (m), 696 (m), 670 (w), 650 (w), 621 (w), 579 (w), 547 (w), 499 (w), 472 (w), 426 (w) cm^{-1}; LRMS (ESI): *m*/*z* = 195.1 $[C_{14}H_{11}O]^+$, 280.1 $[M + H]^+$, 302.1 $[M + Na]^+$; HRMS (ESI): calcd. for $[C_{18}H_{17}NO_2Na]^+$ 302.1151, found $[M + Na]^+$ 302.1151.

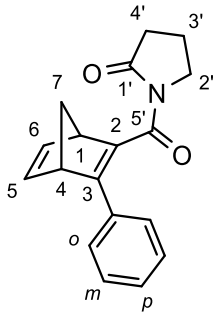

$C_{18}H_{17}NO_2$
279.33 g/mol

14a

1-((1*R*,4*S*)-3-Phenylbicyclo[2.2.1]hepta-2,5-diene-2-carbonyl)piperidin-2-one (14b)

Synthesis according to GP 7; white solid (41 %); recrystallization from hexanes / EtOAc; m.p.: 140 °C (decomposition); $[\alpha]_D^{20}$ = –67.2° [c = 10 mg/mL, CH_2Cl_2]; ^{1}H NMR (500 MHz, $CDCl_3$): *δ* = 7.34–7.29 (m, 2H, *o*-Ar*H*), 7.28–7.23 (m, 1H, *p*-Ar*H*), 7.19–7.14 (m, 2H, *m*-Ar*H*), 7.01 (dd, *J* = 3.0, 4.9 Hz, 1H, 6-H), 6.86 (dd, *J* = 3.0, 4.9 Hz, 1H, 5-H), 3.84–3.77 (m, 2H, 1-H, 4-H), 3.68–3.58 (m, 2H, 2‘-H), 2.50 (dt, *J* = 1.4, 9.8 Hz, 1H, 7-H), 2.08 (dt, *J* = 1.4, 9.8 Hz, 1H, 7-H), 1.92 (t, *J* = 6.9 Hz, 2H, 5‘-H), 1.71–1.56 (m, 4H, 3‘-H, 4‘-H) ppm; ^{13}C NMR (126 MHz, $CDCl_3$): *δ* = 173.1 (C-1‘), 172.2 (C-6‘), 156.1 (C-3), 144.4 (C-2), 143.8 (C-6), 140.1 (C-5), 136.2 (*i*-C_{Ar}), 128.3 (*o*-C_{Ar}), 127.8 (*p*-C_{Ar}), 126.8 (*m*-C_{Ar}), 71.2 (C-7), 56.4 (C-1), 54.5 (C-4), 45.3 (C-2‘), 33.9 (C-5‘), 22.2 (C-3‘), 21.2 (C-4‘) ppm; FTIR (ATR): $\tilde{\nu}$ = 3060 (w), 2993 (w), 2983 (w), 2966 (w), 2935 (w), 2866 (w), 1696 (s), 1656 (vs), 1618 (w), 1593 (w), 1559 (w), 1491 (w), 1479 (w), 1462 (w), 1445 (w), 1392 (w), 1339 (m), 1316 (w), 1295 (s), 1276 (m), 1261 (w), 1243 (m), 1184 (w), 1161 (m), 1148 (m), 1134 (w), 1096 (w), 1079 (w), 1065 (w), 1026 (w), 1001 (w), 977 (w), 945 (w), 918 (w), 890 (w), 864 (w), 825 (w), 809 (w), 767 (m), 747 (m), 725 (m), 702 (m), 677 (w), 665 (w), 637 (w), 604 (w), 564 (w), 552 (w), 507 (w), 441 (w), 424 (w) cm^{-1}; LRMS (ESI): *m*/*z* = 195.1 $[C_{14}H_{11}O]^+$, 294.2 $[M + H]^+$, 316.1 $[M + Na]^+$; HRMS (ESI): calcd. for $[C_{19}H_{20}NO_2]^+$ 294.1489, found $[M + H]^+$ 294.1490.

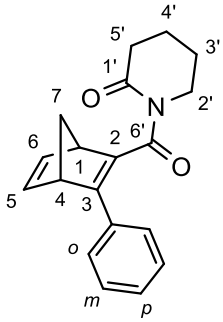

$C_{19}H_{19}NO_2$
293.37 g/mol

14b

1-((1*R*,4*S*)-3-Phenylbicyclo[2.2.1]hepta-2,5-diene-2-carbonyl)azepan-2-one (14c)

Synthesis according to GP 7; colorless oil (45 %); column chromatography on silica (hexanes / EtOAc = 5 : 1); R_f = 0.26 (hexanes / EtOAc = 5 : 1, UV); $[\alpha]_D^{20}$ = –24.0° [c = 10 mg/mL, CH_2Cl_2]; ^{1}H NMR (500 MHz, $CDCl_3$): *δ* = 7.33–7.27 (m, 2H, *o*-Ar*H*), 7.26–7.21 (m, 1H, *p*-Ar*H*), 7.20–7.15 (m, 2H, *m*-Ar*H*), 7.00 (dd, *J* = 3.0, 4.9 Hz, 1H, 6-H), 6.86 (dd, *J* = 3.0, 4.9 Hz, 1H, 5-H), 3.87–3.67 (m, 4H, 1-H, 4-H, 2‘-H), 2.52 (dt, *J* = 1.4, 9.8 Hz, 1H, 7-H), 2.32–

2.23 (m, 2H, 6‘-H), 2.08 (dt, *J* = 1.4, 9.8 Hz, 1H, 7-H), 1.72–1.57 (m, 4H, 3‘-H, 4‘-H), 1.51–1.34 (m, 2H, 5‘-H) ppm; ^{13}C NMR (126 MHz, $CDCl_3$): δ = 177.3 (C-1‘), 171.5 (C-7‘),154.5 (C-3), 144.9 (C-2), 143.6 (C-6), 140.2 (C-5), 136.0 (*i*-C_{Ar}), 128.2 (*o*-C_{Ar}), 127.7 (*p*-C_{Ar}), 126.8 (*m*-C_{Ar}), 71.0 (C-7), 56.0 (C-1), 55.0 (C-4), 43.7 (C-2‘), 38.4 (C-6‘), 29.5 (C-4‘), 28.3 (C-3‘), 23.3 (C-5‘) ppm; FTIR (ATR): $\tilde{\nu}$ = 3062 (w), 2985 (w), 2933 (m), 2860 (w), 1777 (w), 1700 (s), 1662 (s), 1558 (w), 1492 (w), 1443 (m), 1379 (m), 1361 (m), 1348 (m), 1332 (s), 1296 (s), 1253 (s), 1213 (s), 1179 (vs), 1145 (s), 1079 (m), 1046 (w), 1027 (w), 991 (w), 968 (s), 904 (m), 891 (m), 873 (w), 854 (w), 842 (w), 809 (w), 758 (s), 715 (s), 695 (s), 656 (w), 614 (m), 596 (w), 558 (w), 535 (w), 503 (w), 473 (w), 450 (w), 418 (w) cm^{-1}; LRMS (ESI): *m*/*z* = 195.1 $[C_{14}H_{11}O]^+$, 308.2 $[M + H]^+$, 330.2 $[M + Na]^+$; HRMS (ESI): calcd. for $[C_{20}H_{22}NO_2]^+$ 308.1645, found $[M + H]^+$ 308.1641.

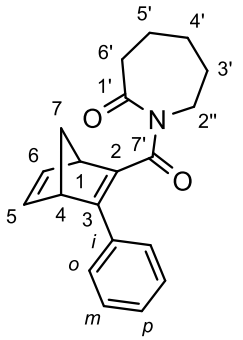

$C_{20}H_{21}NO_2$
307.39 g/mol

14c

1-((1*R*,4*S*)-3-Phenylbicyclo[2.2.1]hepta-2,5-diene-2-carbonyl)azacyclotridecan-2-one (14d)

Synthesis according to GP 7; colorless oil (44 %); column chromatography on silica (hexanes / EtOAc = 20 : 1 to 10 : 1); R_f = 0.29 (hexanes / EtOAc = 20 : 1, UV); $[\alpha]_D^{20}$ = –28.7° [c = 10 mg/mL, CH_2Cl_2]; ^{1}H NMR (500 MHz, $CDCl_3$): δ = 7.34–7.23 (m, 3H, *o*-Ar*H*, *p*-Ar*H*), 7.18–7.11 (m, 2H, *m*-Ar*H*), 7.04 (dd, *J* = 3.0, 4.9 Hz, 1H, 6-H), 6.87 (dd, *J* = 3.0, 4.9 Hz, 1H, 5-H), 3.95–3.85 (m, 2H, 1-H, 4-H), 3.60–3.48 (m, 2H, 2‘-H), 2.39 (dt, *J* = 1.4, 9.8 Hz, 1H, 7-H), 2.36–2.23 (m, 2H, 12‘-H), 2.11 (dt, *J* = 1.4, 9.8 Hz, 1H, 7-H), 1.62–1.55 (m, 2H, 11‘-H), 1.50–1.41 (m, 2H, 3‘-H), 1.13–1.33 (m, 14H, 4‘-H, 5‘-H, 6‘-H, 7‘-H, 8‘-H, 9‘-H, 10‘-H) ppm; ^{13}C NMR (126 MHz, $CDCl_3$): δ = 176.5 (C-1‘), 172.5 (C-13‘), 156.9 (C-3), 144.1 (C-2), 143.4 (C-6), 140.3 (C-5), 135.2 (*i*-C_{Ar}), 128.6 (*o*-C_{Ar}), 128.5 (*p*-C_{Ar}), 126.7 (*m*-C_{Ar}), 71.0 (C-7), 56.5 (C-1), 54.8 (C-4), 45.2 (C-2‘), 38.0 (C-12‘), 26.8 (C-3‘), 26.3, 26.03, 25.99, 25.6, 25.2, 24.9, 24.2, 23.7 (C-4‘, C-5‘, C-6‘, C-7‘, C-8‘, C-9‘, C-10‘, C-11‘),ppm; FTIR (ATR): $\tilde{\nu}$ = 2931 (m), 2861 (w), 1667 (m), 1642 (s), 1573 (w), 1558 (w), 1492 (w), 1461 (w), 1444 (m), 1351 (m), 1295 (m), 1256 (m), 1230 (m), 1215 (m), 1170 (m), 1140 (m), 1121 (w), 1090 (m), 1043 (m), 977 (w), 950 (w), 909 (m), 880 (w), 847 (w), 810 (w), 761 (m), 729 (vs), 695 (s), 647 (m), 630 (w), 556 (w), 527 (w), 504 (w), 474 (w), 431 (w) cm^{-1}; LRMS (ESI): *m*/*z* = 195.1 $[C_{14}H_{11}O]^+$, 392.3 $[M + H]^+$, 414.2 $[M + Na]^+$; HRMS (ESI): calcd. for $[C_{26}H_{34}NO_2]^+$ 392.2584, found $[M + H]^+$ 392.2584.

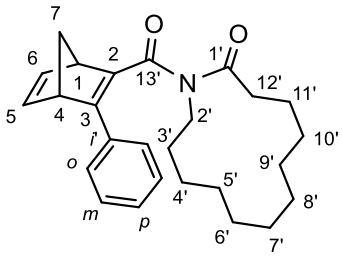

$C_{26}H_{33}NO_2$
391.56 g/mol

14d

(*R*)-2-((*tert*-Butoxycarbonyl)amino)-3-methylbutanoic acid (29)

According to ref.,[14] to a solution of (*D*)-valine (20.0 g, 0.17 mol) in THF (400 mL) was added Di-*tert*-butyl dicarbonate (40.8 g, 0.19 mol) and NaOH (100 mL, 17 wt% in water). The reaction mixture was stirred for 24 h at room temperature, 1 M HCl (100 mL) was added and the aqueous phase was extracted with EtOAc (3 × 150 mL). The combined organic layers were dried over Na_2SO_4 and the solvent was removed under reduced pressure. *N*-boc-protected (*D*)-valine **29** was obtained as a colorless oil (34.1 g, 0.17 mol, quant.) without further purification.

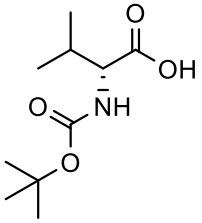

$C_{10}H_{19}NO_4$
217.26 g/mol

29

^{1}H NMR (300 MHz, $CDCl_3$): δ = 11.37 (bs, 1H, COO*H*, COO*H**), 6.32 (d, *J* = 8.6 Hz, 0.32H, N*H**), 5.07 (d, *J* = 8.6 Hz, 0.68H, N*H*), 4.37–4.16 (m, 0.68H, 2-H), 4.11–3.88 (m, 0.32H, 2-H*), 2.28–2.06 (m, 1H, 3-H, 3-H*), 1.43 (s, 9H, C(CH_3)$_3$, C(CH*$_3$)$_3$), 0.98 (d, *J* = 7.3 Hz, 3H, 4-H, 4-H*), 0.91 (d, *J* = 7.3 Hz, 3H, 4-H, 4-H*) ppm; ^{13}C NMR (75 MHz, $CDCl_3$): δ = 177.3 (C-1), 177.1 (C*-1), 157.2 (*C**O_2*t*-Bu), 156.0 (*C*O_2*t*-Bu), 81.7 (*C**(CH_3)$_3$), 80.2 (*C*(CH_3)$_3$), 60.2 (C-2), 58.5 (C*-2), 31.2 (C-3), 31.0 (C*-3), 28.4 (C(*C*H_3)$_3$), 28.3 (C(*C**H_3)$_3$), 19.2 (C*-4), 19.1 (C-4), 17.61 (C*-4), 17.55 (C-4) ppm. The spectroscopic data are in accordance with literature.[14]

(*R*)-*tert*-Butyl-(3-methyl-1-oxo-1-(phenylamino)butan-2-yl)carbamate (30)

According to ref.,[14] in a flame dried Schlenk flask under a nitrogen atmosphere *N*-boc-protected (*D*)-valine **29** (34.1 g, 0.16 mol) was dissolved in abs. CH_2Cl_2 (150 mL) and NEt_3 (23.9 mL, 17.5 g, 0.17 mol) and ethyl chloroformate (16.5 mL, 18.8 g, 0.17 mol) were added dropwise at 0 °C. The reaction mixture was stirred for 30 min at 0 °C, aniline (14.3 mL, 14.6 g, 0.16 mol) was added dropwise and the reaction mixture was stirred for 3 h at room temperature. The reaction mixture was washed with a saturated $NaHCO_3$ solution (50 mL) and brine (50 mL). The organic layer was dried over Na_2SO_4, the solvent was removed under reduced pressure and the crude product was washed with hot hexanes (200 mL) to yield *N*-boc-protected amide **30** as a colorless solid (4.84 g, 16.6 mmol, 11 %).

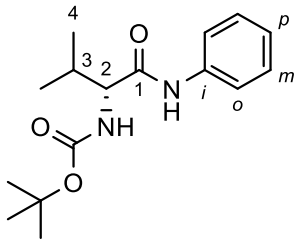

$C_{16}H_{24}N_2O_3$
292.38 g/mol

30

m.p.: 142 °C; ^{1}H NMR (300 MHz, $CDCl_3$): δ = 8.79 (bs, 1H, N*H*), 7.58–7.38 (m, 2H, *o*-Ar*H*), 7.25–7.13 (m, 2H, *m*-Ar*H*), 7.10–6.97 (m, 1H, *p*-Ar*H*), 5.59 (d, *J* = 8.6 Hz, 1H, N*H*), 4.26–4.05 (m, 1H, 2-H), 2.38–1.94 (m, 1H, 3-H), 1.42 (s, 9H, C(CH_3)$_3$), 1.04 (d, *J* = 7.3 Hz, 3H, 4-H), 1.02 (d, *J* = 7.3 Hz, 3H, 4-H) ppm; ^{13}C NMR (75 MHz, $CDCl_3$): δ = 170.9 (C-1), 156.6 (*C*O_2*t*-Bu), 137.9 (*i*-C_{Ar}), 128.9 (*m*-C_{Ar}), 124.3 (*p*-C_{Ar}), 120.1 (*o*-C_{Ar}), 80.2 (*C*(CH_3)$_3$), 61.1 (C-2), 31.1 (C-3), 28.5 (C(*C*H_3)$_3$), 19.4 (C-4), 18.5 (C-4) ppm. The spectroscopic data are in accordance with literature.[14]

(*R*)-2-Amino-3-methyl-*N*^{1}-phenylbutanamide (31)

According to ref.,[14] to a solution of *N*-boc-protected amide **30** (3.00 g, 10.3 mmol) in CH_2Cl_2 (100 mL) trifluoroacetic acid (15.0 mL, 22.2 g, 0.19 mol) was added and the reaction mixture was stirred for 4 h at room temperature. The reaction mixture was diluted with EtOAc (150 mL), 2.5 M NaOH solution (150 mL) was added and the aqueous layer was extracted with EtOAc (3 × 100 mL). The combined organic layers were washed with brine (100 mL) and dried over Na_2SO_4. The solvent was removed under reduced pressure and the amide **31** was obtained as a colorless oil (1.57 g, 8.17 mmol, 79 %) without further purification.

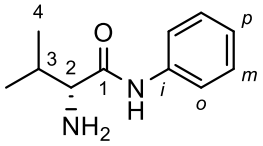

$C_{11}H_{16}N_2O$
192.26 g/mol

31

^{1}H NMR (300 MHz, $CDCl_3$): δ = 9.51 (bs, 1H, N*H*), 7.66–7.54 (m, 2H, o-Ar*H*), 7.38–7.28 (m, 2H, *m*-Ar*H*), 7.14–7.03 (m, 1H, *p*-Ar*H*), 3.39 (d, *J* = 3.4 Hz, 1H, 2-H), 2.52–2.35 (m, 1H, 3-H), 1.78 (bs, 2H, NH_2), 1.04 (d, *J* = 7.3 Hz, 3H, 4-H), 0.87 (d, *J* = 7.3 Hz, 3H, 4-H) ppm; ^{13}C NMR (75 MHz, $CDCl_3$): δ = 172.5 (C-1), 137.7 (*i*-C_{Ar}), 128.9 (*m*-C_{Ar}), 124.0 (*p*-C_{Ar}), 119.5 (*o*-C_{Ar}), 60.4 (C-2), 30.7 (C-3), 19.7 (C-4), 16.0 (C-4) ppm. The spectroscopic data are in accordance with literature.[14]

(*R*)-3-Methyl-*N*^{1}-phenylbutane-1,2-diamine (32)

According to ref.,[14] in a flame dried Schlenk flask under a nitrogen atmosphere to a solution of the amide **31** (1.42 g, 7.40 mmol) in abs. THF (100 mL) was added $LiAlH_4$ (1.12 g, 29.6 mmol) at 0 °C. The reaction mixture was heated for 9 h under reflux and a 2.5 M NaOH solution (100 mL) was slowly added. The mixture was diluted with water (100 mL), filtered through Celite® and the filtrate was extracted with EtOAc (300 mL). The organic layer was washed with brine (200 mL), dried over Na_2SO_4 and the solvent was removed under reduced pressure. The diamine **32** was obtained as a colorless oil (1.02 g, 5.74 mmol, 76 %) without further purification.

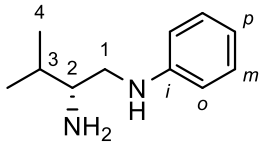

$C_{11}H_{18}N_2$
178.28 g/mol

32

^{1}H NMR (300 MHz, $CDCl_3$): δ = 7.24–7.13 (m, 2H, *m*-Ar*H*), 6.75–6.59 (m, 3H, *p*-Ar*H*, o-Ar*H*), 4.15 (bs, 1H, N*H*), 3.30–3.20 (m, 1H, 2-H), 2.91–2.70 (m, 2H, 1-H), 1.78–1.59 (m, 1H, 3-H), 1.24 (bs, 2H, NH_2), 0.99 (d, *J* = 7.3 Hz, 3H, 4-H), 0.96 (d, *J* = 7.3 H, 3H, 4-H) ppm; ^{13}C NMR (75 MHz, $CDCl_3$): δ = 148.8 (*i*-C_{Ar}), 129.3 (*m*-C_{Ar}), 117.4 (*p*-C_{Ar}), 113.1 (*o*-C_{Ar}), 56.2 (C-2), 48.2 (C-1), 32.7 (C-3), 19.4 (C-4), 17.9 (C-4) ppm. The spectroscopic data are in accordance with literature.[14]

(*R*)-4-Isopropyl-1-phenylimidazolidin-2-one (11)

According to ref.,[14] to a solution of diamine **32** (1.00 g, 5.65 mmol) in toluene (10 mL) a solution of K_2CO_3 (1.56 g, 11.3 mmol) in water (10 mL) was added and the reaction mixture was cooled to 0 °C. A solution of triphosgene (0.84 g, 2.83 mmol) in toluene (2 mL) was added dropwise and the reaction mixture was stirred for 2 h at room temperature. The organic layer was washed with brine (20 mL) and dried over Na_2SO_4. The solvent was removed under reduced pressure and the crude product was recrystallized from a mixture of hexanes and EtOAc. The imidazolidinone **11** was isolated as a colorless solid (0.72 g, 3.52 mmol, 62 %).

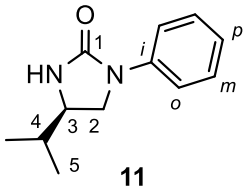

$C_{12}H_{16}N_2O$
204.27 g/mol

11

$[\alpha]_D^{20}$ = –10.0 ° [c = 10 mg/mL, CH_2Cl_2]; m.p.: 135 °C; ^{1}H NMR (500 MHz, $CDCl_3$): δ = 7.59–7.51 (m, 2H, *o*-Ar*H*), 7.37–7.29 (m, 2H, *m*-Ar*H*), 7.07–7.01 (m, 1H, *p*-Ar*H*), 5.51 (bs, 1H, N*H*), 3.97–3.91 (m, 1H, 2-H), 3.62–3.48 (m, 2H, 2-H, 3-H), 1.81–1.71 (m, 1H, 4-H), 0.99 (d, *J* = 7.3 Hz, 3H, 5-H), 0.96 (d, *J* = 7.3 Hz, 3H, 5-H) ppm; ^{13}C NMR (126 MHz, $CDCl_3$): δ = 159.3 (C-1), 140.2 (*i*-C_{Ar}), 128.9 (*m*-C_{Ar}), 122.6 (*p*-C_{Ar}), 117.8 (*o*-C_{Ar}), 55.0 (C-3), 49.2 (C-2), 33.3 (C-4), 18.2 (C-5), 17.9 (C-5) ppm; FTIR (ATR): $\tilde{\nu}$ = 3222 (m), 3099 (w), 2957 (m), 2870 (w), 1701 (s), 1599 (m), 1500 (s), 1474 (s), 1408 (s), 1389 (s), 1367 (s), 1344 (m), 1315 (s), 1259 (s), 1164 (m), 1148 (m), 1091 (w), 1076 (w), 1040 (m), 991 (w), 908 (w), 892 (w), 845 (w), 748 (vs), 687 (s), 675 (m), 616 (w), 604 (m), 508 (m), 480 (w), 435 (w) cm^{-1}; HRMS (ESI): calcd. for $[C_{12}H_{16}N_2O]^+$ 205.1335, found $[M + H]^+$ 205.1335; LRMS (ESI): *m*/*z* = 205.1 $[M + H]^+$, 227.1 $[M + Na]^+$.

(*R*)-4-Isopropyl-1-phenyl-3-((1*R*,4*S*)-3-phenylbicyclo[2.2.1]hepta-2,5-diene-2-carbonyl)-imidazolidin-2-one (12)

Synthesis according to GP 8; colorless solid (46 %); recrystallization from hexanes / EtOAc; $[\alpha]_D^{20}$ = –142.1° [c = 10 mg/mL, CH_2Cl_2]; m.p.: 126 °C; ^{1}H NMR (500 MHz, $CDCl_3$): δ = 7.49–7.44 (m, 2H, *o*'-Ar*H*), 7.38–7.31 (m, 4H, *o*-Ar*H*, *m*'-Ar*H*), 7.30–7.24 (m, 2H, *m*-Ar*H*), 7.22–7.17 (m, 1H, *p*-Ar*H*), 7.15–7.09 (m, 1H, *p*'-Ar*H*), 7.01 (dd, *J* = 3.0, 4.9 Hz, 1H, 6-H), 6.94 (dd, *J* = 3.0, 4.9 Hz, 1H, 5-H), 4.49–4.42 (m, 1H, 2'-H), 3.95–3.91 (m, 1H, 4-H), 3.90–3.84 (m, 1H, 5'-H), 3.82–3.78 (m, 1H, 1-H), 3.57–3.51 (m, 1H, 5'-H), 2.61 (dt, *J* = 1.4, 9.8 Hz, 1H, 7-H), 2.57–2.48 (m, 1H, 3'-H), 2.09 (dt, *J* = 1.4, 9.8 Hz, 1H, 7-H), 0.97 (d, *J* = 7.3 H, 3H, 4'-H), 0.88 (d, *J* = 7.3 Hz, 3H, 4'-H) ppm; ^{13}C NMR (126 MHz, $CDCl_3$): δ = 168.8 (C-6'), 156.4 (C-3), 152.2 (C-1'), 143.5 (C-6), 143.3 (C-2), 141.1 (C-5), 138.7 (*i*'-C_{Ar}), 135.9 (*i*-C_{Ar}), 129.1 (*m*'-C_{Ar}), 128.3 (*m*-C_{Ar}), 127.8 (*p*-C_{Ar}), 126.5 (*o*-C_{Ar}), 124.4 (*p*'-C_{Ar}), 119.3 (*o*'-C_{Ar}), 71.2 (C-7), 55.7 (C-1), 55.5 (C-4), 55.3 (C-2'), 43.4 (C-5'), 29.0 (C-3'), 18.4 (C-4'), 14.8 (C-4') ppm; FTIR (ATR): $\tilde{\nu}$ = 3064 (w), 2962 (w), 2936 (w), 2872 (w), 1731 (s), 1655 (m), 1599 (m), 1558 (w), 1503 (m), 1489 (m), 1459 (w), 1404 (m), 1366 (s), 1341 (m), 1297 (s), 1263 (vs), 1239 (m), 1180 (w), 1115 (w), 1075 (w), 1025 (w), 955 (w), 911 (w), 868 (w), 831 (w), 759 (m), 731 (m), 710 (m), 691 (m), 641 (w), 540 (w), 510 (w) cm^{-1}; LRMS (ESI): *m*/*z* = 399.2 $[M + H]^+$, 421.2 $[M + Na]^+$; HRMS (ESI): calcd. for $[C_{26}H_{26}N_2O_2]^+$ 399.2067, found $[M + H]^+$ 399.2068.

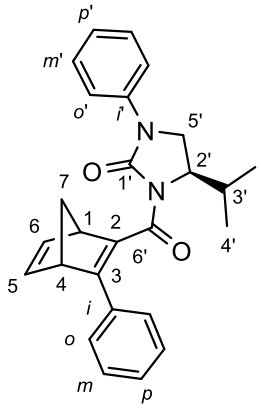

$C_{26}H_{26}N_2O_2$
398.50 g/mol

12

1-(2-Chlorethyl)-3-(prop-2-in-1-yl)urea (33)

According to ref.,[15] in a flame dried Schlenk flask under a nitrogen atmosphere to a solution of 3-amino-1-propyne (1.4 mL, 1.20 g, 21.8 mmol) and NEt_3 (0.21 mL, 0.15 g, 1.40 mmol) in abs. THF (40 mL) was added 2-chloroethyl isocyanate dropwise and the reaction mixture was stirred for 3 h at room temperature. The solvent was removed under reduced pressure and the residue was washed with CH_3Cl (50 mL). The urea derivative **33** was obtained as a colorless solid (2.50 g, 15.6 mmol, 67 %) without further purification.

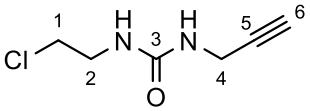

$C_6H_9ClN_2O$
160.60 g/mol

33

m.p.: 93 °C; ^{1}H NMR (300 MHz, CD_3OD): δ = 4.84 (s, 2H, N*H*), 3.89 (d, *J* = 2.5 Hz, 2H, 4-H), 3.57 (t, *J* = 6.0 Hz, 2H, 1-H), 3.44 (t, *J* = 6.0 Hz, 2H, 2-H), 2.54 (t, *J* = 2.2 Hz, 1H, 6-H) ppm; ^{13}C NMR (75 MHz, CD_3OD): δ = 160.2 (C-3), 81.7 (C-5), 71.7 (C-6), 44.7 (C-1), 43.0 (C-2), 30.2 (C-4) ppm. The spectroscopic data are in accordance with literature.[15]

1-(Prop-2-yn-1-yl)imidazolidin-2-one (10)

According to ref.,[15] in a flame dried Schlenk under a nitrogen atmosphere to a solution of the urea derivative **33** (1.50 g, 9.34 mmol) in abs. THF (40 mL) were added tetrabutylammonium bromide (0.60 g, 1.87 mmol) and powdered KOH (0.66 g, 11.7 mmol) at 0 °C. The reaction mixture was stirred for 4 h at room temperature, filtrated over Celite® and the solvent was removed under reduced pressure. The crude product was purified by column chromatography on silica (hexanes / EtOAc = 1 : 1 to Et_2O /CH_3Cl = 1 : 1) and the imidazolidinone **10** was obtained as a colorless solid (0.60 g, 4.83 mmol, 52 %).

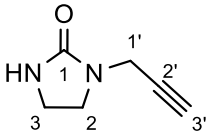

$C_6H_8N_2O$
124.14 g/mol

10

m.p.: 126 °C; ^{1}H NMR (300 MHz, $CDCl_3$): δ = 4.01 (d, *J* = 2.3 Hz, 2H, 1‘-H), 3.57–3.49 (m, 2H, 3-H), 3.48–3.40 (m, 2H, 2-H), 2.23 (t, *J* = 2.3 Hz, 1H, 3‘-H) ppm; ^{13}C NMR (75 MHz, $CDCl_3$): δ = 162.3 (C-1), 78.2 (C-2‘), 72.4 (C-3‘), 44.5 (C-3), 38.1 (C-2), 33.5 (C-1‘) ppm. The spectroscopic data are in accordance with literature.[15]

1-((1*R*,4*S*)-3-Phenylbicyclo[2.2.1]hepta-2,5-diene-2-carbonyl)-3-(prop-2-yn-1-yl)-imidazolidin-2-one (Ph(ImC_1))

Synthesis according to GP 8; colorless oil (51 %); column chromatography on silica (hexanes / EtOAc = 3 : 1); R_f = 0.25 (hexanes / EtOAc = 2 : 1, UV); $[\alpha]_D^{20}$ = –48.4° [c = 10 mg/mL, CH_2Cl_2]; ^{1}H NMR (700 MHz, $CDCl_3$): δ = 7.33–7.24 (m, 4H, *o*-Ar*H*, *m*-Ar*H*), 7.23–7.18 (m, 1H, *p*-Ar*H*), 6.96 (dd, *J* = 3.0, 4.9 Hz, 1H, 6-H), 6.93 (dd, *J* = 3.0, 4.9 Hz, 1H, 5-H), 4.05–3.95 (m, 2H, 1‘‘-H), 3.94–3.87 (m, 3H, 1-H, 2‘-H), 3.86–3.80 (m, 1H, 4-H), 3.55–3.41 (m, 2H, 3‘-H), 2.64 (dt, *J* = 1.4, 6.3 Hz, 1H, 7-H), 2.27–2.23 (m, 1H, 3‘‘-H), 2.11 (dt, *J* = 1.4, 6.3 Hz, 1H, 7-H) ppm; ^{13}C NMR (176 MHz, $CDCl_3$): δ = 168.6 (C-4‘), 157.6 (C-3), 153.5 (C-1‘),143.4 (C-6), 142.4 (C-2), 141.7 (C-5), 135.7 (*i*-C_{Ar}), 128.3 (*o*-C_{Ar}), 127.9 (*p*-C_{Ar}), 126.5 (*o*-C_{Ar}), 77.1 (C-2‘’), 73.2 (C-3‘‘), 71.4 (C-7), 55.8 (C-4), 55.6 (C-1), 40.7 (C-3‘), 40.0 (C-2‘), 33.3 (C-1‘‘) ppm; FTIR (ATR): $\tilde{\nu}$ = 3254 (w), 3063 (w), 2987 (w), 2938 (w), 2871 (w), 1730 (s), 1649 (m), 1558 (w), 1492 (m), 1480 (m), 1433 (m), 1344 (s), 1297 (m), 1249 (vs), 1154 (w), 1107 (w), 1079 (w), 1029 (w), 991 (w), 950 (w), 911 (m), 875 (w), 844 (w), 811 (w), 799 (w),

763 (m), 749 (m), 727 (s), 710 (s), 694 (s), 646 (m), 550 (w), 498 (w), 473 (w), 442 (w) cm^{-1}; LRMS (ESI): *m*/*z* = 319.1 $[M + H]^+$, 341.1 $[M + Na]^+$; HRMS (ESI): calcd. for $[C_{20}H_{19}N_2O_2]^+$ 319.1441, found $[M + H]^+$ 319.1442.

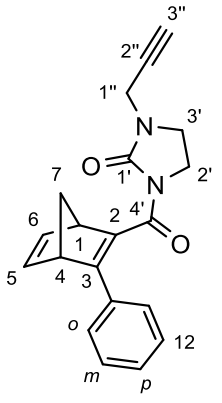

$C_{20}H_{18}N_2O_2$
318.37 g/mol

Ph(ImC$_1$)

1.4 Synthesis of alcohols, alkynes, alkynones and triazoles

General remark about the synthesis of the alcohol 3c, alkyne Ph(*i*PrC$_1$OC$_1$) and triazole Ph(*i*PrC$_1$OC$_1$)click

The chiral alcohol **3c**, alkyne **Ph(*i*PrC$_1$OC$_1$)** and triazole **Ph(*i*PrC$_1$OC$_1$)click** were synthesized according to a literature protocol from our previous publication.[16] The analytical data was in good agreement with our previous results.

General procedure for the synthesis of the alcohols through ring-opening of oxazolidinones (3a,b, 7, 8) [GP 9]

According to ref.,[16] the respective norbornadiene **2a,b**, **5** or **6** (0.65 mmol) was dissolved in dioxane (20 mL) and 3.1 M KOH (1.22 mL, 3.78 mmol) was added. The reaction mixture was stirred for 24 h at 60 °C, dried over $MgSO_4$ and the solvent was removed under reduced pressure. The crude product was purified by column chromatography on silica.

General procedure for the synthesis of the propargylic ether derived alkynes (Ph(R^{1}C$_1$OC$_1$), 1-Naph(*i*PrC$_1$OC$_1$), 2-Naph(*i*PrC$_1$OC$_1$)) [GP 10]

According to ref.,[17] under a nitrogen atmosphere to a solution of the respective alcohol **3a,b, 7** or **8** (63.3 µmol) in abs. THF (15 mL) was added NaH (6.33 mg, 0.16 mmol) at 0 °C. The reaction mixture was stirred for 30 min at 0 °C and propargylic bromide (10.9 µL, 14.1 mg, 95.0 mmol, 80 wt% in toluene) was added. The reaction mixture was stirred for 24 h at room temperature, a saturated aqueous NH_4Cl solution (10 mL) was added and the aqueous layer was extracted with EtOAc (2 × 15 mL). The combined organic layers were dried over $MgSO_4$, the solvent was removed under reduced pressure and the product was purified by column chromatography on silica.

General procedure for the ring-opening of the lactams with ethinyl magnesium bromide (Ph(C$_n$CO)) [GP 11]

Under a nitrogen atmosphere a solution of the respective lactam derivative **14a–d** (0.16 mmol) in abs. THF (5 mL) was charged with ethinyl magnesium bromide (3.2 mL, 3.01 g, 1.60 mmol, 0.5 M in THF) at -78 °C. The reaction mixture was slowly heated to room temperature over a time period of 1.5 h and subsequently stirred for 30 min at room temperature. A saturated aqueous NH_4Cl solution (10 mL) was added, the aqueous phase was extracted with EtOAc

(3 × 20 mL) and the combined organic layers were dried over $MgSO_4$. The crude product was purified by column chromatography on silica.

General procedure for the click reaction of alkynes and alkynones with benzyl azide (Ph($R^1C_1OC_1$)click, Ph(*i*PrC_1OC_4)click, 1-Naph(*i*PrC_1OC_1)click, Ph(ImC_1)click, Ph(*i*PrC_1amide)click, Ph(C_nCO)click) [GP 12]

According to ref.,[18] under a nitrogen atmosphere the respective alkyne **Ph($R^1C_1OC_1$), Ph(*i*PrC_1OC_4)**, **1-Naph(*i*PrC_1OC_1)**, **Ph(ImC_1)**, or alkynone **Ph(C_nCO)**, **Ph(*i*PrC_1amide)** (0.13 mmol) and benzyl azide **1** (19.6 µL, 20.9 mg, 0.16 mmol) were dissolved in abs. CH_2Cl_2 (2 mL). Degassed water (2 mL), $CuSO_4 \cdot 5\ H_2O$ (3.25 mg, 13.0 µmol) and sodium ascorbate (5.15 mg, 26.0 µmol) were added and the reaction mixture was stirred for 24 h at room temperature in the dark. A saturated EDTA solution (5 mL) was added, the aqueous layer was extracted with CH_2Cl_2 (3 × 10 mL) and the combined organic layers were dried over $MgSO_4$. The solvent was removed under reduced pressure and the crude product was purified by column chromatography on silica or neutral aluminium oxide.

(1*R*,4*S*)-*N*-((*R*)-1-Hydroxy-3-methylbutan-2-yl)-3-(naphthalen-1-yl)bicyclo[2.2.1]hepta-2,5-diene-2-carboxamide (7)

Synthesis according to GP 9; colorless oil (45 %); column chromatography on silica (hexanes / EtOAc = 1 : 1) followed by preparative HPLC on a Orbit 100 Sil column (250 × 20 mm, 5 µm, hexanes / *i*PrOH 93 : 7, flow rate: 19 mL/min, λ = 245 nm, R_t = 15.29 min); R_f = 0.26 (hexanes / EtOAc = 1 : 1, UV); $[\alpha]_D^{20}$ = –9.1° [c = 10 mg/mL, CH_2Cl_2]; ^{1}H NMR (700 MHz, $CDCl_3$): δ = 7.92–7.80 (m, 2H, 4'-H, 8'-H), 7.60–7.21 (m, 5H, 2'-H, 3'-H, 5'-H, 6'-H, 7'-H), 7.17 (dd, *J* = 3.0, 4.8 Hz, 1H, 6-H), 7.01 (dd, *J* = 3.0, 4.8 Hz, 1H, 5-H), 5.22 (bs, 1H, N*H*), 4.34–4.21 (m, 1H, 4-H), 3.84–3.70 (m, 1H, 1-H), 3.61–3.11 (m, 3H, 2''-H, 5''-H), 2.61–2.46 (m, 1H, 7-H), 2.18 (dt, *J* = 1.7, 6.3 Hz, 1H, 7-H), 1.79 (bs, 1H, O*H*), 1.37–0.99 (m, 1H, 3''-H), 0.44 – -0.06 (m, 6H, 4''-H), ppm; ^{13}C NMR (176 MHz, $CDCl_3$): δ = 166.6 (C-1''), 147.4 (C-3), 144.7 (C-2), 141.7 (C-6), 136.3 (C-5), 135.4, 135.2, 134.0, 130.4, 128.8, 127.1, 128.5, 126.8, 125.8, 125.4 (10 × C_{Ar}), 72.4 (C-7), 65.3 (C-1''), 60.0 (C-1), 57.6 (C-2''), 52.5 (C-4), 28.6 (C-3''), 18.8 (C-4''), 16.9 (C-4'') ppm; FTIR (ATR): $\tilde{\nu}$ = 3410 (m), 3059 (w), 2960 (m), 2934 (m), 2870 (w), 2242 (w), 2123 (w), 1997 (w), 1786 (w), 1745 (w), 1641 (s), 1609 (s), 1556 (w), 1507 (s), 1464 (m), 1392 (m), 1369 (m), 1333 (w), 1293 (m), 1264 (w), 1240 (m), 1183 (w), 1155 (w), 1117 (w), 1075 (m), 1053 (m), 1018 (m), 976 (w), 909 (w), 877 (w), 800 (s), 776 (vs), 721 (s), 669 (w), 646 (m), 617 (w), 555 (m), 495 (w), 426 (w) cm^{-1}; LRMS (ESI): *m*/*z* = 245.1 $[C_{18}H_{13}O]^+$, 348.2 $[M + H]^+$, 370.2 $[M + Na]^+$; HRMS (ESI): calcd. for $[C_{23}H_{26}NO_3]^+$ 348.1958, found $[M + H]^+$ 348.1965.

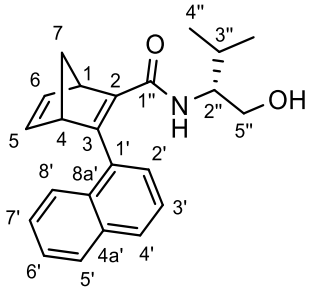

$C_{23}H_{25}NO_2$
347.46 g/mol

7

(1*R*,4*S*)-*N*-((*R*)-3-Methyl-1-(prop-2-yn-1-yloxy)butan-2-yl)-3-(naphthalen-1-yl)bicyclo-[2.2.1]hepta-2,5-diene-2-carboxamide (1-Naph(*i*PrC_1OC_1))

Synthesis according to GP 10; colorless oil (62 %); column chromatography on silica (hexanes / EtOAc = 7 : 1); R_f = 0.18 (hexanes / EtOAc = 7 : 1, UV); $[\alpha]_D^{20}$ = –21.0° [c = 10 mg/mL, CH_2Cl_2]; ^{1}H NMR (500 MHz, $CDCl_3$): δ = 8.01–7.20 (m, 7H, 2'-H, 3'-H, 4'-H, 5'-

H, 6‘-H, 7‘-H, 8‘-H), 7.17 (dd, *J* = 3.0, 4.8 Hz, 1H, 6-H), 7.00 (dd, *J* = 3.0, 4.8 Hz, 1H, 5-H), 5.23 (d, *J* = 9.4 Hz, 1H, N*H*), 4.33–4.21 (m, 1H, 4-H), 4.00–3.50 (m, 4H, 1-H, 2‘‘-H, 5‘‘-H), 3.39–2.71 (m, 2H, 6‘‘-H), 2.60–2.45 (m, 1H, 7-H), 2.31 (bs, 1H, 8‘‘-H), 2.16 (dt, *J* = 1.7, 6.3 Hz, 1H, 7-H), 1.41–1.22 (m, 1H, 3‘‘-H), 0.62 – -0.03 (m, 6H, 4‘‘-H), ppm; ^{13}C NMR (126 MHz, $CDCl_3$): δ = 164.9 (C-1‘‘), 158.6 (C-3), 147.6 (C-2), 144.5 (C-6), 141.7 (C-5), 135.4, 134.0, 130.6, 128.7, 128.5, 126.9, 126.6, 125.7, 125.6, 123.9 (10 × C_{Ar}), 79.7 (C-7‘‘), 74.4 (C-8‘‘), 72.3 (C-7), 69.4 (C-6‘‘), 59.8 (C-1), 59.8 (C-1), 58.1 (C-2‘‘), 53.2 (C-5‘‘), 52.5 (C-4), 28.6 (C-3‘‘), 19.0 (C-4‘‘), 17.4 (C-4‘‘) ppm; FTIR (ATR): $\tilde{\nu}$ = 3413 (w), 3295 (w), 3228 (w), 3059 (w), 2961 (m), 2934 (w), 2870 (w), 2113 (w), 1649 (vs), 1617 (m), 1556 (w), 1508 (s), 1466 (w), 1392 (w), 1358 (w), 1294 (w), 1264 (w), 1238 (w), 1183 (w), 1142 (w), 1104 (m), 1020 (w), 953 (w), 877 (w), 801 (m), 778 (s), 717 (m), 669 (w), 646 (w), 558 (w), 488 (w), 427 (w) cm^{-1}; LRMS (ESI): *m*/*z* = 245.1 $[C_{18}H_{13}O]^{+\cdot}$,386.2 [M + H]$^+$, 408.2 [M + Na]$^+$; HRMS (ESI): calcd. for $[C_{26}H_{28}NO_3]^+$ 386.2115, found [M +H]$^+$ 386.2109.

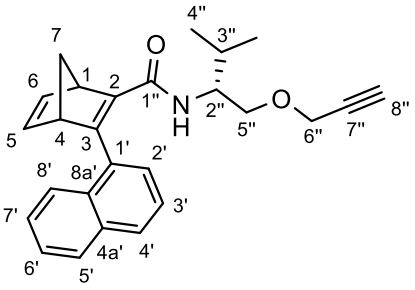

$C_{26}H_{27}NO_2$
385.51 g/mol

1-Naph(*i*PrC$_1$OC$_1$)

(1*R*,4*S*)-*N*-((*R*)-1-((1-Benzyl-1*H*-1,2,3-triazol-4-yl)methoxy)-3-methylbutan-2-yl)-3-(naphthalen-1-yl)bicyclo[2.2.1]hepta-2,5-diene-2-carboxamide (1-Naph(*i*PrC$_1$OC$_1$)click)

Synthesis according to GP 12; colorless oil (60 %); column chromatography on neutral aluminium oxide (hexanes / EtOAc = 1 : 3) followed by preparative HPLC on a Orbit 100 Sil column (250 × 20 mm, 5 µm, hexanes / *i*PrOH 85 : 15, flow rate: 19 mL/min, λ = 245 nm, R_t = 90.00 min); R_f = 0.48 (hexanes/ EtOAc = 1 : 3, UV);$[\alpha]_D^{20}$ = –31.7° [c = 3 mg/mL, CH_2Cl_2]; ^{1}H NMR (700 MHz, $CDCl_3$): δ = 7.84–7.77 (d, *J* = 7.1 Hz, 1H, 8‘-H), 7.74–7.67 (m, 1H, 4‘-H), 7.51–7.33 (m, 6H, 3’-H, 5’-H, 6’-H, 7’-H, *m*-ArH), 7.29–7.01 (m, 6H, 6-H, 8’’-H, 2’-H, o-Ar*H*, *p*-Ar*H*), 6.98 (dd, *J* = 3.0, 4.8 Hz, 1H, 5-H), 5.50 (s, 2H, 9’’-H), 5.17 (d, *J* = 9.4 Hz, 1H, N*H*), 4.42–4.01 (m, 3H, 1-H, 6’’-H), 3.76–3.71 (m, 1H, 4-H), 3.69–3.63 (m, 1H, 2’’-H), 3.26–2.65 (m, 2H, 5’’-H), 2.60–2.38 (m, 1H, 7-H), 2.14 (dt, *J* = 1.7, 6.3 Hz, 1H, 7-H), 1.43–1.16 (m, 1H, 3’’-H), 0.60 – -0.20 (m, 6H, 4’’-H) ppm; ^{13}C NMR (176 MHz, $CDCl_3$): δ = 164.9 (C-1’’), 158.4 (C-3), 147.5 (C-2), 145.7 (C-7’’), 144.4 (C-6), 141.7 (C-5), 135.3 134.8, 133.9, 130.5, 129.3, 128.9, 128.6, 128.5, 128.2, 126.8, 126.6, 125.7, 125.5, 123.9 (14 × C_{Ar}), 122.2 (C-8’’), 72.2 (C-7), 70.1 (C-5’’), 64.6 (C-6’’), 59.8 (C-4), 54.2 (C-9’’), 53.2 (C-2’’), 52.5 (C-1), 28.4 (C-3’’), 19.0 (C-4’’), 17.0 (C-4’’) ppm; FTIR (ATR): $\tilde{\nu}$ = 3416 (w), 2960 (w), 2933 (w), 2868 (w), 1646 (s), 1615 (m), 1506 (s), 1456 (m), 1392 (w), 1369 (w), 1330 (w), 1294 (m), 1262 (w), 1225 (w), 1102 (m), 1048 (m), 1020 (w), 911 (w), 877 (w), 800 (m), 778 (s), 721 (vs), 670 (w), 646 (w), 617 (w), 553 (w), 520 (w), 473 (w), 427 (w) cm^{-1}; LRMS (ESI): *m*/*z* = 519.3 [M + H]$^+$, 541.3 [M + Na]$^+$; HRMS (ESI): calcd. for $[C_{33}H_{35}N_4O_2]^+$ 519.2755, found [M +H]$^+$ 519.2759.

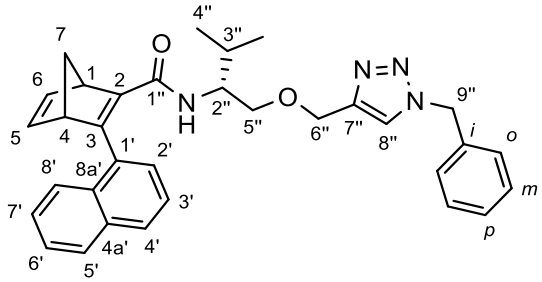

$C_{33}H_{34}N_4O_2$
518.66 g/mol

1-Naph(*i*PrC$_1$OC$_1$)click

(1*R*,4*S*)-*N*-((*R*)-1-Hydroxy-3-methylbutan-2-yl)-3-(naphthalen-1-yl)bicyclo[2.2.1]hepta-2,5-diene-2-carboxamide (8)

Synthesis according to GP 9; colorless oil (62 %); column chromatography on silica (hexanes / EtOAc = 1 : 1) followed by preperative HPLC on Orbit 100 Sil column (250 ×20 mm, 5 µm, hexanes / *i*PrOH 99 : 1, flow rate: 12 mL/min, λ = 245 nm, R_t = 52.35 min); R_f = 0.35 (PE/EtOAc = 1 : 1, UV); $[\alpha]_D^{20}$ = –16.3° [c = 10 mg/mL, CH_2Cl_2]; ^{1}H NMR (700 MHz, $CDCl_3$): δ = 7.87–7.78 (m, 4H, 1‘-H, 4‘-H, 5‘-H, 6‘-H), 7.53–7.47 (m, 2H, 6‘-H, 7‘-H), 7.46–7.42 (dd, *J* = 1.6, 8.5 Hz, 1H, 3‘-H), 7.05 (dd, *J* = 3.0, 4.8 Hz, 1H, 6-H), 7.00 (dd, *J* = 3.0, 4.8 Hz, 1H, 5-H), 5.56 (bs, 1H, N*H*), 4.17–4.10 (m, 1H, 4-H), 3.92–3.88 (m, 1H, 1-H), 3.76–3.68 (m, 1H, 2‘‘-H), 3.61 (dd, *J* = 6.6, 8.6 Hz, 1H, 5‘‘-H), 3.49 (dd, *J* = 6.6, 8.6 Hz, 1H, 5‘‘-H), 2.79 (bs, 1H, O*H*), 2.39 (dt, *J* = 1.7, 6.3 Hz, 1H, 7-H), 2.11 (dt, *J* = 1.7, 6.3 Hz, 1H, 7-H), 1.61-1.51 (m, 1H, 3‘‘-H), 0.61 (d, *J* = 6.9 Hz, 4‘‘-H), 0.52 (d, *J* = 6.9 Hz, 4‘‘-H) ppm; ^{13}C NMR (176 MHz, $CDCl_3$): δ = 167.7 (C-1‘‘), 159.2 (C-3), 144.7 (C-2), 144.1 (C-6), 141.7 (C-5), 133.7, 133.3, 133.1, 128.7, 128.1, 127.9, 126.9, 126.8, 126.0 (9 × C_{Ar}), 124.8 (1-C_{Ar}), 71.9 (C-7), 64.8 (C-5‘‘), 58.3 (C-1), 57.6 (C-2‘‘), 53.5 (C-4), 29.0 (C-3‘‘), 19.2 (C-4‘‘), 18.2 (C-4‘‘) ppm; FTIR (ATR): $\tilde{\nu}$ = 3415 (m), 3057 (w), 2962 (m), 2936 (m), 2870 (w), 2300 (w), 2257 (w), 2211 (w), 2175 (w), 2161 (w), 2112 (w), 2034 (w), 2019 (w), 1978 (w), 1956 (w), 1906 (w), 1631 (vs), 1557 (m), 1509 (s), 1466 (m), 1388 (w), 1369 (w), 1325 (w), 1295 (m), 1239 (w), 1190 (w), 1150 (w), 1127 (w), 1079 (w), 1055 (w), 1020 (w), 962 (w), 894 (w), 859 (w), 819 (m), 790 (w), 749 (m), 716 (m), 670 (w), 578 (w), 539 (w), 476 (m), 455 (w), 431 (w), 413 (w) cm^{-1}; LRMS (ESI): *m*/*z* = 245.1 $[C_{18}H_{13}O]^+$, 348.2 $[M + H]^+$, 370.2 $[M + Na]^+$; HRMS (ESI): calcd. for $[C_{23}H_{25}NO_3Na]^+$ 370.1777, found $[M + Na]^+$ 370.1779.

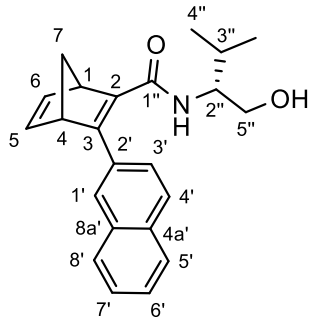

$C_{23}H_{25}NO_2$
347.46 g/mol

8

(1*R*,4*S*)-*N*-((*R*)-3-Methyl-1-(prop-2-yn-1-yloxy)butan-2-yl)-3-(naphthalen-2-yl)bicyclo-[2.2.1]hepta-2,5-diene-2-carboxamide (2-Naph(*i*PrC$_1$OC$_1$))

Synthesis according to GP 10; colorless oil (58 %); column chromatography on silica (hexanes / EtOAc = 7 : 1); R_f = 0.23 (hexanes / EtOAc = 7 : 1, UV); $[\alpha]_D^{20}$ = –47.9° [c = 10 mg/mL, CH_2Cl_2]; ^{1}H NMR (700 MHz, $CDCl_3$): δ = 7.84–7.78 (m, 4H, 2‘-H, 4‘-H, 5‘-H, 8‘-H), 7.54–7.42 (m, 3H, 3‘-H, 6‘-H, 7‘-H), 7.04 (dd, *J* = 3.0 Hz, 4.8 Hz, 1H, 6-H), 7.01 (dd, *J* = 3.0 Hz, 4.8 Hz, 1H, 5-H), 5.58 (d, *J* = 9.4 Hz, 1H, N*H*), 4.17–4.09 (m, 1H, 4-H), 3.91–3.85

(m, 2H, 1-H, 1‘‘-H), 3.81–3.71 (m, 2H, 5‘‘-H), 3.51 (dd, *J* = 4.0 Hz, 9.8 Hz, 1H, 2‘‘-H), 3.31 (dd, *J* = 4.0 Hz, 9.8 Hz, 1H, 2‘‘-H), 2.38 (dt, *J* = 1.7 Hz, 6.3 Hz, 1H, 7-H), 2.29 (t, *J* = 2.0 Hz, 1H, 7‘‘-H), 2.10 (dt, *J* = 1.7 Hz, 6.3 Hz, 1H, 7-H), 1.67–1.59 (m, 1H, 3‘‘-H), 0.76 (d, *J* = 6.9 Hz, 3H, 4‘‘-H), 0.64 (d, *J* = 6.9 Hz, 3H, 4‘‘-H) ppm; ^{13}C NMR (176 MHz, $CDCl_3$): δ = 166.2 (C-1‘‘), 157.9 (C-3), 144.8 (C-2), 143.9 (C-6), 141.8 (C-5), 133.7, 133.3, 133.0, 128.4, 128.18, 128.17, 127.8, 126.6, 126.5, 125.9 (9 × C_{Ar}), 125.1 (1’-C_{Ar}), 79.5 (C-6‘‘), 74.5 (C-7‘‘), 71.8 (C-7), 69.4 (C-2‘‘), 58.03 (C-1), 58.00 (C-1‘‘), 53.7 (C-4), 29.2 (C-3‘‘), 19.3 (C-4‘‘), 18.7 (C-4‘‘) ppm; FTIR (ATR): $\tilde{\nu}$ = 3423 (w), 3296 (w), 3056 (w), 2962 (m), 2934 (w), 2870 (w), 2241 (w), 2114 (w), 1753 (w), 1640 (s), 1610 (s) 1557 (w), 1502 (s), 1466 (m), 1408 (w), 1389 (w), 1357 (m), 1295 (m), 1259 (m), 1234 (m), 1188 (w), 1144 (w), 1100 (s), 1036 (m), 1020 (m), 951 (w), 909 (m), 859 (m), 791 (w), 748 (m), 715 (vs), 669 (m), 645 (m), 629 (m), 578 (m), 523 (w), 475 (s) cm^{-1}; LRMS (ESI): *m*/*z* = 245.1 $[C_{18}H_{13}O]^+$, 386.2 $[M + H]^+$, 408.2 $[M + Na]^+$; HRMS (ESI): calcd. for $[C_{26}H_{28}NO_3]^+$ 386.2115, found $[M + H]^+$ 386.2125.

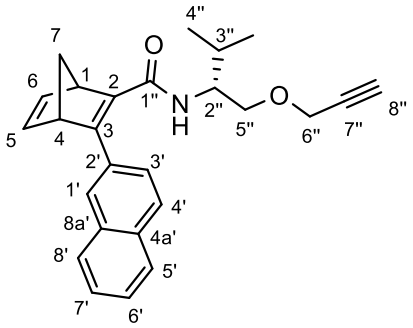

$C_{26}H_{27}NO_2$
385.51 g/mol

2-Naph(*i*PrC$_1$OC$_1$)

(1*R*,4*S*)-*N*-(2-Hydroxyethyl)-3-phenylbicyclo[2.2.1]hepta-2,5-diene-2-carboxamide (3a)
Synthesis according to GP 9; colorless oil (72 %); filtration through silica (EtOAc); $[\alpha]_D^{20}$ = −39.5 ° [c = 10 mg/mL, CH_2Cl_2]; ^{1}H NMR (500 MHz, $CDCl_3$): δ = 7.41–7.36 (m, 2H, *o*-Ar*H*), 7.35–7.29 (m, 3H, *m*-Ar*H*, *p*-Ar*H*), 7.00 (dd, *J* = 3.0, 4.9 Hz, 1H, 6-H), 6.92 (dd, *J* = 3.0, 4.9 Hz, 1H, 5-H), 5.83–5.66 (m, 1H, N*H*), 4.09–4.03 (m, 1H, 4-H), 3.83–3.78 (m, 1H, 4-H), 3.62 (t, *J* = 5.0 Hz, 2H, 3‘-H), 3.40–3.25 (m, 2H, 2‘-H), 2.30 (dt, *J* = 1.3, 6.9 Hz, 1H, 7-H), 2.07 (dt, *J* = 1.3, 6.9 Hz, 1H, 7-H), 1.67 (bs, 1H, O*H*) ppm; ^{13}C NMR (126 MHz, $CDCl_3$): δ = 167.8 (C-1‘), 159.4 (C-3), 143.9 (C-6), 143.8 (C-2), 141.6 (C-5), 136.0 (*i*-C_{Ar}), 128.8 (*o*-C_{Ar}), 128.6 (*p*-C_{Ar}), 127.1 (*m*-C_{Ar}), 71.7 (C-7), 62.7 (C-3’), 58.0 (C-4), 53.4 (C-1), 42.7 (C-2‘) ppm; FTIR (ATR): $\tilde{\nu}$ = 3324 (m), 3064 (w), 2978 (w), 2936 (m), 2869 (w), 1631 (s), 1607 (s), 1572 (m), 1557 (m), 1519 (vs), 1444 (m), 1361 (w), 1331 (m), 1295 (s), 1263 (m), 1157 (w), 1117 (w), 1066 (m), 881 (w), 811 (w), 760 (s), 717 (s), 696 (s), 656 (m), 601 (w), 535 (w) cm^{-1}; LRMS (ESI): *m*/*z* = 195.1 $[C_{14}H_{11}O]^+$, 256.1 $[M + H]^+$, 278.1 $[M + Na]^+$; HRMS (ESI): calcd. for $[C_{16}H_{17}NO_2Na]^+$ 278.1151, found $[M + Na]^+$ 278.1151.

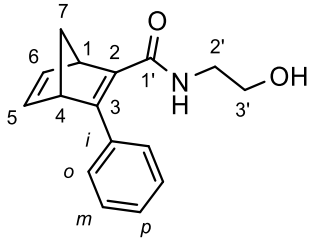

$C_{16}H_{17}NO_2$
255.32 g/mol

3a

(1*R*,4*S*)-3-Phenyl-*N*-(2-(prop-2-yn-1-yloxy)ethyl)bicyclo[2.2.1]hepta-2,5-diene-2-carboxamide (Ph(HC$_1$OC$_1$))

Synthesis according to GP 10; colorless oil (44 %); column chromatography on silica (hexanes / EtOAc = 3 : 1); R_f = 0.20 (hexane / EtOAc = 5 : 1, UV); $[\alpha]_D^{20}$ = – 23.3° [c = 10 mg/mL, CH_2Cl_2]; ^{1}H NMR (700 MHz, $CDCl_3$): δ = 7.40–7.32 (m, 4H, *o*-Ar*H*, *m*-Ar*H*), 7.31–7.27 (m, 1H, *p*-Ar*H*), 7.00 (dd, *J* = 3.0, 4.9 Hz, 1H, 6-H), 6.92 (dd, *J* = 3.0, 4.9 Hz, 1H, 5-H), 5.73 (bs, 1H, N*H*), 4.05–4.08 (m, 1H, 1-H), 3.98 (d, *J* = 2.4 Hz, 2H, 4'-H), 3.84–3.78 (m, 1H, 4-H), 3.57–3.33 (m, 4H, 2'-H, 3'-H), 2.38 (t, *J* = 2.4 Hz, 1H, 6'-H), 2.29 (dt, *J* = 1.3, 6.9 Hz, 1H, 7-H), 2.05 (dt, *J* = 1.3, 6.9 Hz, 1H, 7-H); ^{13}C NMR (176 MHz, $CDCl_3$): δ = 166.3 (C-1'), 158.7 (C-3), 143.90 (C-2), 143.90 (C-2), 143.86 (C-6), 141.6 (C-5), 136.1 (*i*-C_{Ar}), 128.7 (*o*-C_{Ar}), 128.3 (*p*-C_{Ar}), 127.2 (*m*-C_{Ar}), 79.4 (C-5'), 74.8 (C-6'), 71.6 (C-7), 68.6 (C-3'), 58.2 (C-4'), 58.0 (C-4), 53.4 (C-1), 39.0 (C-2') ppm; FTIR (ATR): $\tilde{\nu}$ = 3424 (w), 3290 (w), 2981 (w), 2936 (w), 2867 (w), 1640 (s), 1612 (s), 1557 (m), 1513 (s), 1443 (m), 1352 (w), 1328 (w), 1295 (s), 1260 (m), 1199 (w), 1157 (w), 1099 (vs), 1027 (m), 1002 (w), 951 (w), 919 (w), 874 (w), 846 (w), 811 (w), 761 (s), 716 (s), 696 (s), 657 (m), 519 (w) cm^{-1}; LRMS (ESI): *m*/*z* = 195.1 $[C_{14}H_{11}O]^+$, 294.2 $[M + H]^+$, 316.1 $[M + Na]^+$; HRMS (ESI): calcd. for $[C_{19}H_{19}NO_2Na]^+$ 316.1308, found $[M + Na]^+$ 316.1309.

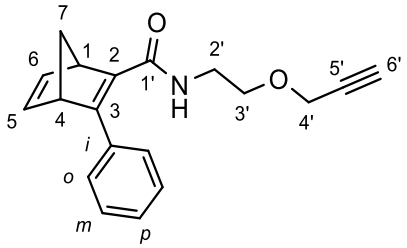

$C_{19}H_{19}NO_2$
293.37 g/mol

Ph(HC$_1$OC$_1$)

(1*R*,4*S*)-*N*-(2-((1-Benzyl-1*H*-1,2,3-triazol-4-yl)methoxy)ethyl)-3-phenylbicyclo[2.2.1]-hepta-2,5-diene-2-carboxamide (Ph(HC$_1$OC$_1$)click)

Synthesis according to GP 12; colorless oil (45 %, >80 % purity according to ^{1}H NMR); column chromatography on neutral aluminium oxide (hexanes / EtOAc = 1 : 1 to pure EtOAc); R_f = 0.43 (PE / EtOAc = 1 : 2, UV, neutral aluminium oxide); $[\alpha]_D^{20}$ = –18.2° [c = 3 mg/mL, CH_2Cl_2]; ^{1}H NMR (700 MHz, $CDCl_3$): δ = 7.42–7.36 (m, 4H, *m*'-Ar*H*, *o*-Ar*H*), 7.31–7.23 (m, 6H, *m*-Ar*H*, *o*'-Ar*H*, *p*-Ar*H*, 6'-H), 7.18–7.14 (m, 1H, *p*'-Ar*H*), 6.98 (dd, *J* = 3.0, 4.9 Hz, 1H, 6-H), 6.90 (dd, *J* = 3.0, 4.9 Hz, 1H, 5-H), 5.81–5.72 (m, 1H, N*H*), 5.50 (s, 2H, 7'-H), 4.45 (s, 2H, 4'-H), 4.06–4.02 (m, 1H, 1-H), 3.81–3.76 (m, 1H, 4-H), 3.50–3.33 (m, 4H, 2'-H, 3'-H), 2.27 (dt, *J* = 1.3, 6.9 Hz, 1H, 7-H), 2.04 (dt, *J* = 1.3, 6.9 Hz, 1H, 7-H) ppm; ^{13}C NMR (176 MHz, $CDCl_3$): δ = 166.3 (C-1'), 158.6 (C-3), 145.3 (C-5'), 143.89 (C-2), 143.86 (C-6), 141.6 (C-5), 136.0 (*i*-C_{Ar}), 134.6 (*i*'-C_{Ar}), 129.3 (*m*'-C_{Ar}), 129.0 (*p*'-C_{Ar}), 128.6 (*o*-C_{Ar}), 128.27 (*o*'-C_{Ar}), 128.26 (*p*-C_{Ar}), 127.1 (*m*-C_{Ar}), 122.3 (C-6'), 71.6 (C-7), 69.2 (C-3'), 64.5 (C-4'), 58.0 (C-4), 54.3 (C-7'), 53.5 (C-1), 39.1 (C-2') ppm; FT-IR (ATR): $\tilde{\nu}$ = 3422 (w), 3308 (w), 2922 (m), 2868 (m), 1713 (w), 1642 (vs), 1556 (m), 1518 (s), 1456 (m), 1331 (m), 1295 (s), 1258 (m), 1221 (m), 1125 (s), 1098 (s), 1050 (m), 1029 (m), 916 (w), 877 (w), 812 (w), 761 (m), 719 (s), 697 (s), 657 (w), 583 (w), 526 (w), 474 (w), 462 (w) cm^{-1}; LRMS (ESI): *m*/*z* = 427.2 $[M + H]^+$, 449.2 $[M + Na]^+$; HRMS (ESI): calcd. for $[C_{26}H_{26}N_4O_2Na]^+$ 449.1948, found $[M + Na]^+$ 449.1937.

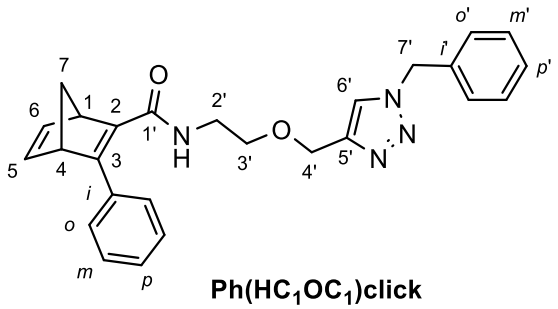

$C_{26}H_{26}N_4O_2$
426.52 g/mol

Ph(HC$_1$OC$_1$)click

(1*R*,4*S*)-*N*-((*R*)-1-Hydroxy-3-phenylpropan-2-yl)-3-phenylbicyclo[2.2.1]hepta-2,5-diene-2-carboxamide (3b)

Synthesis according to GP 9; colorless oil (62 %, 78 % purity according to ^{1}H NMR); column chromatography on silica (hexanes / EtOAc = 2 : 1 to 1 : 1); R_f = 0.33 (hexanes / EtOAc = 1 : 1, UV); $[\alpha]_D^{20}$ = –12.7° [c = 10 mg/mL, CH_2Cl_2]; ^{1}H NMR (500 MHz, $CDCl_3$): δ = 7.37–7.25 (m, 5H, *m*-Ar*H*, *m'*-Ar*H*, *p*'-Ar*H*), 7.24–7.14 (m, 3H, *o*-Ar*H*, *p*-Ar*H*), 7.01–6.96 (m, 2H, *o*'-Ar*H*), 6.95 (dd, *J* = 3.0 Hz, 4.9 Hz, 1H, 6-H), 6.90 (dd, *J* = 3.0 Hz, 4.9 Hz, 1H, 5-H), 5.58 (d, *J* = 9.6 Hz, 1H, N*H*), 4.16–4.09 (m, 1H, 2'-H), 4.00–3.96 (m, 1H, 1-H), 3.80–3.75 (m, 1H, 4-H), 3.62–3.55 (m, 1H, 4'-H), 3.51–3.43 (m, 1H, 4'-H), 2.91–2.84 (m, 1H, O*H*), 2.66 (d, *J* = 7.3 Hz, 2H, 3'-H), 2.27 (dt, *J* = 1.4 Hz, 6.3 Hz, 1H, 7-H), 2.03 (dt, *J* = 1.4 Hz, 6.3 Hz, 1H, 7-H) ppm; ^{13}C NMR (126 MHz, $CDCl_3$): δ = 167.1 (C-1'), 159.3 (C-3), 143.9 (C-2), 143.8 (C-6), 141.6 (C-5), 137.5 (*i'*-C_{Ar}), 136.0 (*i*-C_{Ar}), 129.2 (*o'*-C_{Ar}), 128.8 (*m'*-C_{Ar}), 128.7 (*o*-C_{Ar}), 128.6 (*p*-C_{Ar}), 127.1 (*m*-C_{Ar}), 126.7 (*p'*-C_{Ar}), 71.6 (C-7), 64.6 (C-4'), 58.1 (C-4), 53.9 (C-2'), 53.2 (C-1), 36.8 (C-3') ppm; FTIR (ATR): $\tilde{\nu}$ = 3408 (w), 2936 (w), 1744 (m), 1633 (m), 1605 (m), 1557 (w), 1495 (s), 1454 (m), 1443 (m), 1406 (w), 1356 (w), 1294 (m), 1239 (m), 1155 (w), 1065 (w), 1031 (m), 910 (m), 874 (w), 810 (w), 756 (m), 729 (s), 697 (vs), 655 (m), 600 (w), 505 (m) cm^{-1}; LRMS (ESI): *m*/*z* = 195.1 $[C_{14}H_{11}O]^+$, 346.2 $[M + H]^+$, 368.2 $[M + Na]^+$; HRMS (ESI): calcd. for $[C_{23}H_{23}NO_2Na]^+$ 368.1621, found $[M + Na]^+$ 368.1622.

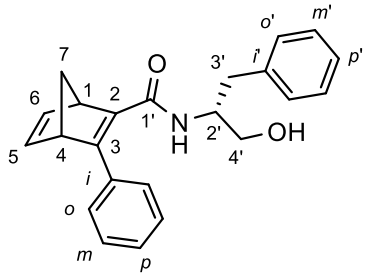

$C_{23}H_{23}NO_2$
345.44 g/mol

3b

(1*R*,4*S*)-3-Phenyl-*N*-((*R*)-1-phenyl-3-(prop-2-yn-1-yloxy)propan-2-yl)bicyclo[2.2.1]hepta-2,5-diene-2-carboxamide (Ph(BnC$_1$OC$_1$))

Synthesis according to GP 10; colorless oil (57 %); column chromatography on silica (hexanes / EtOAc = 8 : 1 to 4 : 1); R_f = 0.36 (hexanes / EtOAc = 4 : 1, UV); $[\alpha]_D^{20}$ = –11.5° [c = 10 mg/mL, CH_2Cl_2]; ^{1}H NMR (500 MHz, $CDCl_3$): δ = 7.38–7.27 (m, 5H, *m*-Ar*H*, *m'*-Ar*H*, *p*'-Ar*H*), 7.26–7.15 (m, 3H, *o*-Ar*H*, *p*-Ar*H*), 7.12–7.07 (m, 2H, *o*'-Ar*H*), 6.98 (dd, *J* = 3.0, 4.9 Hz, 1H, 6-H), 6.92 (dd, *J* = 3.0, 4.9 Hz, 1H, 5-H), 5.69 (d, *J* = 9.6 Hz, 1H, N*H*), 4.32–4.23 (m, 1H, 2'-H), 4.06–4.02 (m, 1H, 1-H), 4.01–3.93 (m, 2H, 5'-H), 3.81–3.76 (m, 1H, 4-H), 3.37–3.27 (m, 2H, 4'-H), 2.78 (dd, *J* = 5.9, 13.0 Hz, 1H, 3'-H), 2.64 (dd, *J* = 8.8, 13.0 Hz, 1H, 3'-H), 2.37 (t, *J* = 2.5 Hz, 1H, 7'-H), 2.28 (dt, *J* = 1.4 Hz, 6.3 Hz, 1H, 7-H), 2.03 (dt, *J* = 1.4 Hz, 6.3 Hz, 1H, 7-H) ppm; ^{13}C NMR (126 MHz, $CDCl_3$): δ = 165.7 (C-1'), 158.5 (C-3), 144.0 (C-2), 143.8 (C-6),

141.6 (C-5), 137.9 (*i*'-C_{Ar}), 136.0 (*i*-C_{Ar}), 129.5 (*o*'-C_{Ar}), 128.7 (*o*-C_{Ar}), 128.4 (*m*'-C_{Ar}), 128.3 (*p*-C_{Ar}), 127.1 (*m*-C_{Ar}), 126.4 (*p*'-C_{Ar}), 79.4 (C-6'), 74.7 (C-7'), 71.5 (C-7), 69.2 (C-5'), 58.3 (C-4'), 58.0 (C-4), 53.4 (C-1), 50.0 (C-2'), 37.0 (C-3') ppm; FTIR (ATR): $\tilde{\nu}$ = 3417 (w), 3293 (w), 3062 (w), 3027 (w), 2937 (w), 2867 (w), 1753 (m), 1641 (m), 1612 (m), 1557 (w), 1496 (s), 1454 (m), 1443 (m), 1407 (w), 1357 (w), 1295 (m), 1236 (m), 1156 (w), 1090 (m), 1066 (m), 1030 (m), 911 (w), 810 (w), 745 (m), 718 (m), 697 (vs), 655 (m), 507 (m) cm^{-1}; LRMS (ESI): *m*/*z* = 195.1 $[C_{14}H_{11}O]^+$, 384.2 [M + H], 406.2 $[M + Na]^+$; HRMS (ESI): calcd. for $[C_{26}H_{26}NO_2]^+$ 384.1958, found $[M + Na]^+$ 384.1956.

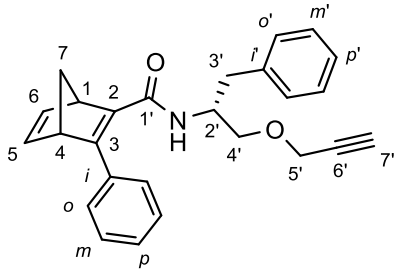

$C_{26}H_{25}NO_2$
383.49 g/mol

Ph(BnC_1OC_1)

(1*R*,4*S*)-*N*-((*R*)-1-((1-Benzyl-1*H*-1,2,3-triazol-4-yl)methoxy)-3-phenylpropan-2-yl)-3-phenylbicyclo[2.2.1]hepta-2,5-diene-2-carboxamide (Ph(BnC_1OC_1)click)

Synthesis according to GP 12; colorless oil (72 %); column chromatography on neutral aluminum oxide (hexanes / EtOAc = 1 : 1 to pure EtOAc); R_f = 0.45 (hexane / EtOAc = 1 : 1, UV); $[\alpha]_D^{20}$ = –9.3° [c = 10 mg/mL, CH_2Cl_2]; ^{1}H NMR (500 MHz, $CDCl_3$): δ = 7.41–7.34 (m, 3H, *m*''-Ar*H*, *p*''-Ar*H*), 7.31–7.11 (m, 11H, *o*-Ar*H*, *o*''-Ar*H*, *m*-Ar*H*, *m*'-Ar*H*, *p*-Ar*H*, *p*'-Ar*H*, 7'-H), 7.04–6.98 (m, 2H, *o*'-Ar*H*), 6.97 (dd, *J* = 3.0, 4.9 Hz, 1H, 6-H), 6.90 (dd, *J* = 3.0, 4.9 Hz, 1H, 5-H), 5.69 (d, *J* = 9.6 Hz 1H, N*H*), 5.55–5.45 (m, 2H, 9'-H), 4.48–4.39 (m, 2H, 5'-H), 4.31–4.21 (m, 1H, 2'-H), 4.03–3.97 (m, 1H, 1-H), 3.80–3.74 (m, 1H, 4-H), 3.32–3.22 (m, 2H, 4'-H), 2.74 (dd, *J* = 8.8, 13.0 Hz, 1H, 3'-H), 2.60 (dd, *J* = 8.8, 13.0 Hz, 1H, 3'-H), 2.26 (dt, *J* = 1.3, 6.9 Hz, 1H, 7-H), 2.02 (dt, *J* = 1.3, 6.9 Hz, 1H, 7-H) ppm; ^{13}C NMR (126 MHz, $CDCl_3$): δ = 165.7 (C-1'), 158.4 (C-3), 145.3 (C-6'), 144.0 (C-2), 143.8 (C-6), 141.5 (C-5), 137.8 (*i*'-C_{Ar}), 136.0 (*i*-C_{Ar}), 134.7 (*i*''-C_{Ar}), 129.4 (*o*'-C_{Ar}), 129.2 (*m*''-C_{Ar}), 128.9 (*p*''-C_{Ar}), 128.5 (*o*-C_{Ar}), 128.4 (*m*'-C_{Ar}), 128.2 (*p*-C_{Ar}), 128.1 (*o*''-C_{Ar}), 127.1 (*m*-C_{Ar}), 126.4 (*p*'-C_{Ar}), 122.3 (C-7'), 71.5 (C-7), 69.7 (C-4'), 64.6 (C-5'), 58.0 (C-4), 54.2 (C-8'), 53.4 (C-1), 50.0 (C-2'), 37.1 (C-3') ppm; FTIR (ATR): $\tilde{\nu}$ = 2918 (m), 2850 (w), 1641 (m), 1613 (w), 1557 (w), 1496 (m), 1467 (w), 1454 (m), 1331 (w), 1295 (w), 1260 (m), 1223 (w), 1156 (w), 1120 (m), 1088 (w), 1048 (m), 1029 (m), 909 (m), 808 (w), 721 (s), 696 (vs), 649 (m), 619 (w), 576 (m), 510 (w), 469 (w) cm^{-1}; LRMS (ESI): *m*/*z* = 517.3 $[M + H]^+$, 539.2 $[M + Na]^+$; HRMS (ESI): calcd. for $[C_{33}H_{33}N_4O_2]^+$ 517.2598, found $[M + H]^+$ 517.2592;

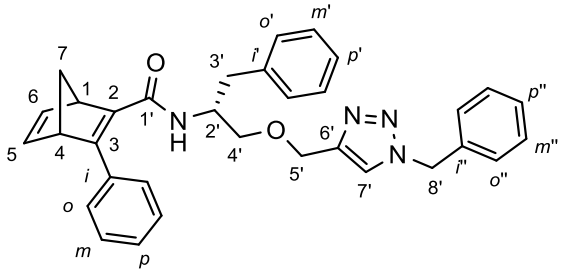

$C_{33}H_{32}N_4O_2$
516.65 g/mol

Ph(BnC_1OC_1)click

(1*R*,4*S*)-*N*-((*R*)-1-(Hex-5-yn-1-yloxy)-3-methylbutan-2-yl)-3-phenylbicyclo-[2.2.1]hepta-2,5-diene-2-carboxamide (Ph(*i*PrC$_1$OC$_4$))

To a solution of the alcohol **2c** (0.21 g, 0.69 mmol) in abs. THF (10 mL) was added sodium hydride (69.3 mg, 1.73 mmol, 60 wt% in mineral oil) at 0 °C and the reaction mixture was stirred for 1 h at 0 °C. 6-Iodo-hex-1-yne (0.22 g, 1.04 mmol) was added and the reaction mixture was stirred for 24 h at room temperature. A saturated aqueous NH_4Cl solution (10 mL) was added, the aqueous phase was extracted with EtOAc (3 × 30 mL) and the combined organic layers were dried over $MgSO_4$. The solvent was removed under reduced pressure and the crude product was purified by column chromatography (hexanes / EtOAc = 3 : 1). The alkyne **Ph(*i*PrC$_1$OC$_4$)** was obtained as a colorless oil (68.0 mg, 0.18 mmol, 26 %).

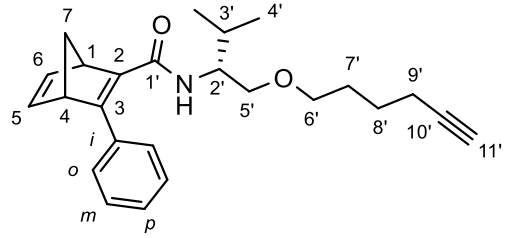

$C_{25}H_{31}NO_2$
377.53 g/mol

Ph(*i*PrC$_1$OC$_4$)

R_f = 0.90 (hexanes / EtOAc = 1 : 1, UV); $[\alpha]_D^{20}$ = –16.8° [c = 10 mg/mL, CH_2Cl_2]; ^{1}H NMR (500 MHz, $CDCl_3$): δ = 7.41–7.25 (m, 5H, *o*-Ar*H*, *m*-Ar*H*, *p*-Ar*H*), 7.01 (dd, *J* = 3.0, 4.9 Hz, 1H, 6-H), 6.94 (dd, *J* = 3.0, 4.9 Hz, 1H, 5-H), 5.54 (d, *J* = 9.6 Hz, 1H, N*H*), 4.11–4.03 (m, 1H, 1-H), 3.87–3.80 (m, 1H, 2‘-H), 3.79–3.75 (m, 1H, 4-H), 3.40 (dd, *J* = 4.0, 9.6 Hz, 1H, 5‘-H), 3.32–3.19 (m, 3H, 5‘-H, 6‘-H), 2.30 (dt, *J* = 1.3, 6.9 Hz, 1H, 7-H), 2.19–2.12 (m, 2H, 9‘-H), 2.04 (dt, *J* = 1.3, 6.9 Hz, 1H, 7-H), 1.94 (t, *J* = 2.5 Hz, 1H, 11‘-H), 1.74–1.64 (m, 1H, 3‘-H), 1.58–1.41 (m, 4H, 7‘-H, 8‘-H), 0.78 (d, *J* = 7.3 Hz, 3H, 4‘-H), 0.68 (d, *J* = 7.3 Hz, 3H, 4‘-H) ppm; ^{13}C NMR (126 MHz, $CDCl_3$): δ = 166.0 (C-1‘), 158.0 (C-3), 144.6 (C-2), 143.9 (C-6), 141.7 (C-5), 136.4 (*i*-C_{Ar}), 128.7 (*o*-C_{Ar}), 128.2 (*p*-C_{Ar}), 127.0 (*m*-C_{Ar}), 84.4 (C-10‘), 71.7 (C-7), 70.6 (C-6‘), 70.3 (C-5‘), 68.5 (C-11‘), 58.1 (C-4), 53.8 (C-2‘), 53.5 (C-1), 29.3 (C-3‘), 28.7 (C-7‘), 25.2 (C-8‘), 19.5 (C-4‘), 18.6 (C-4‘), 18.3 (C-9‘) ppm; FTIR (ATR): $\tilde{\nu}$ = 3425 (w), 3306 (w), 2958 (m), 2935 (m), 2868 (m), 1645 (s), 1615 (s), 1557 (w), 1502 (s), 1444 (m), 1387 (w), 1368 (m), 1295 (m), 1237 (m), 1184 (w), 1116 (s), 1031 (w), 946 (w), 922 (w), 876 (w), 842 (w), 810 (w), 759 (s), 715 (s), 697 (vs), 653 (s), 628 (s), 515 (m), 496 (w) cm^{-1}; LRMS (ESI): *m*/*z* = 195.1 $[C_{14}H_{11}O]^+$, 378.2 $[M + H]^+$, 400.2 $[M + Na]^+$; HRMS (ESI): calcd. for $[C_{25}H_{32}NO_2]^+$ 378.2428, found $[M + H]^+$ 378.2429.

(1*R*,4*S*)-*N*-((*R*)-1-(4-(1-Benzyl-1*H*-1,2,3-triazol-4-yl)butoxy)-3-methylbutan-2-yl)-3-phenyl-bicyclo[2.2.1]hepta-2,5-diene-2-carboxamide (Ph(*i*PrC$_1$OC$_4$)click)

Synthesis according to GP 12; colorless oil (76 %); column chromatography on silica (hexanes / EtOAc = 1 : 1 to 1 : 2); R_f = 0.40 (hexanes / EtOAc = 1 : 1, UV); $[\alpha]_D^{20}$ = –7.6 [c = 10 mg/mL, CH_2Cl_2]; ^{1}H NMR (500 MHz, $CDCl_3$): δ = 7.38–7.28 (m, 7H, *o*-Ar*H*, *m*-Ar*H*, *m*‘-Ar*H*, *p*-Ar*H*), 7.27–7.22 (m, 3H, *o*‘-Ar*H*, *p*‘-Ar*H*), 7.18 (s, 1H, 11‘-H), 6.98 (dd, *J* = 3.0, 4.9 Hz, 1H, 6-H), 6.92 (dd, *J* = 3.0, 4.9 Hz, 1H, 5-H), 5.50 (d, *J* = 9.8 Hz, 1H, N*H*), 5.48 (s, 2H, 12‘-H), 4.07–4.02 (m, 1H, 1-H), 3.87–3.80 (m, 1H, 2‘-H), 3.78–3.72 (m, 1H, 4-H), 3.36 (dd, *J* = 4.0, 9.6 Hz, 5‘-H), 3.27 (t, *J* = 6.3 Hz, 2H, 6‘-H), 3.21 (dd, *J* = 4.0, 9.6 Hz, 1H, 5‘-H), 2.66 (t, *J* = 7.8 Hz, 2H, 9‘-H), 2.27 (dt, *J* = 1.3, 6.9 Hz, 1H, 7-H), 2.02 (dt, *J* = 1.3, 6.9 Hz, 1H, 7-H), 1.73–1.55 (m, 3H, 3‘-H, 8‘-H), 1.50–1.41 (m, 2H, 7‘-H), 0.76 (d, *J* = 7.3 Hz, 3H, 4‘-H), 0.65 (d, *J* = 7.3 Hz, 3H, 4‘-H) ppm; ^{13}C NMR (126 MHz, $CDCl_3$): δ = 165.9 (C-1’), 157.9 (C-3), 148.6 (C-10’), 144.5 (C-2), 143.8 (C-6), 141.7 (C-5), 136.3 (*i*-C_{Ar}), 135.1 (*i*’-C_{Ar}), 129.2 (*o*-C_{Ar}), 128.71 (*p*-C_{Ar}), 128.66 (*m*-C_{Ar}), 128.2 (*p*’-C_{Ar}), 128.1 (*o*’-C_{Ar}), 127.0 (*m*’-C_{Ar}), 120.6 (C-11’), 71.6 (C-7),

70.8 (C-6'), 70.3 (C-5'), 58.1 (C-4), 54.1 (C-12'), 53.7 (C-1), 53.5 (C-2'), 29.22 (C-7'), 29.17 (C-3'), 26.1 (C-8'), 25.6 (C-9'), 19.5 (C-4'), 18.5 (C-4') ppm; FTIR (ATR): $\tilde{\nu}$ = 2935 (m), 2867 (m), 1643 (s), 1615 (m), 1556 (w), 1498 (s), 1457 (m), 1386 (w), 1367 (m), 1296 (m), 1252 (m), 1219 (m), 1180 (w), 1116 (s), 1075 (m), 1046 (m), 1030 (m), 1002 (w), 921 (w), 875 (w), 810 (w), 760 (m), 716 (s), 697 (vs), 656 (m), 602 (w), 579 (w), 519 (w), 461 (w) cm^{-1}; LRMS (ESI): *m*/*z* = 511.3 $[M + H]^+$, 533.3 $[M + Na]^+$; HRMS (ESI): calcd. for $[C_{32}H_{38}N_4O_2]^+$ 511.3068, found $[M + H]^+$ 511.3073.

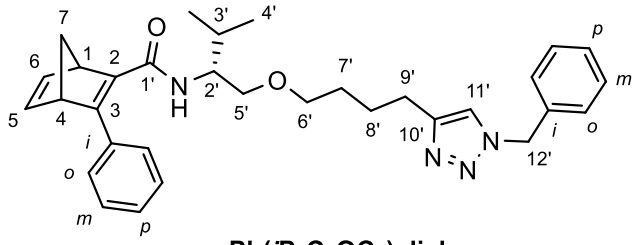

$C_{32}H_{38}N_4O_2$
510.68 g/mol

Ph(*i*PrC_1OC_4)click

(1*R*,4*S*)-*N*-(4-Oxohex-5-yn-1-yl)-3-phenylbicyclo[2.2.1]hepta-2,5-diene-2-carboxamide (Ph(C_2CO))

Synthesis according to GP 11; colorless oil (52 %); column chromatography on silica (hexanes / EtOAc = 2 : 1); R_f = 0.33 (hexanes / EtOAc = 2 : 1, UV); $[\alpha]_D^{20}$ = –18.9° [c = 10 mg/mL, CH_2Cl_2]; ^{1}H NMR (500 MHz, $CDCl_3$): δ = 7.41–7.35 (m, 2H, *o*-Ar*H*), 7.34–7.27 (m, 3H, *m*-Ar*H*, *p*-Ar*H*), 7.00 (dd, *J* = 3.0, 4.9 Hz, 1H, 6-H), 6.92 (dd, *J* = 3.0, 4.9 Hz, 1H, 5-H), 5.47–5.36 (m, 1H, N*H*), 4.10–4.01 (m, 1H, 1-H), 3.84–3.76 (m, 1H, 4-H), 3.22 (s, 1H, 7'-H), 3.22–3.15 (m, 2H, 2'-H), 2.50 (t, *J* = 7.7 Hz, 2H, 4'-H), 2.28 (dt, *J* = 1.3, 6.9 Hz, 1H, 7-H), 2.04 (dt, *J* = 1.3, 6.9 Hz, 1H, 7-H), 1.76–1.69 (m, 2H, 3'-H) ppm; ^{13}C NMR (126 MHz, $CDCl_3$): δ = 186.5 (C-5'), 166.5 (C-1'), 158.6 (C-3), 144.2 (C-2), 143.8 (C-6), 141.6 (C-5), 136.1 (*i*-C_{Ar}), 128.8 (*o*-C_{Ar}), 128.5 (*p*-C_{Ar}), 127.0 (*m*-C_{Ar}), 81.3 (C-6'), 79.0 (C-7'), 71.7 (C-7), 57.9 (C-4), 53.4 (C-1), 42.9 (C-4'), 38.5 (C-2'), 23.4 (C-3') ppm; FTIR (ATR): $\tilde{\nu}$ = 3271 (w), 3065 (w), 2974 (w), 2936 (w), 2868 (w), 2087 (m), 1678 (s), 1635 (s), 1572 (w), 1557 (m), 1515 (vs), 1443 (m), 1402 (w), 1370 (w), 1329 (m), 1295 (s), 1261 (m), 1224 (m), 1157 (w), 1119 (m), 1065 (w), 1032 (w), 913 (w), 881 (w), 811 (w), 761 (s), 715 (s), 696 (s), 657 (m), 600 (w), 528 (w) cm^{-1}; LRMS (ESI): *m*/*z* = 195.1 $[C_{14}H_{11}O]^+$, 306.2 $[M + H]^+$, 329.1 $[M + Na]^+$; HRMS (ESI): calcd. for $[C_{20}H_{19}NO_2Na]^+$ 328.1308, found $[M + Na]^+$ 328.1308.

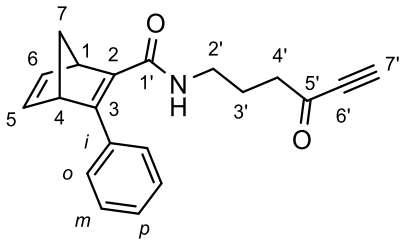

$C_{20}H_{19}NO_2$
305.38 g/mol

Ph(C_2CO)

(1*R*,4*S*)-*N*-(4-(1-Benzyl-1*H*-1,2,3-triazol-4-yl)-4-oxobutyl)-3-phenylbicyclo[2.2.1]-hepta-2,5-diene-2-carboxamide (Ph(C_2CO)click)

Synthesis according to GP 12; colorless oil (60 %); column chromatography on silica (hexanes / EtOAc = 1 : 1 to 1 : 2); R_f = 0.32 (hexanes / EtOAc = 1 : 1, UV); $[\alpha]_D^{20}$ = –4.7 [c = 10 mg/mL, CH_2Cl_2]; ^{1}H NMR (500 MHz, $CDCl_3$): δ = 7.90 (s, 1H, 7'-H), 7.43–7.36 (m, 3H, *p*'-Ar*H*, *o*-Ar*H*), 7.35–7.27 (m, 6H, *o*'-Ar*H*, *m*-Ar*H*, *m*'-Ar*H*), 7.24–7.18 (m, 1H, *p*'-Ar*H*), 6.99 (dd, *J* = 3.0, 4.9 Hz, 1H, 6-H), 6.90 (dd, *J* = 3.0, 4.9 Hz, 1H, 5-H), 5.58 (s, 1H, N*H*), 5.55 (s,

2H, 8‘-H), 4.05–4.00 (m, 1H, 1-H), 3.81–3.77 (m, 1H, 4-H), 3.32–3.20 (m, 2H, 2‘-H), 3.00 (t, *J* = 6.9 Hz, 2H, 4‘-H), 2.27 (dt, *J* = 1.3, 6.9 Hz, 1H, 7-H), 2.03 (dt, *J* = 1.3, 6.9 Hz, 1H, 7-H), 1.80 (q, *J* = 6.9 Hz, 2H, 3‘-H) ppm; ^{13}C NMR (126 MHz, $CDCl_3$): δ = 194.5 (C-5’), 166.5 (C-1‘), 158.3 (C-3), 148.0 (C-6’), 144.1 (C-2), 143.8 (C-6), 141.6 (C-5), 136.0 (*i*-C_{Ar}), 133.7 (*i’*-C_{Ar}), 129.5 (*o*-C_{Ar}), 129.3 (*p*-C_{Ar}), 128.7 (*m*’-C_{Ar}), 128.5 (*o*’-C_{Ar}), 128.3 (*p*’-C_{Ar}), 127.1 (*m*-C_{Ar}), 125.4 (C-7’), 71.6 (C-7), 57.8 (C-4), 54.6 (C-8’), 53.5 (C-1), 38.9 (C-2’), 36.9 (C-4’), 23.5 (C-3’) ppm; FTIR (ATR): $\tilde{\nu}$ = 3351 (w), 3065 (w), 2976 (w), 2936 (w), 2868 (w), 1684 (m), 1638 (s), 1612 (m), 1556 (w), 1523 (s), 1455 (m), 1443 (m), 1403 (w), 1374 (w), 1331 (w), 1295 (m), 1242 (m), 1171 (m), 1124 (w), 1078 (w), 1032 (m), 1002 (w), 967 (w), 911 (m), 880 (w), 810 (w), 761 (m), 718 (vs), 697 (s), 657 (w), 619 (w), 585 (w), 506 (w), 426 (w) cm^{-1}; LRMS (ESI): *m*/*z* = 195.1 $[C_{14}H_{11}O]^+$, 439.2 $[M + H]^+$, 461.2 $[M + Na]^+$; HRMS (ESI): calcd. for $[C_{27}H_{27}N_4O_2]^+$ 439.2129, found $[M + H]^+$ 439.2135.

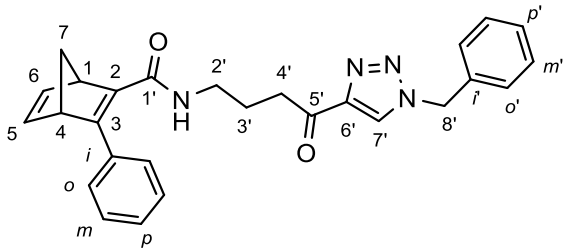

$C_{27}H_{26}N_4O_2$
438.53 g/mol

Ph(C_2CO)click

(1*R*,4*S*)-*N*-(5-Oxohept-6-yn-1-yl)-3-phenylbicyclo[2.2.1]hepta-2,5-diene-2-carboxamide (Ph(C_3CO))

Synthesis according to GP 11; colorless oil (74 %); column chromatography on silica (hexanes / EtOAc = 2 : 1); R_f = 0.45 (hexanes / EtOAc = 2 : 1, UV); $[\alpha]_D^{20}$ = –67.2° [c = 10 mg/mL, CH_2Cl_2]; ^{1}H NMR (500 MHz, $CDCl_3$): δ = 7.39–7.34 (m, 2H, *o*-Ar*H*), 7.33–7.27 (m, 3H, *m*-Ar*H*, *p*-Ar*H*), 6.99 (dd, *J* = 3.0, 4.9 Hz, 1H, 6-H), 6.91 (dd, *J* = 3.0, 4.9 Hz, 1H, 5-H), 5.38 (bs, 1H, N*H*), 4.07–4.01 (m, 1H, 1-H), 3.81–3.74 (m, 1H, 4-H), 3.21 (s, 1H, 8‘-H), 3.20–3.11 (m, 2H, 2‘-H), 2.53 (t, *J* = 7.7 Hz, 2H, 5‘-H), 2.28 (dt, *J* = 1.3, 6.9 Hz, 1H, 7-H), 2.03 (dt, *J* = 1.3, 6.9 Hz, 1H, 7-H), 1.56–1.46 (m, 2H, 4‘-H), 1.33–1.41 (m, 2H, 3‘-H) ppm; ^{13}C NMR (126 MHz, $CDCl_3$): δ = 186.9 (C-6‘), 166.4 (C-1‘), 158.2 (C-3), 144.3 (C-2), 143.8 (C-6), 141.6 (C-5), 136.1 (*i*-C_{Ar}), 128.7 (*o*-C_{Ar}), 128.4 (*p*-C_{Ar}), 127.0 (*m*-C_{Ar}), 81.4 (C-7‘), 78.7 (C-8‘), 71.6 (C-7), 57.9 (C-4), 53.4 (C-1), 44.9 (C-5‘), 38.9 (C-2‘), 28.5 (C-3‘), 20.9 (C-4‘) ppm; FTIR (ATR): $\tilde{\nu}$ = 3273 (w), 3066 (w), 2936 (m), 2868 (w), 2087 (m), 1678 (s), 1636 (s), 1612 (s), 1557 (m), 1516 (vs), 1443 (m), 1403 (w), 1366 (w), 1328 (m), 1295 (s), 1261 (m), 1224 (m), 1156 (w), 1119 (m), 1076 (m), 1031 (w), 911 (w), 870 (w), 810 (w), 760 (s), 715 (s), 696 (s), 657 (m), 599 (w), 558 (w), 506 (w) cm^{-1}; LRMS (ESI): *m*/*z* = 195.1 $[C_{14}H_{11}O]^+$, 320.2 $[M + H]^+$, 342.2 $[M + Na]^+$; HRMS (ESI): calcd. for $[C_{21}H_{22}NO_2]^+$ 320.1645, found $[M + H]^+$ 320.1646.

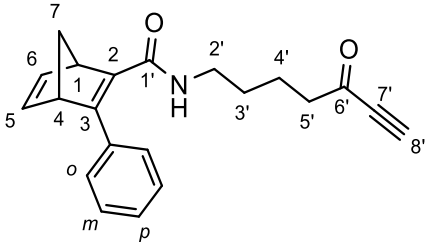

$C_{21}H_{21}NO_2$
319.40 g/mol

Ph(C_3CO)

(1*R*,4*S*)-*N*-(5-(1-Benzyl-1*H*-1,2,3-triazol-4-yl)-5-oxopentyl)-3-phenylbicyclo[2.2.1]-hepta-2,5-diene-2-carboxamide (Ph(C_2CO)click)

Synthesis according to GP 12; colorless oil (53 %); column chromatography on silica (hexanes / EtOAc = 1 : 1); R_f = 0.27 (hexanes / EtOAc = 1 : 1, UV); $[\alpha]_D^{20}$ = –19.2° [c = 10 mg/mL, CH_2Cl_2]; ^{1}H NMR (500 MHz, $CDCl_3$): δ = 7.92 (s, 1H, 8‘-H), 7.42–7.20 (m, 10H, *o*-Ar*H*, *o*‘-Ar*H*, *m*-Ar*H*, *m*‘-Ar*H*, *p*-Ar*H*, *p*‘-Ar*H*), 6.99 (dd, *J* = 3.0, 4.9 Hz, 1H, 6-H), 6.90 (dd, *J* = 3.0, 4.9 Hz, 1H, 5-H), 5.54 (s, 2H, 9‘-H), 5.41 (s, 1H, N*H*), 4.08–4.02 (m, 1H, 1-H), 3.83–3.74 (m, 1H, 4-H), 3.27–3.13 (m, 1H, 2‘-H), 3.03 (t, *J* = 6.9 Hz, 2H, 5‘-H), 2.27 (dt, *J* = 1.3, 6.9 Hz, 1H, 7-H), 2.03 (dt, *J* = 1.3, 6.9 Hz, 1H, 7-H), 1.63–1.53 (m, 2H, 4‘-H), 1.47–1.37 (m, 2H, 3‘-H) ppm; ^{13}C NMR (126 MHz, $CDCl_3$): δ = 194.8 (C-6’), 166.3 (C-1’), 158.0 (C-3), 148.1 (C-7’), 144.3 (C-2), 143.9 (C-6), 141.6 (C-5), 136.1 (*i*-C_{Ar}), 133.7 (*i*’-C_{Ar}), 129.4 (*o*-C_{Ar}), 129.3 (*p*-C_{Ar}), 128.7 (*m*’-C_{Ar}), 128.5 (*o*’-C_{Ar}), 128.3 (*p*’-C_{Ar}), 127.0 (*m*-C_{Ar}), 125.4 (C-8’), 71.6 (C-7), 57.8 (C-4), 54.6 (C-9’), 53.5 (C-1), 39.1 (C-2’), 39.0 (C-5’), 28.9 (C-3’), 21.1 (C-4’) ppm; FTIR (ATR): $\tilde{\nu}$ = 3348 (w), 3064 (w), 2935 (w), 2866 (w), 1684 (m), 1637 (m), 1612 (m), 1557 (w), 1522 (s), 1455 (m), 1442 (m), 1404 (w), 1369 (w), 1330 (w), 1295 (m), 1240 (m), 1168 (m), 1124 (w), 1077 (w), 1033 (m), 1002 (w), 952 (w), 911 (w), 810 (w), 760 (m), 716 (vs), 695 (s), 656 (m), 620 (w), 599 (w), 509 (w), 471 (w) cm^{-1}; LRMS (ESI): *m*/*z* = 195.1 $[C_{14}H_{11}O]^+$, 453.2 $[M + H]^+$, 475.2 $[M + Na]^+$; HRMS (ESI): calcd. for $[C_{28}H_{29}N_4O_2]^+$ 453.2285, found $[M + H]^+$ 453.2286.

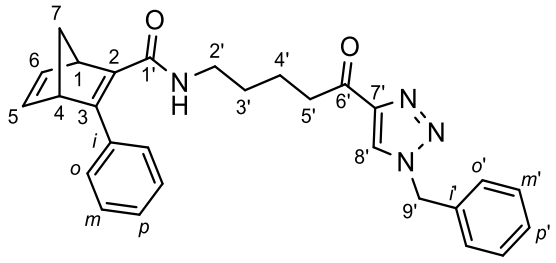

$C_{28}H_{28}N_4O_2$
452.56 g/mol

Ph(C_3CO)click

(1*R*,4*S*)-*N*-(6-Oxooct-7-yn-1-yl)-3-phenylbicyclo[2.2.1]hepta-2,5-diene-2-carbox-amide (Ph(C_4CO))

Synthesis according to GP 11; colorless oil (56 %); column chromatography on silica (hexanes / EtOAc = 1 : 1); R_f = 0.76 (hexanes / EtOAc = 1 : 1, UV); $[\alpha]_D^{20}$ = –21.8 [c = 10 mg/mL, CH_2Cl_2]; ^{1}H NMR (500 MHz, $CDCl_3$): δ = 7.40–7.34 (m, 2H, *o*-Ar*H*), 7.33–7.28 (m, 3H, *m*-Ar*H*, *p*-Ar*H*), 7.00 (dd, *J* = 3.0, 4.9 Hz, 1H, 6-H), 6.91 (dd, *J* = 3.0, 4.9 Hz, 1H, 5-H), 5.32 (bs, 1H, N*H*), 4.11–4.01 (m, 1H, 1-H), 3.83–3.74 (m, 1H, 4-H), 3.21 (s, 1H, 9‘-H), 3.20–3.12 (m, 2H, 2‘-H), 2.52 (t, *J* = 7.7 Hz, 2H, 6‘-H), 2.29 (dt, *J* = 1.3, 6.9 Hz, 1H, 7-H), 2.04 (dt, *J* = 1.3, 6.9 Hz, 1H, 7-H), 1.65–1.56 (m, 2H, 5‘-H), 1.40–1.30 (m, 2H, 3‘-H), 1.21–1.08 (m, 2H, 4‘-H) ppm; ^{13}C NMR (126 MHz, $CDCl_3$): δ = 187.2 (C-7‘), 166.3 (C-1‘), 158.1 (C-3), 144.4 (C-2), 143.9 (C-6), 141.6 (C-5), 136.1 (*i*-C_{Ar}), 128.7 (*o*-C_{Ar}), 128.3 (*p*-C_{Ar}), 127.0 (*m*-C_{Ar}), 81.4 (C-8‘), 78.6 (C-9‘), 71.7 (C-7), 57.9 (C-4), 53.4 (C-1), 45.2 (C-6‘), 39.1 (C-2‘), 29.0 (C-3‘), 26.2 (C-4‘), 23.3 (C-5‘) ppm; FTIR (ATR): $\tilde{\nu}$ = 3275 (w), 3064 (w), 2934 (m), 2865 (w), 2086 (m), 1678 (s), 1636 (s), 1557 (m), 1517 (s), 1443 (m), 1402 (w), 1366 (w), 1329 (m), 1295 (s), 1260 (m), 1200 (w), 1156 (w), 1120 (m), 1075 (m), 1031 (w), 912 (w), 874 (w), 810 (w), 760 (s), 715 (s), 696 (vs), 657 (m), 599 (w), 526 (w), 420 (w) cm^{-1}; LRMS (ESI): *m*/*z* = 195.1 $[C_{14}H_{11}O]^+$, 334.2 $[M + H]^+$, 356.2 $[M + Na]^+$; HRMS (ESI): calcd. for $[C_{22}H_{24}NO_2]^+$ 334.1802, founs $[M + H]^+$ 334.1801.

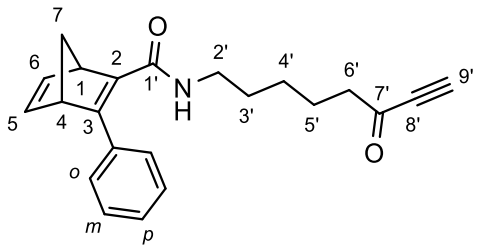

$C_{22}H_{23}NO_2$
333.43 g/mol

Ph(C_4CO)

(1*R*,4*S*)-*N*-(6-(1-Benzyl-1*H*-1,2,3-triazol-4-yl)-6-oxohexyl)-3-phenylbicyclo[2.2.1]hepta-2,5-diene-2-carboxamide (Ph(C_4CO)click)

Synthesis according to GP 12; colorless oil (48 %); column chromatography on silica (hexanes / EtOAc = 1 : 1); R_f = 0.30 (hexanes / EtOAc = 1 : 1, UV); $[\alpha]_D^{20}$ = –96.3° [c = 10 mg/mL, CH_2Cl_2]; ^{1}H NMR (700 MHz, $CDCl_3$): δ = 7.93 (s, 1H, 9‘-H), 7.41–7.38 (m, 3H, *o*-Ar*H*, *p*-Ar*H*), 7.37–7.34 (m, 2H, *m*‘-Ar*H*), 7.31–7.26 (m, 5H, *m*-Ar*H*, *o*‘-Ar*H*, *p*‘-Ar*H*), 6.99 (dd, *J* = 3.0, 4.9 Hz, 1H, 6-H), 6.91 (dd, *J* = 3.0, 4.9 Hz, 1H, 5-H), 5.55 (s, 2H, 10‘-H), 5.32 (bs, 1H, N*H*), 4.07–4.02 (m, 1H, 1-H), 3.81–3.75 (m, 1H, 4-H), 3.22–3.10 (m, 2H, 2‘-H), 3.03 (t, *J* = 6.9 Hz, 2H, 6‘-H), 2.28 (dt, *J* = 1.3, 6.9 Hz, 1H, 7-H), 2.03 (dt, *J* = 1.3, 6.9 Hz, 1H, 7-H), 1.68–1.59 (m, 2H, 5‘-H), 1.40–1.34 (m, 2H, 3‘-H), 1.22–1.16 (m, 2H, 4‘-H) ppm; ^{13}C NMR (176 MHz, $CDCl_3$): δ = 195.2 (C-7’), 166.3 (C-1’), 158.0 (C-3), 148.3 (C-8’), 144.5 (C-2), 144.0 (C-6), 141.6 (C-5), 136.2 (*i*-C_{Ar}), 133.8 (*i*'-C_{Ar}), 129.5 (*o*-C_{Ar}), 129.3 (*p*-C_{Ar}), 128.8 (*m*’-C_{Ar}), 128.5 (*o*’-C_{Ar}), 128.4 (*p*’-C_{Ar}), 127.1 (*m*-C_{Ar}), 125.4 (C-9’), 71.7 (C-7), 57.9 (C-4), 54.6 (C-10’), 53.4 (C-1), 39.4 (C-6’), 39.2 (C-2’), 29.1 (C-3’), 26.6 (C-4’), 23.6 (C-5’) ppm; FTIR (ATR): $\tilde{\nu}$ = 3338 (w), 3064 (w), 2933 (m), 2864 (w), 1683 (s), 1637 (s), 1612 (m), 1556 (w), 1525 (s), 1456 (m), 1442 (m), 1404 (w), 1372 (w), 1331 (w), 1295 (m), 1241 (m), 1167 (m), 1124 (w), 1078 (w), 1035 (m), 1002 (w), 957 (w), 912 (w), 872 (w), 810 (w), 761 (m), 717 (vs), 696 (s), 657 (m), 619 (w), 600 (w), 511 (w), 471 (w) cm^{-1}; LRMS (ESI): *m*/*z* = 195.1 $[C_{14}H_{11}O]^+$, 467.2 $[M + H]^+$, 489.2 $[M + Na]^+$; HRMS (ESI): calcd. for $[C_{29}H_{31}N_4O_2]^+$ 467.2442, found $[M + H]^+$ 467.2445.

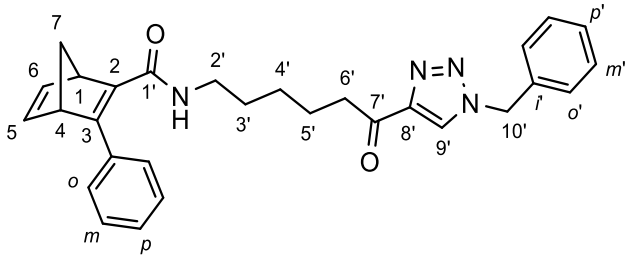

$C_{29}H_{30}N_4O_2$
466.59 g/mol

Ph(C_4CO)click

(1*R*,4*S*)-*N*-(12-Oxotetradec-13-in-1-yl)-3-phenylbicyclo[2.2.1]hepta-2,5-diene-2-carboxamide (Ph(C_{10}CO))

Synthesis according to GP 11; colorless oil (50 %); column chromatography on silica (hexanes / EtOAc = 5 : 1); R_f = 0.30 (hexanes / EtOAc = 5 : 1, UV); $[\alpha]_D^{20}$ = –47.3 [c = 10 mg/mL, CH_2Cl_2]; ^{1}H NMR (500 MHz, $CDCl_3$): δ = 7.39–7.34 (m, 2H, *o*-Ar*H*), 7.33–7.27 (m, 3H, *m*-Ar*H*, *p*-Ar*H*), 7.00 (dd, *J* = 3.0, 4.9 Hz, 1H, 6-H), 6.91 (dd, *J* = 3.0, 4.9 Hz, 1H, 5-H), 5.31 (bs, 1H, N*H*), 4.09–4.03 (m, 1H, 1-H), 3.84–3.76 (m, 1H, 4-H), 3.21 (s, 1H, 15‘-H), 3.20–3.09 (m, 2H, 2‘-H), 2.57 (t, *J* = 7.7 Hz, 2H, 12‘-H), 2.29 (dt, *J* = 1.3, 6.9 Hz, 1H, 7-H), 2.04 (dt, *J* = 1.3, 6.9 Hz, 1H, 7-H), 1.36–1.05 (m, 16H, 3‘-H, 4‘-H, 5‘-H, 6‘-H, 7‘-H, 8‘-H, 9‘-H, 10‘-H,), 1.73–1.62 (m, 2H, 11‘-H) ppm; ^{13}C NMR (126 MHz, $CDCl_3$): δ = 187.7 (C-13‘), 166.3 (C-1‘), 157.8 (C-3), 144.5 (C-2), 144.0 (C-6), 141.6 (C-5), 136.2 (*i*-C_{Ar}), 128.7 (*o*-C_{Ar}), 128.3 (*p*-C_{Ar}), 127.1 (*m*-C_{Ar}), 81.6 (C-14‘), 78.4 (C-15‘), 71.7 (C-7), 57.9 (C-4), 53.5 (C-1), 45.6 (C-12‘), 39.5

(C-2‘), 29.56, 29.54, 29.46, 29.4, 29.34, 29.29, 29.0, 27.0 (C-3‘, C-4‘, C-5‘, C-6‘, C-7‘, C-8‘ C-9‘, C-10‘), 23.9 (C-11‘) ppm; FTIR (ATR): $\tilde{\nu}$ =3296 (w), 3064 (w), 2925 (s), 2853 (m), 2086 (m), 1679 (s), 1638 (s), 1613 (s), 1557 (m), 1516 (s), 1464 (m), 1444 (m), 1403 (w), 1369 (w), 1329 (w), 1295 (s), 1259 (m), 1156 (w), 1125 (w), 1086 (m), 1032 (w), 910 (w), 875 (w), 810 (w), 760 (s), 715 (s), 695 (vs), 656 (m), 598 (w), 506 (w) cm^{-1}; LRMS (ESI): *m*/*z* = 418.3 $[M + H]^+$, 440.3 $[M + Na]^+$; HRMS (ESI): calcd. for $[C_{28}H_{36}NO_2]^+$ 418.2741, found $[M + H]^+$ 418.2737.

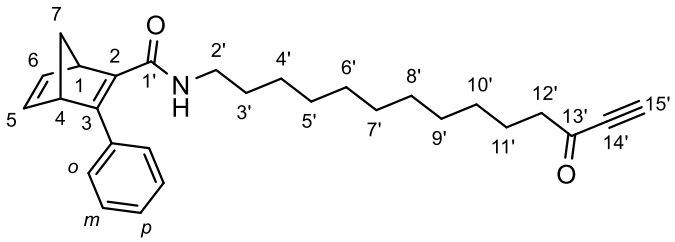

Ph(C$_{10}$CO)

(1*R*,4*S*)-*N*-(12-(1-Benzyl-1*H*-1,2,3-triazol-4-yl)-12-oxododecyl)-3-phenylbicyclo[2.2.1]-hepta-2,5-diene-2-carboxamide (Ph(C$_{10}$CO)click)

Synthesis according to GP 12; colorless oil (48 %); column chromatography on silica (hexanes / EtOAc = 1 : 1); R_f = 0.68 (hexanes / EtOAc = 1 : 1, UV); $[\alpha]_D^{20}$ = –12.4° [c = 10 mg/mL, CH_2Cl_2]; ^{1}H NMR (500 MHz, $CDCl_3$): δ = 7.94 (s, 1H, 15‘-H), 7.42–7.33 (m, 5H, *o*-Ar*H*, *m*‘-Ar*H*, *p*-Ar*H*), 7.33–7.27 (m, 5H, *m*-Ar*H*, *o*‘-Ar*H*, *p*‘-Ar*H*), 6.99 (dd, *J* = 3.0, 4.9 Hz, 1H, 6-H), 6.91 (dd, *J* = 3.0, 4.9 Hz, 1H, 5-H), 5.55 (s, 2H, 16‘-H), 5.35–5.28 (m, 1H, N*H*), 4.08–4.04 (m, 1H, 1-H), 3.81–3.76 (m, 1H, 4-H), 3.22–3.06 (m, 4H, 12‘-H, 2‘-H), 2.28 (dt, *J* = 1.3, 6.9 Hz, 1H, 7-H), 2.03 (dt, *J* = 1.3, 6.9 Hz, 1H, 7-H), 1.76–1.67 (m, 2H, 11‘-H), 1.40–1.14 (m, 14H, 3‘-H, 4‘-H, 5‘-H, 6‘-H, 8‘-H, 9‘-H, 10‘-H), 1.12–1.02 (m, 2H, 7‘-H) ppm; ^{13}C NMR (126 MHz, $CDCl_3$): δ = 195.6 (C-13’), 166.3 (C-1’), 157.8 (C-3), 148.3 (C-14’), 144.5 (C-2), 143.9 (C-6), 141.6 (C-5), 136.1 (*i*-C_{Ar}), 133.7 (*i*’-C_{Ar}), 129.4 (*o*-C_{Ar}), 129.3 (*p*-C_{Ar}), 128.7 (*m*’-C_{Ar}), 128.4 (*o*’-C_{Ar}), 128.3 (*p*’-C_{Ar}), 127.1 (*m*-C_{Ar}), 125.4 (C-15’), 71.7 (C-7), 57.8 (C-4), 54.5 (C-16’), 53.4 (C-1), 39.6 (C-12’), 39.4 (C-2’), 29.57, 29.53, 29.51, 29.46, 29.33, 29.32, 29.2 (C-3’, C-4’, C-5’, C-6’, C-8’, C-9’, C-10’), 27.0 (C-7’), 24.0 (C-11’) ppm; FTIR (ATR): $\tilde{\nu}$ = 3344 (w), 2925 (s), 2853 (m), 1685 (s), 1638 (s), 1614 (m), 1557 (w), 1526 (s), 1456 (m), 1443 (m), 1404 (w), 1371 (w), 1330 (w), 1295 (m), 1241 (m), 1174 (m), 1116 (w), 1077 (w), 1033 (m), 1002 (w), 961 (w), 873 (w), 811 (w), 761 (m), 717 (vs), 696 (s), 657 (w), 600 (w), 521 (w), 473 (w) cm-1; LRMS (ESI): *m*/*z* = 195.1 $[C_{14}H_{11}O]$+, 551.3 [M + H]+, 573.3 [M + Na]+; HRMS (ESI): calcd. for $[C_{35}H_{43}N_4O_2]$ 551.3381, found $[M + H]^+$ 551.3386.

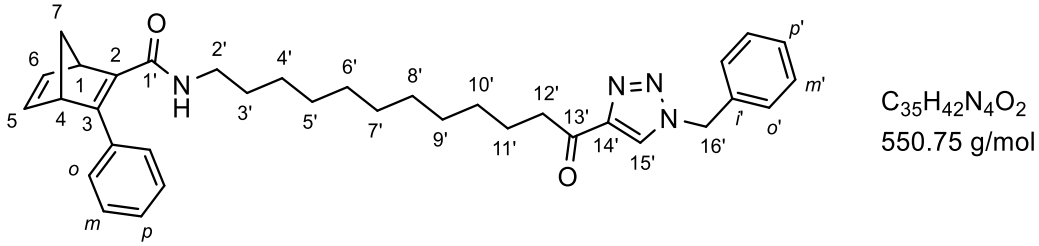

Ph(C$_{10}$CO)click

(1*R*,4*S*)-*N*-((*R*)-3-Methyl-1-(*N*-phenylpropiolamido)butan-2-yl)-3-phenylbicyclo[2.2.1]-hepta-2,5-diene-2-carboxamide (Ph(*i*PrC$_1$amide))

Under a nitrogen atmosphere a solution of the imidazolidinone **12** (30.0 mg, 75.3 mmol) in abs. THF (4 mL) was charged with ethinyl magnesium bromide (0.26 mL, 0.24 g, 0.13 mmol, 0.5 M in THF) at -78 °C. The reaction mixture was slowly heated to room temperature over a time period of 30 min. A saturated aqueous NH_4Cl solution (10 mL) was added, the aqueous phase

was extracted with EtOAc (3 × 20 mL) and the combined organic layers were dried over $MgSO_4$. The crude product was purified by column chromatography on silica (hexanes / EtOAc = 3 : 1 to 2 : 1) and the alkynone **Ph(*i*PrC$_1$amide)** was obtained as a yellow oil (11.0 mg, 25.9 µmol, 35 %).

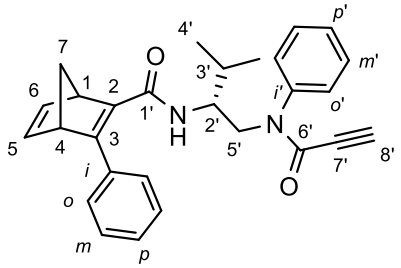

$C_{28}H_{28}N_2O_2$
424.54 g/mol

Ph(*i*PrC$_1$amide)

R_f = 0.37 (hexanes / EtOAc = 3 : 1, UV); $[\alpha]_D^{20}$ = –29.4° [c = 10 mg/mL, CH_2Cl_2]; ^{1}H NMR (500 MHz, $CDCl_3$): δ = 7.40–7.33 (m, 7H, *m*-Ar*H*, *p*'-Ar*H*, *o*'-Ar*H*, *o*-Ar*H*), 7.32–7.27 (m, 1H, *p*-Ar*H*), 7.26–7.18 (m, 2H, *m*'-Ar*H*), 7.07 (dd, *J* = 3.0, 4.9 Hz, 1H, 6-H), 6.92 (dd, *J* = 3.0, 4.9 Hz, 1H, 5-H), 5.74 (d, *J* = 9.6 Hz, 1H, N*H*), 4.24–4.15 (m, 1H, 5'-H), 4.11–4.02 (m, 1H, 2'-H), 4.00–3.95 (m, 1H, 1-H), 3.83–3.78 (m, 1H, 4-H), 3.26 (dd, *J* = 4.2, 13.6 Hz, 1H, 5'-H), 2.77 (s, 1H, 8'-H), 2.28 (dt, *J* = 1.3, 6.9 Hz, 1H, 7-H), 2.04 (dt, *J* = 1.3, 6.9 Hz, 1H, 7-H), 1.71–1.62 (m, 1H, 3'-H), 0.75 (d, *J* = 7.3 Hz, 3H, 4'-H), 0.65 (d, *J* = 7.3 Hz, 3H, 4'-H) ppm; ^{13}C NMR (126 MHz, $CDCl_3$): δ = 166.5 (C-1'), 159.5 (C-6'), 154.2 (C-3), 144.0 (C-2), 143.7 (C-6), 141.5 (C-5), 141.0 (*i*'-C_{Ar}), 136.5 (*i*-C_{Ar}), 129.5 (*o*-C_{Ar}), 128.7 (*p*'-C_{Ar}), 128.6 (*m*'-C_{Ar}), 128.5 (*o*'-C_{Ar}), 128.2 (*p*-C_{Ar}), 127.3 (*m*-C_{Ar}), 80.4 (C-7'), 76.1 (C-8'), 70.9 (C-7), 58.2 (C-4), 53.4 (C-1), 52.7 (C-2'), 50.0 (C-5'), 30.7 (C-3'), 19.1 (C-4'), 17.4 (C-4') ppm; FTIR (ATR): $\tilde{\nu}$ = 3412 (w), 3207 (w), 3063 (w), 2963 (w), 2936 (w), 2871 (w), 2102 (w), 1633 (vs), 1594 (m), 1557 (w), 1494 (s), 1433 (w), 1399 (m), 1369 (m), 1296 (s), 1281 (m), 1251 (w), 1226 (w), 1183 (w), 1157 (w), 1130 (w), 1075 (w), 1024 (w), 913 (w), 875 (w), 808 (w), 760 (m), 734 (m), 718 (m), 697 (s), 655 (w), 606 (w), 511 (w) cm^{-1}; LRMS (ESI): *m*/*z* = 195.1 $[C_{14}H_{11}O]^+$, 425.2 $[M + H]^+$, 447.2 $[M + Na]^+$; HRMS (ESI): calcd. for $[C_{29}H_{28}N_2O_2]^+$ 425.2224, found $[M + H]^+$ 425.2220.

1-Benzyl-*N*-((*R*)-3-methyl-2-((1*R*,4*S*)-3-phenylbicyclo[2.2.1]hepta-2,5-diene-2-carboxamido)butyl)-*N*-phenyl-1*H*-1,2,3-triazol-4-carboxamide (Ph(*i*PrC$_1$amide)click)

Synthesis according to GP 12; colorless oil (86 %), column chromatography on silica (hexanes / EtOAc = 1 : 1) followed by preparative HPLC on a Orbit 100 Sil column (250 × 20 mm, 5 µm, hexanes / *i*PrOH 90 : 10, flow rate: 19 mL/min, λ = 245 nm, R_t = 14.12 min); R_f = 0.47 (hexanes / EtOAc = 1 : 1, UV); $[\alpha]_D^{20}$ = –25.4° [c = 10 mg/mL, CH_2Cl_2]; ^{1}H NMR (700 MHz, $CDCl_3$): δ = 7.39–7.28 (m, 8H, *o*''-Ar*H*, *o*'-Ar*H*, *m*-Ar*H*, *p*-Ar*H*, *p*'-Ar*H*), 7.25–7.17 (m, 4H, *m*''-Ar*H*, *m*'-Ar*H*), 7.09–6.95 (m, 4H, 6-H, *o*'-Ar*H*, *p*''-Ar*H*), 6.80–6.76 (m, 1H, 5-H), 6.52 (s, 1H, 8'-H), 6.04 (d, *J* = 9.6 Hz, 1H, N*H*), 5.28 (s, 2H, 9'-H), 4.47–4.39 (m, 1H, 5'-H), 4.16–4.08 (m, 1H, 2'-H), 3.86–3.79 (m, 1H, 1-H), 3.76–3.70 (m, 1H, 4-H), 3.35–3.27 (m, 1H, 5'-H), 2.15 (dt, *J* = 1.3, 6.9 Hz, 1H, 7-H), 1.94 (dt, *J* = 1.3, 6.9 Hz, 1H, 7-H), 1.70–1.79 (m, 2H, 3'-H), 0.80 (d, *J* = 7.3 Hz, 3H, 4'-H), 0.73 (d, *J* = 7.3 Hz, 3H, 4'-H) ppm; ^{13}C NMR (176 MHz, $CDCl_3$): δ = 166.7 (C-1'), 162.1 (C-6'), 159.3 (C-3), 143.9 (C-2), 143.5 (C-6), 142.5 (C-7'), 142.1 (*i*'-C_{Ar}), 141.3 (C-5), 136.4 (*i*-C_{Ar}), 133.9 (*i*''-C_{Ar}), 129.63, 129.62 (*m*''-C_{Ar}, *o*-C_{Ar}), 129.22 (*o*''-C_{Ar}), 129.0 (*m*'-C_{Ar}), 128.6 (*p*'-C_{Ar}), 128.4 (*o*'-C_{Ar}), 128.2 (*p*''-C_{Ar}), 128.1 (*p*-C_{Ar}), 127.4 (*m*-C_{Ar}), 125.6 (C-8'), 70.7 (C-7), 57.9 (C-4), 54.0 (C-9'), 53.5 (C-1), 53.0 (C-2'), 50.9 (C-5'), 30.9 (C-3'), 19.1 (C-4'), 17.7 (C-4') ppm; FTIR (ATR): $\tilde{\nu}$ = 2963 (w), 1639 (m), 1594 (m), 1510 (m), 1494 (m), 1455 (w), 1433 (w), 1407 (m), 1369 (w), 1294 (w), 1258 (m), 1223 (m), 1157 (w), 1130 (w), 1075 (w), 1048 (m), 1000 (w), 908 (m), 837 (w), 824 (w),

808 (w), 759 (m), 719 (vs), 694 (s), 645 (m), 599 (w), 578 (w), 545 (w), 528 (w), 508 (w), 470 (w) cm^{-1}; LRMS (ESI): *m*/*z* = 558.3 $[M + H]^+$, 580.3 $[M + Na]^+$; HRMS (ESI): calcd. for $[C_{35}H_{36}N_5O_2]^+$ 558.2864, found $[M + H]^+$ 558.2862.

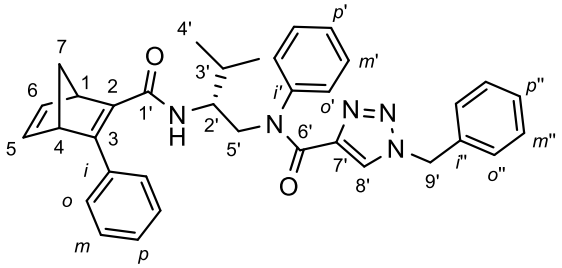

$C_{35}H_{35}N_5O_2$
557.70 g/mol

Ph(*i*PrC$_1$amide)click

1-((1-Benzyl-1*H*-1,2,3-triazol-4-yl)methyl)-3-((1*R*,4*S*)-3-phenylbicyclo[2.2.1]hepta-2,5-diene-2-carbonyl)imidazolidin-2-one (Ph(ImC$_1$)click)

Synthesis according to GP 12; colorless oil (80 %); column chromatography on silica (hexanes / EtOAc = 1 : 3); R_f = 0.31 (hexanes / EtOAc = 1 : 1, UV); $[\alpha]_D^{20}$ = –46.2° [c = 10 mg/mL, CH_2Cl_2]; ^{1}H NMR (700 MHz, $CDCl_3$): *δ* = 7.40–7.34 (m, 3H, *p*-Ar*H*, *m*-Ar*H*), 7.28–7.20 (m, 7H, *o*'-Ar*H*, *m*'-Ar*H*, *o*-Ar*H*, 3''-H), 7.18–7.13 (m, 1H, *p*'-Ar*H*), 6.95 (dd, *J* = 3.0, 4.9 Hz, 1H, 5-H), 6.92 (dd, *J* = 3.0, 4.9 Hz, 1H, 6-H), 5.48 (d, *J* = 6.3 Hz, 2H, 4''-H), 4.40 (d, *J* = 2.6 Hz, 2H, 1''-H), 3.93–3.89 (m, 1H, 1-H), 3.86–3.77 (m, 3H, 3'-H, 4-H), 3.48–3.41 (m, 2H, 2'-H), 2.59 (dt, *J* = 1.4, 9.8 Hz, 1H, 7-H), 2.09 (dt, *J* = 1.4, 9.8 Hz, 1H, 7-H) ppm; ^{13}C NMR (176 MHz, $CDCl_3$): *δ* = 168.5 (C-4'), 157.3 (C-3), 153.7 (C-1'), 143.5 (C-2), 143.3 (C-4), 142.4 (C-2''), 141.5 (C-6), 135.8 (*i*-C_{Ar}), 134.4 (*i*'-C_{Ar}), 129.3 (*o*-C_{Ar}), 129.0 (*p*'-C_{Ar}), 128.24 (*o*'-C_{Ar}), 128.19 (*m*'-C_{Ar}), 127.7 (*p*-C_{Ar}), 126.5 (*m*-C_{Ar}), 122.4 (C-3''), 71.3 (C-7), 55.7 (C-4), 55.5 (C-1), 54.3 (C-4''), 41.4 (C-2'), 40.1 (C-3'), 38.8 (C-1'') ppm; FTIR (ATR): $\tilde{\nu}$ = 3135 (w), 3064 (w), 2985 (w), 2937 (w), 2245 (w), 1727 (s), 1646 (m), 1557 (w), 1493 (m), 1480 (m), 1439 (m), 1355 (s), 1298 (m), 1251 (vs), 1156 (w), 1120 (w), 1078 (w), 1050 (m), 1028 (w), 988 (w), 948 (w), 911 (m), 876 (w), 846 (w), 798 (w), 763 (w), 723 (vs), 711 (s), 696 (w), 647 (m), 620 (w), 608 (w), 572 (w), 548 (w), 498 (w), 466 (w) cm^{-1}; LRMS (ESI): *m*/*z* = 452.2 $[M + H]^+$, 474.2 $[M + Na]^+$; HRMS (ESI): calcd. for $[C_{27}H_{26}N_5O_2]^+$ 452.2081, found $[M + H]^+$ 452.2081.

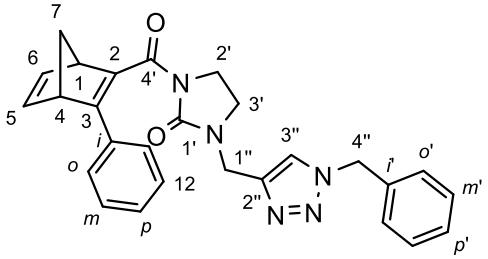

$C_{27}H_{25}N_5O_2$
451.52 g/mol

Ph(ImC$_1$)click

1.5 Rh-catalyzed 1,2-additions

General procedure for the Rh-catalyzed 1,2-additions with soluble catalysts (17) [GP 13]

According to ref.,[19] under a nitrogen atmosphere the diene ligand (10.0 µmol) and $[Rh(C_2H_4)_2Cl]_2$ (1.94 mg, 5.00 µmol) were dissolved in degassed dioxane (1.6 mL) and the reaction mixture was stirred for 15 min at room temperature. Degassed 3.1 M KOH (12.9 µL, 40 µmol) was added and the reaction mixture was stirred for 5 min at room temperature. The solution was heated to 60 °C and triphenylboroxine **16** (74.8 mg, 0.24 mmol) and the

N-tosyl imine **15** (58.8 mg, 0.20 mmol) were added. The reaction mixture was stirred for 24 h at 60 °C, filtered over a pad of silica and flushed with EtOAc (10 mL). The solvent was removed under reduced pressure, the NMR yield was determined using mesitylene as the internal standard and the crude product was purified by column chromatography on silica (hexanes / EtOAc = 10 : 1).

General procedure for Rh-catalyzed 1,2-additions with immobilized dienes (17) [GP 14]
According to ref.,[16] under a nitrogen atmosphere to a suspension of the respective immobilized diene (10.0 µmol diene) in degassed dioxane (1.6 mL) was added $[Rh(C_2H_4)_2Cl]_2$ (1.94 mg, 5.00 µmol). The reaction mixture was stirred for 30 min at room temperature, 3.1 M KOH (12.9 µL, 40.0 µmol) was added and the suspension was stirred for another 20 min at room temperature. The reaction mixture was heated to 60 °C, triphenylboroxine **16** (74.8 mg, 0.24 mmol) and *N*-tosyl imine **15** (58.8 mg, 0.20 mmol) were added and the reaction mixture was stirred for 24 h at 60 °C. EtOAc (2 mL) was added and the reaction mixture was filtered over a pad of silica. The solvent was removed under reduced pressure, the NMR yield was determined using mesitylene as the internal standard and the crude product was purified by column chromatography on silica (hexanes / EtOAc = 10 : 1).

***N*-((4-Chlorophenyl)(phenyl)methyl)-4-methylbenzenesulfonamide (17)**
Synthesis according to GP 14; colorless solid (53 %, 98 %*ee* (*S*) according to chiral HPLC); column chromatography on silica (hexanes/EtOAc 10 : 1); R_f = 0.55 (hexanes/EtOAc 5 : 1, UV); m.p.: 115 °C; ^{1}H NMR (300 MHz, $CDCl_3$): δ = 2.39 (s, 3H, C*H*$_3$), 5.30 (d, *J* = 7.2 Hz, 1H, N*H*), 5.54 (d, *J* = 7.2 Hz, 1H, C*H*), 7.02–7.11 (m, 4H, *m*-Ar*H*, *m*''-Ar*H*), 7.12–7.25 (m, 7H, *o*-Ar*H*, *m*'-Ar*H*, *o*''-Ar*H*, *p*''-Ar*H*), 7.51–7.59 (m, 2H, *o*'-Ar*H*) ppm; ^{13}C NMR (75 MHz, $CDCl_3$): δ = 21.6 (*C*H$_3$), 60.9 (*C*H), 127.3 (*o*'-C$_{Ar}$), 127.4 (*m*''-C$_{Ar}$), 128.0 (*p*''-C$_{Ar}$), 128.7 (*o*''-C$_{Ar}$), 128.8 (*m*'-C$_{Ar}$), 128.9 (*m*'-C$_{Ar}$), 129.5 (*m*-C$_{Ar}$), 133.6 (*i*-C$_{Ar}$), 137.3 (*i*'-C$_{Ar}$), 139.1 (*p*'-C$_{Ar}$), 140.2 (*i*''-C$_{Ar}$), 143.6 (*p*-C$_{Ar}$) ppm. The spectroscopic data were in accordance with the literature.[19] Analytical HPLC: Daicel Chiralcel® OD-H (250 × 4.6 mm, 5 µm), heptane/isopropanol 93 : 7, flow rate: 1.0 mL/min, λ = 235 nm, R_t ((*S*)-**17**) = 15.78 min, R_t ((*R*)-**17**) = 20.01 min.

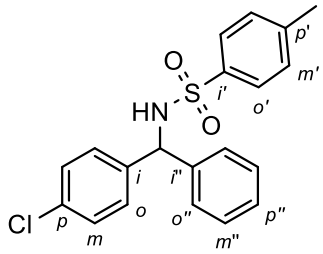

17

$C_{20}H_{18}ClNO_2S$
371.88 g/mol

2 NMR spectra

2.1 Synthesis of the naphthyl-substituted norbornadienes

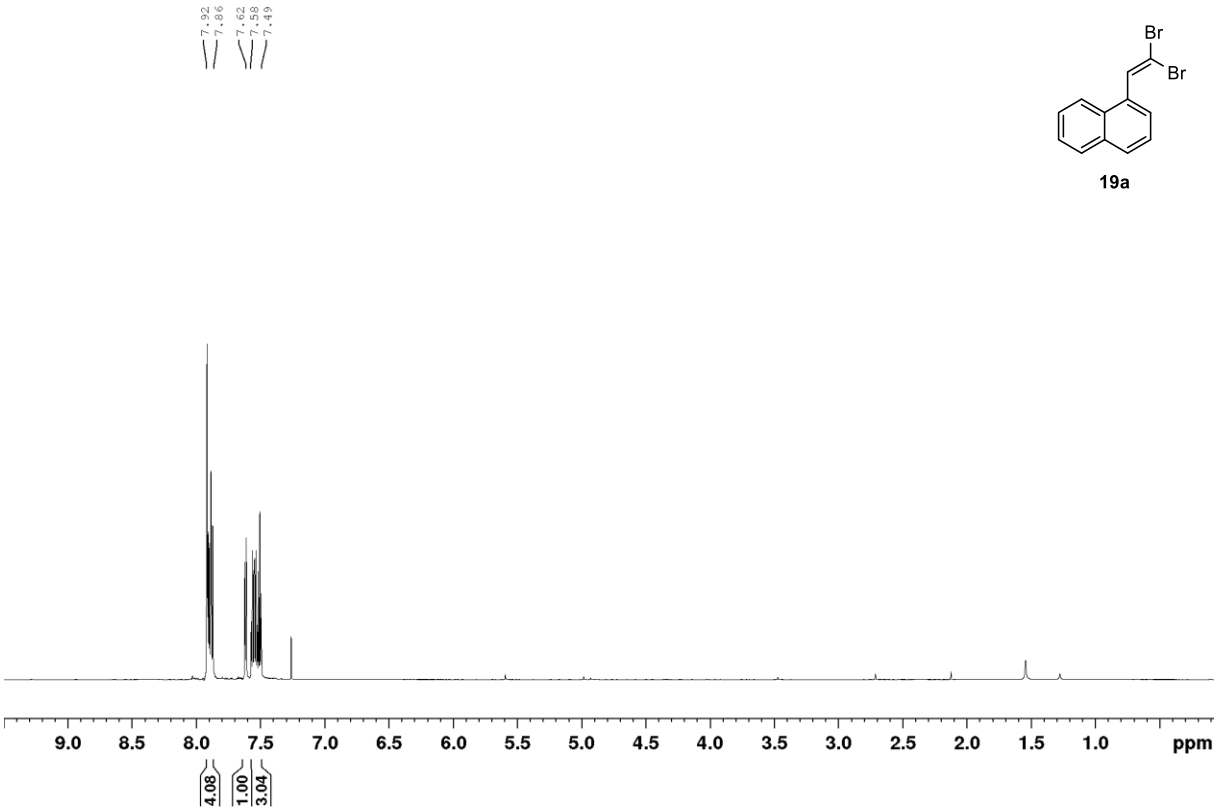

Figure S2. ^{1}H NMR spectrum (700 MHz, $CDCl_3$) of dibromo alkene **19a**.

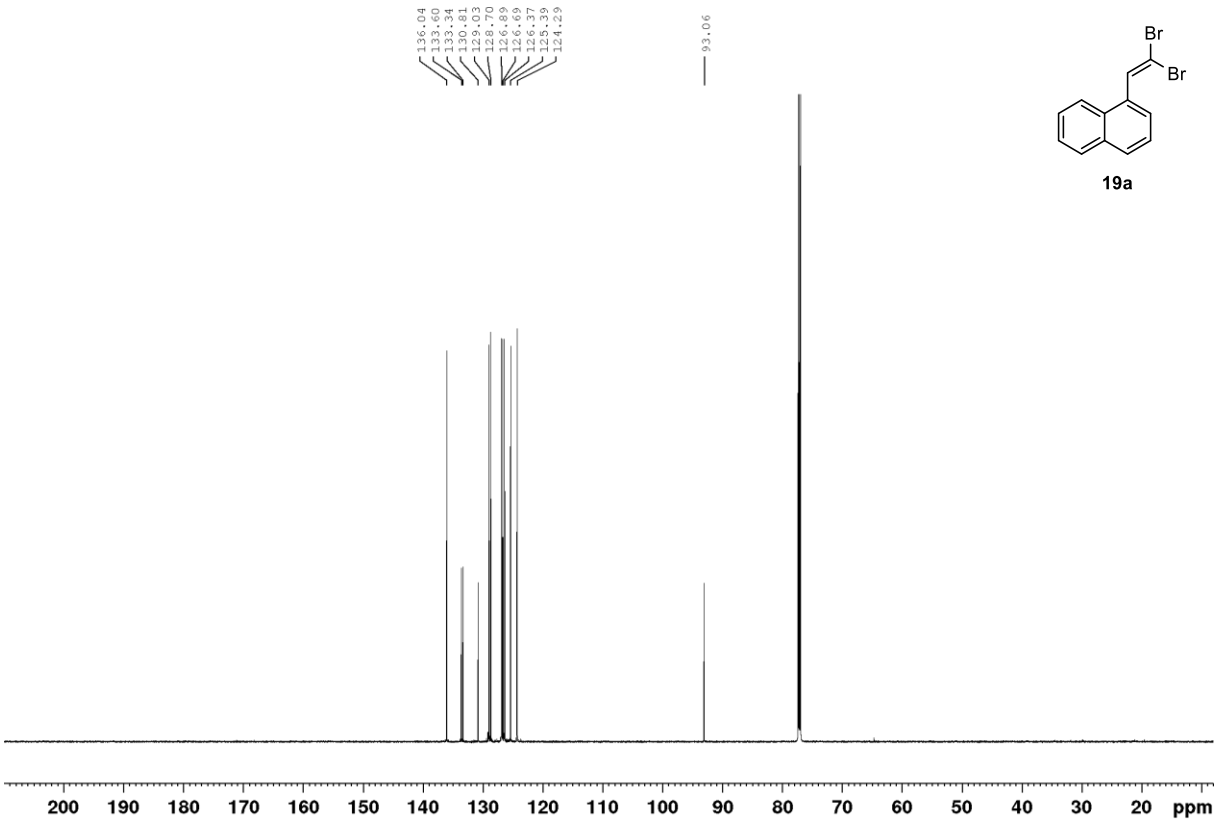

Figure S3. ^{13}C NMR spectrum (176 MHz, $CDCl_3$) of dibromo alkene **19a**.

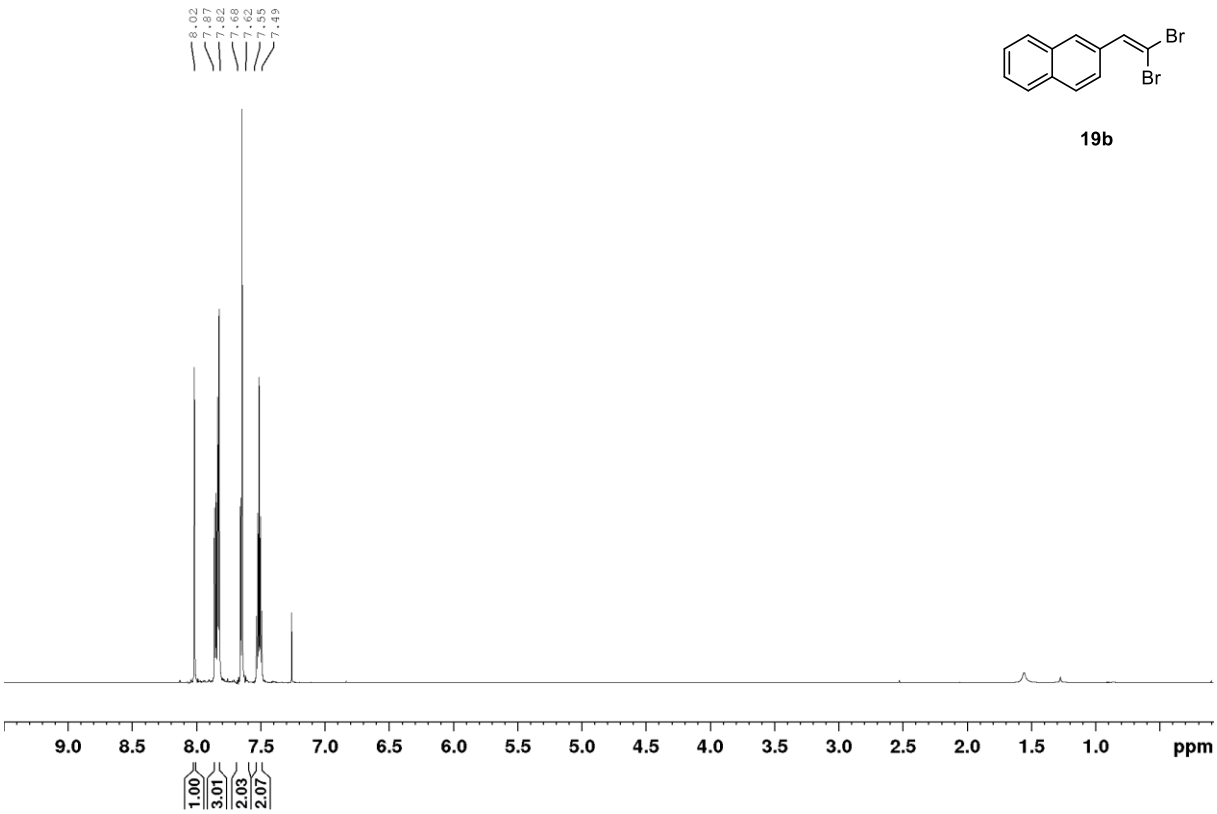

Figure S4. ^{1}H NMR spectrum (700 MHz, $CDCl_3$) of dibromo alkene **19b**.

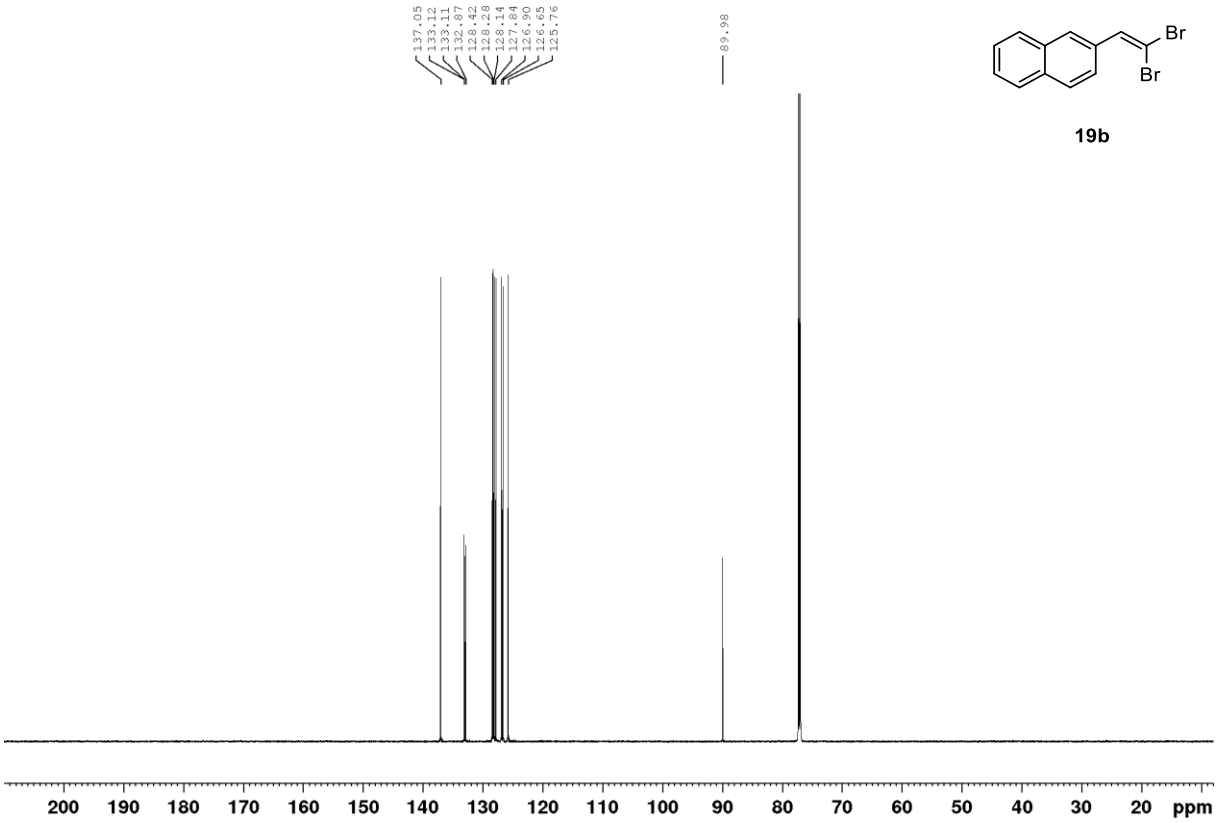

Figure S5. ^{13}C NMR spectrum (176 MHz, $CDCl_3$) of dibromo alkene **19b**.

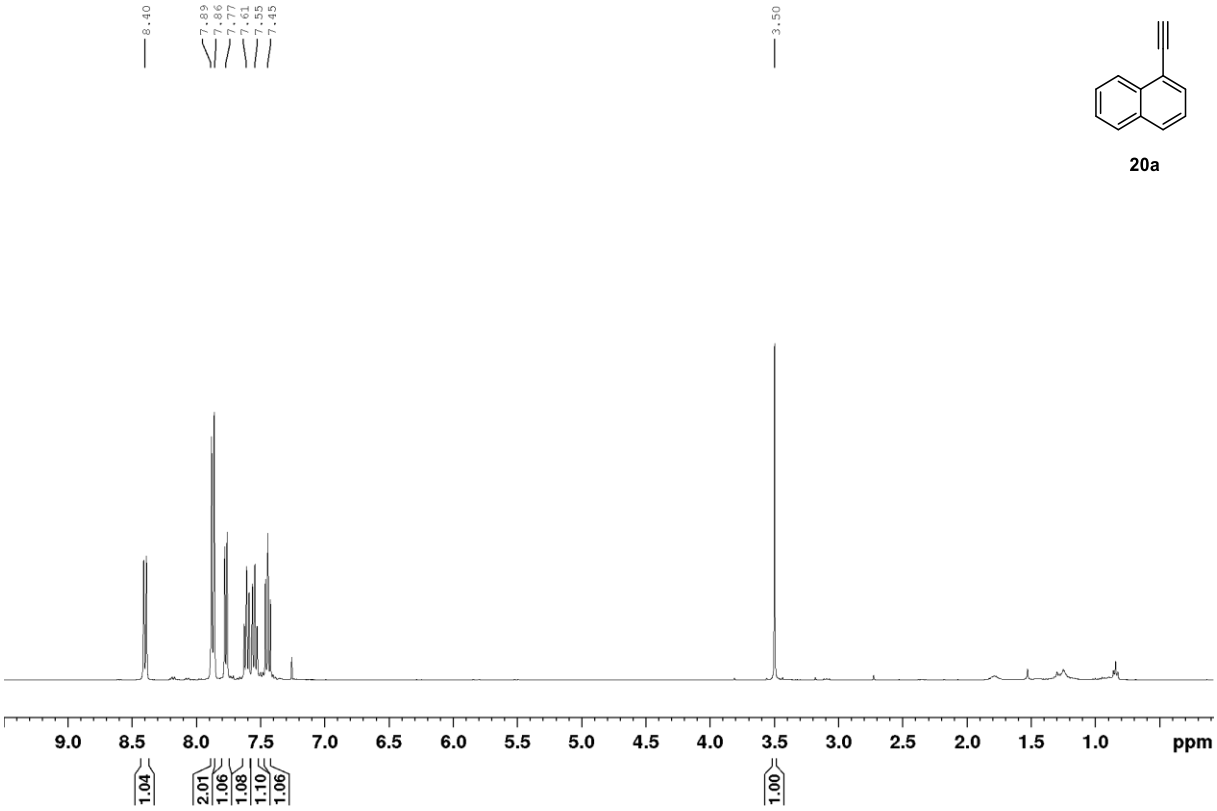

Figure S6. ^{1}H NMR spectrum (400 MHz, $CDCl_3$) of alkyne **20a**.

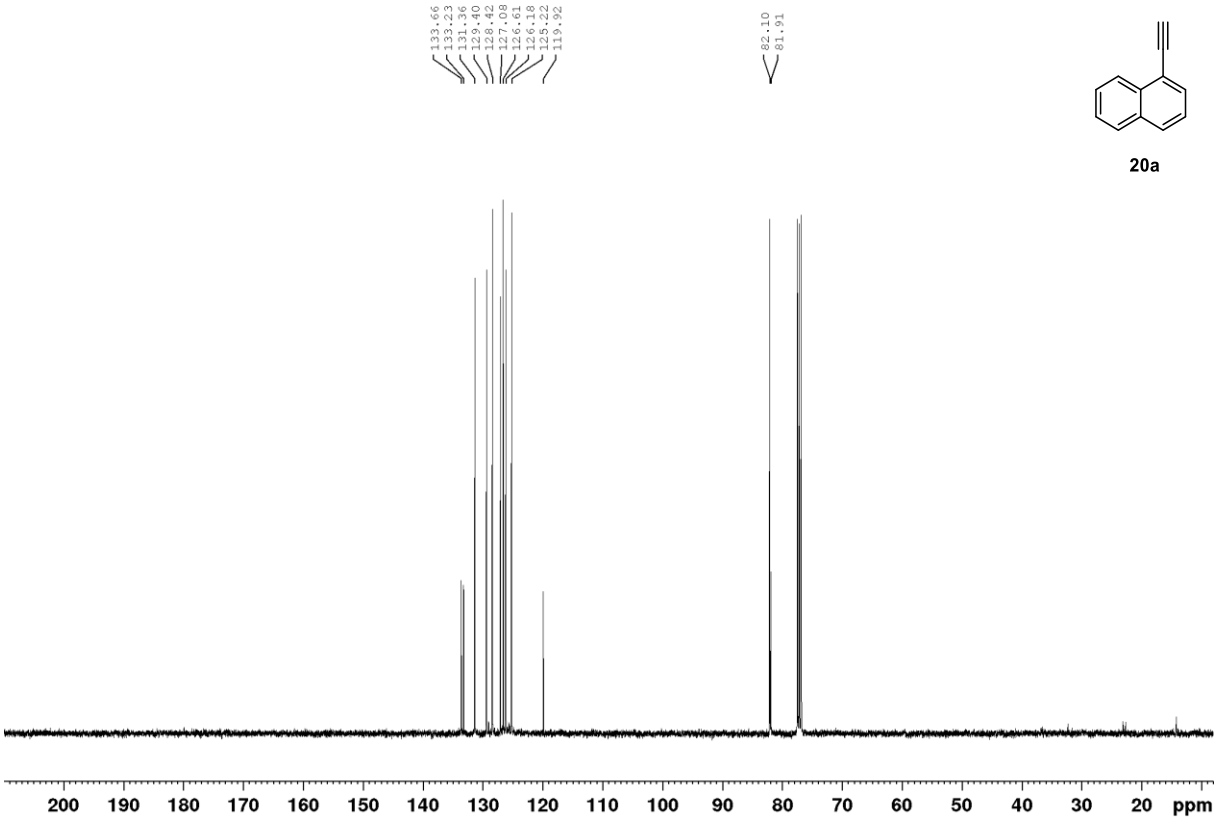

Figure S7. ^{13}C NMR spectrum (101 MHz, $CDCl_3$) of alkyne **20a**.

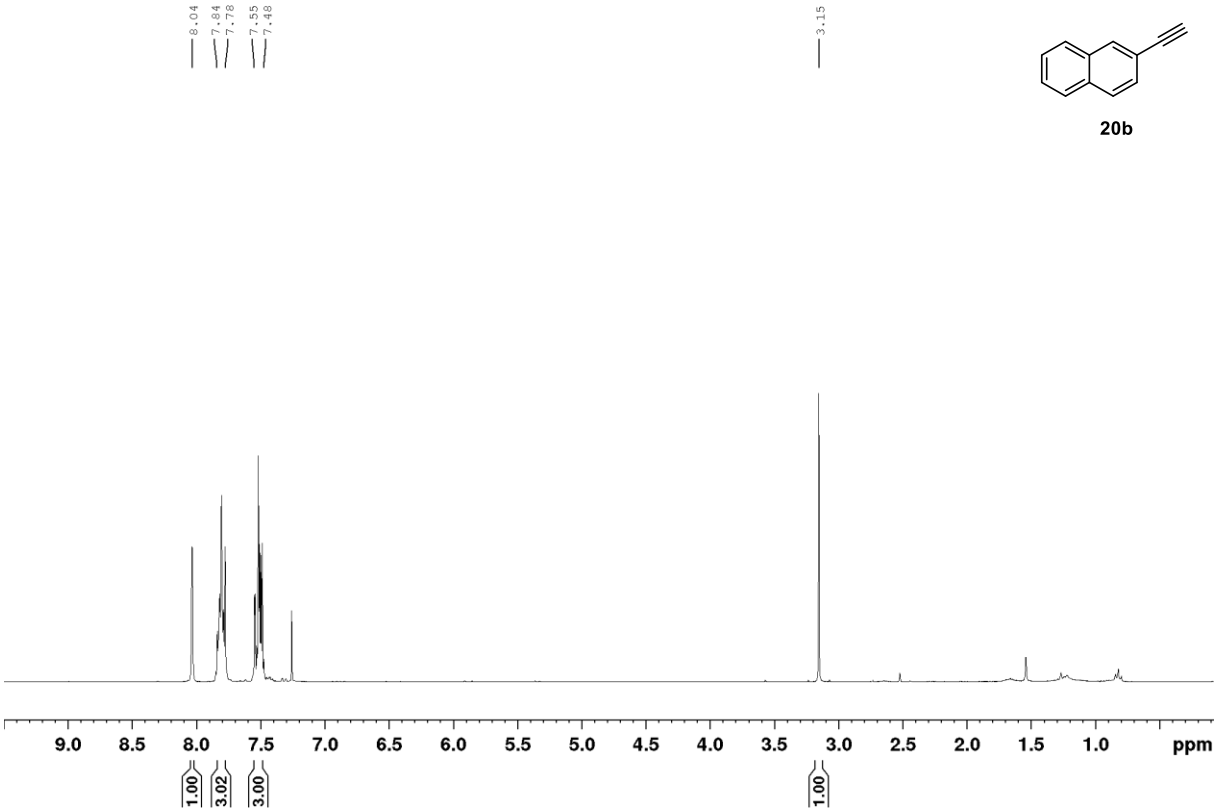

Figure S8. ^{1}H NMR spectrum (300 MHz, $CDCl_3$) of alkyne **20b**.

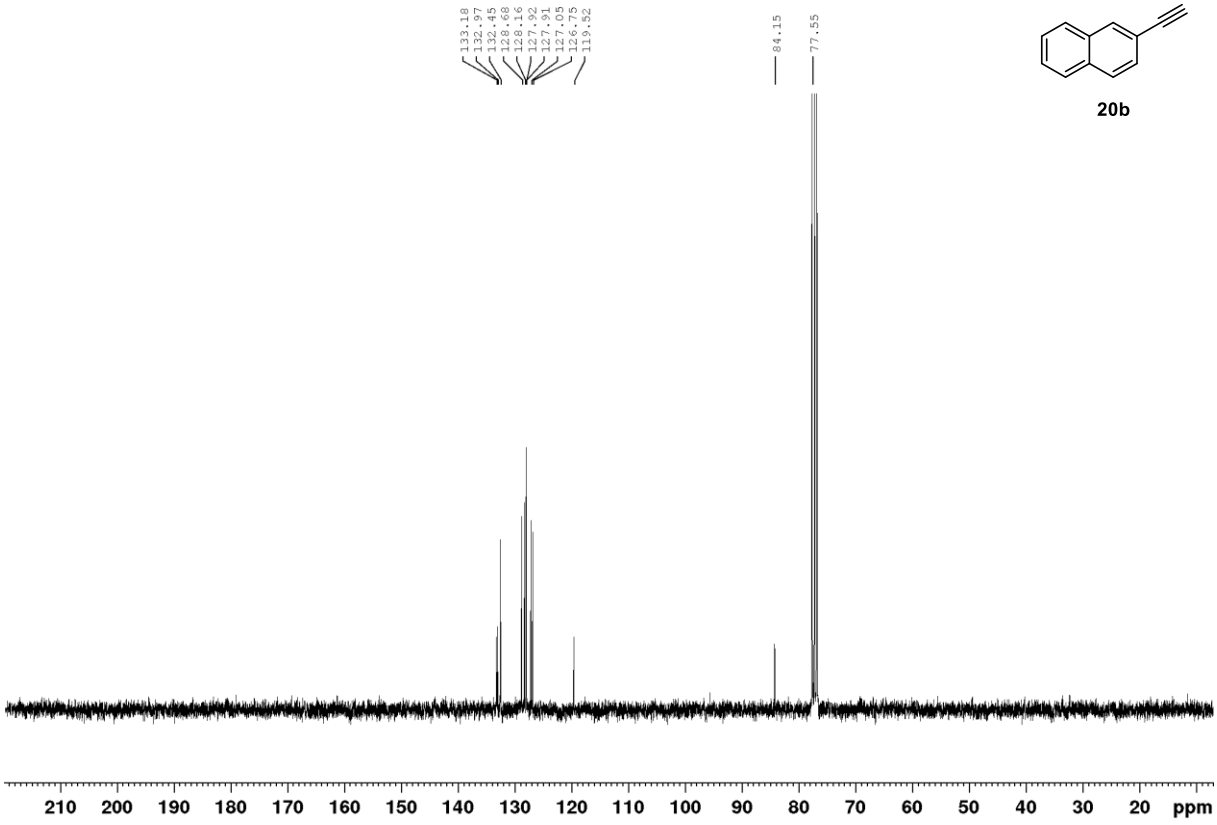

Figure S9. ^{13}C NMR spectrum (75 MHz, $CDCl_3$) of alkyne **20b**.

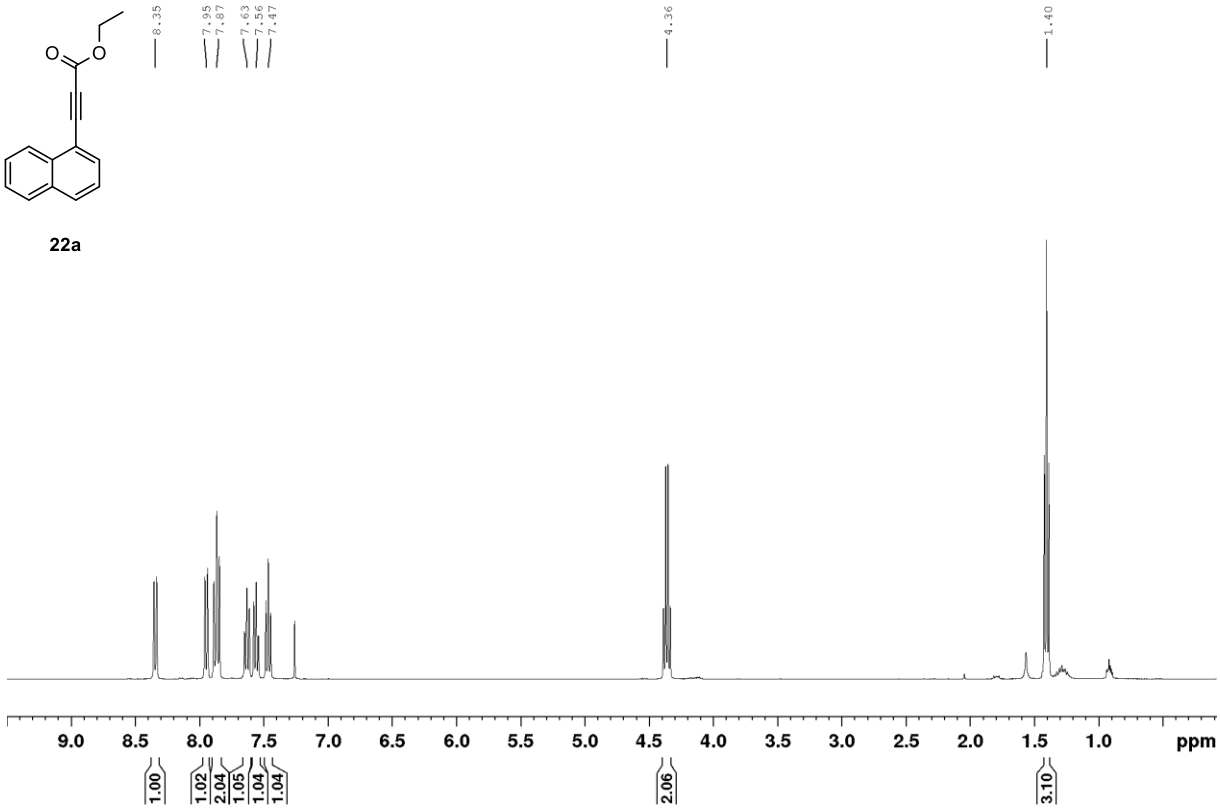

Figure S10. ^{1}H NMR spectrum (400 MHz, $CDCl_3$) of ester **22a**.

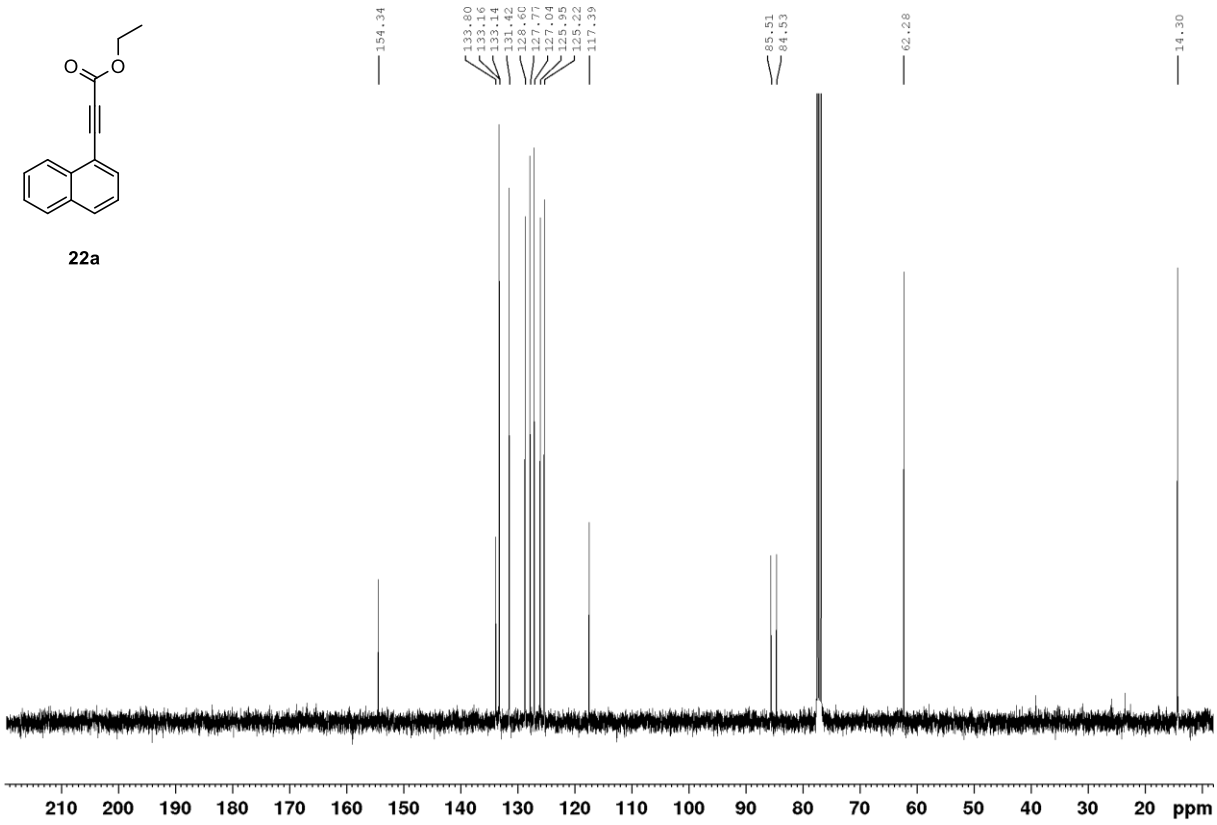

Figure S11. ^{13}C NMR spectrum (101 MHz, $CDCl_3$) of ester **22a**.

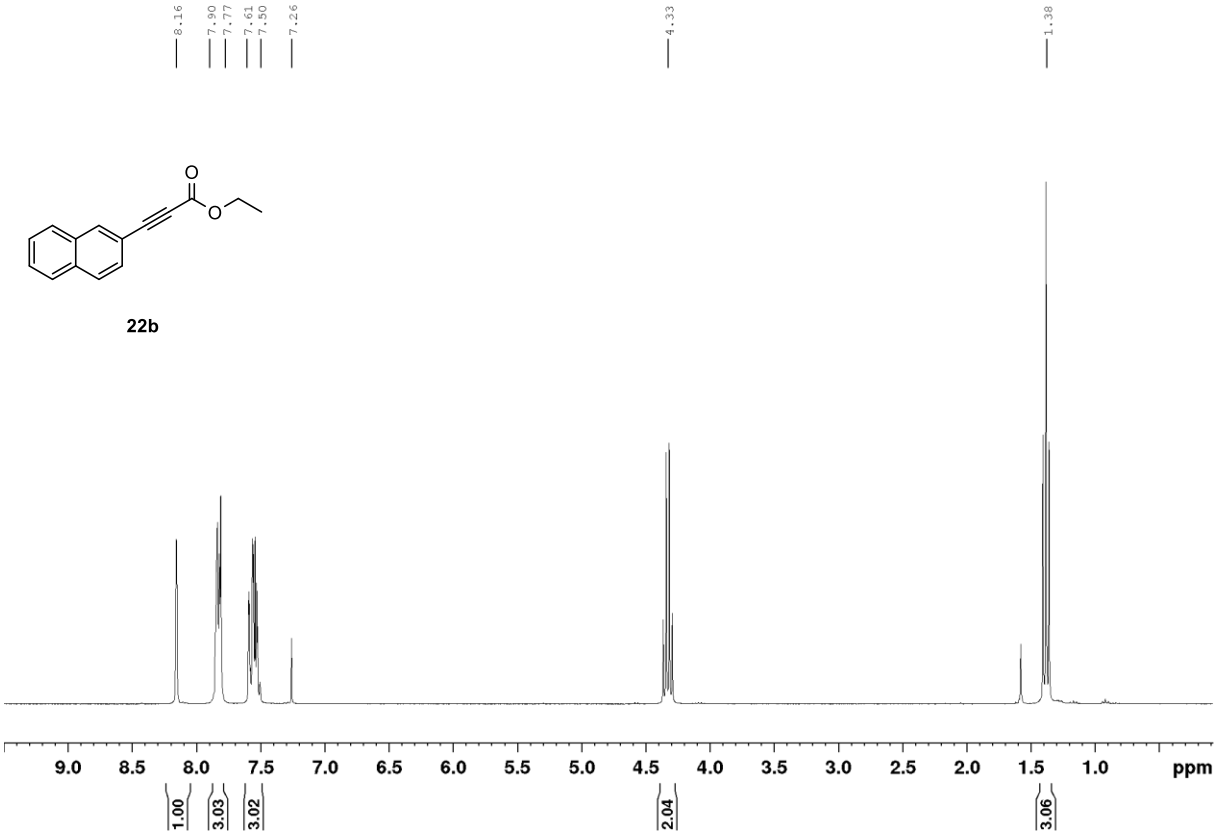

Figure S12. ^{1}H NMR spectrum (300 MHz, $CDCl_3$) of ester **22b**.

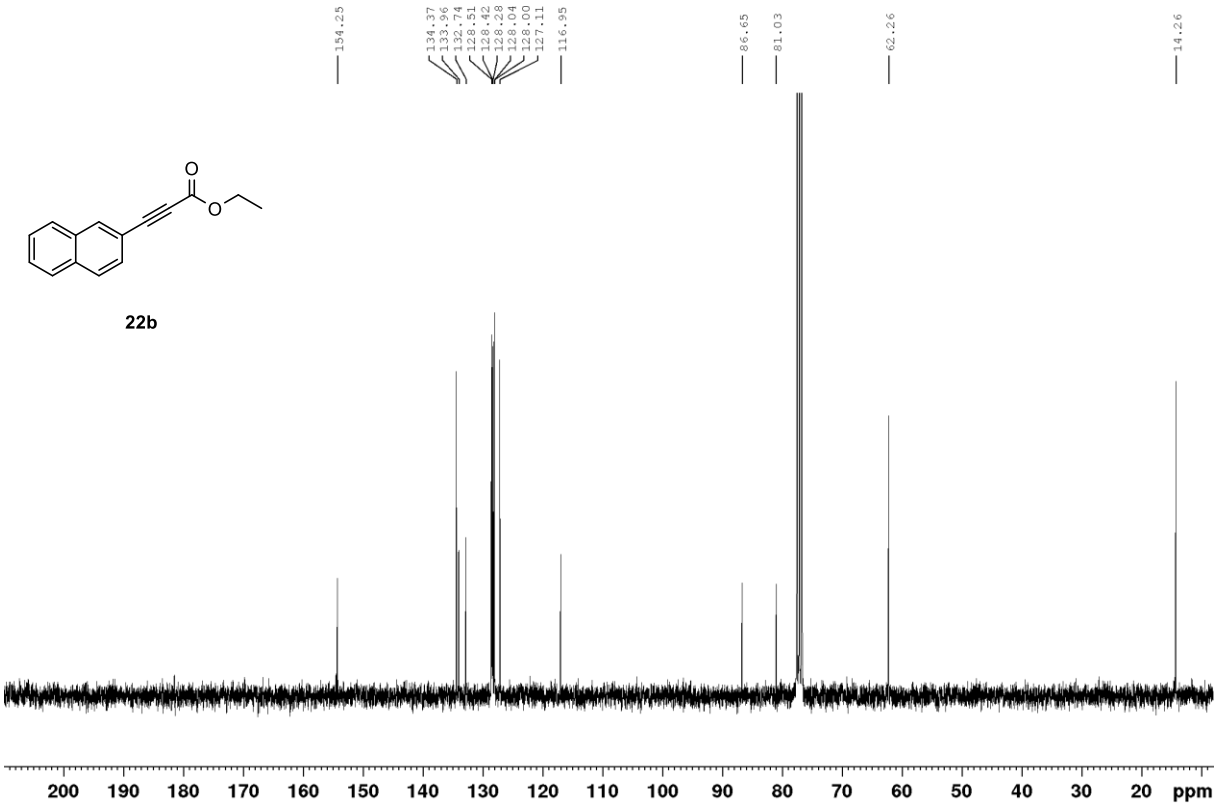

Figure S13. ^{13}C NMR spectrum (75 MHz, $CDCl_3$) of ester **22b**.

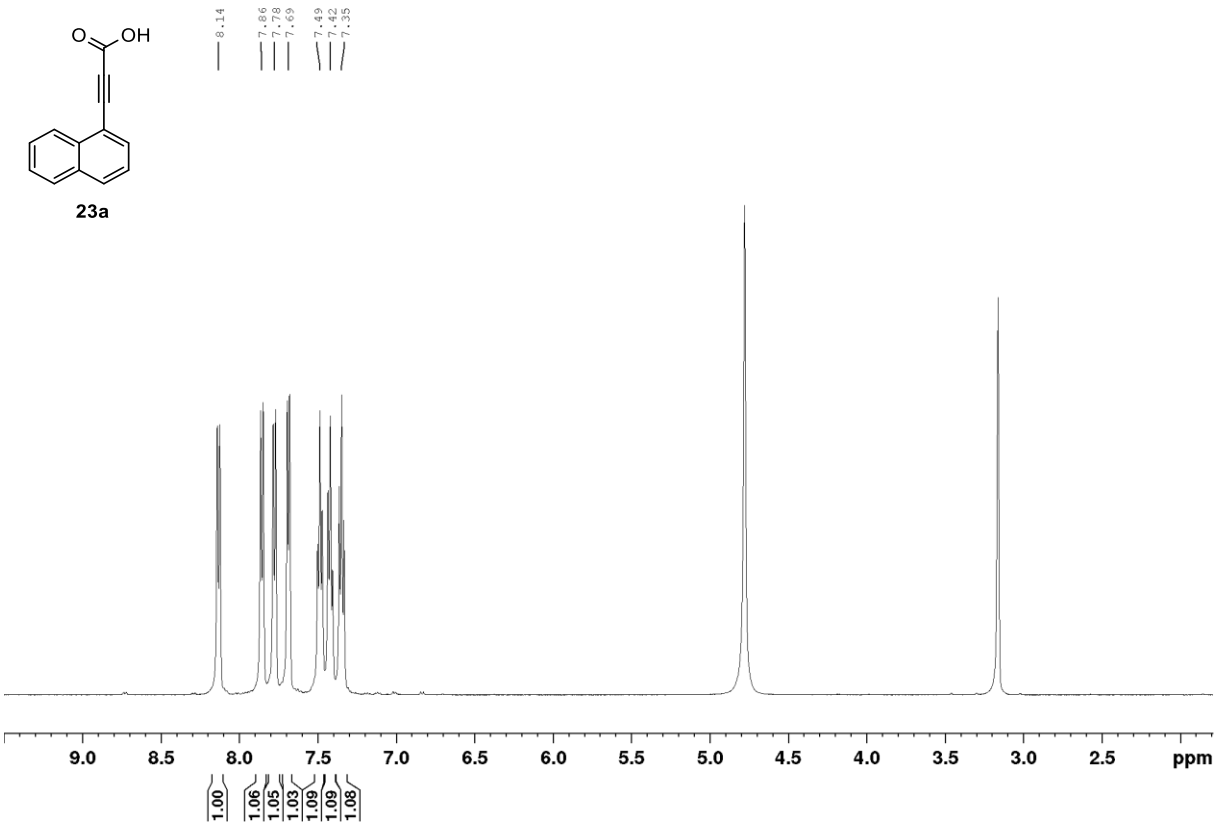

Figure S14. ^{1}H NMR spectrum (500 MHz, CD_3OD) of alkynoic acid **23a**.

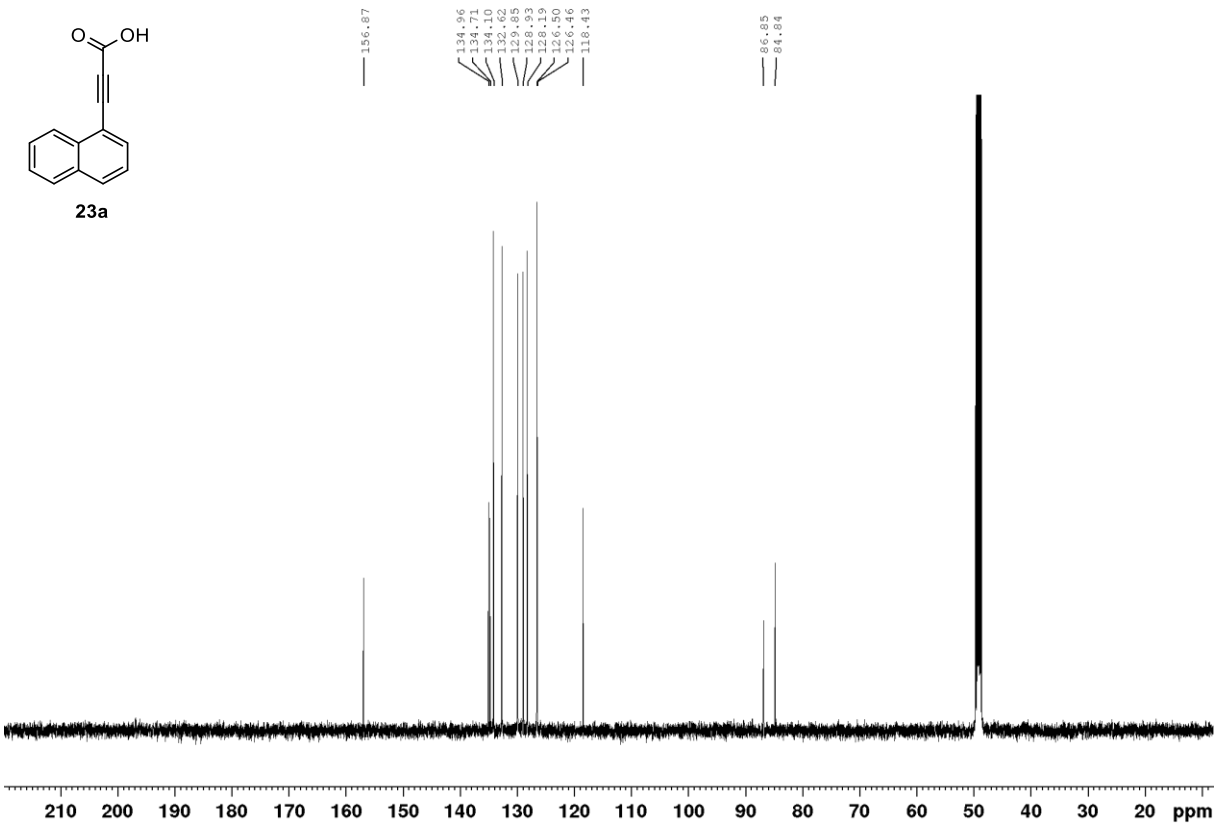

Figure S15. ^{13}C NMR spectrum (126 MHz, CD_3OD) of alkynoic acid **23a**.

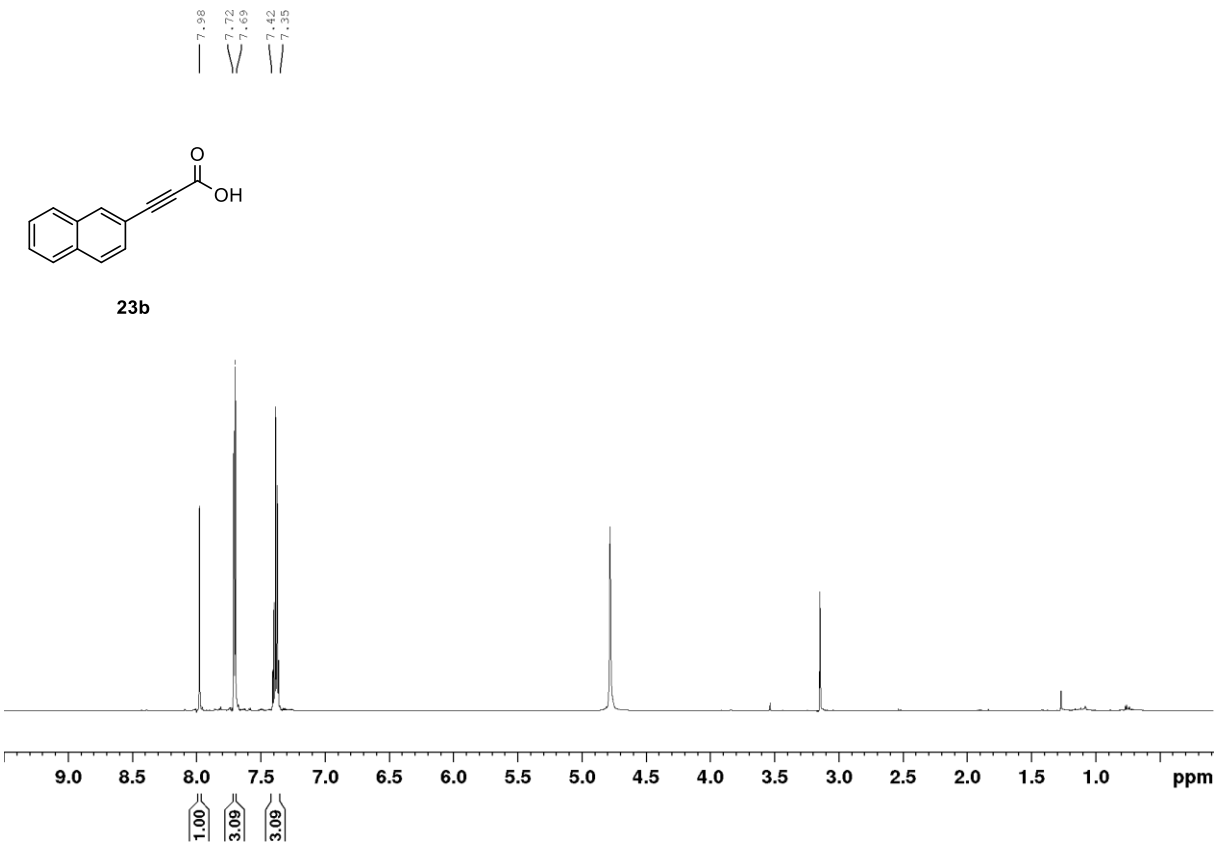

Figure S16. ^{1}H NMR spectrum (700 MHz, CD_3OD) of alkynoic acid **23b**.

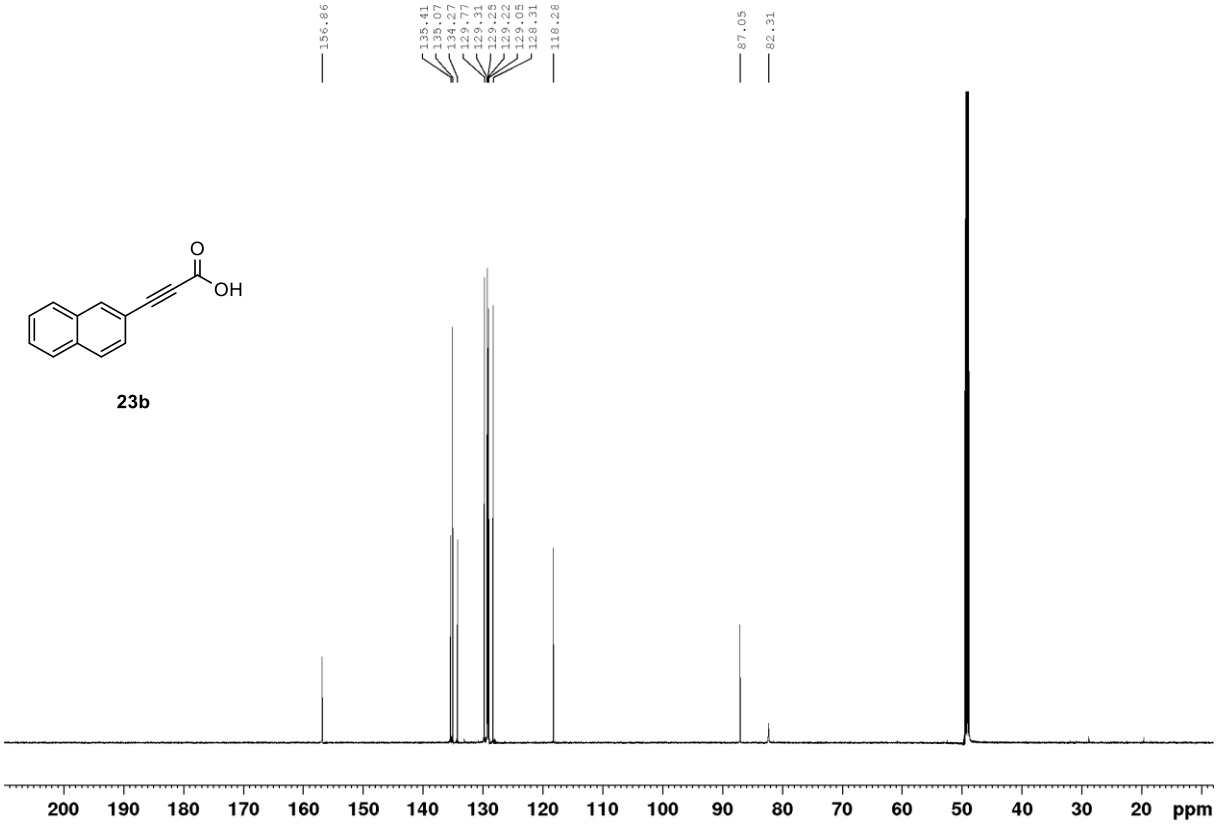

Figure S17. ^{13}C NMR spectrum (176 MHz, CD_3OD) of alkynoic acid **23b**.

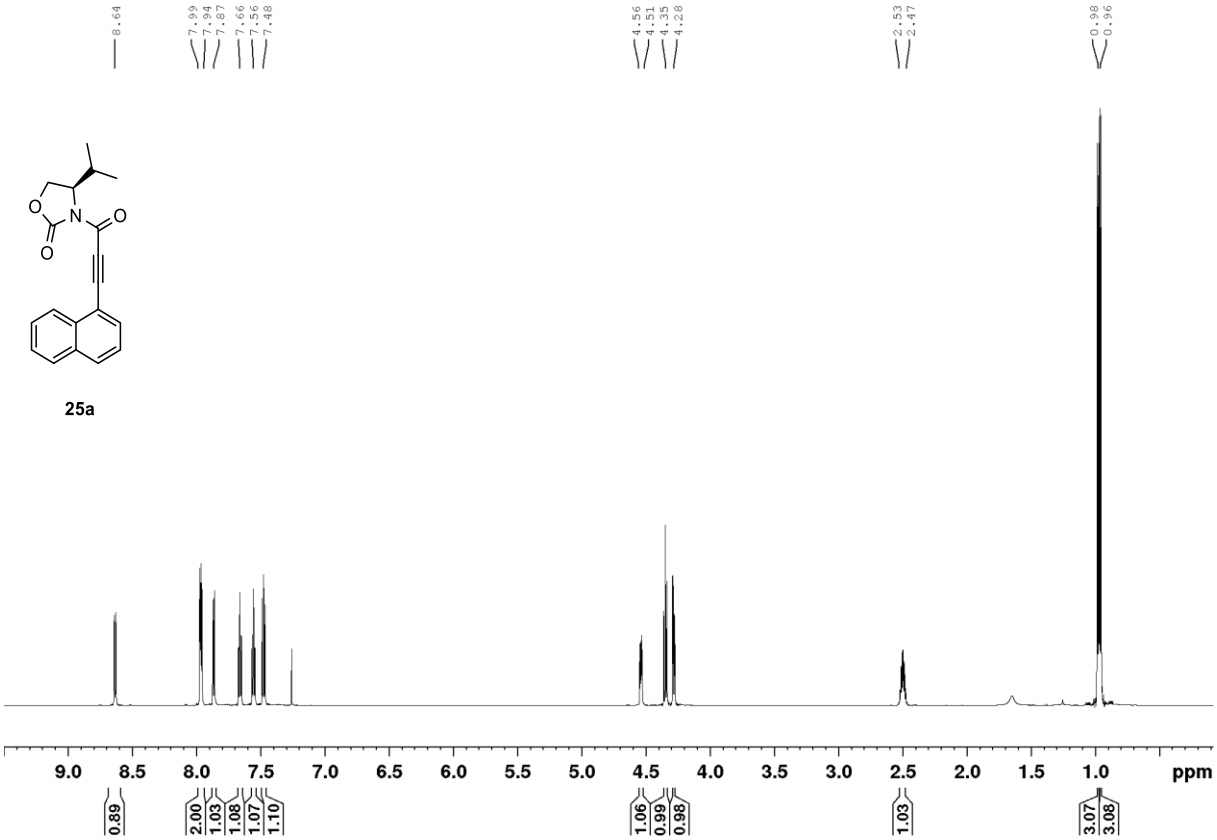

Figure S18. ^{1}H NMR spectrum (700 MHz, $CDCl_3$) of imide **25a**.

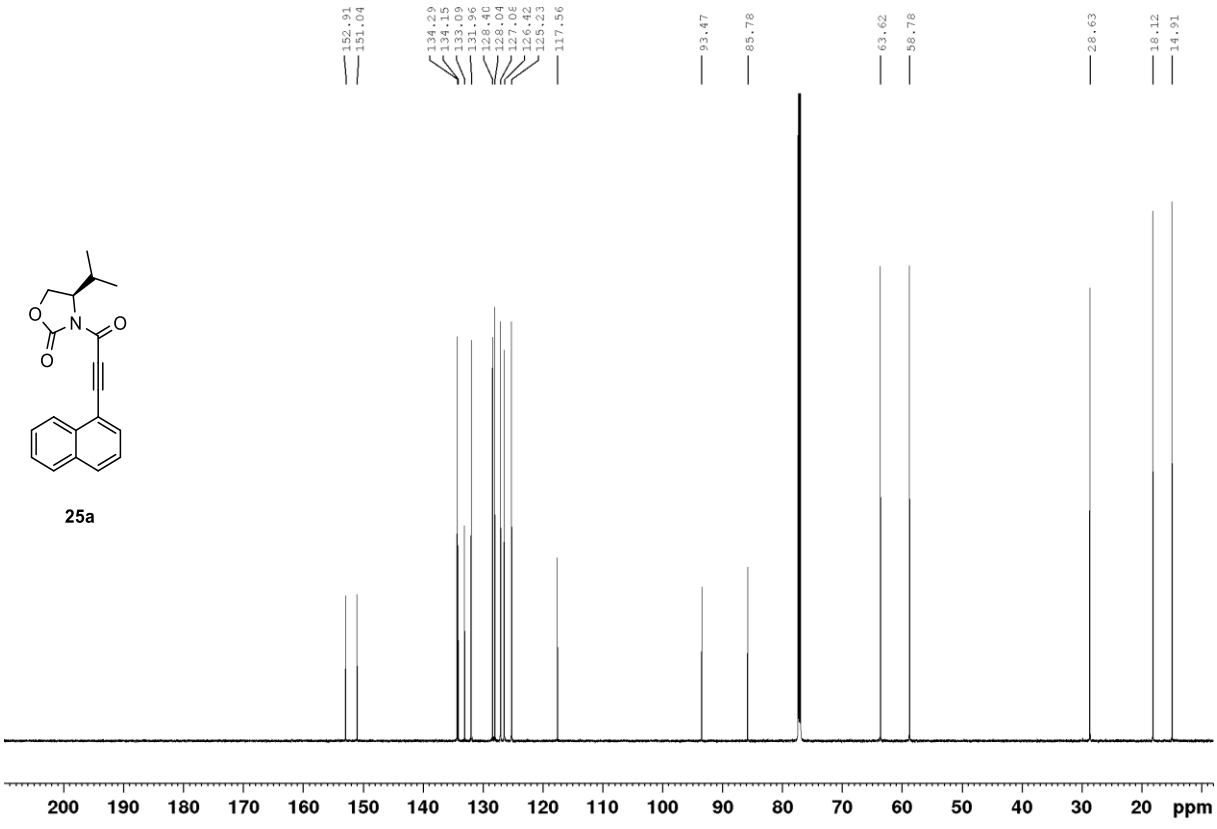

Figure S19. ^{1}H NMR spectrum (176 MHz, $CDCl_3$) of imide **25a**.

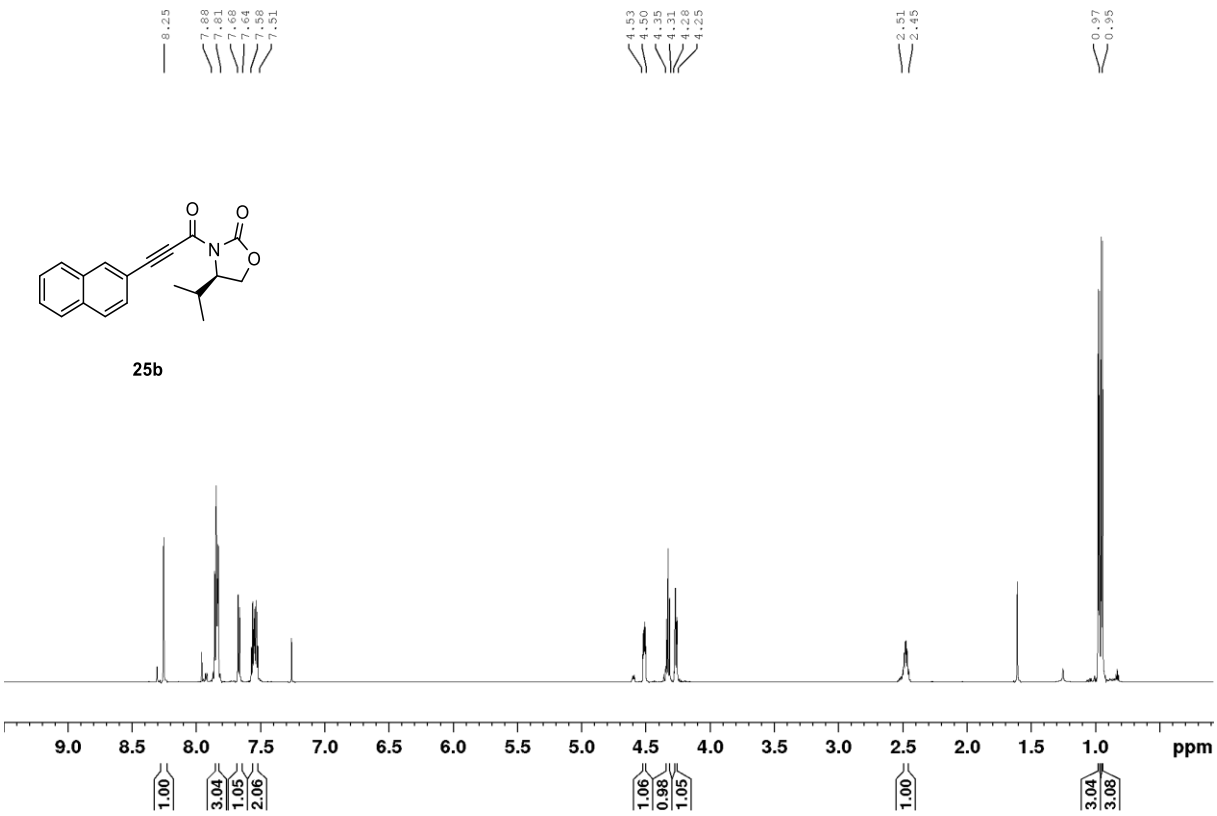

Figure S20. ^{1}H NMR spectrum (700 MHz, $CDCl_3$) of imide **25b**.

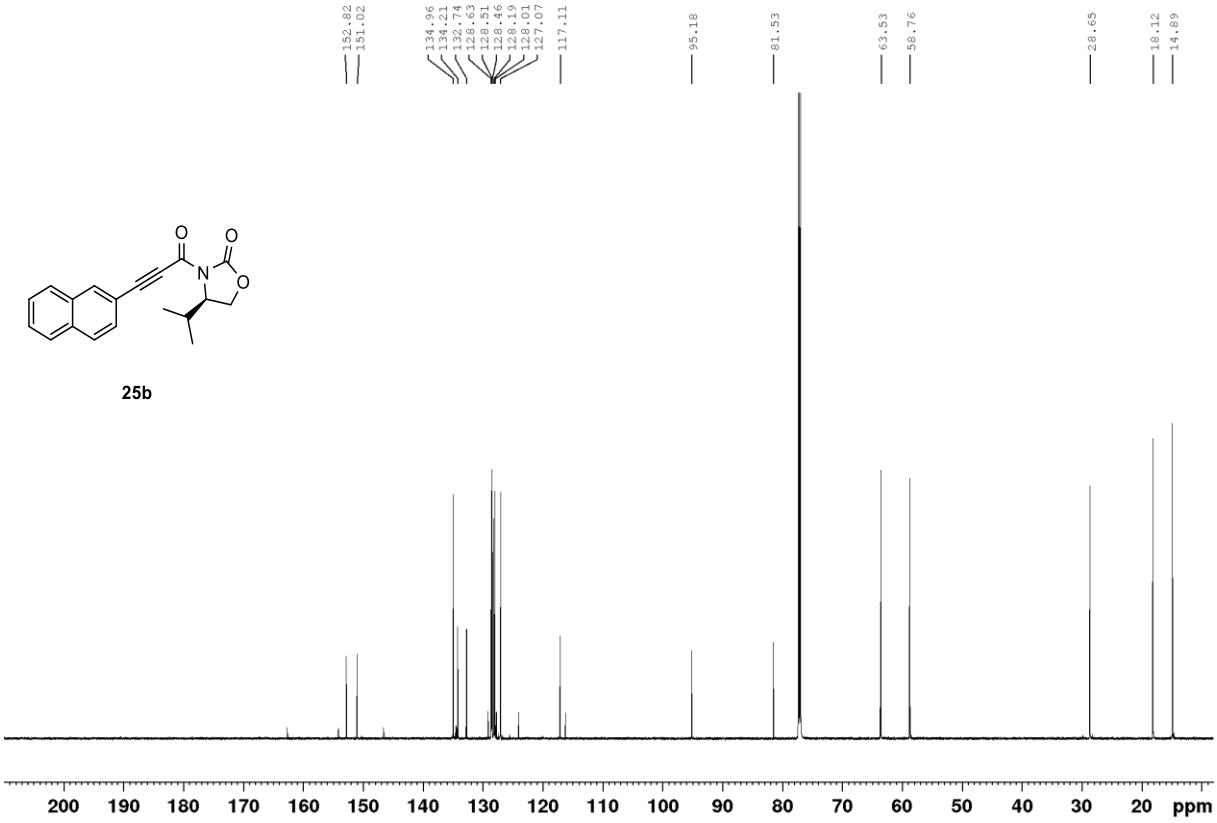

Figure S21. ^{13}C NMR spectrum (176 MHz, $CDCl_3$) of imide **25b**.

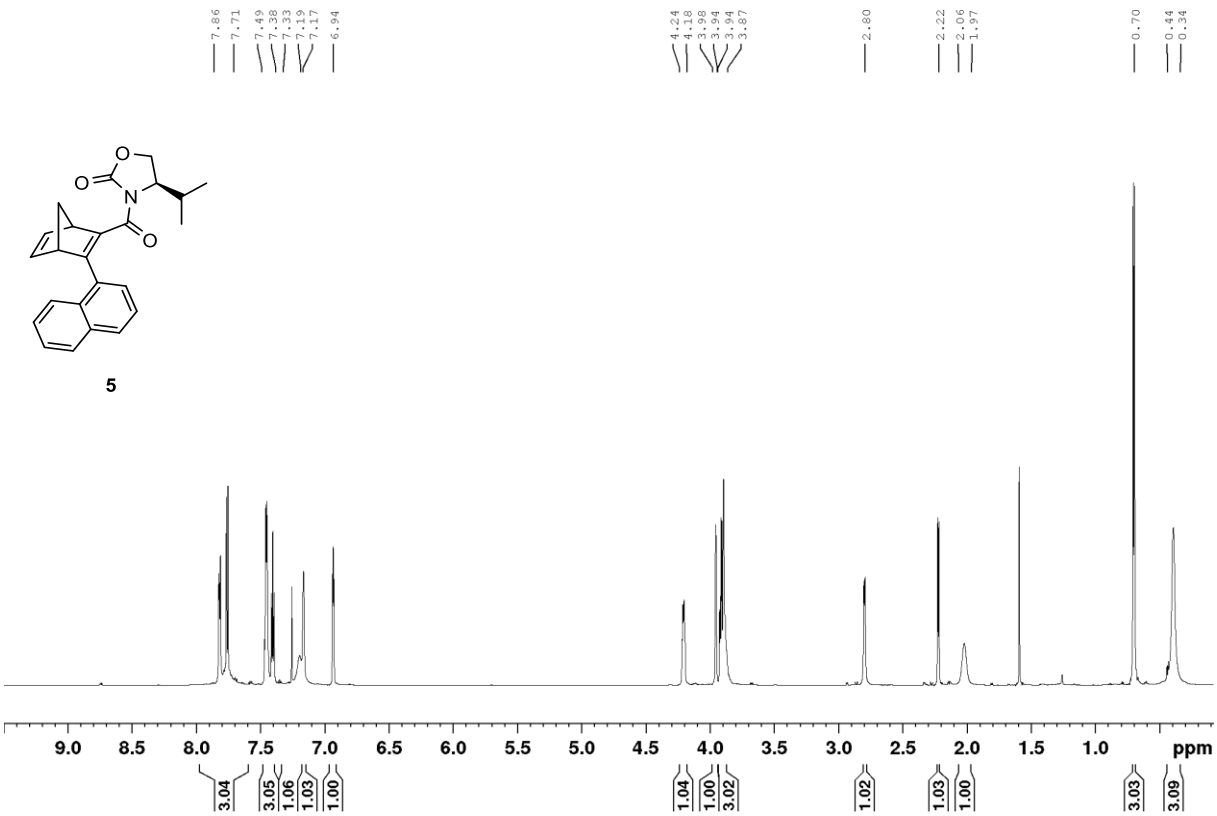

Figure S22. ^{1}H NMR spectrum (700 MHz, $CDCl_3$) of norbornadiene **5**.

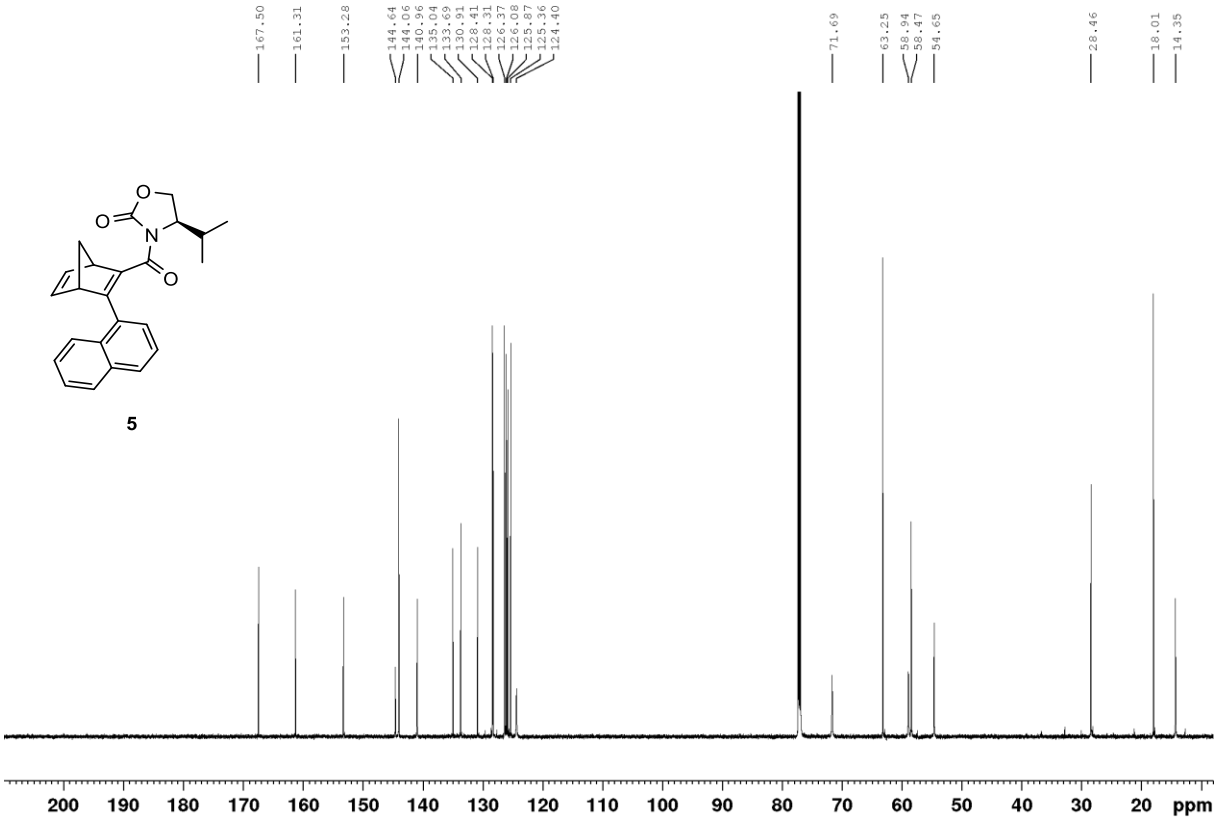

Figure S23. ^{13}C NMR spectrum (176 MHz, $CDCl_3$) of norbornadiene **5**.

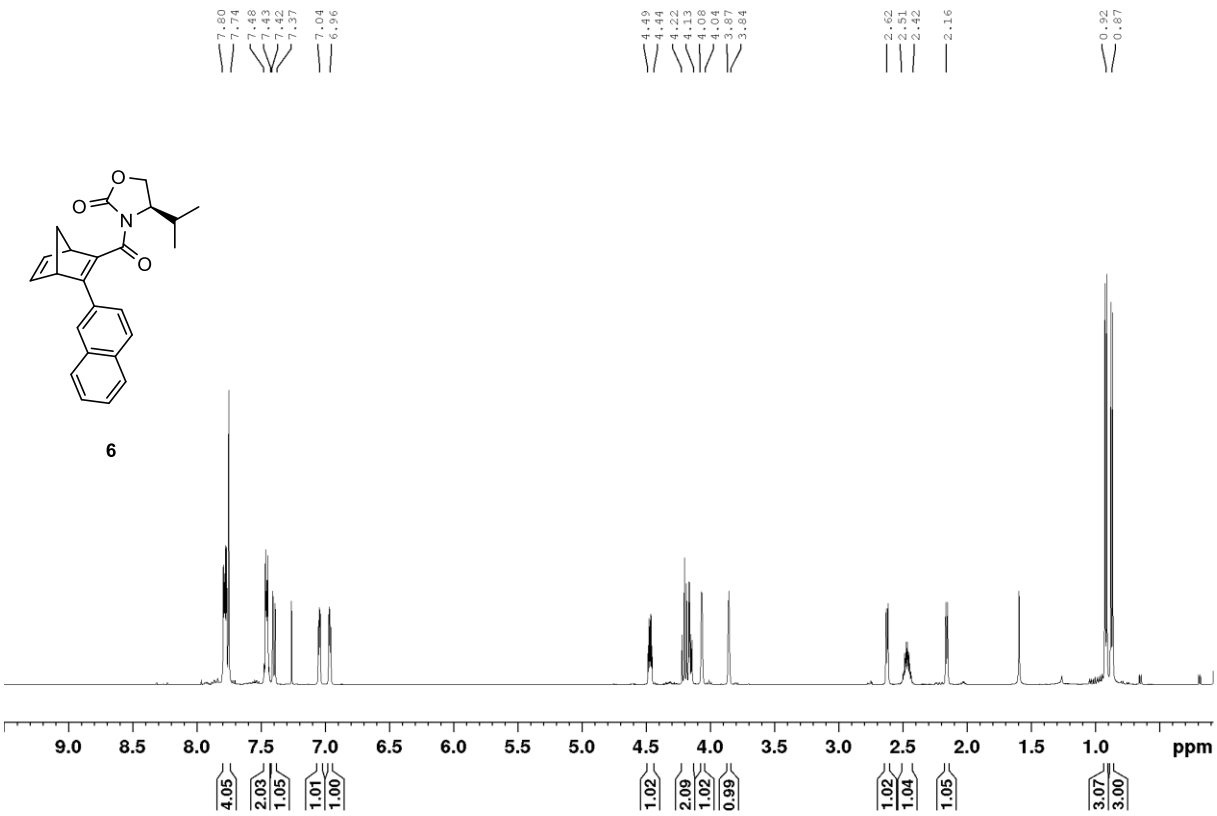

Figure S24. ^{1}H NMR spectrum (700 MHz, $CDCl_3$) of norbornadiene **6**.

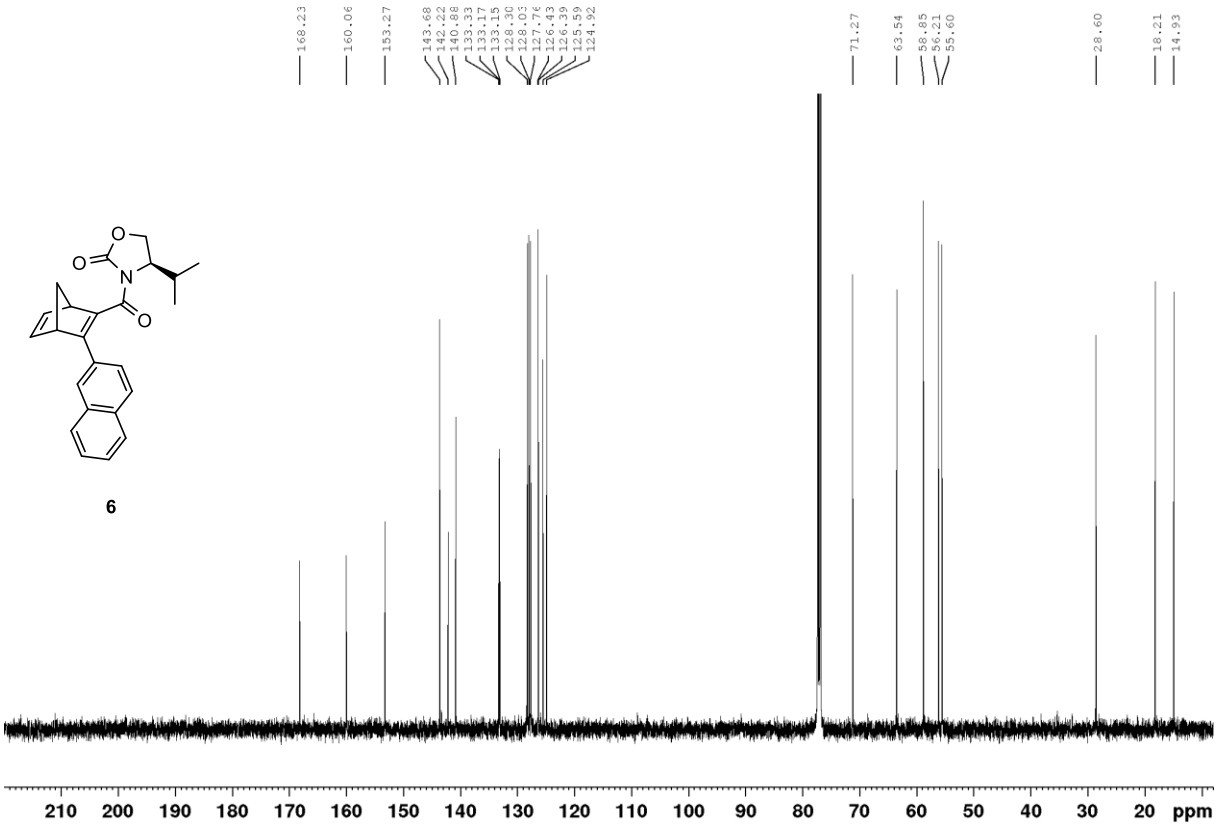

Figure S25. ^{13}C NMR spectrum (176 MHz, $CDCl_3$) of norbornadiene **6**.

2.2 Synthesis of the phenyl-substituted norbornadienes

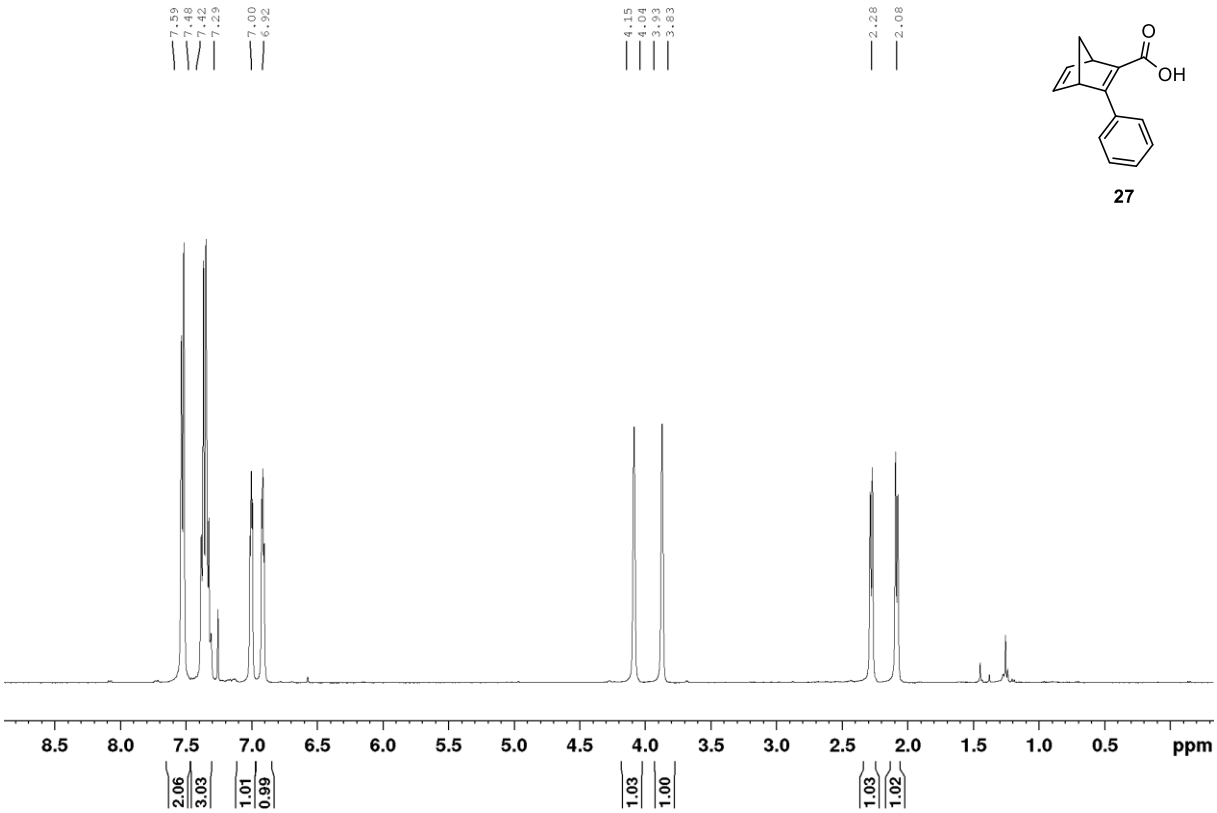

Figure S26. ^{1}H NMR spectrum (400 MHz, $CDCl_3$) of norbornadiene acid **27**.

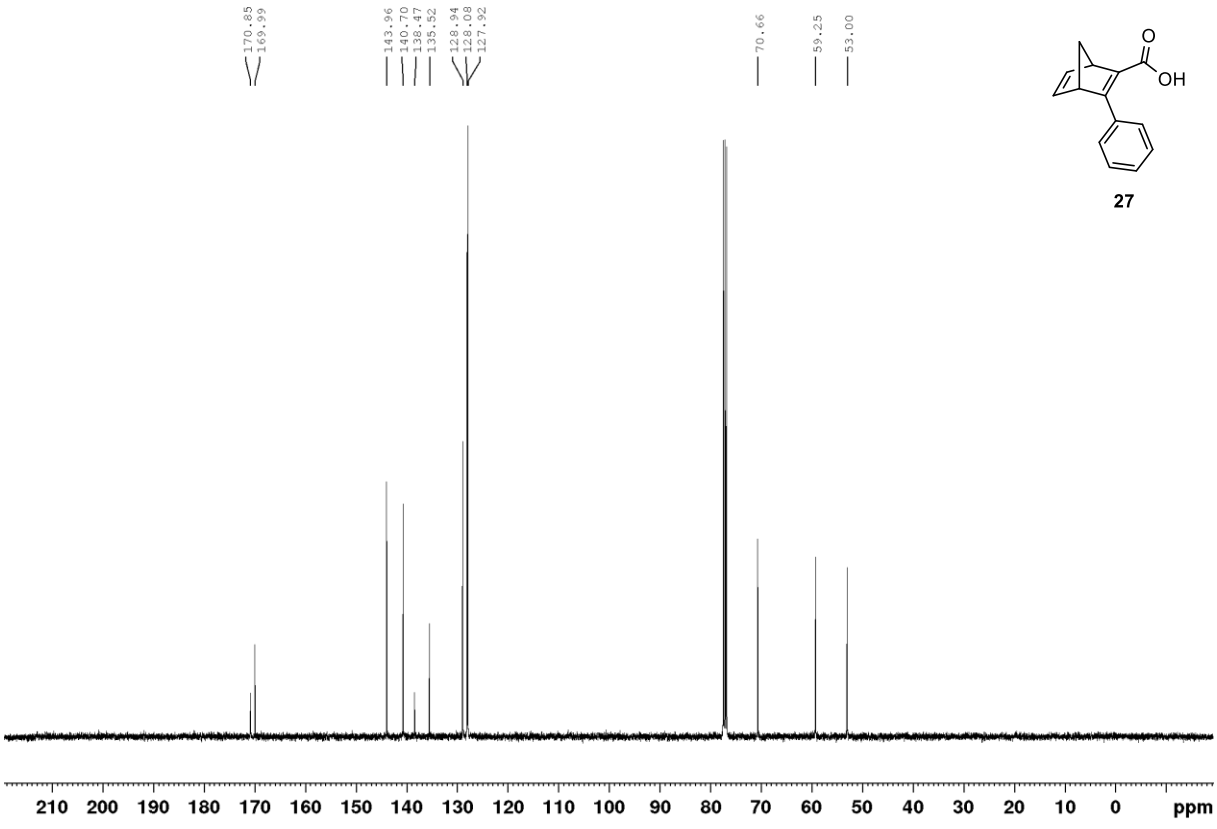

Figure S27. ^{13}C NMR spectrum (101 MHz, $CDCl_3$) of norbornadiene acid **27**.

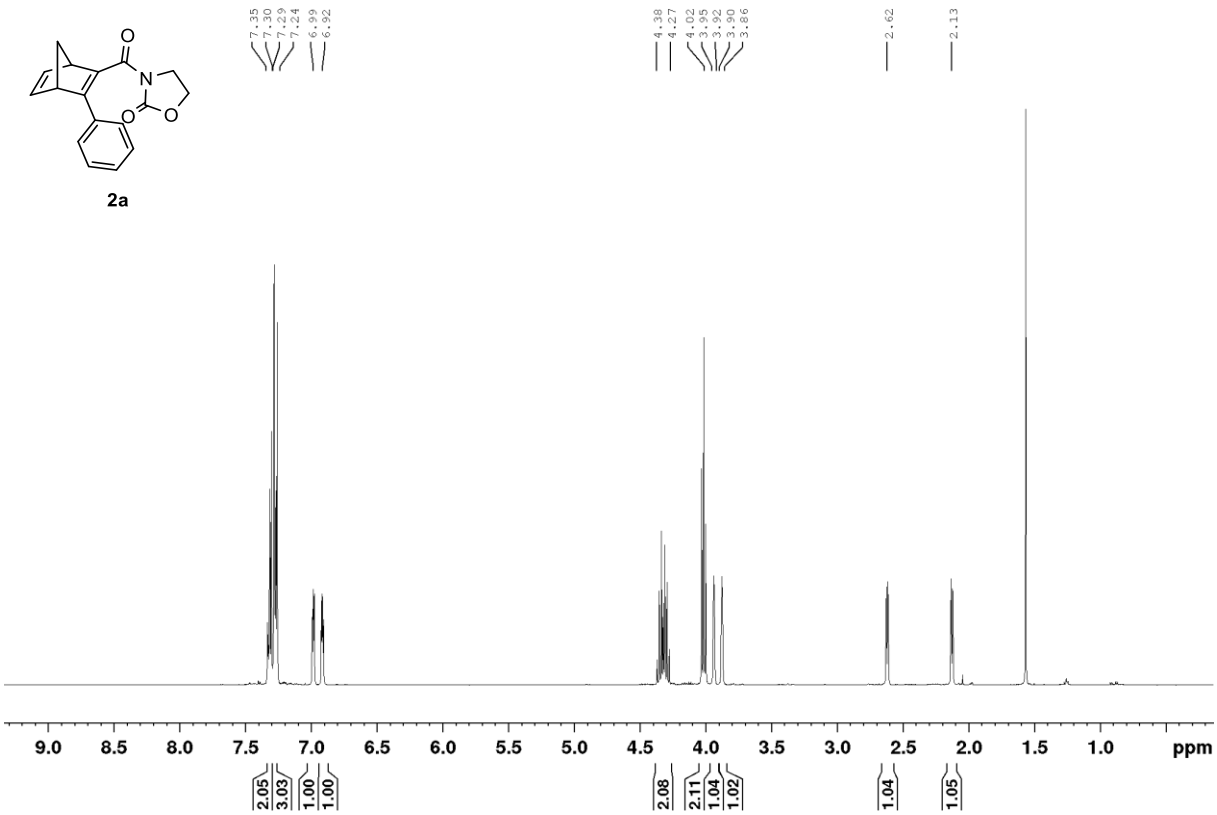

Figure S28. ^{1}H NMR spectrum (500 MHz, $CDCl_3$) of oxazolidinone derivative **2a**.

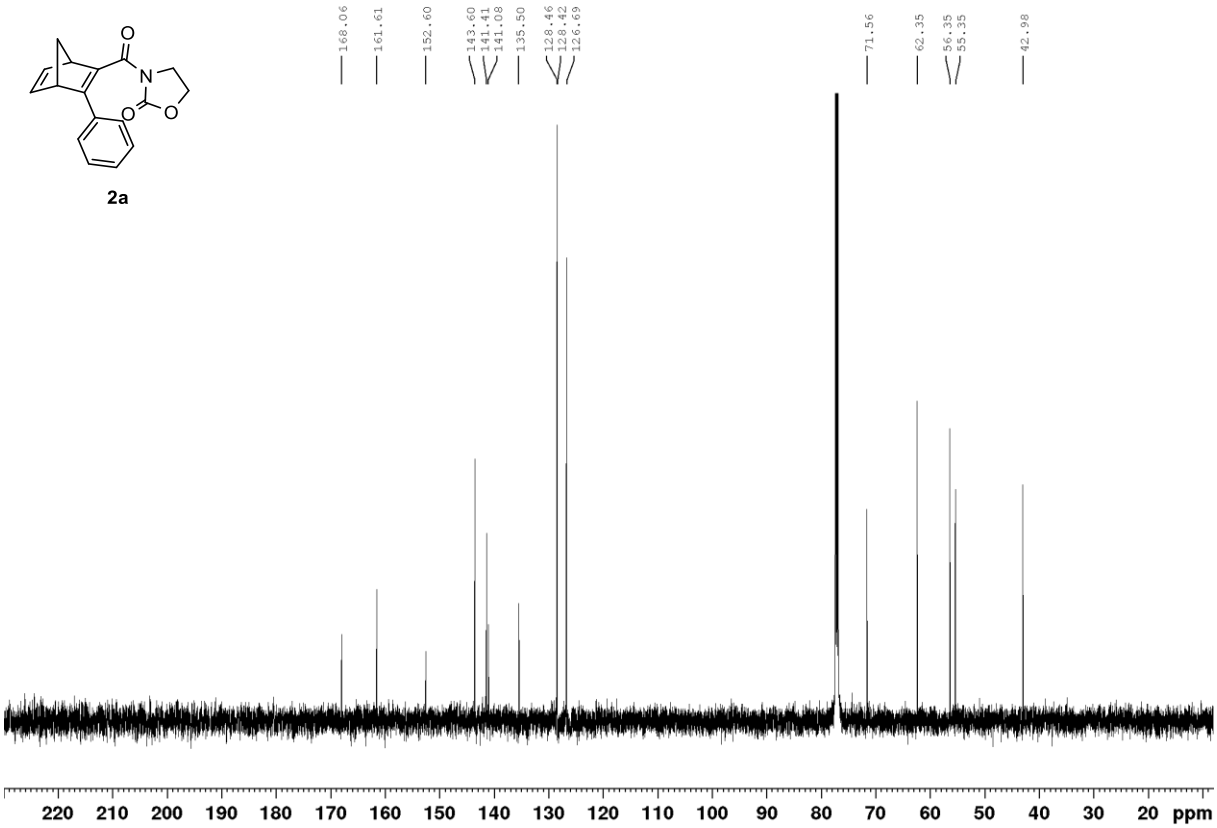

Figure S29. ^{13}C NMR spectrum (126 MHz, $CDCl_3$) of oxazolidinone derivative **2a**.

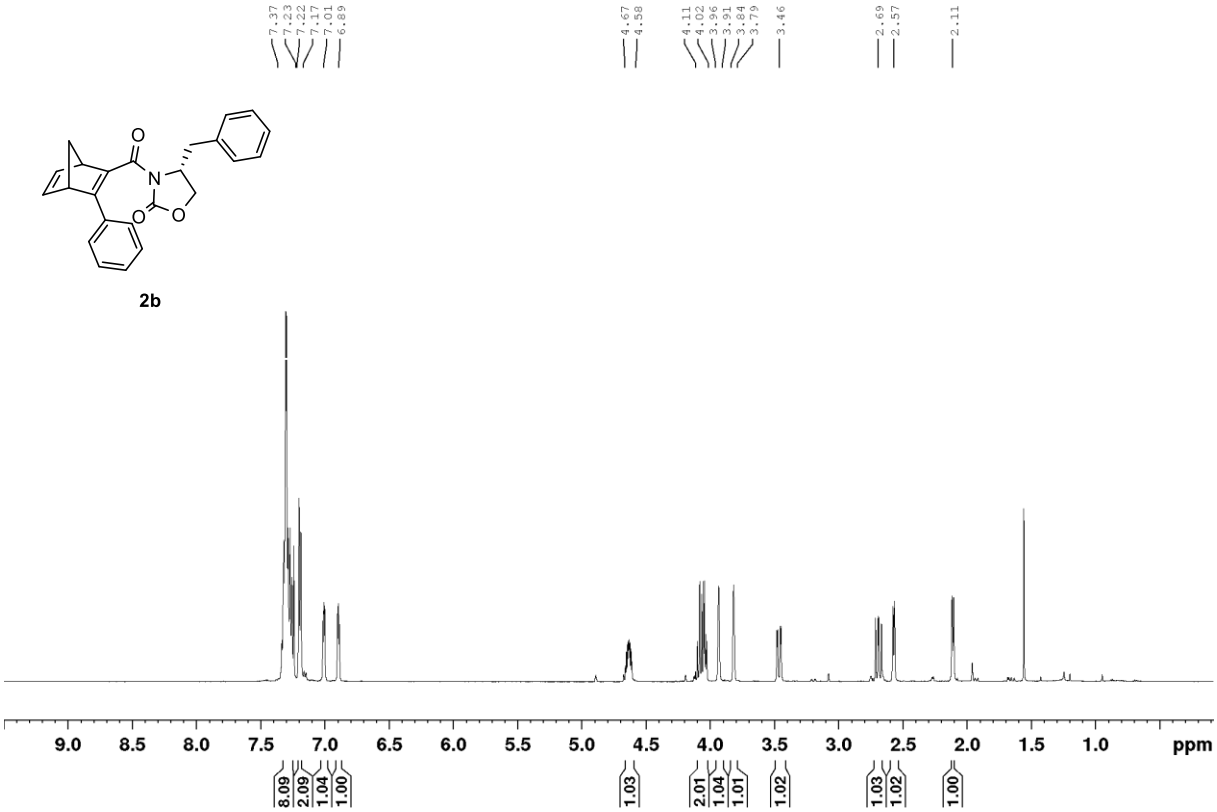

Figure S30. ^{1}H NMR spectrum (500 MHz, $CDCl_3$) of norbornadiene **2b**.

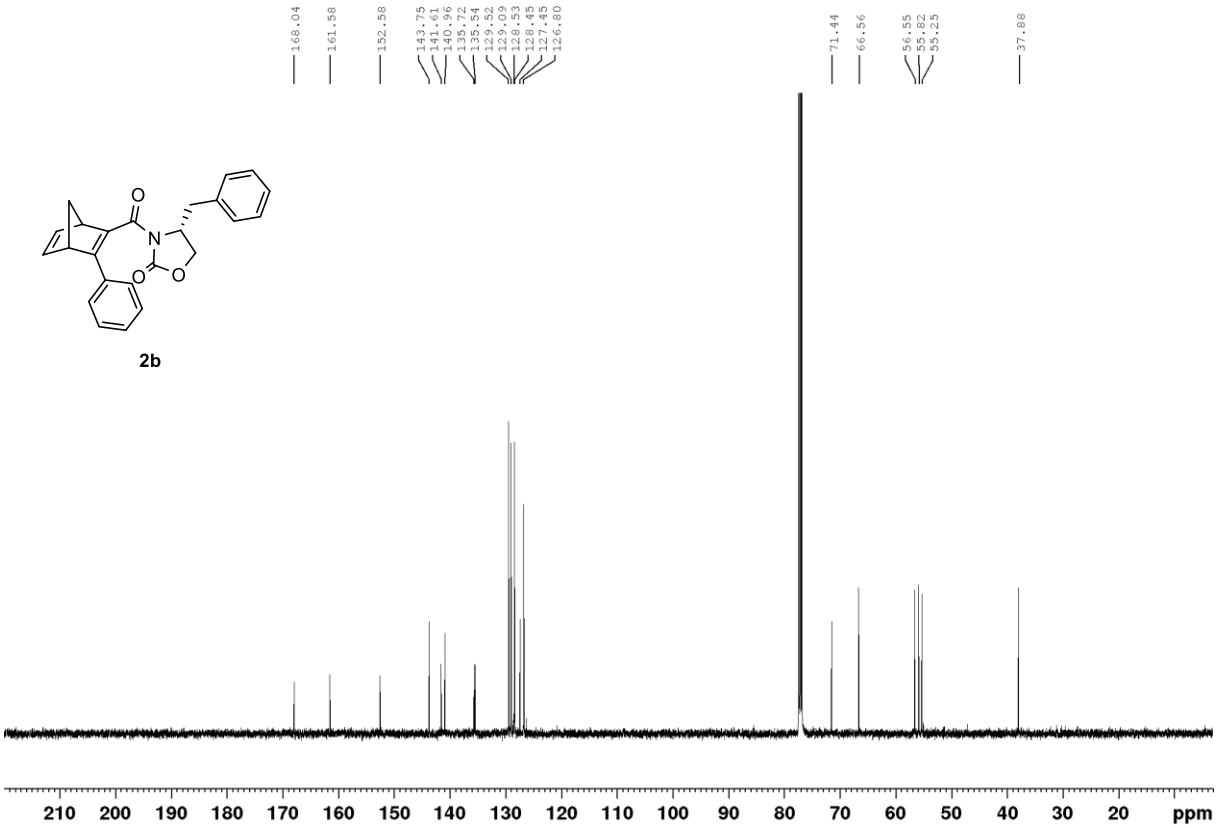

Figure S31. ^{13}C NMR spectrum (126 MHz, $CDCl_3$) of norbornadiene **2b**.

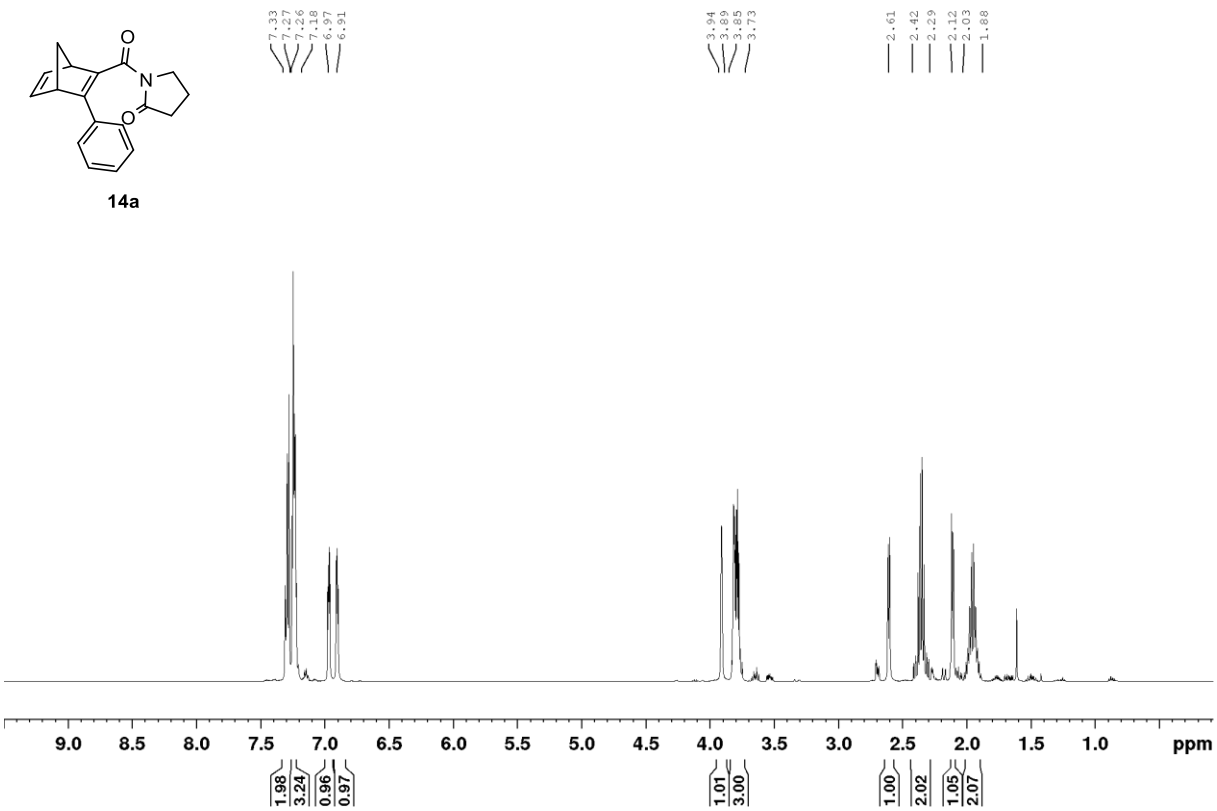

Figure S32. ^{1}H NMR spectrum (500 MHz, $CDCl_3$) of lactam derivative **14a**.

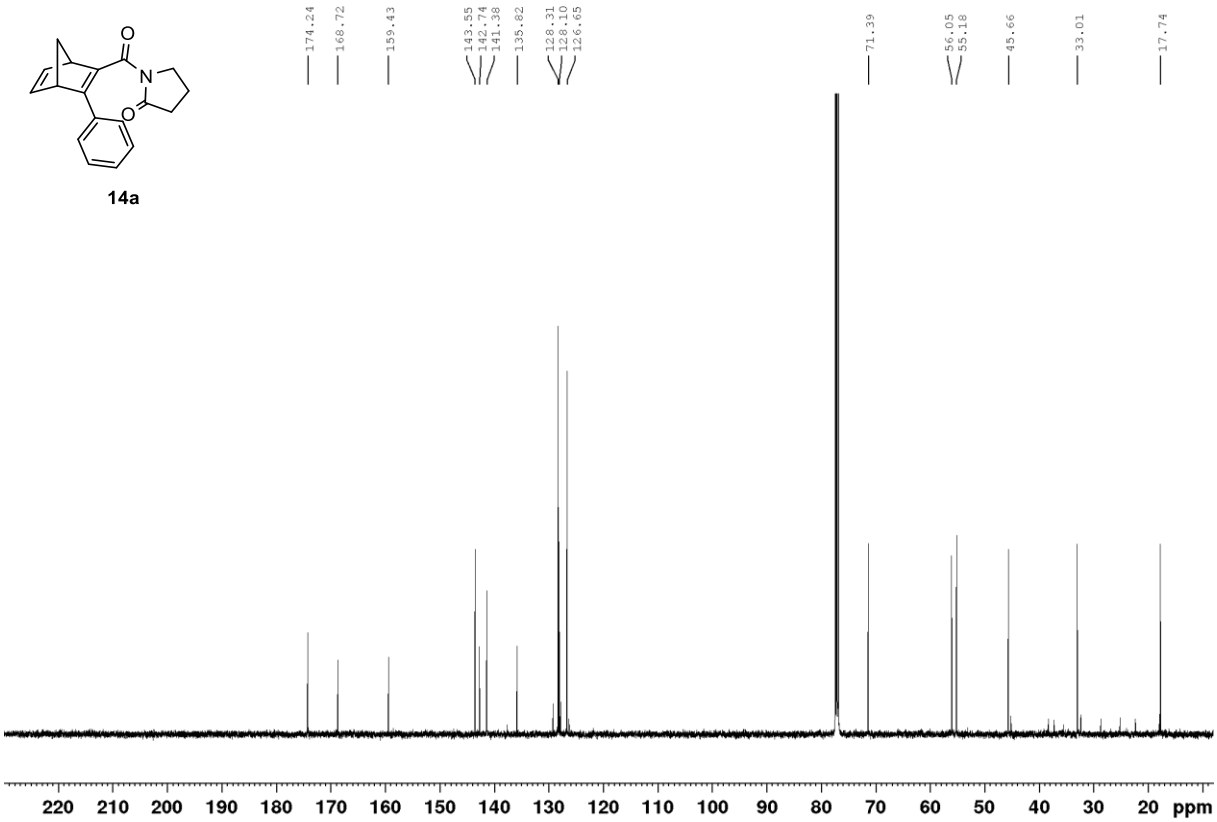

Figure S33. ^{13}C NMR spectrum (126 MHz, $CDCl_3$) of lactam derivative **14a**.

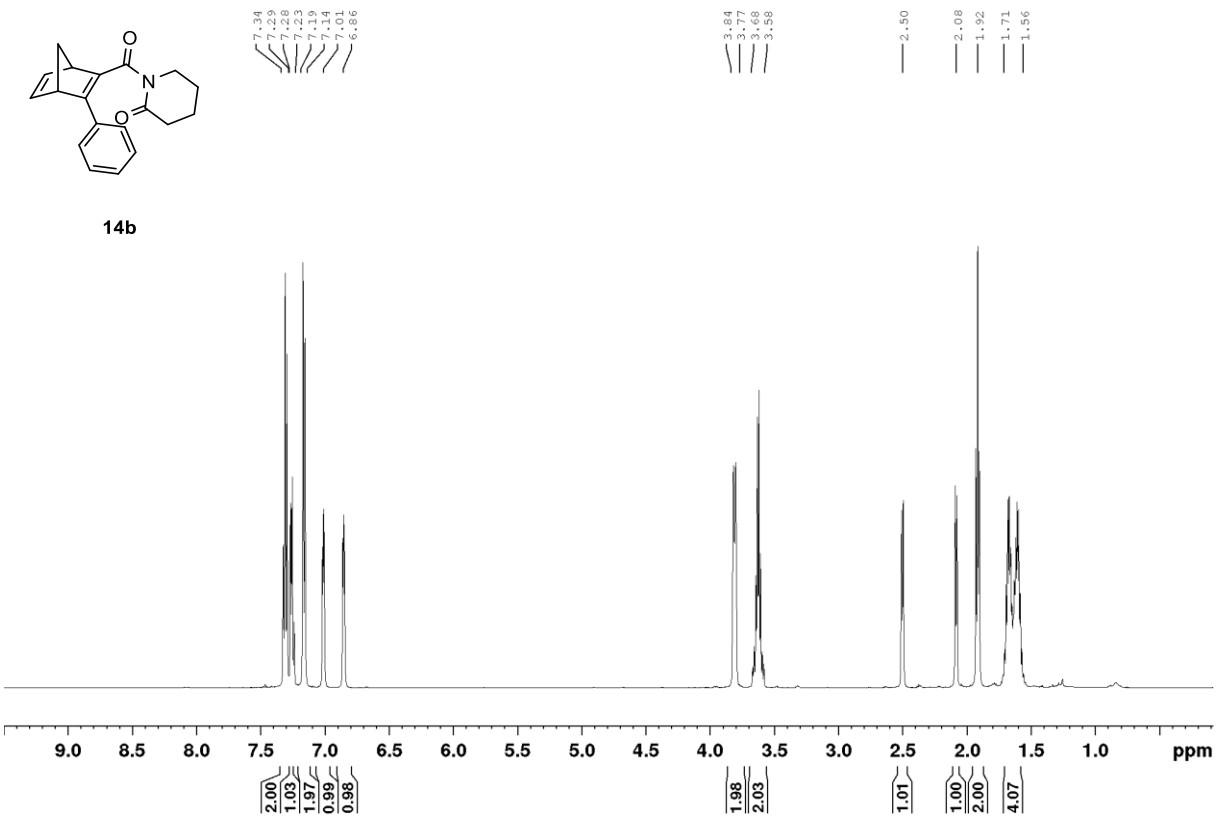

Figure S34. ^{1}H NMR spectrum (500 MHz, $CDCl_3$) of lactam derivative **14b**.

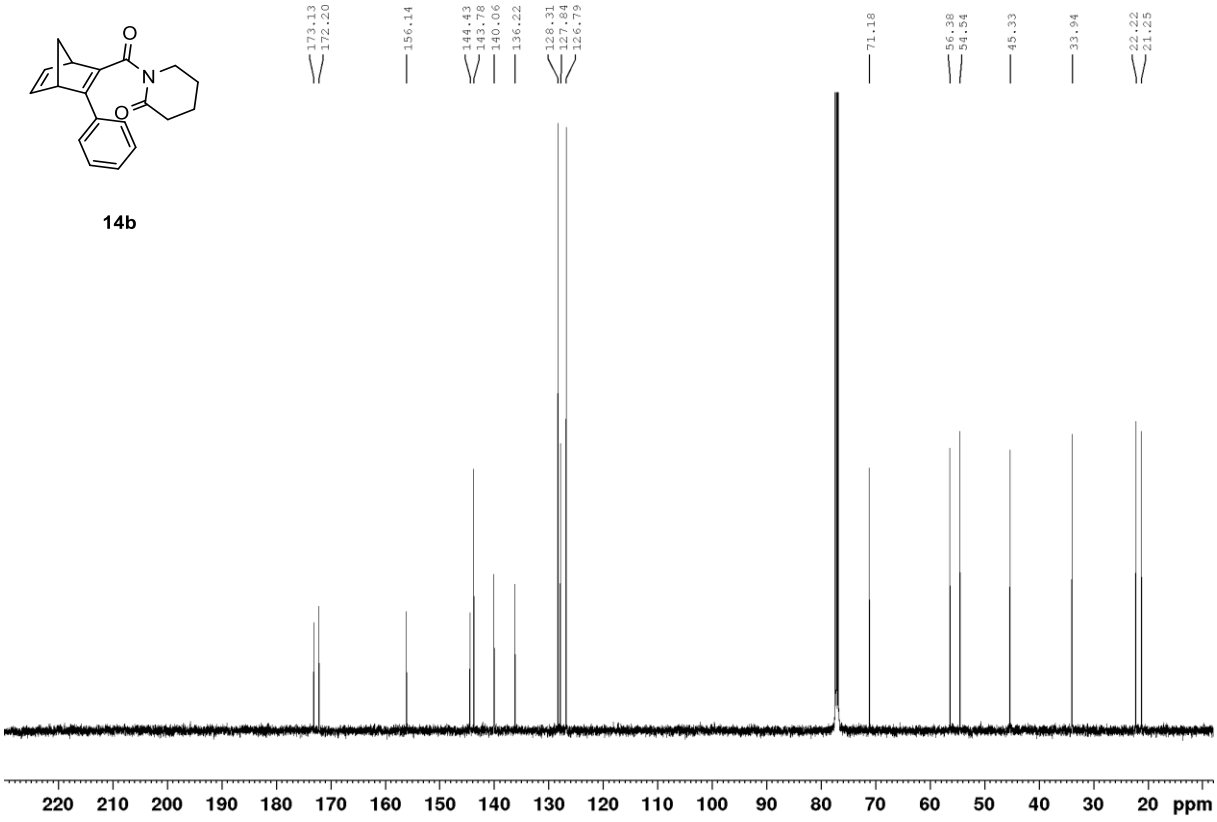

Figure S35. ^{13}C NMR spectrum (126 MHz, $CDCl_3$) of lactam derivative **14b**.

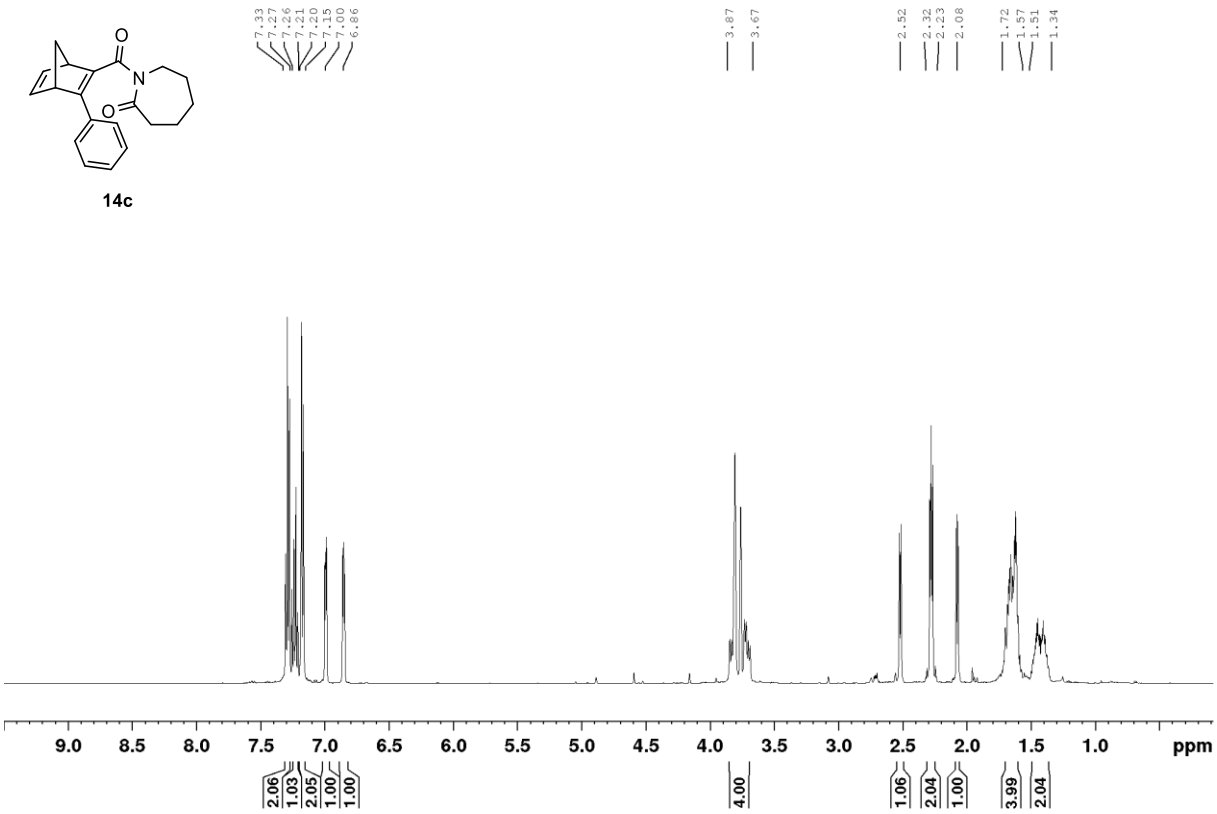

Figure S36. ^{1}H NMR spectrum (500 MHz, $CDCl_3$) of lactam derivative **14c**.

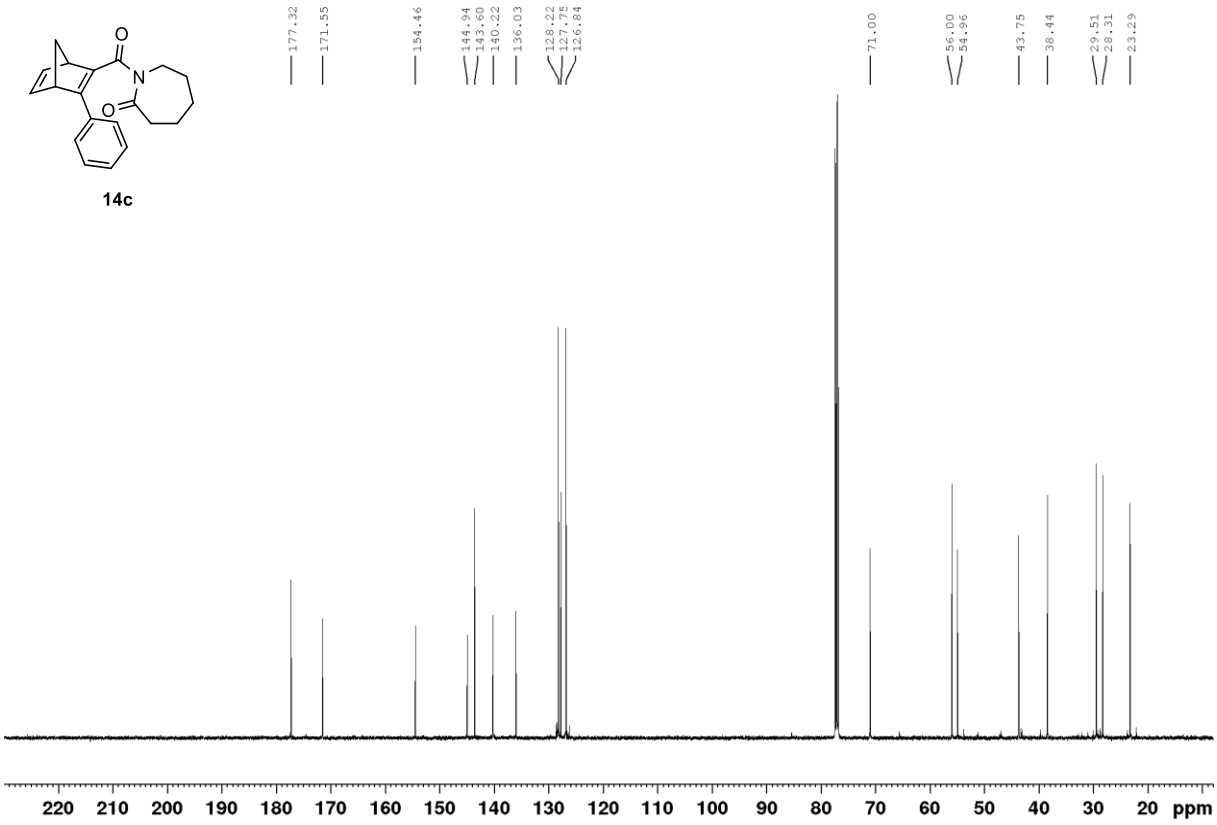

Figure S37. ^{13}C NMR spectrum (126 MHz, $CDCl_3$) of lactam derivative **14c**.

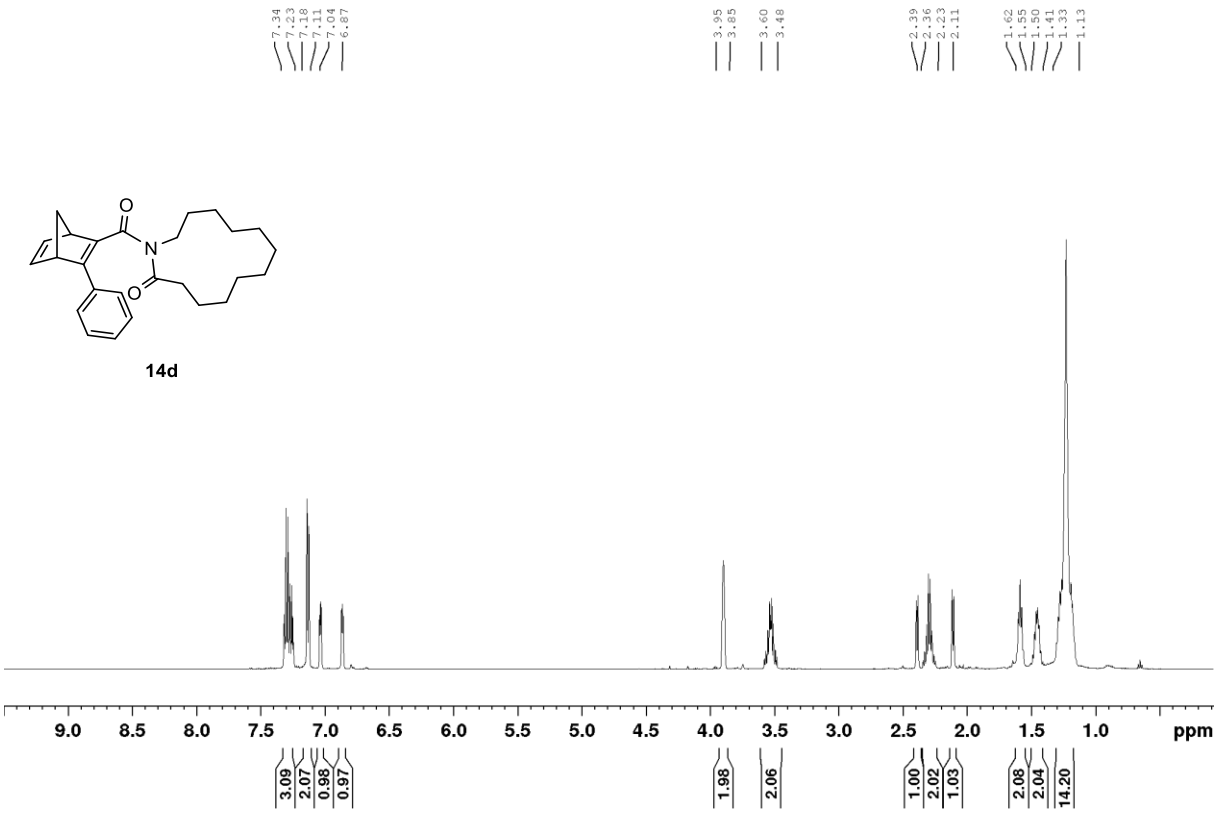

Figure S38. ^{1}H NMR spectrum (500 MHz, $CDCl_3$) of lactam derivative **14d**.

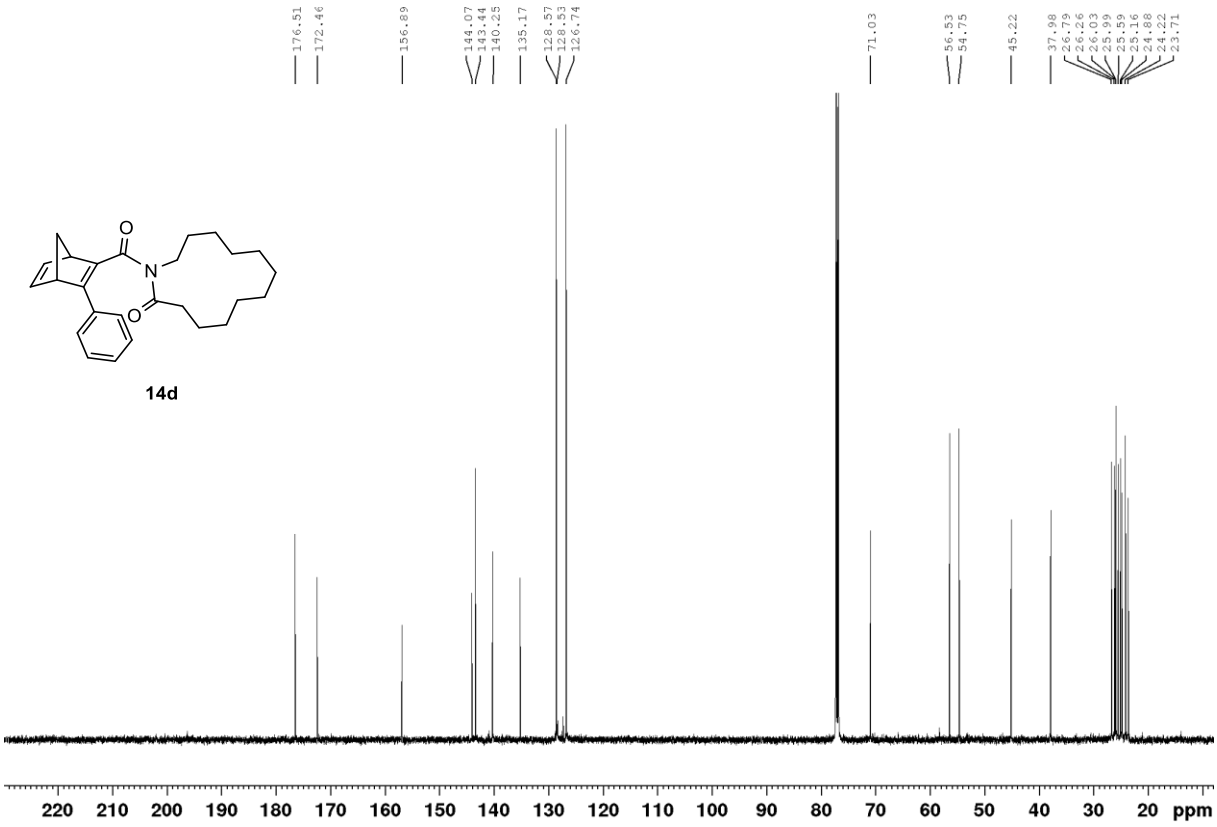

Figure S39. ^{13}C NMR spectrum (126 MHz, $CDCl_3$) of lactam derivative **14d**.

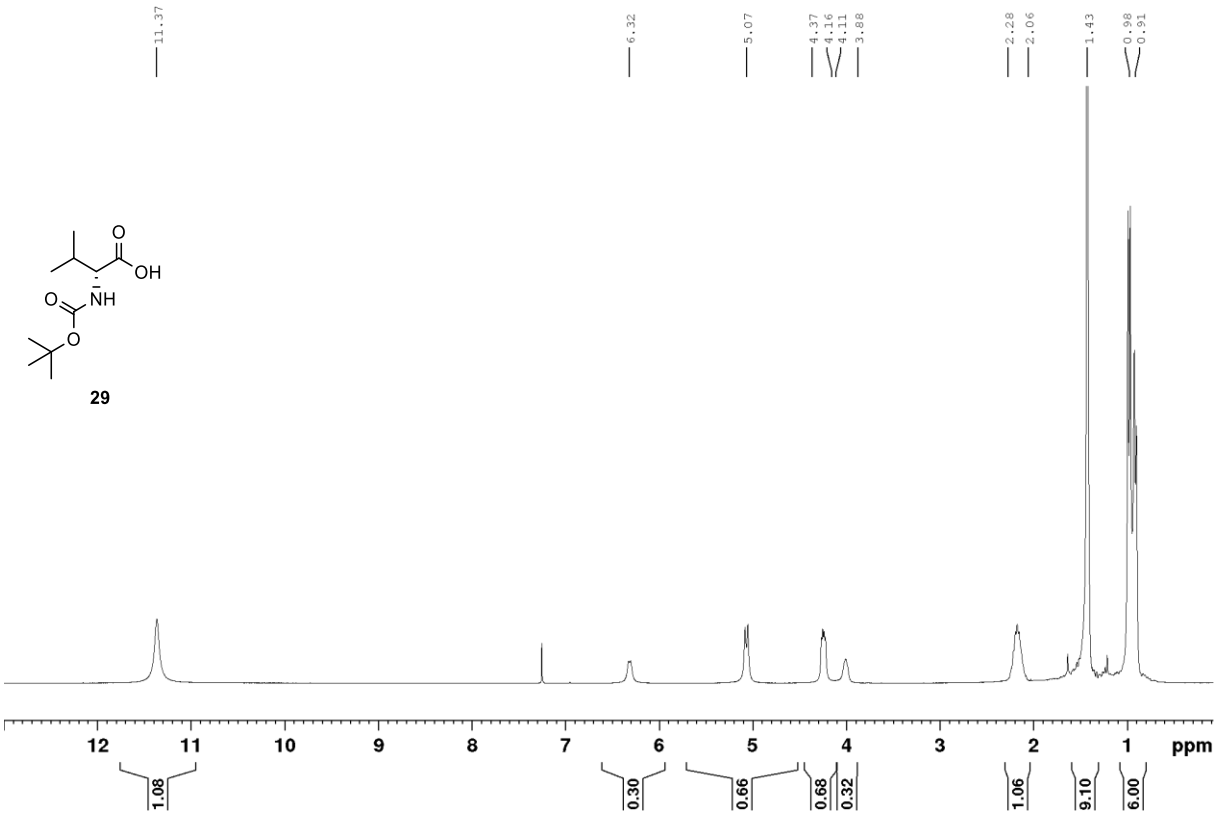

Figure S40. ^{1}H NMR spectrum (300 MHz, $CDCl_3$) of *N*-boc-protected (*D*)-valine **29**.

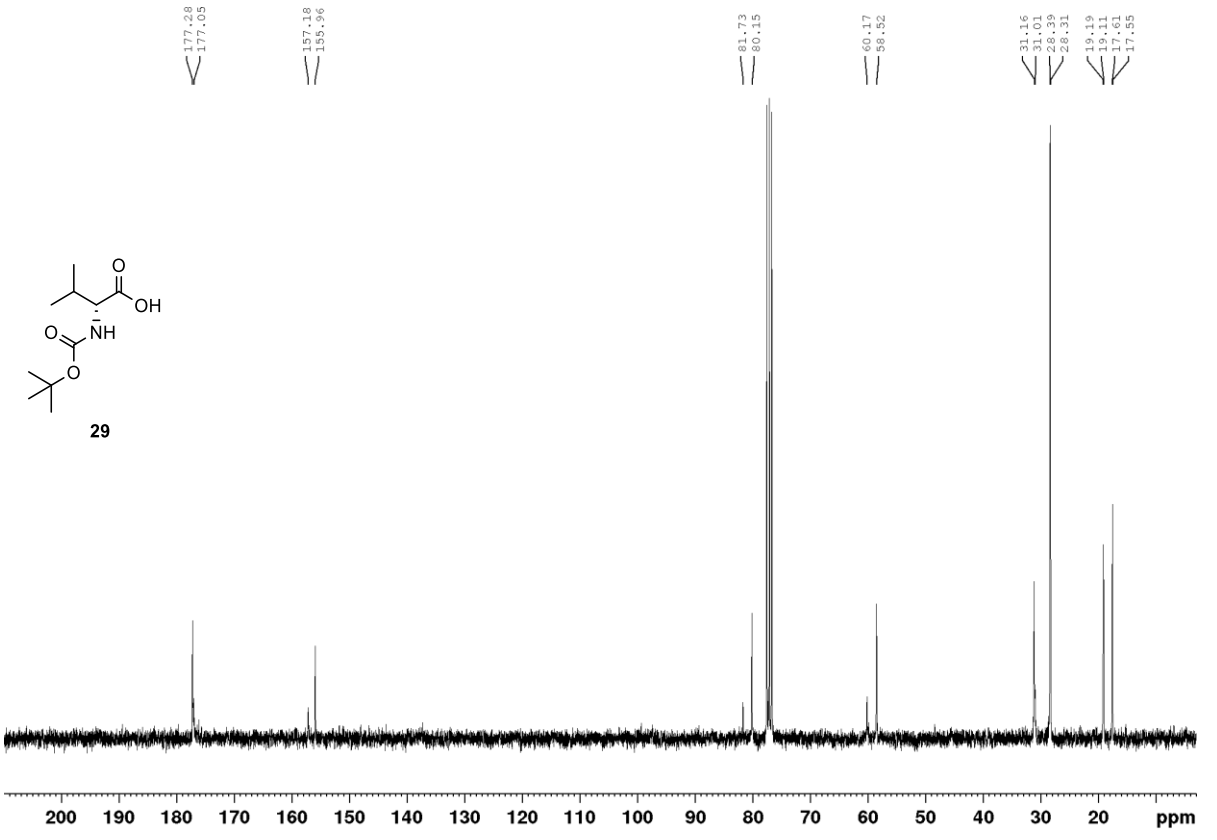

Figure S41. ^{13}C NMR spectrum (75 MHz, $CDCl_3$) of *N*-boc-protected (*D*)-valine **29**.

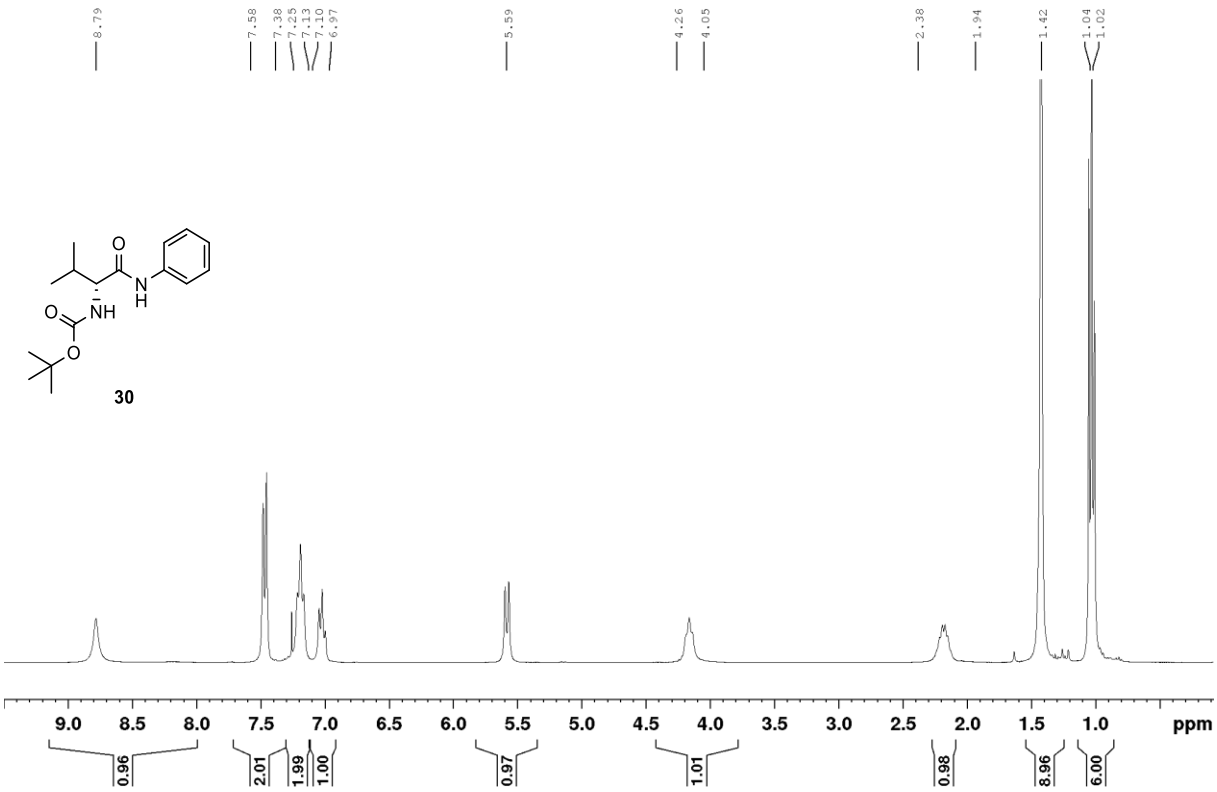

Figure S42. ^{1}H NMR spectrum (300 MHz, $CDCl_3$) of *N*-boc-protected Amide **30**.

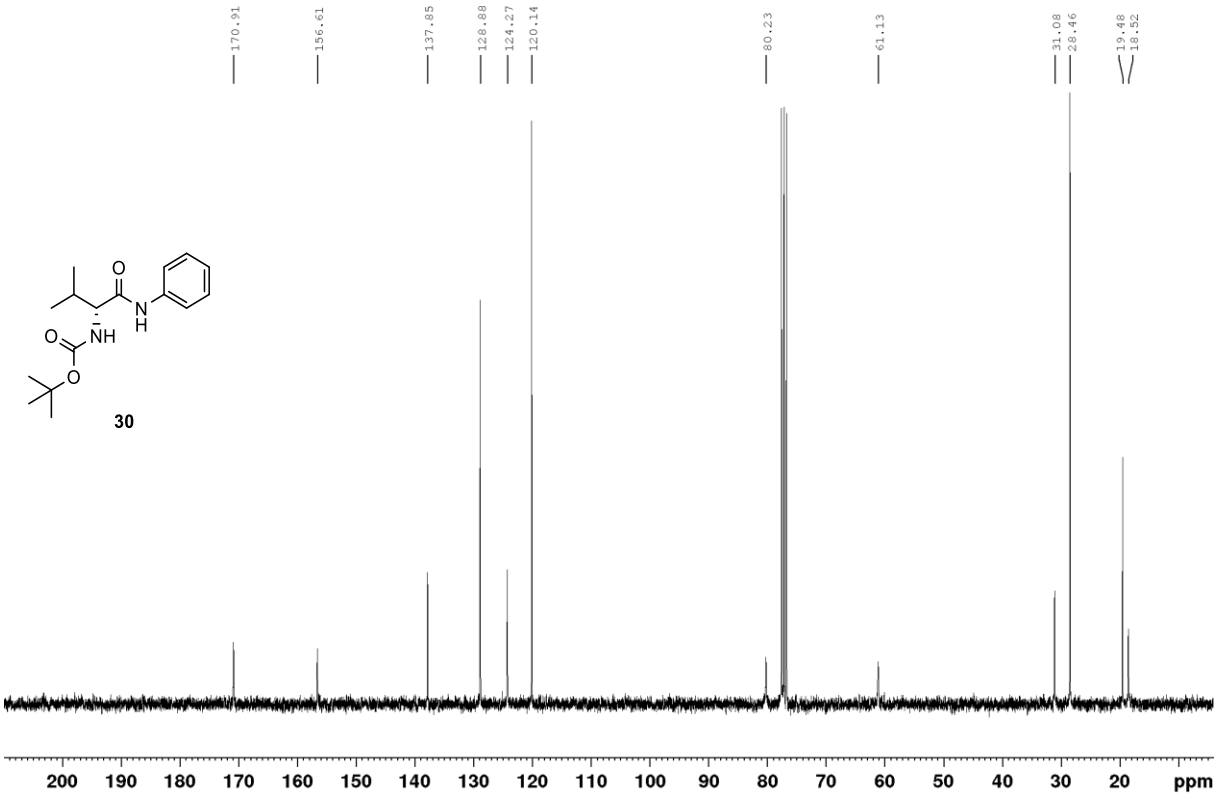

Figure S43. ^{13}C NMR spectrum (75 MHz, $CDCl_3$) of *N*-boc-protected Amide **30**.

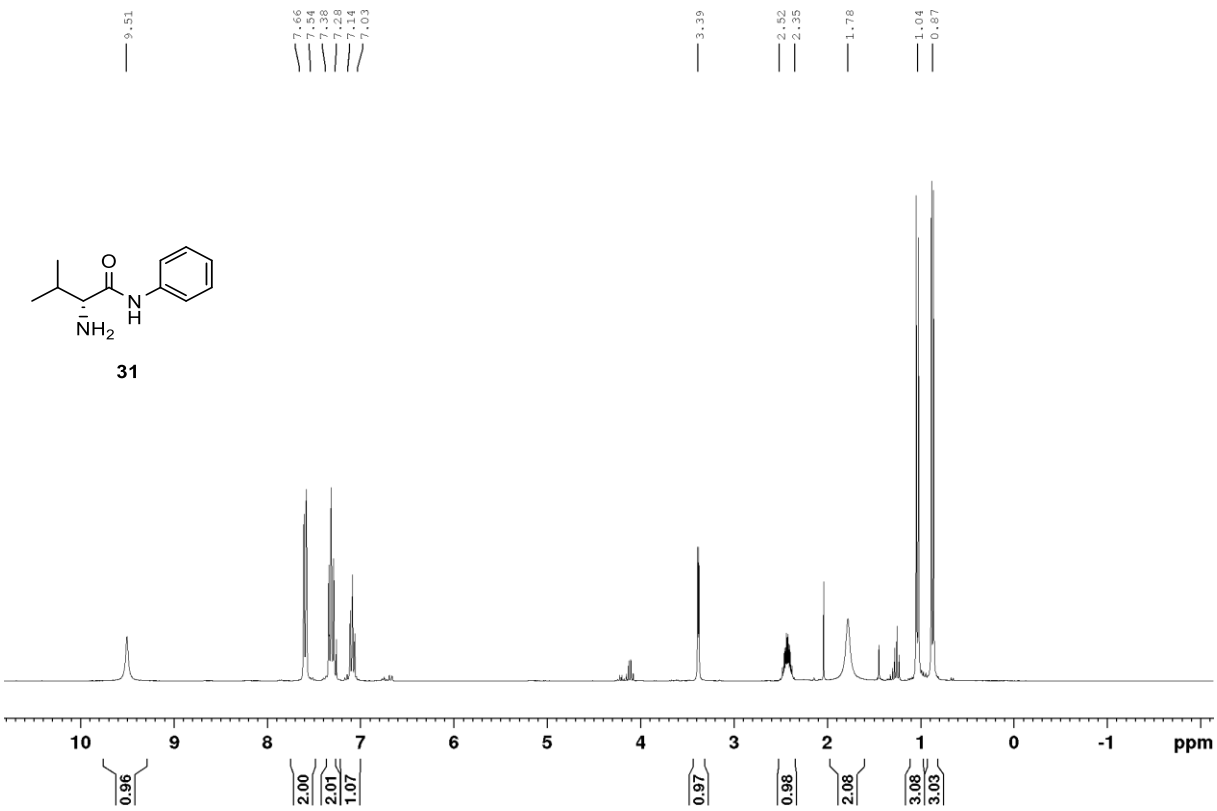

Figure S44. ^{1}H NMR spectrum (300 MHz, $CDCl_3$) of amide **31**.

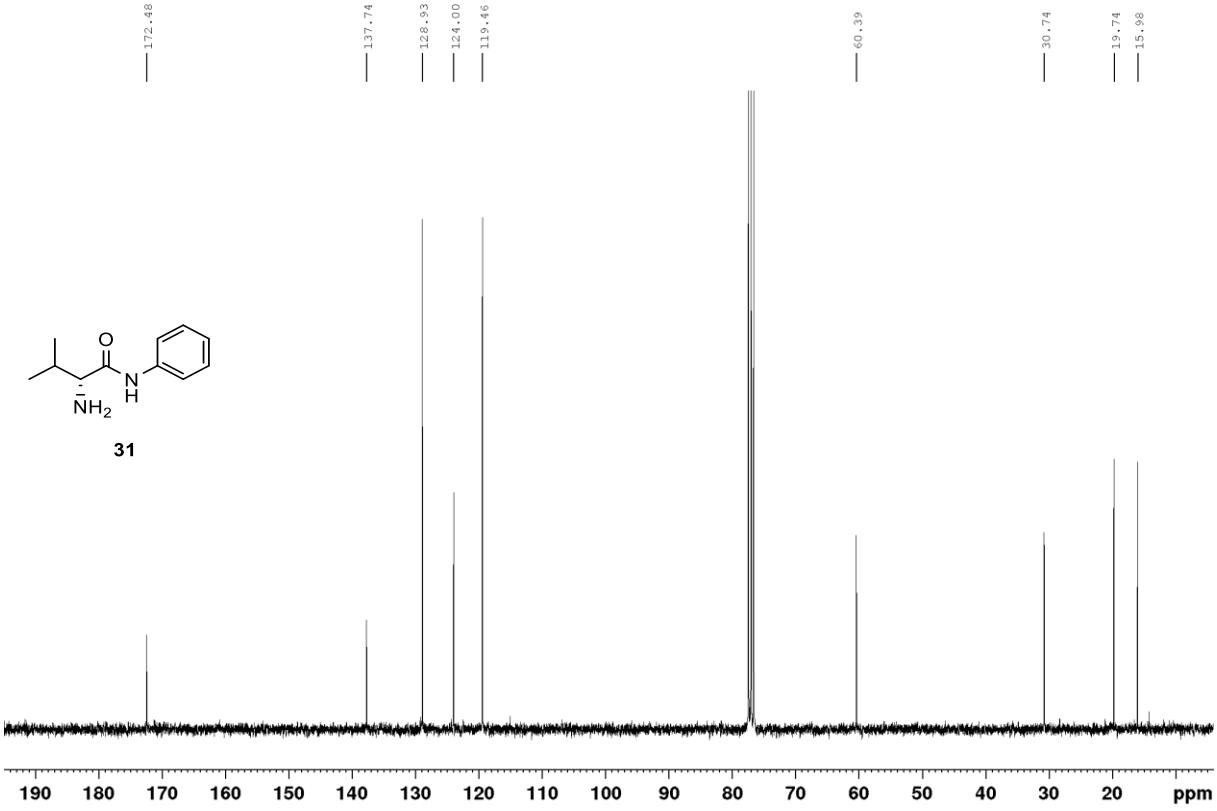

Figure S45. ^{13}C NMR spectrum (75 MHz, $CDCl_3$) of amide **31**.

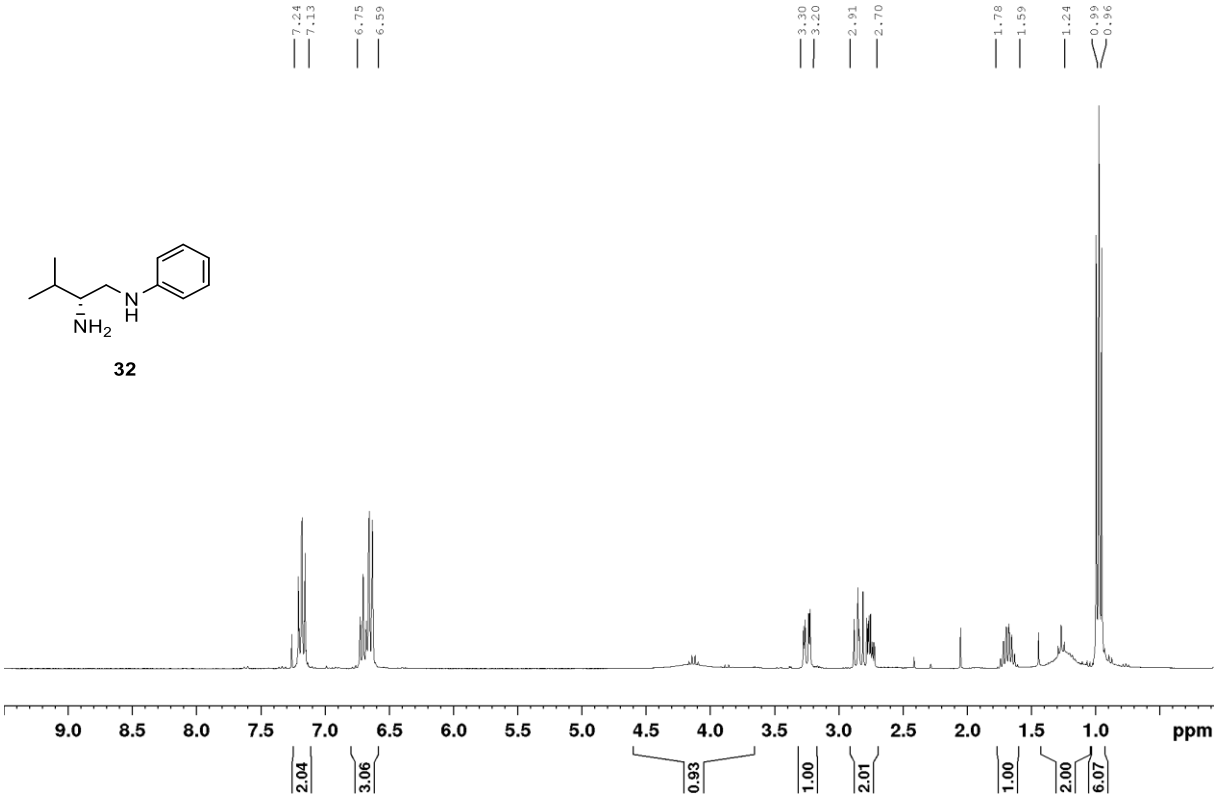

Figure S46. ^{1}H NMR spectrum (300 MHz, $CDCl_3$) of diamine **32**.

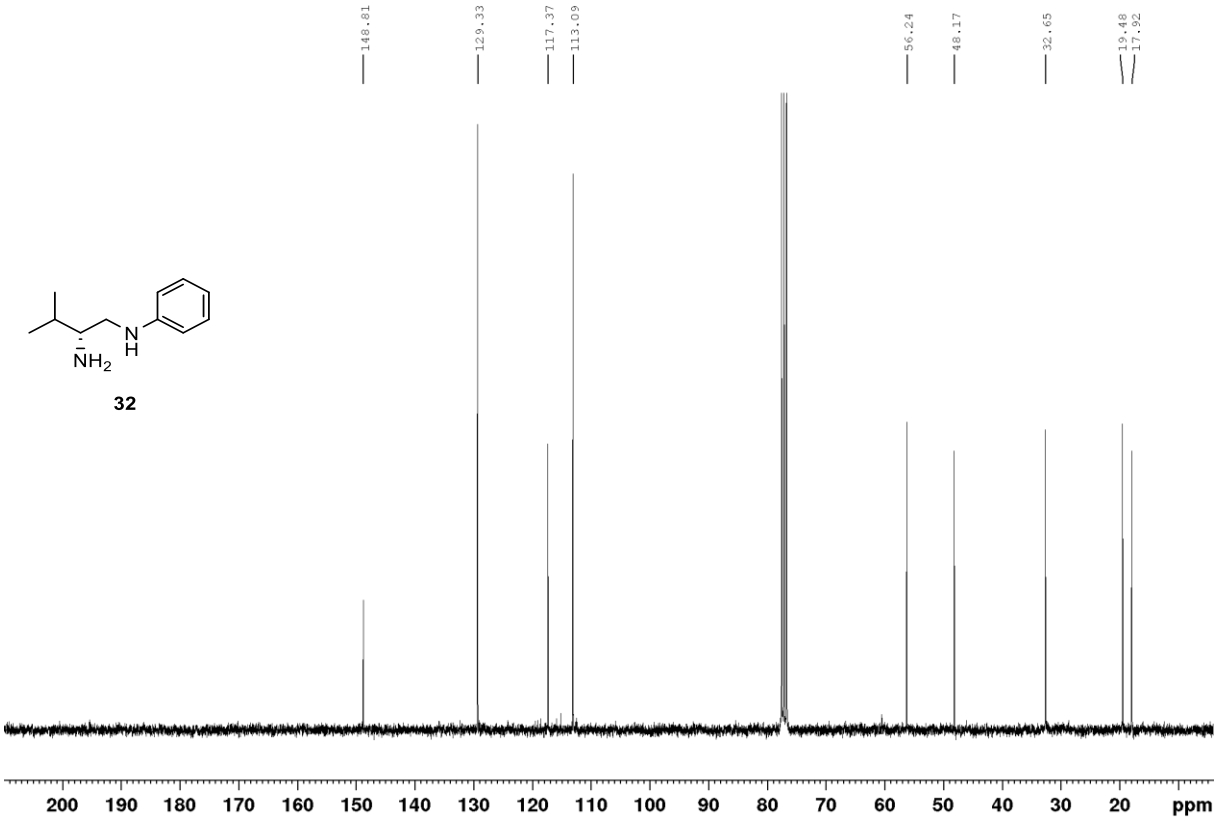

Figure S47. ^{13}C NMR spectrum (300 MHz, $CDCl_3$) of diamine **32**.

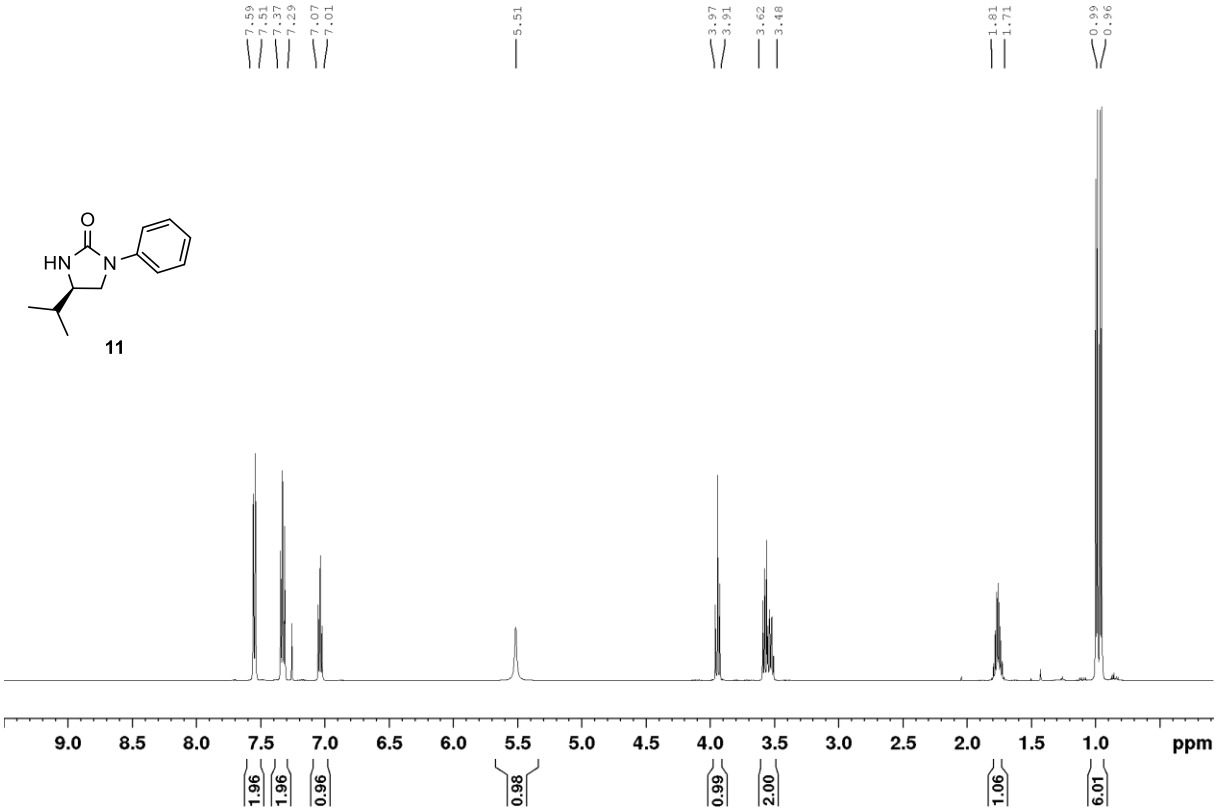

Figure S48. ^{1}H NMR spectrum (500 MHz, $CDCl_3$) of imidazolidinone **11**.

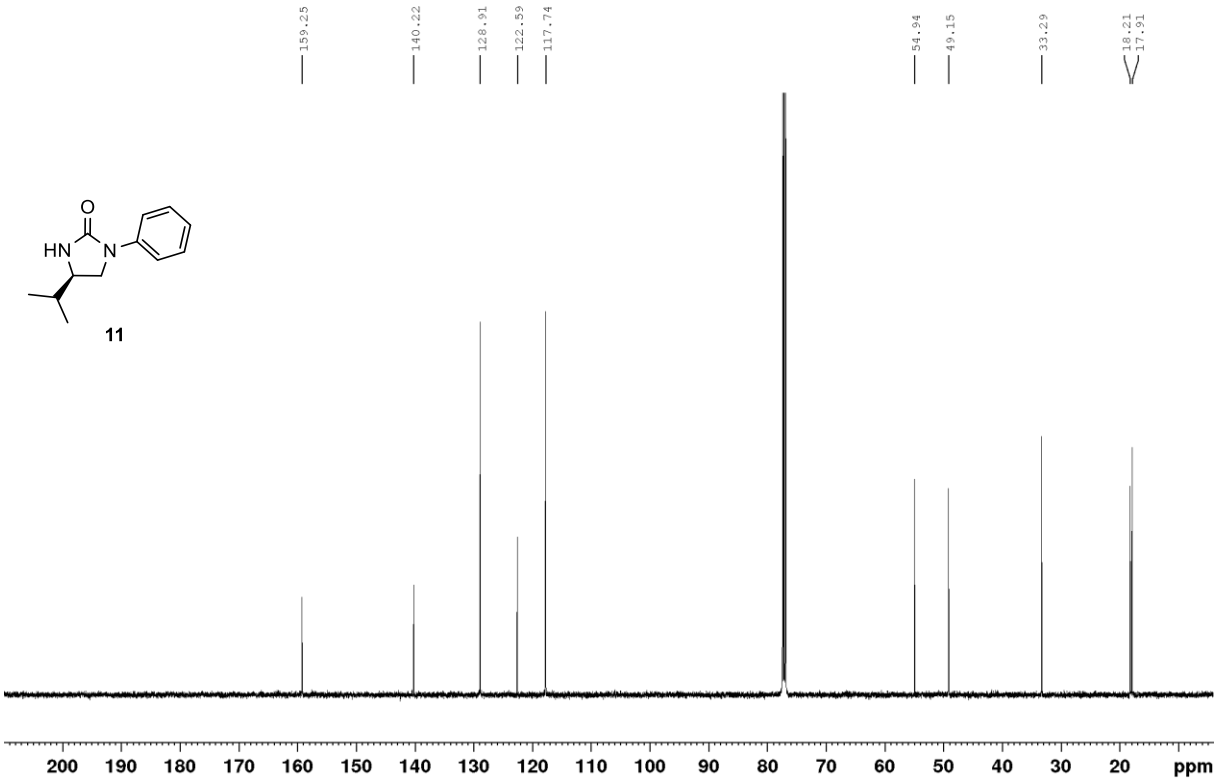

Figure S49. ^{13}C NMR spectrum (126 MHz, $CDCl_3$) of imidazolidinone **11**.

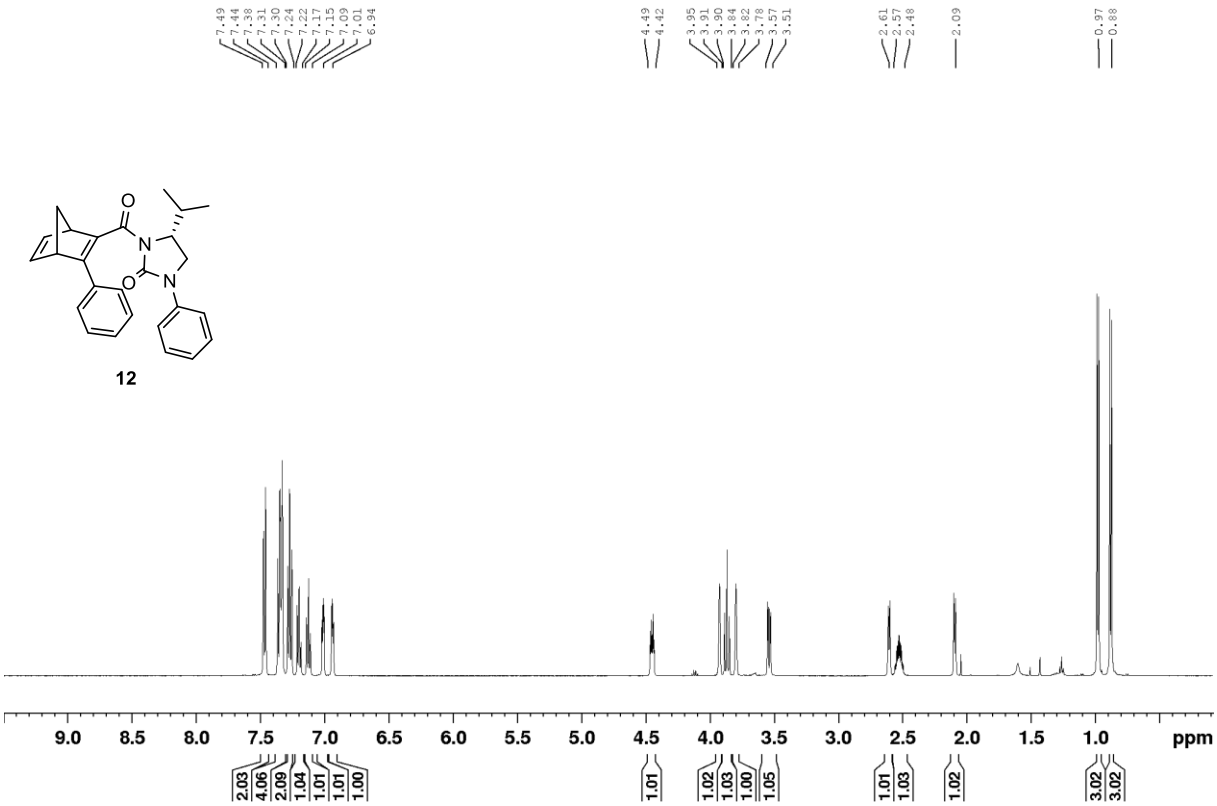

Figure S50. ^{1}H NMR spectrum (500 MHz, $CDCl_3$) of norbornadiene **12**.

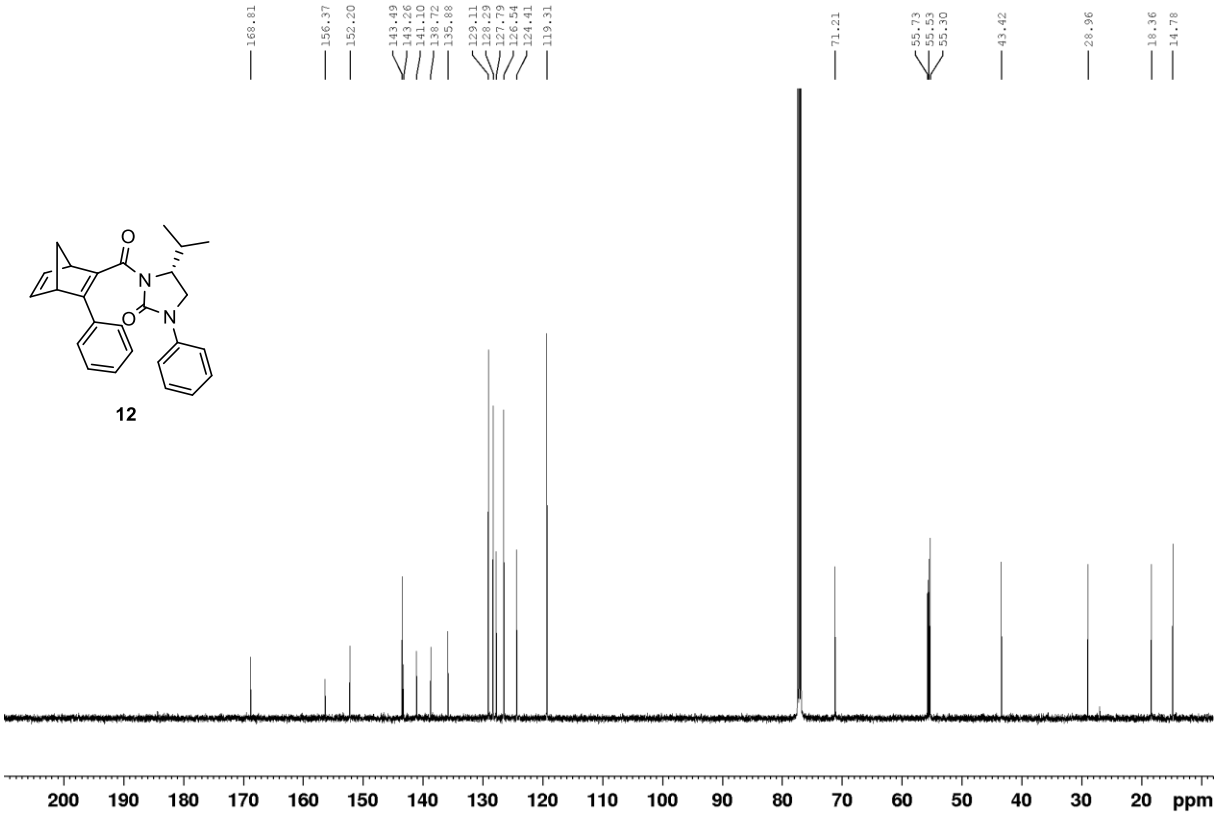

Figure S51. ^{13}C NMR spectrum (126 MHz, $CDCl_3$) of imidazolidinone **12**.

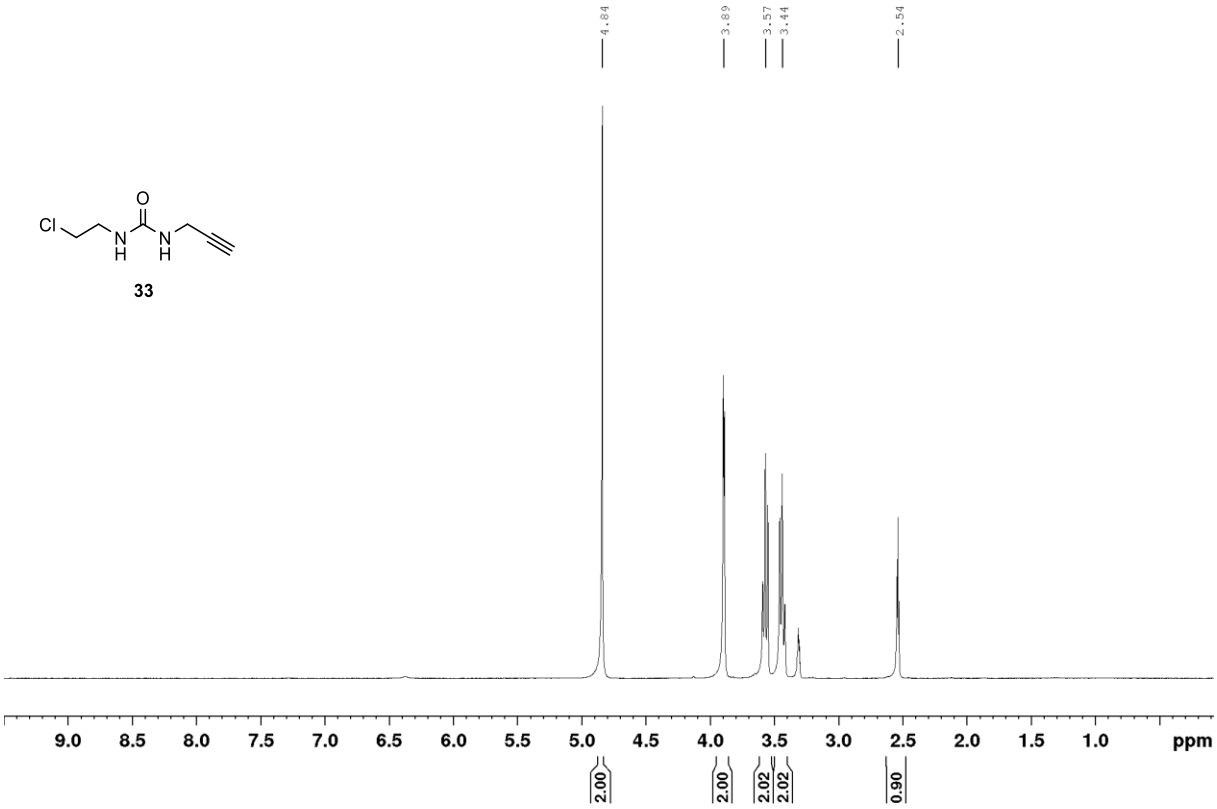

Figure S52. ^{1}H NMR spectrum (300 MHz, CD_3OD) of urea derivative **33**.

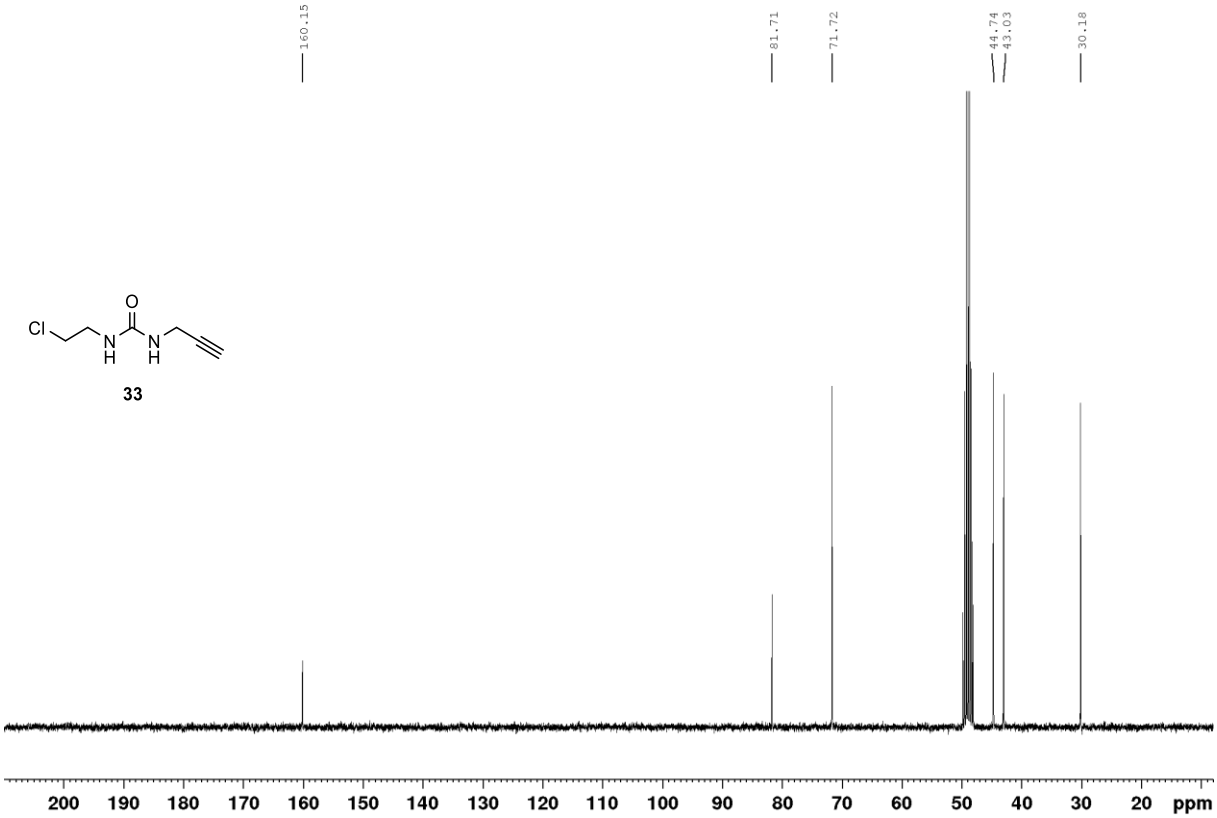

Figure S53. ^{13}C NMR spectrum (75 MHz, CD_3OD) of urea derivative **33**.

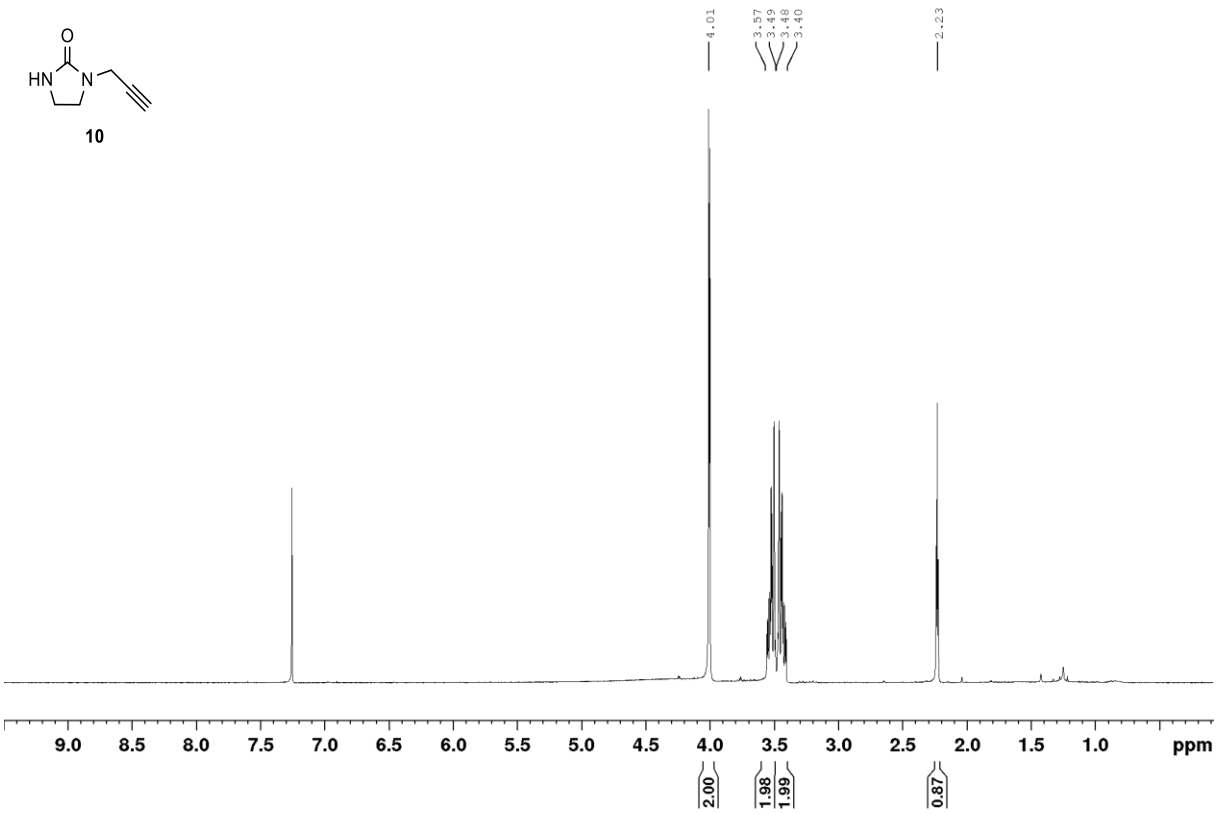

Figure S54. ^{1}H NMR spectrum (300 MHz, $CDCl_3$) of imidazolidinone **10**.

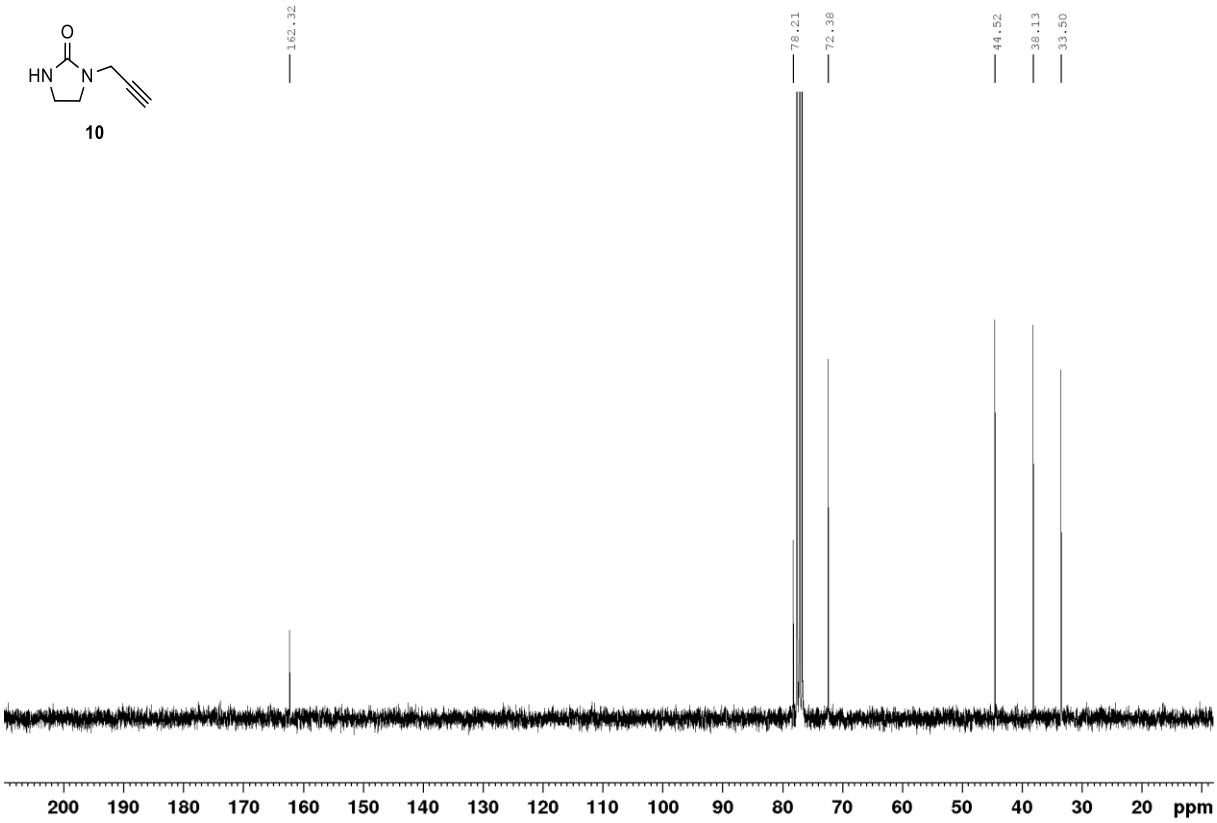

Figure S55. ^{13}C NMR spectrum (75 MHz, $CDCl_3$) of imidazolidinone **10**.

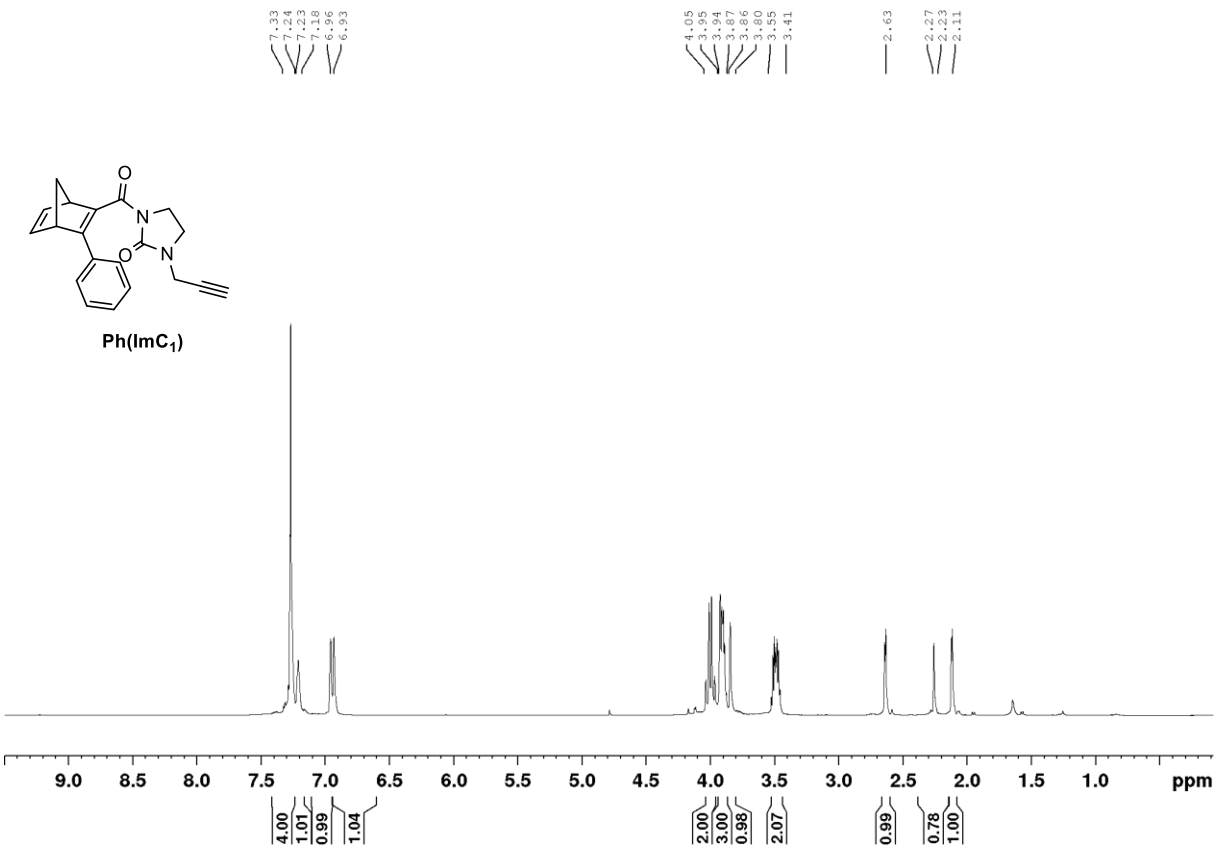

Figure S56. ^{1}H NMR spectrum (700 MHz, $CDCl_3$) of alkyne **Ph(ImC$_1$)**.

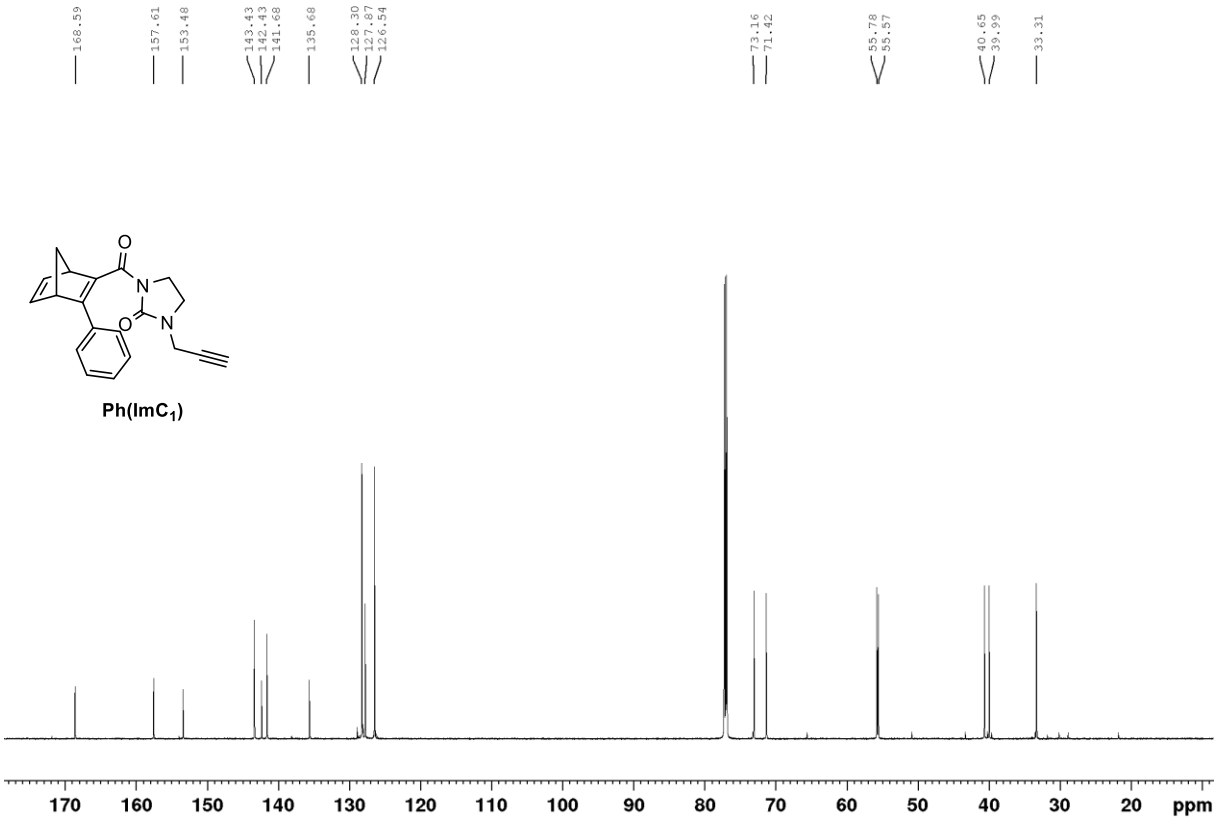

Figure S57. ^{13}C NMR spectrum (176 MHz, $CDCl_3$) of alkyne **Ph(ImC$_1$)**.

2.3 Synthesis of alcohols, alkynes, alkynones and triazoles

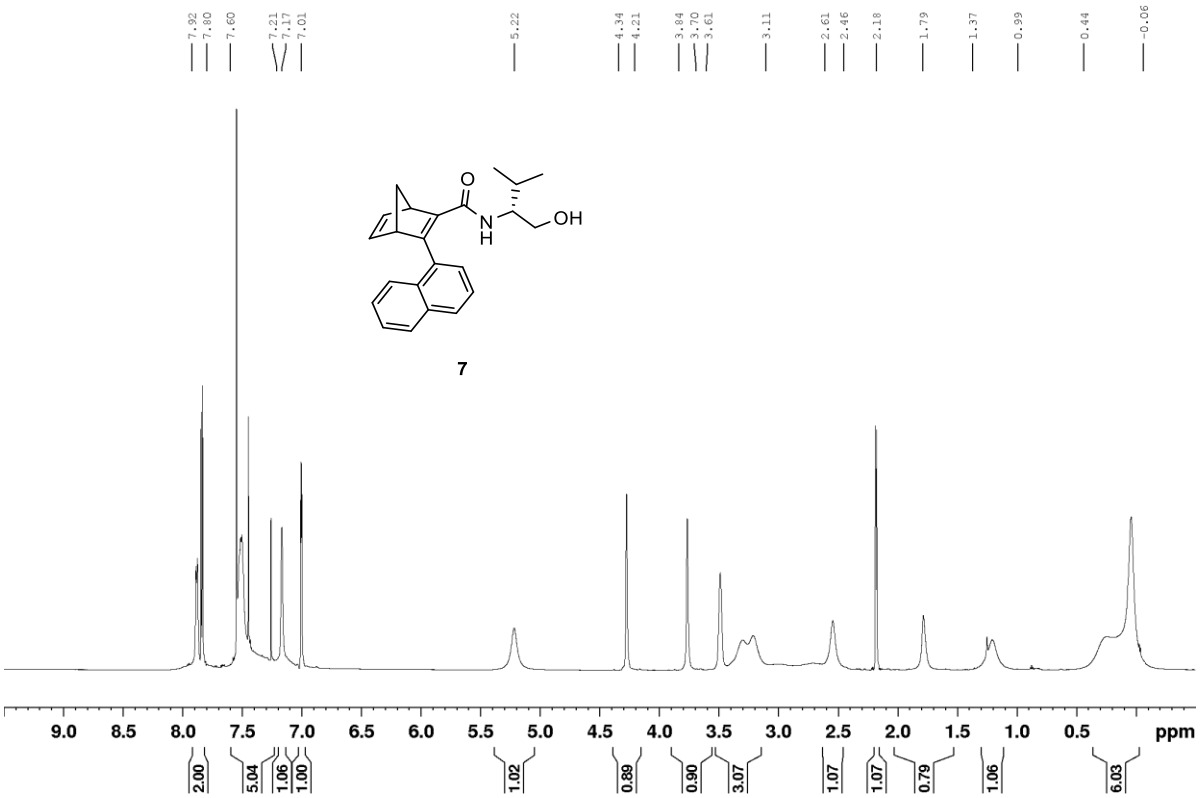

Figure S58. ^{13}C NMR spectrum (700 MHz, $CDCl_3$) of alcohol **7**.

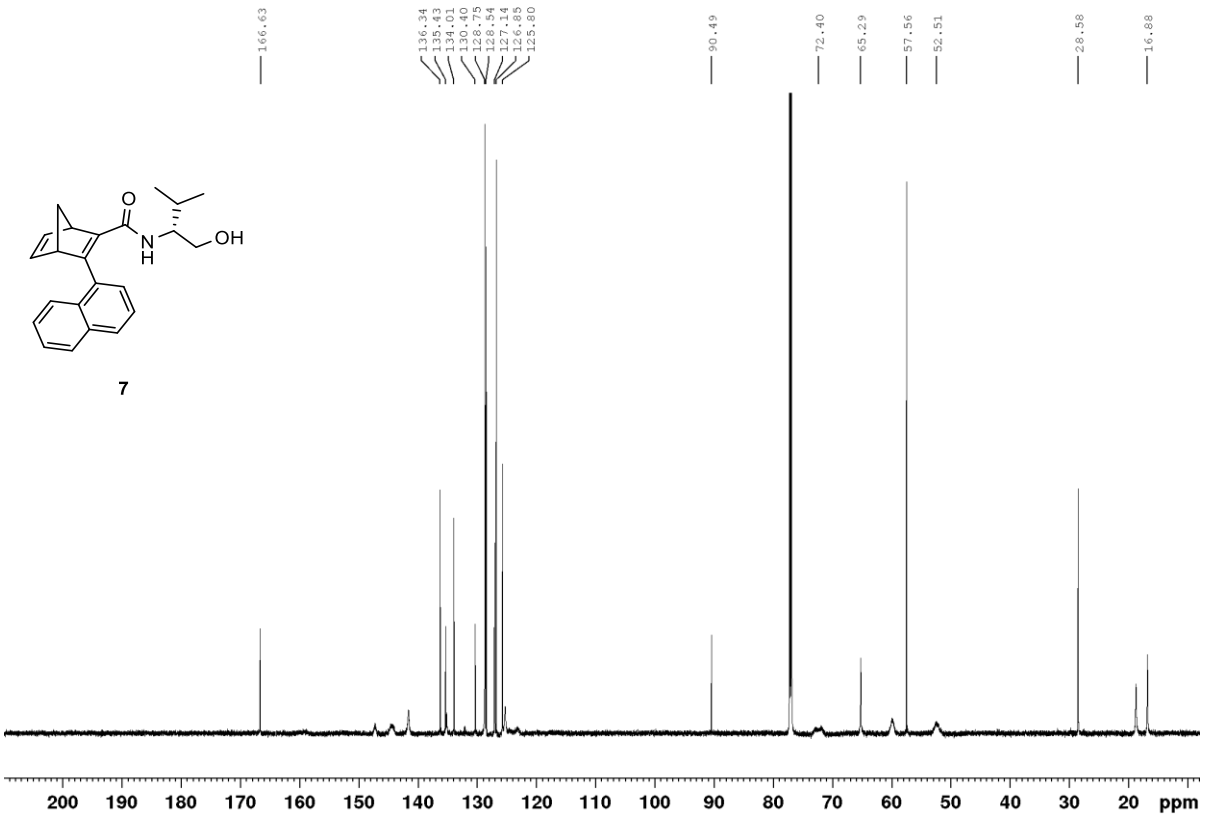

Figure S59. ^{13}C NMR spectrum (176 MHz, $CDCl_3$) of alcohol **7**.

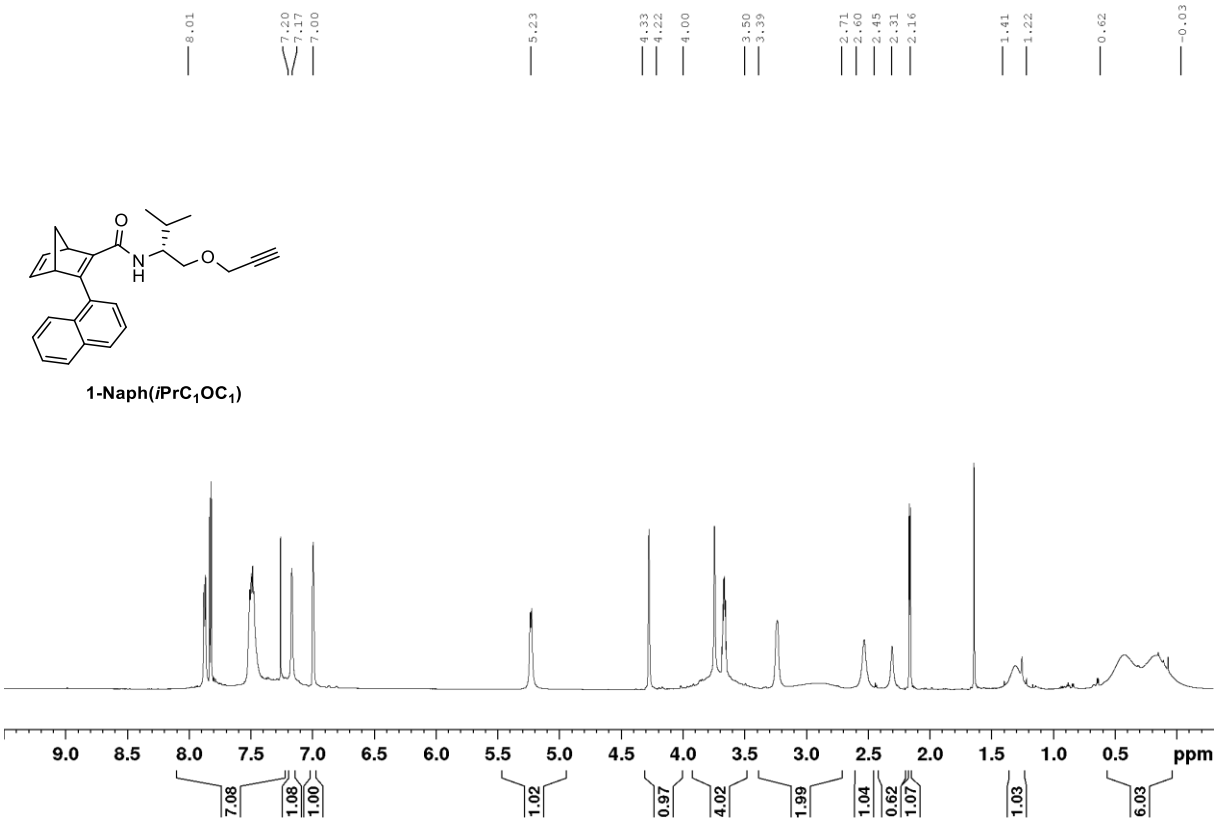

Figure S60. ^{1}H NMR spectrum (700 MHz, $CDCl_3$) of alkyne **1-Naph(*i*PrC$_1$OC$_1$)**.

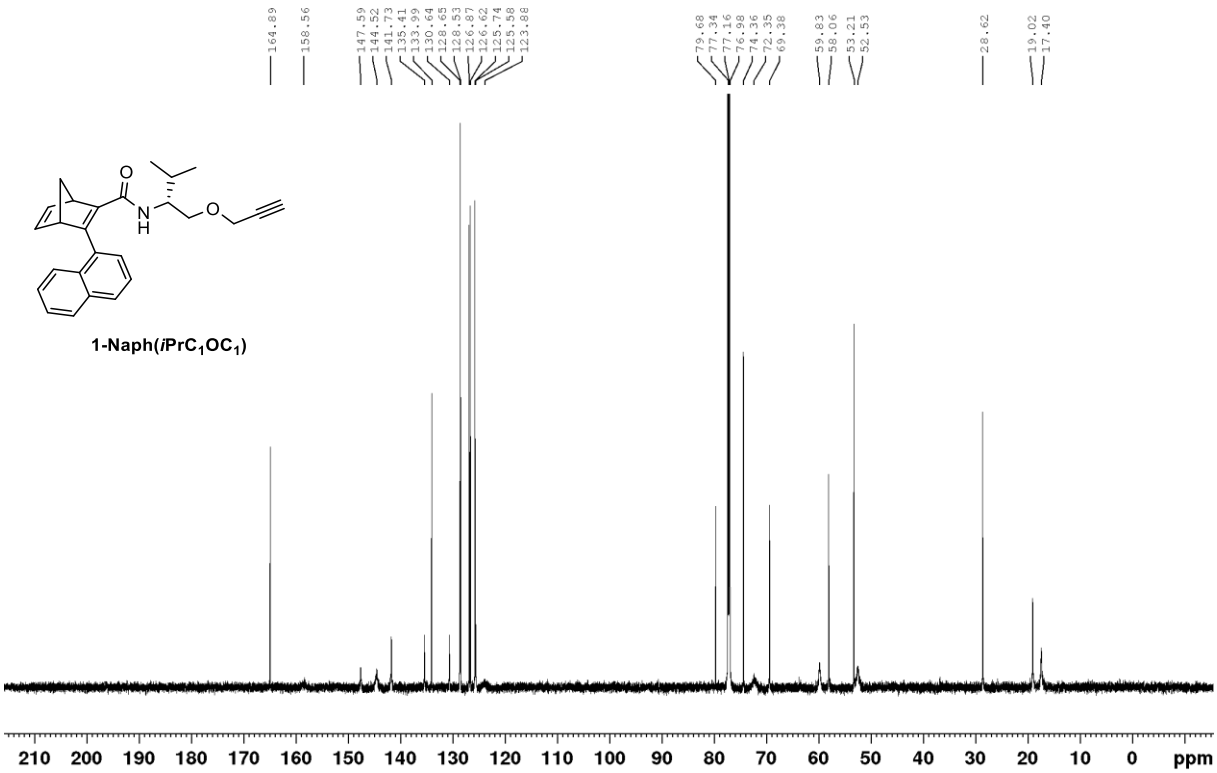

Figure S61. ^{13}C NMR spectrum (176 MHz, $CDCl_3$) of alkyne **1-Naph(*i*PrC$_1$OC$_1$)**.

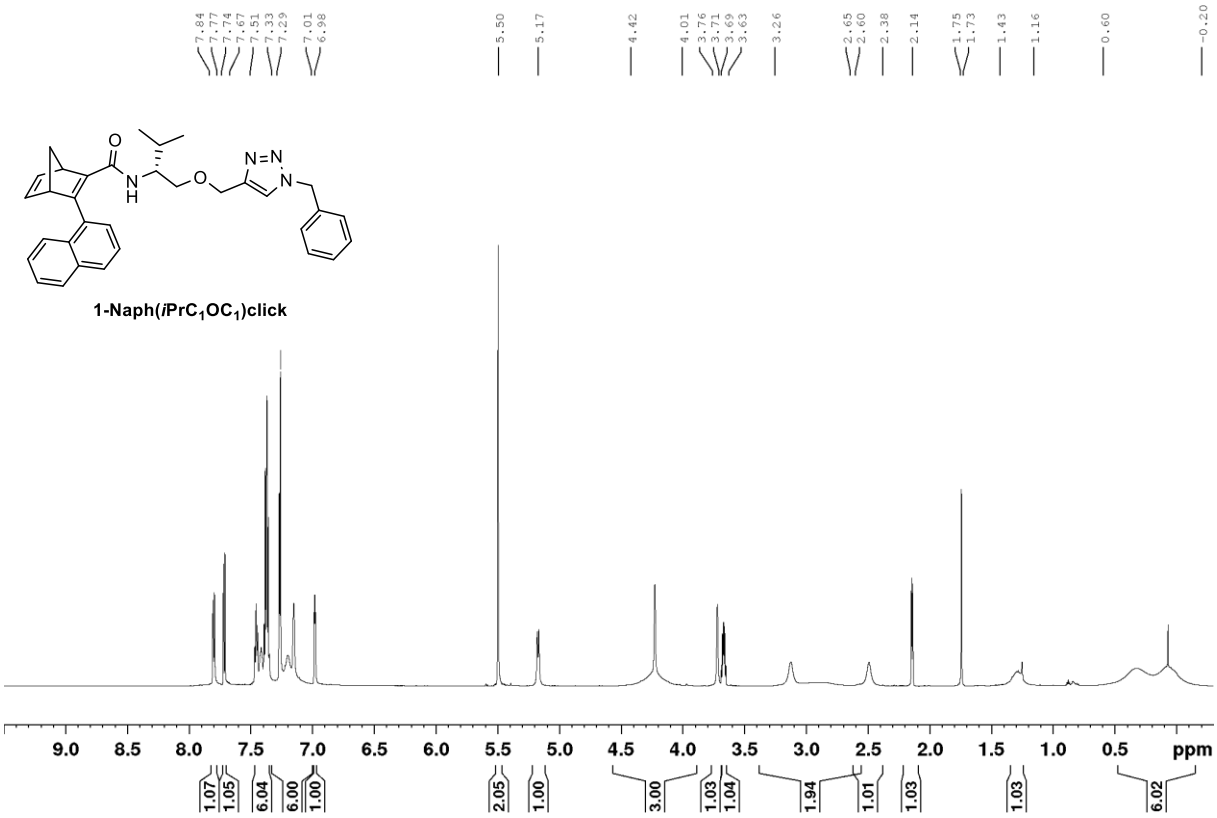

Figure S62. ^{1}H NMR spectrum (700 MHz, $CDCl_3$) of triazole **1-Naph(*i*PrC$_1$OC$_1$)click**.

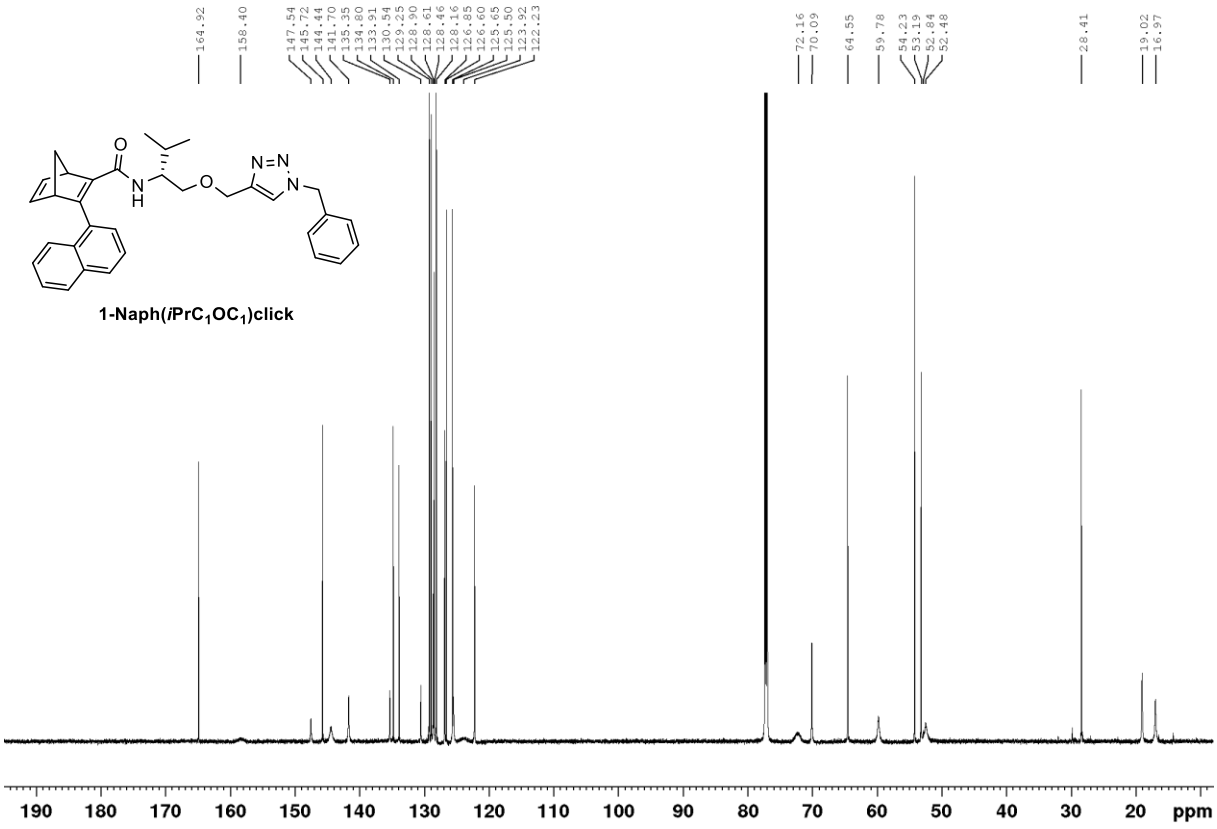

Figure S63. ^{13}C NMR spectrum (176 MHz, $CDCl_3$) of triazole **1-Naph(*i*PrC$_1$OC$_1$)click**.

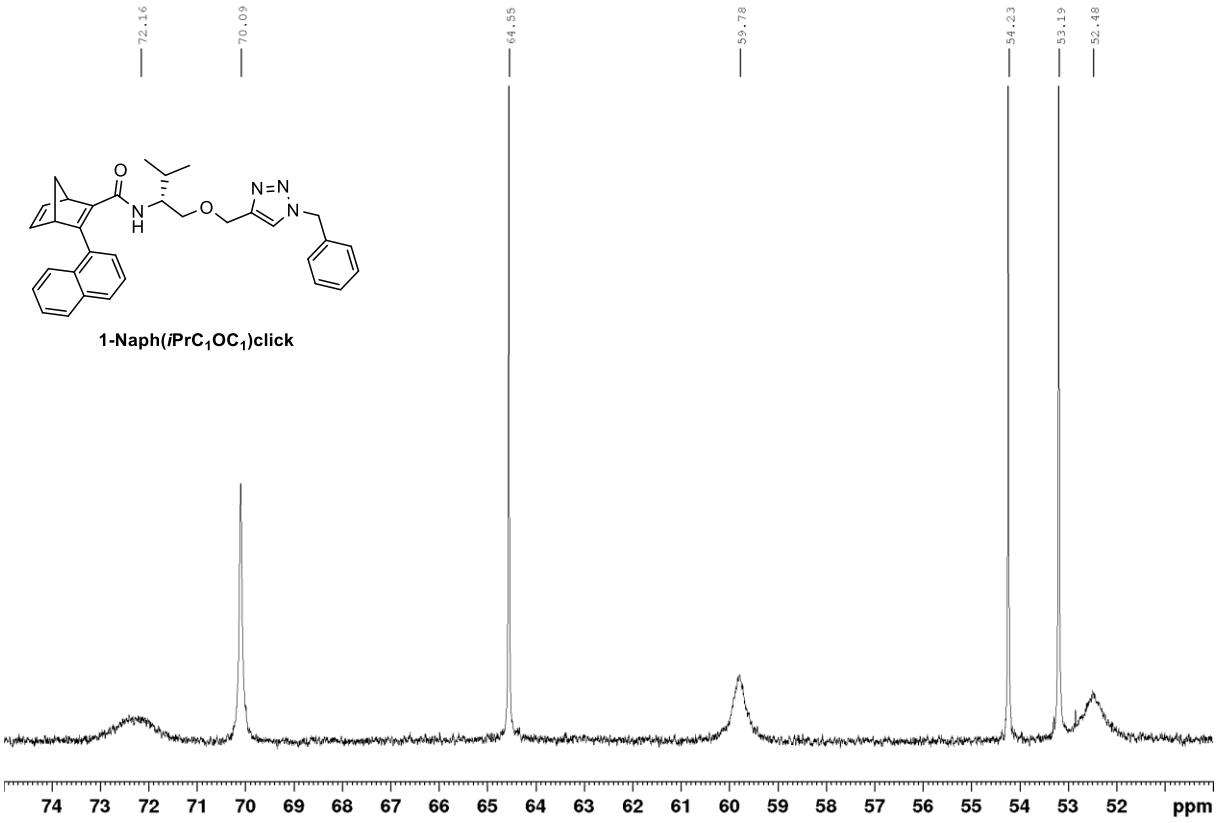

Figure S64. ^{13}C NMR spectrum (176 MHz, $CDCl_3$, δ = 50 – 75 ppm) of triazole **1-Naph(*i*PrC$_1$OC$_1$)click**.

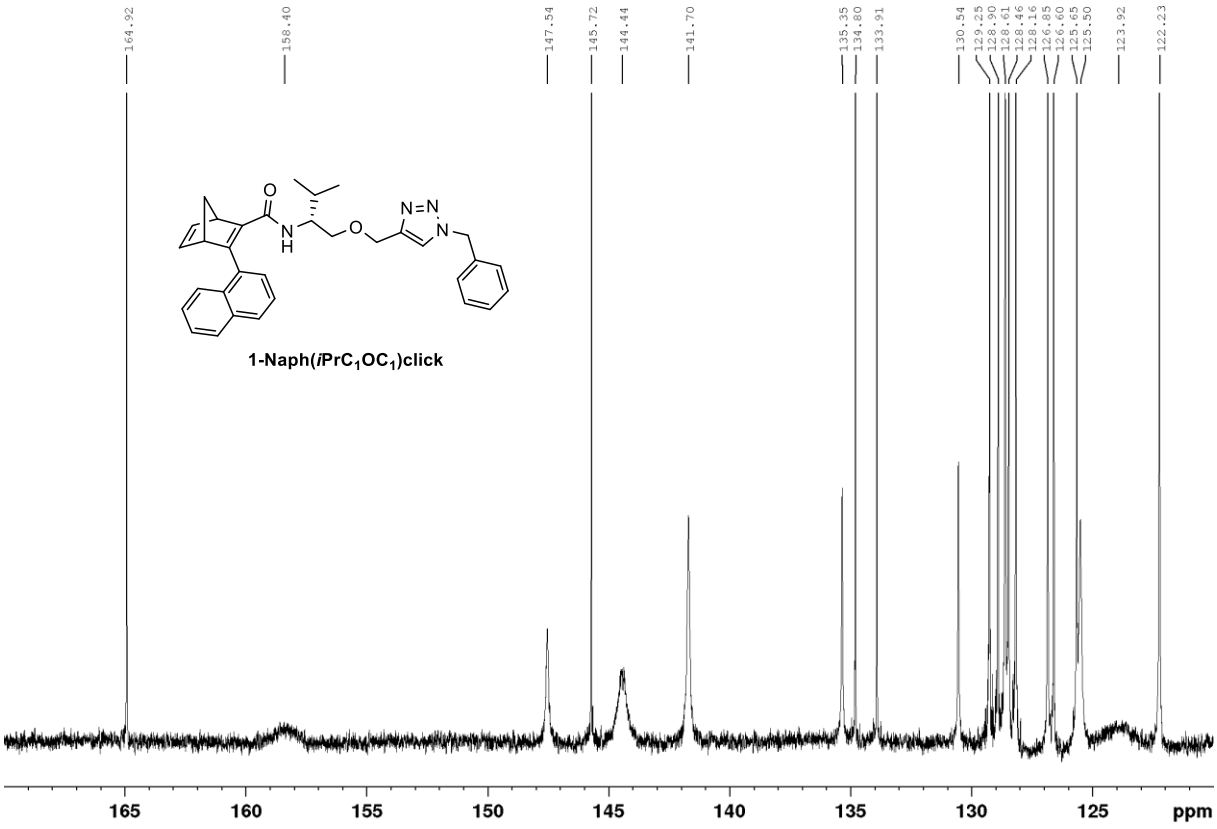

Figure S65. ^{13}C NMR spectrum (176 MHz, $CDCl_3$, δ = 120 – 170 ppm) of triazole **1-Naph(*i*PrC$_1$OC$_1$)click**.

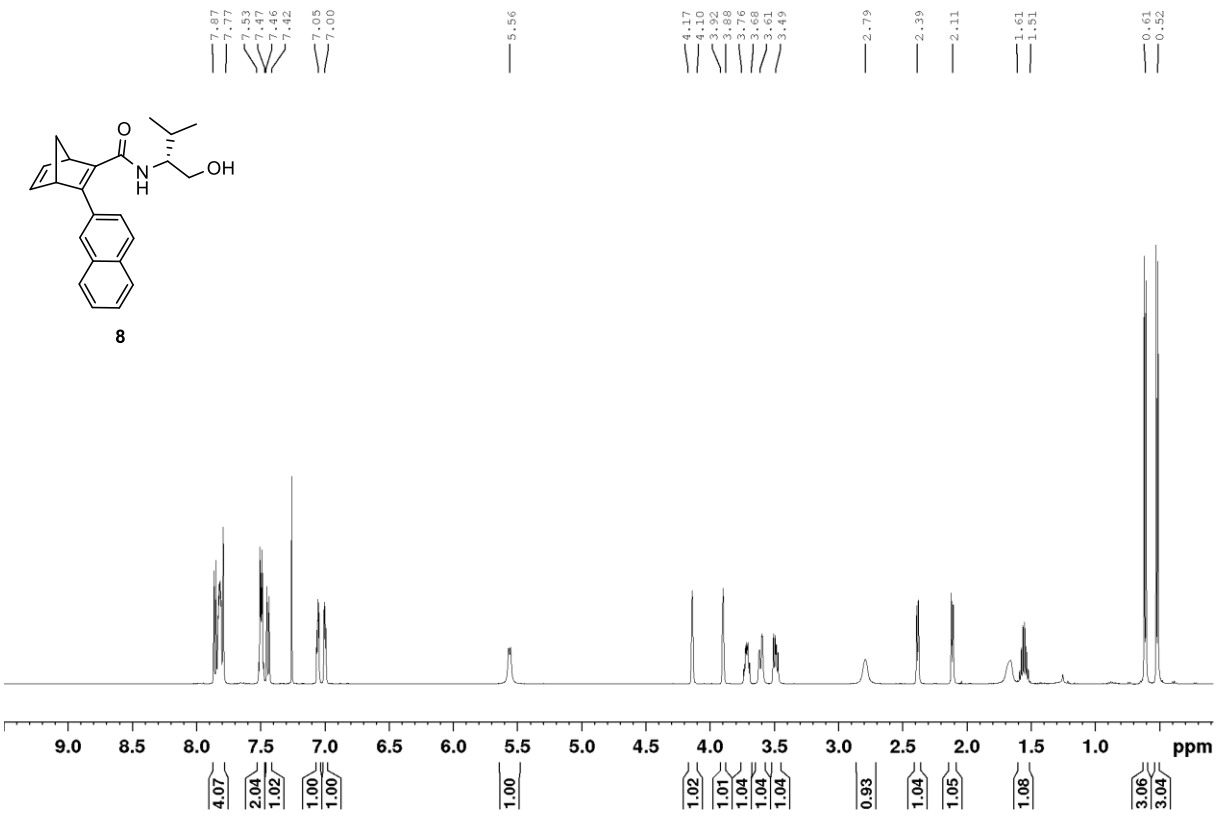

Figure S66. ^{1}H NMR spectrum (500 MHz, $CDCl_3$) of alcohol **8**.

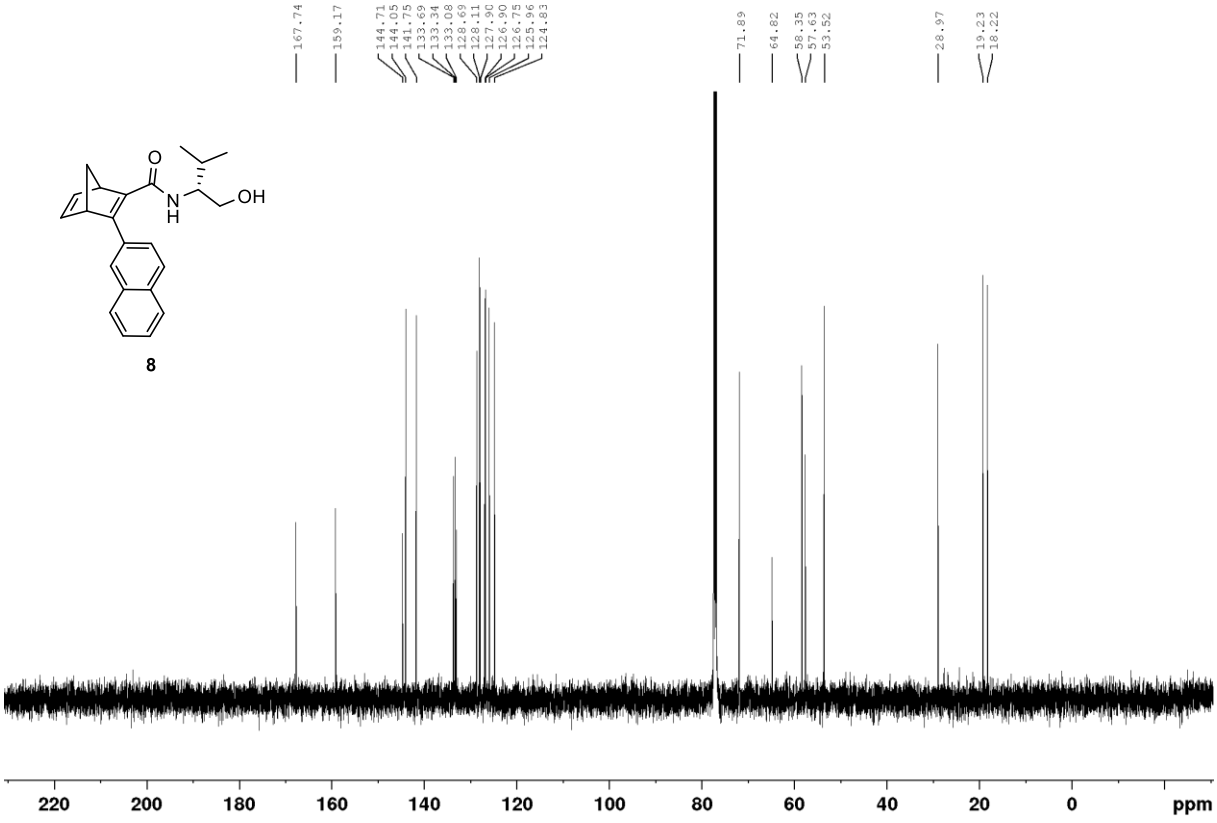

Figure S67. ^{13}C NMR spectrum (126 MHz, $CDCl_3$) of alcohol **8**.

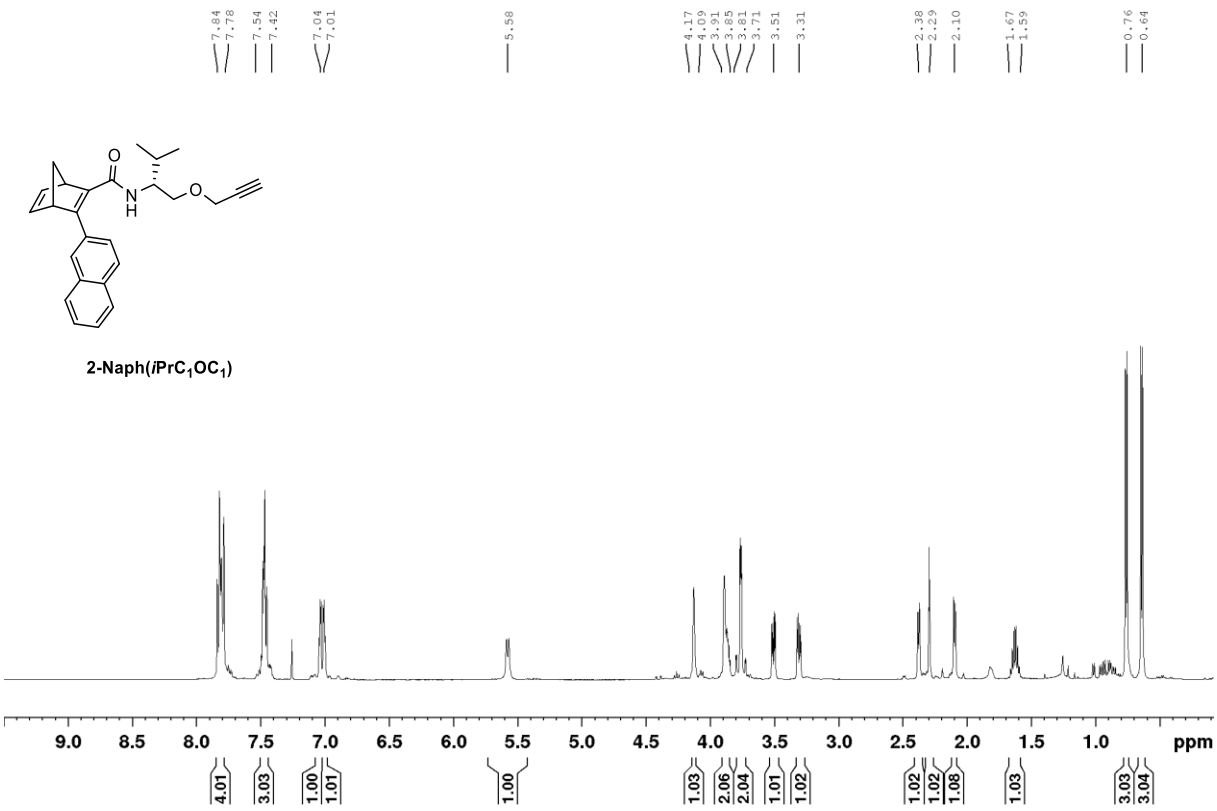

Figure S68. ^{1}H NMR spectrum (500 MHz, $CDCl_3$) of alkyne **2-Naph(*i*PrC$_1$OC$_1$)**.

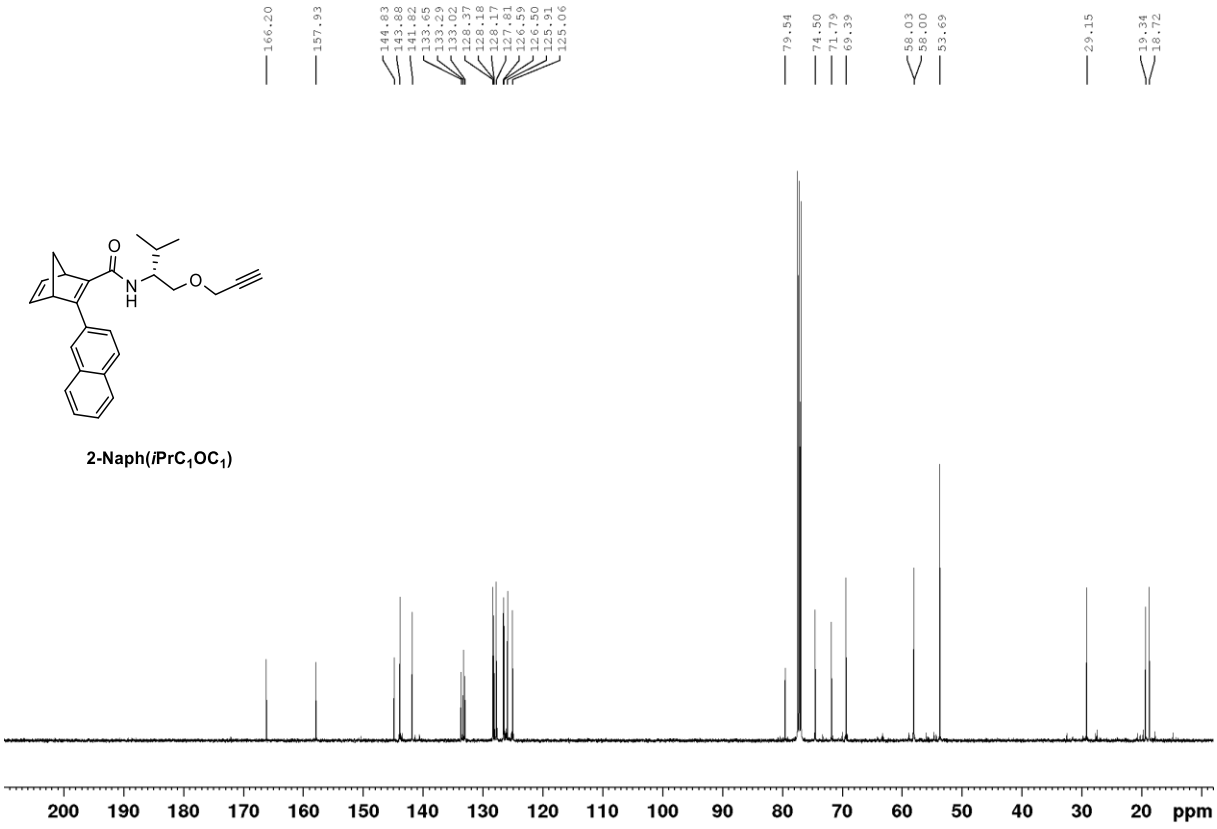

Figure S69. ^{13}C NMR spectrum (126 MHz, $CDCl_3$) of alkyne **2-Naph(*i*PrC$_1$OC$_1$)**.

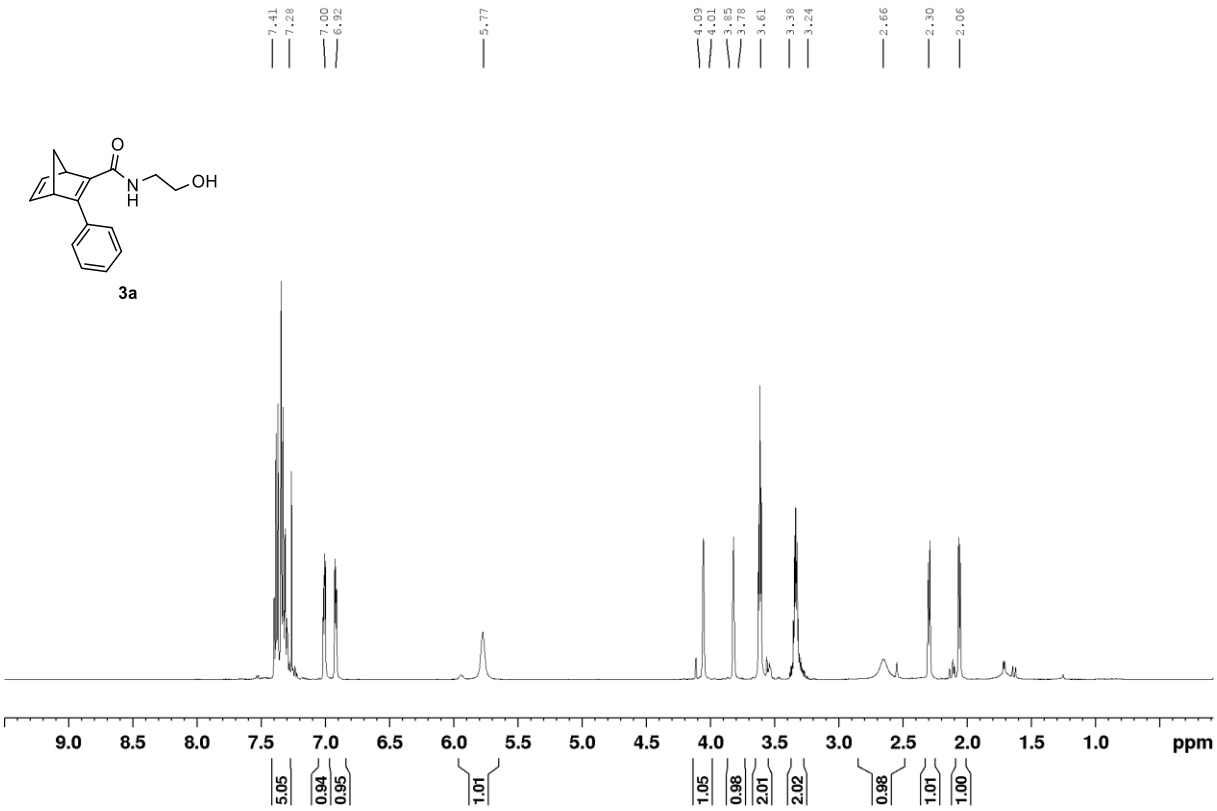

Figure S70. ^{1}H NMR spectrum (500 MHz, $CDCl_3$) of alcohol **3a**.

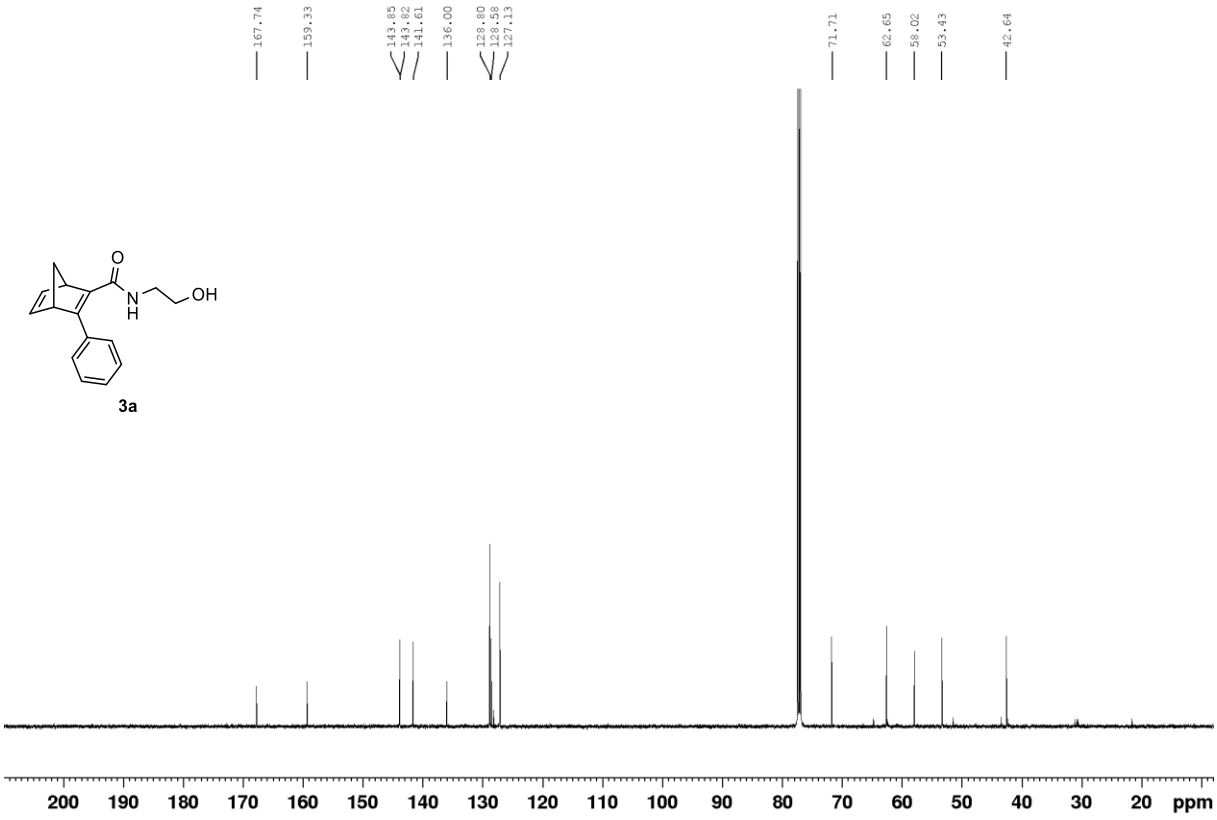

Figure S71. ^{1}H NMR spectrum (126 MHz, $CDCl_3$) of alcohol **3a**.

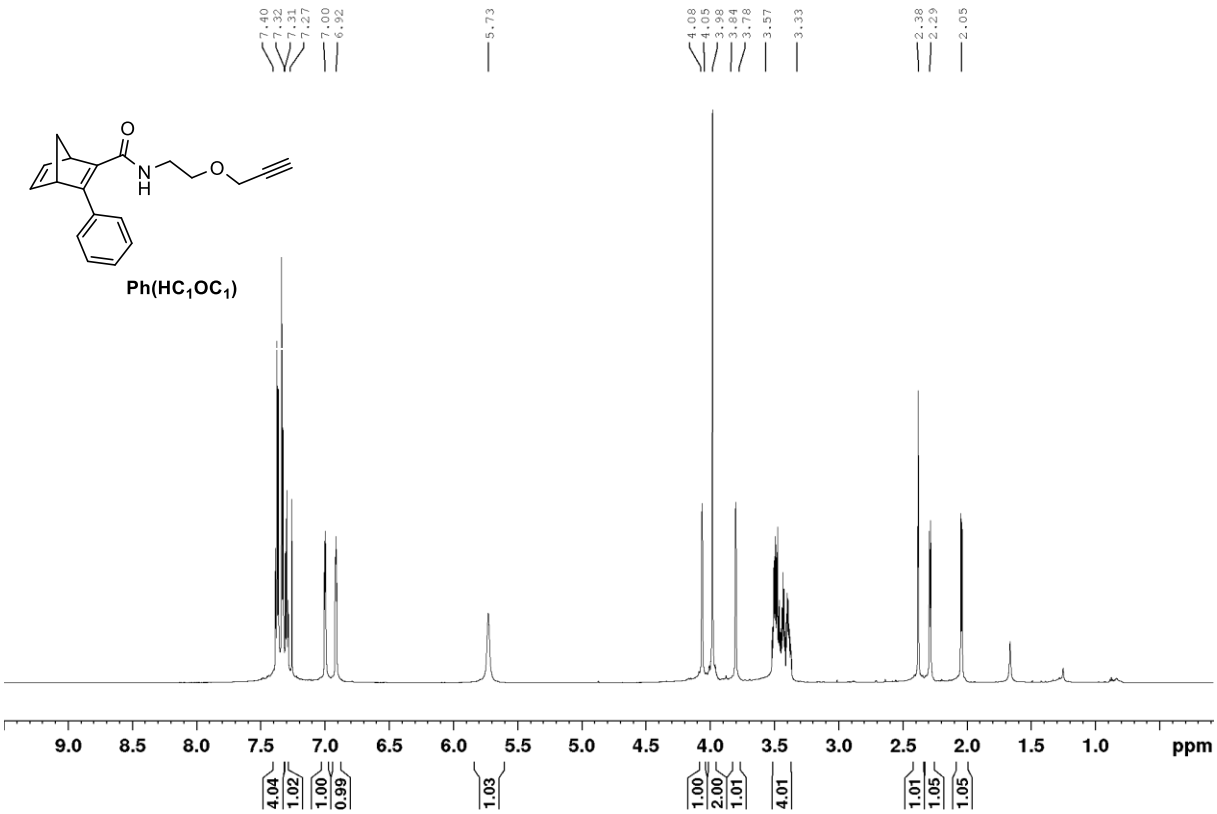

Figure S72. ^{1}H NMR spectrum (700 MHz, $CDCl_3$) of alkyne **Ph(HC$_1$OC$_1$)**.

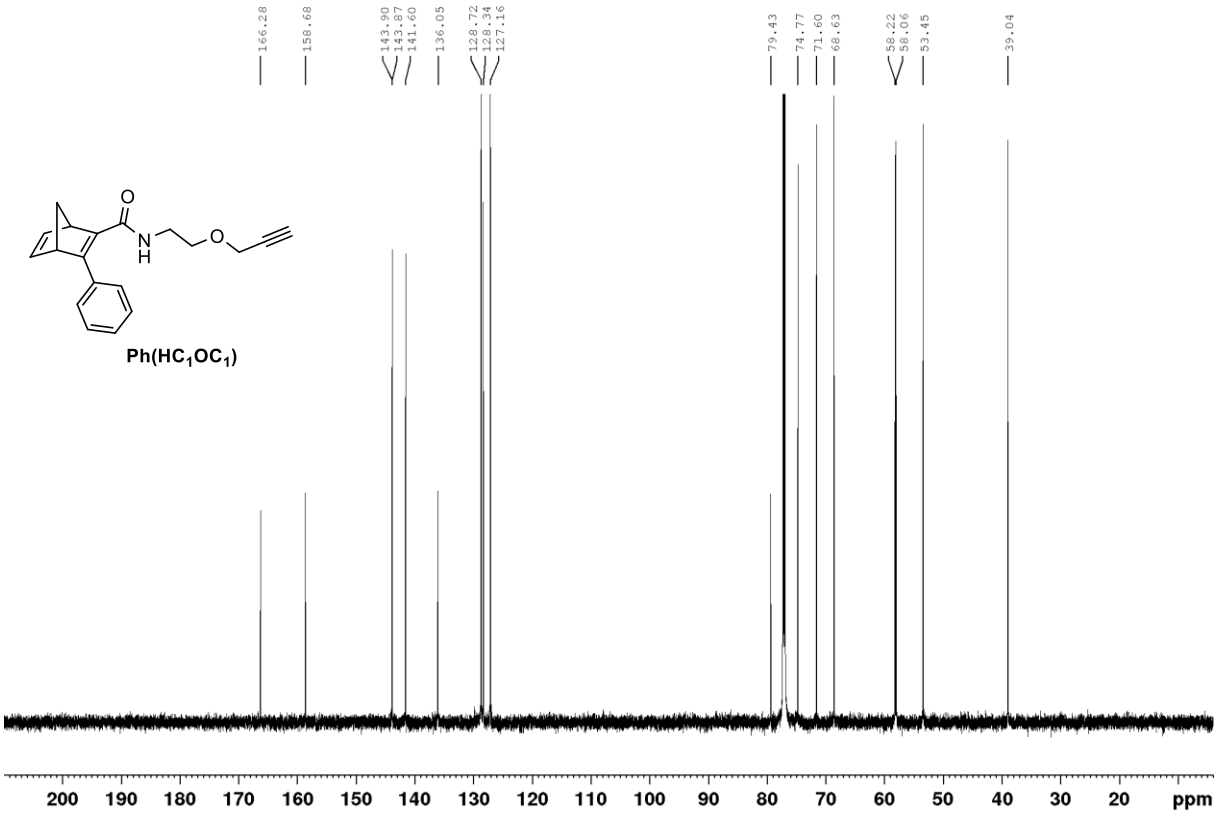

Figure S73. ^{13}C NMR spectrum (176 MHz, $CDCl_3$) of alkyne **Ph(HC$_1$OC$_1$)**.

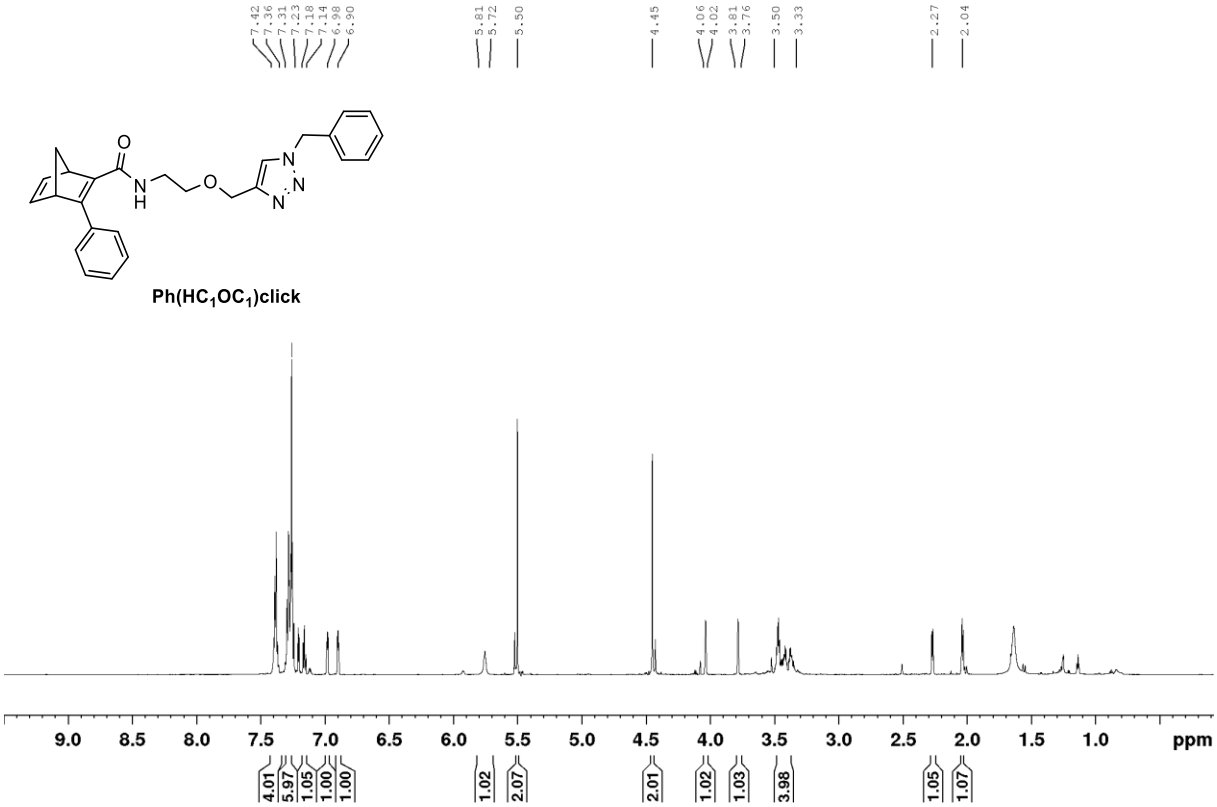

Figure 74 ^{1}H NMR spectrum (700 MHz, $CDCl_3$) of triazole **Ph(HC$_1$OC$_1$)click**.

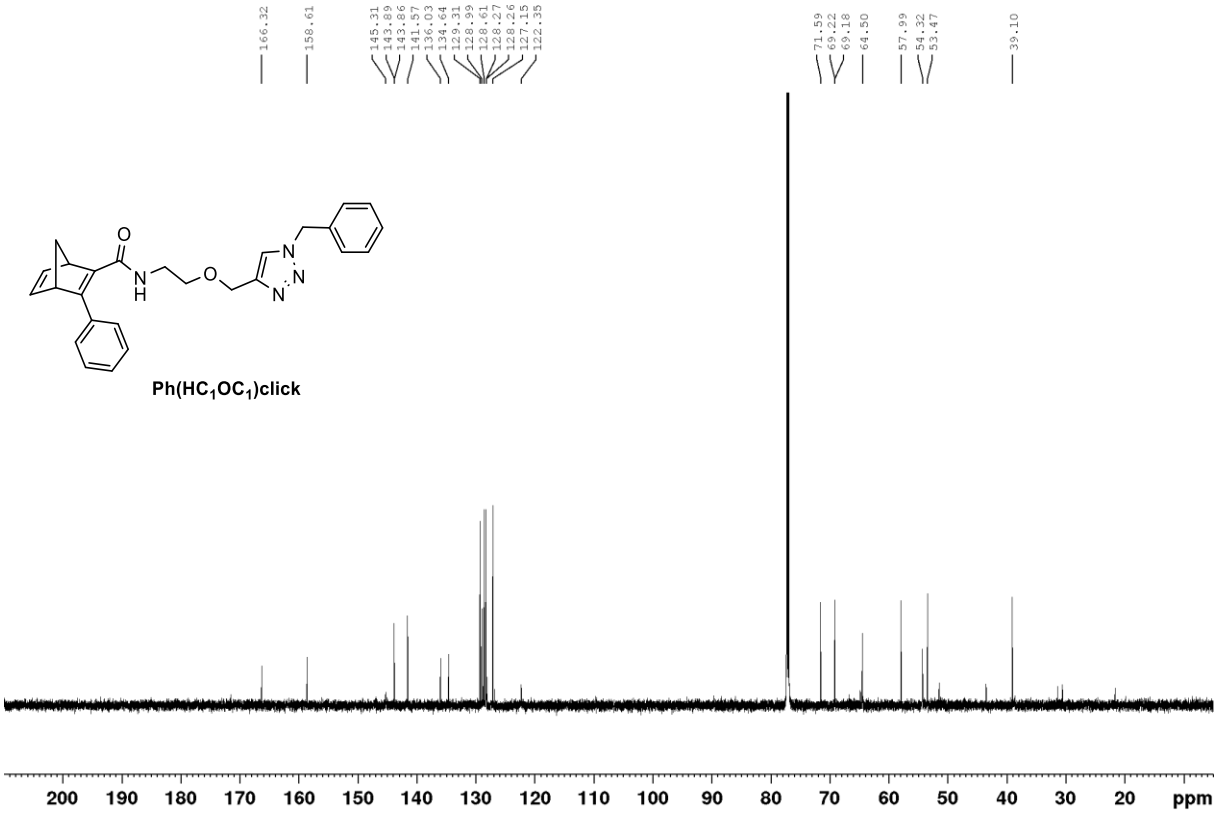

Figure S75. ^{13}C NMR spectrum (176 MHz, $CDCl_3$) of triazole **Ph(HC$_1$OC$_1$)click**.

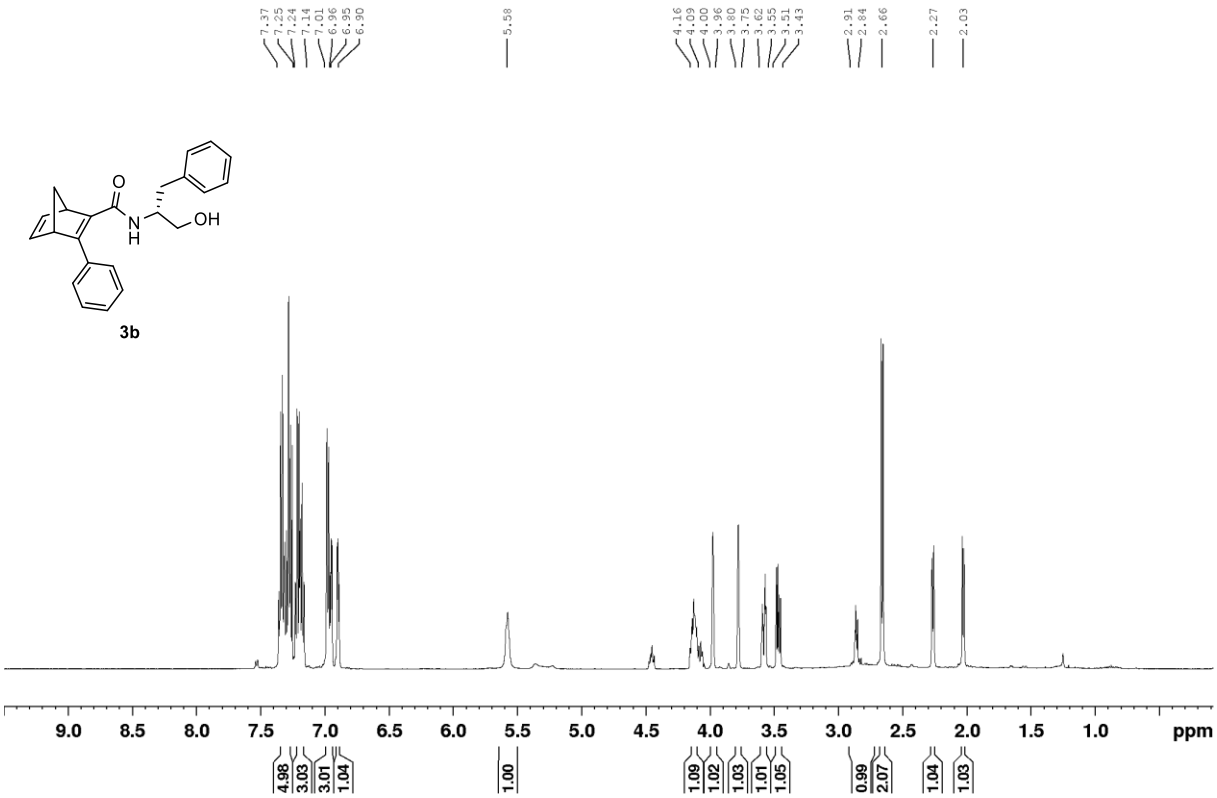

Figure S76. ^{1}H NMR spectrum (500 MHz, $CDCl_3$) of alcohol **3b**.

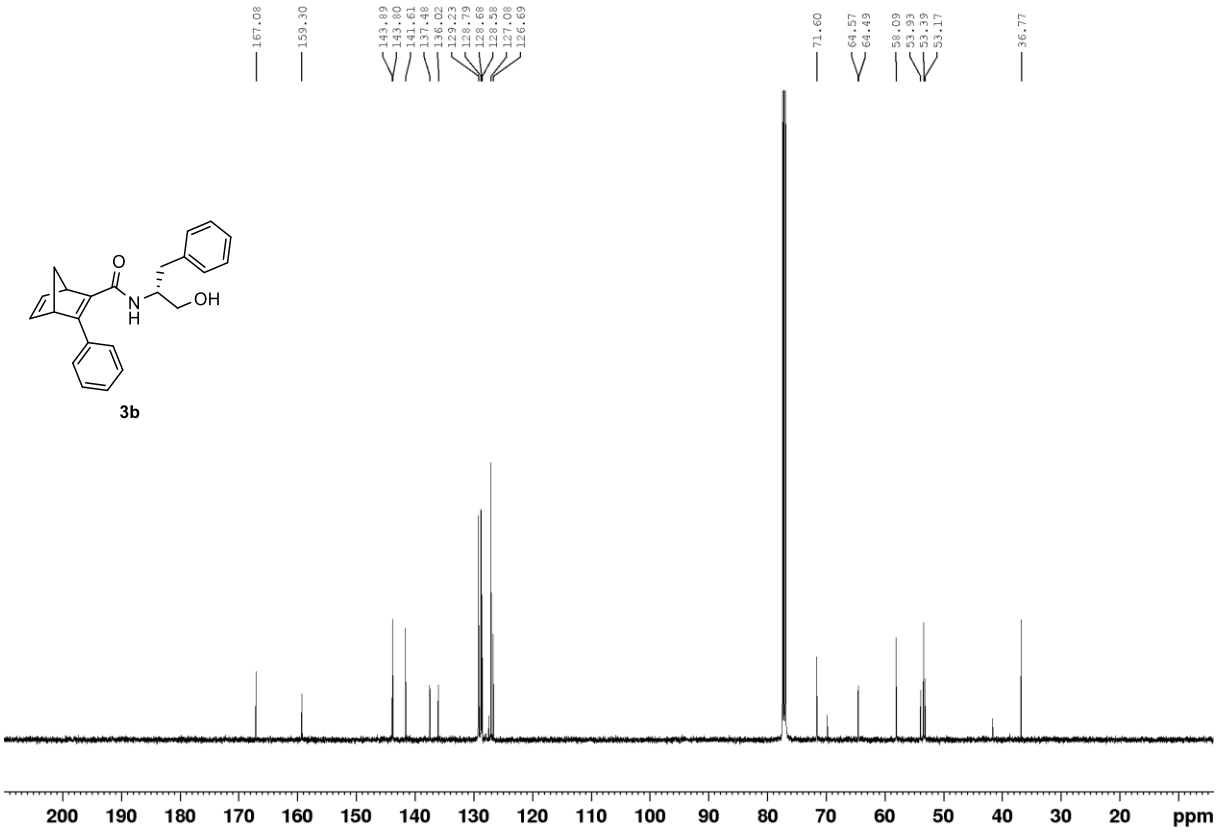

Figure S77. ^{13}C NMR spectrum (126 MHz, $CDCl_3$) of alcohol **3b**.

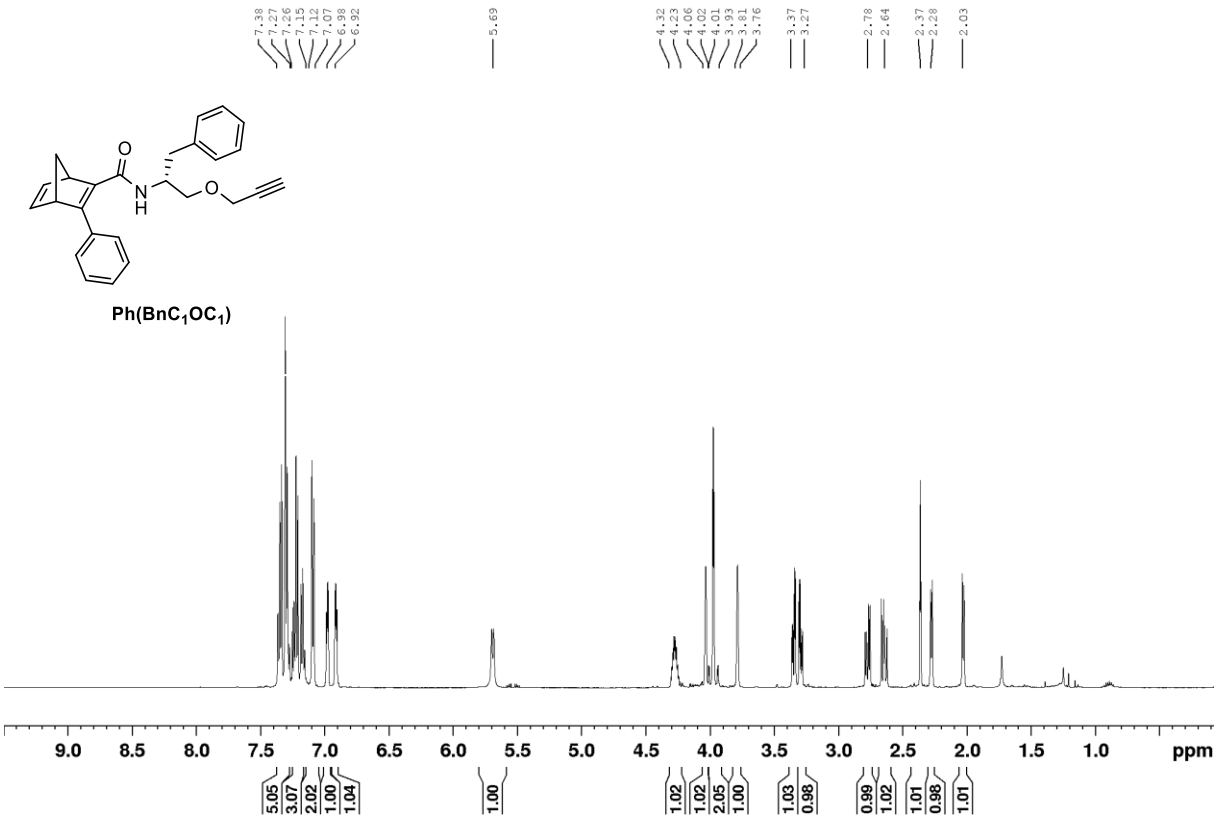

Figure S78. ^{1}H NMR spectrum (500 MHz, $CDCl_3$) of alkyne **Ph(BnC$_1$OC$_1$)**.

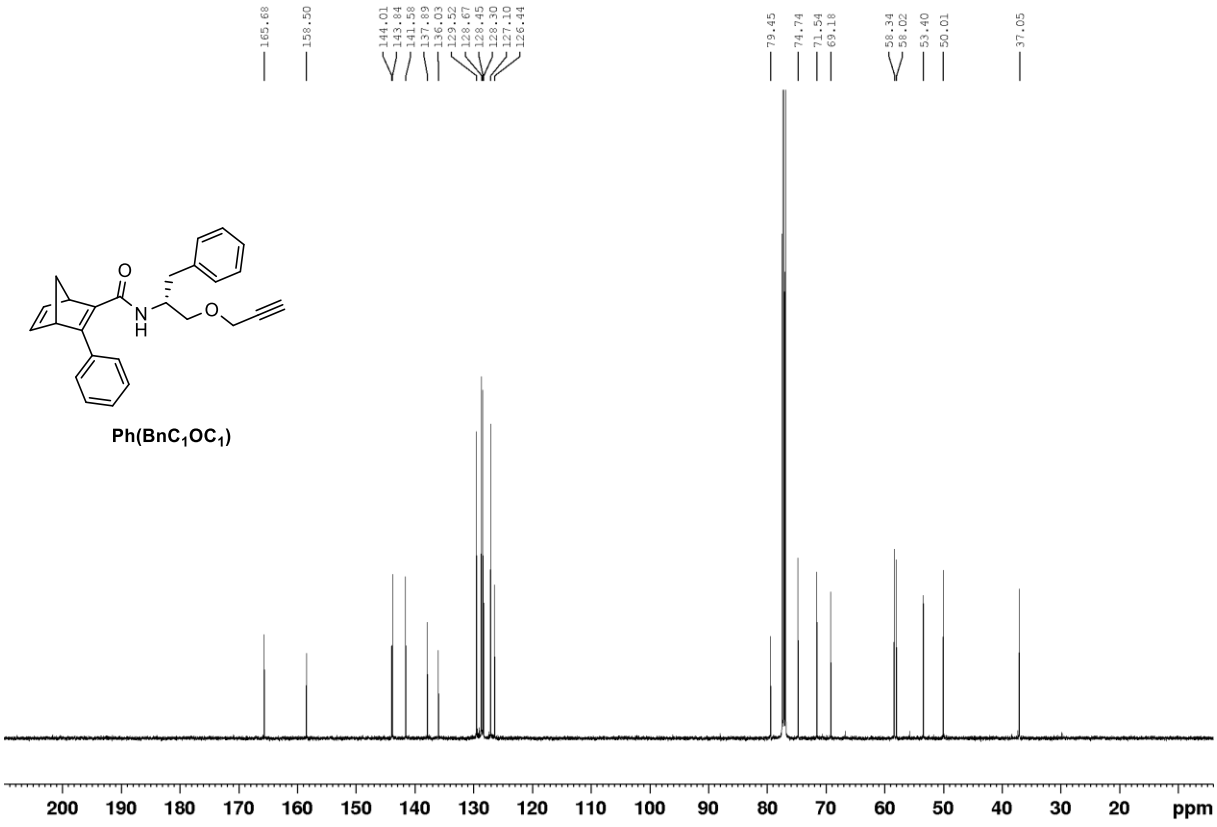

Figure S79. ^{13}C NMR spectrum (126 MHz, $CDCl_3$) of alkyne **Ph(BnC$_1$OC$_1$)**.

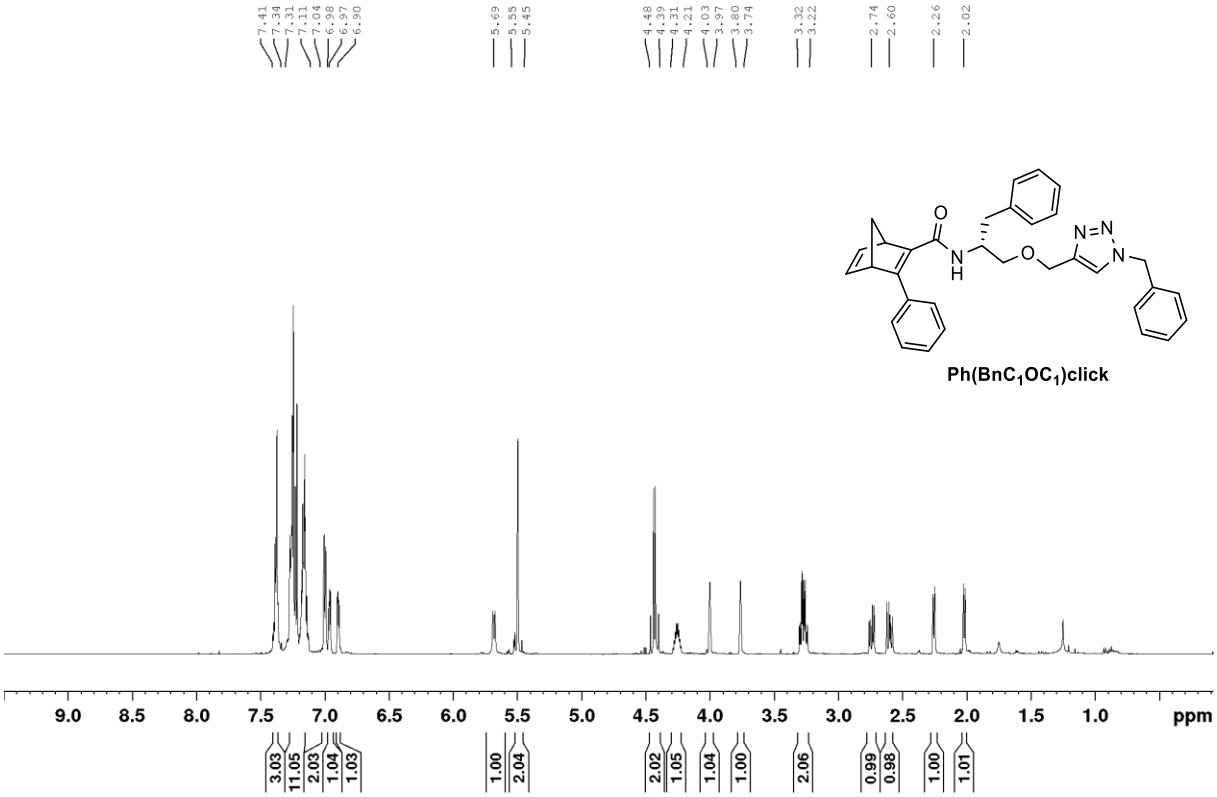

Figure S80. ^{1}H NMR spectrum (500 MHz, $CDCl_3$) of triazole **Ph(BnC$_1$OC$_1$)click.**

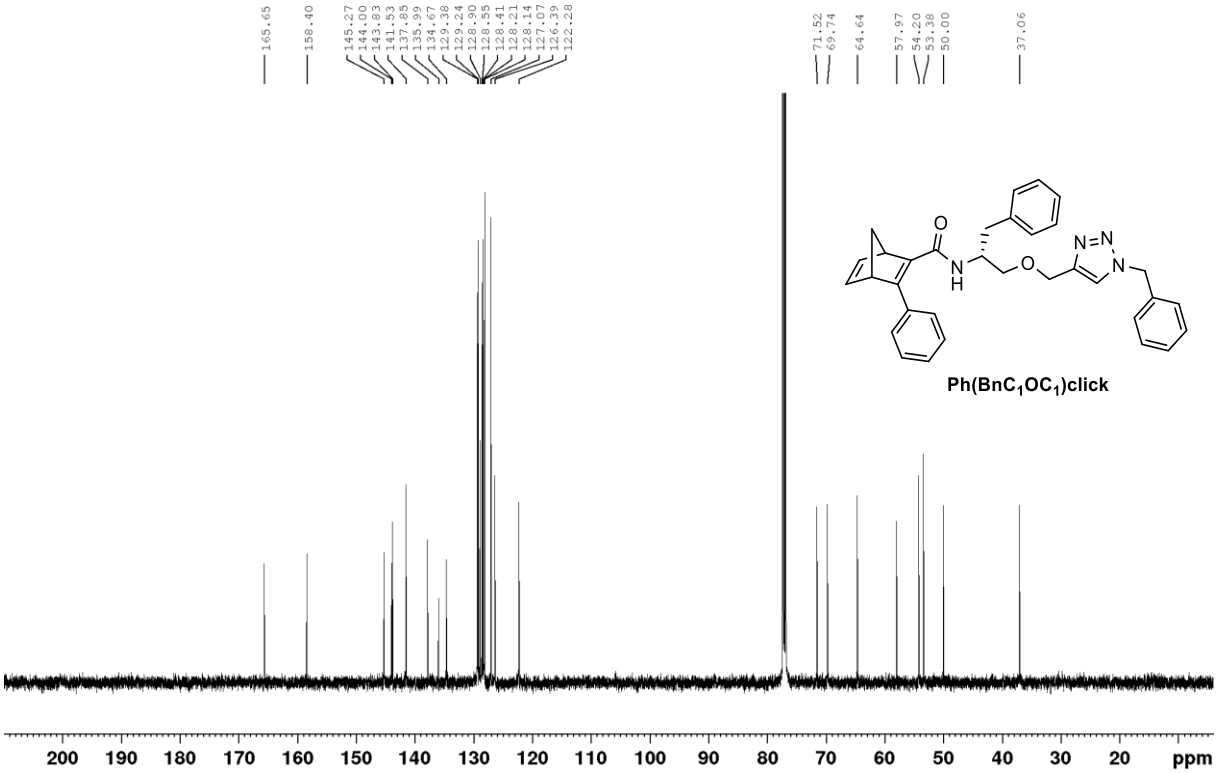

Figure S81. ^{13}C NMR spectrum (126 MHz, $CDCl_3$) of triazole **Ph(BnC$_1$OC$_1$)click.**

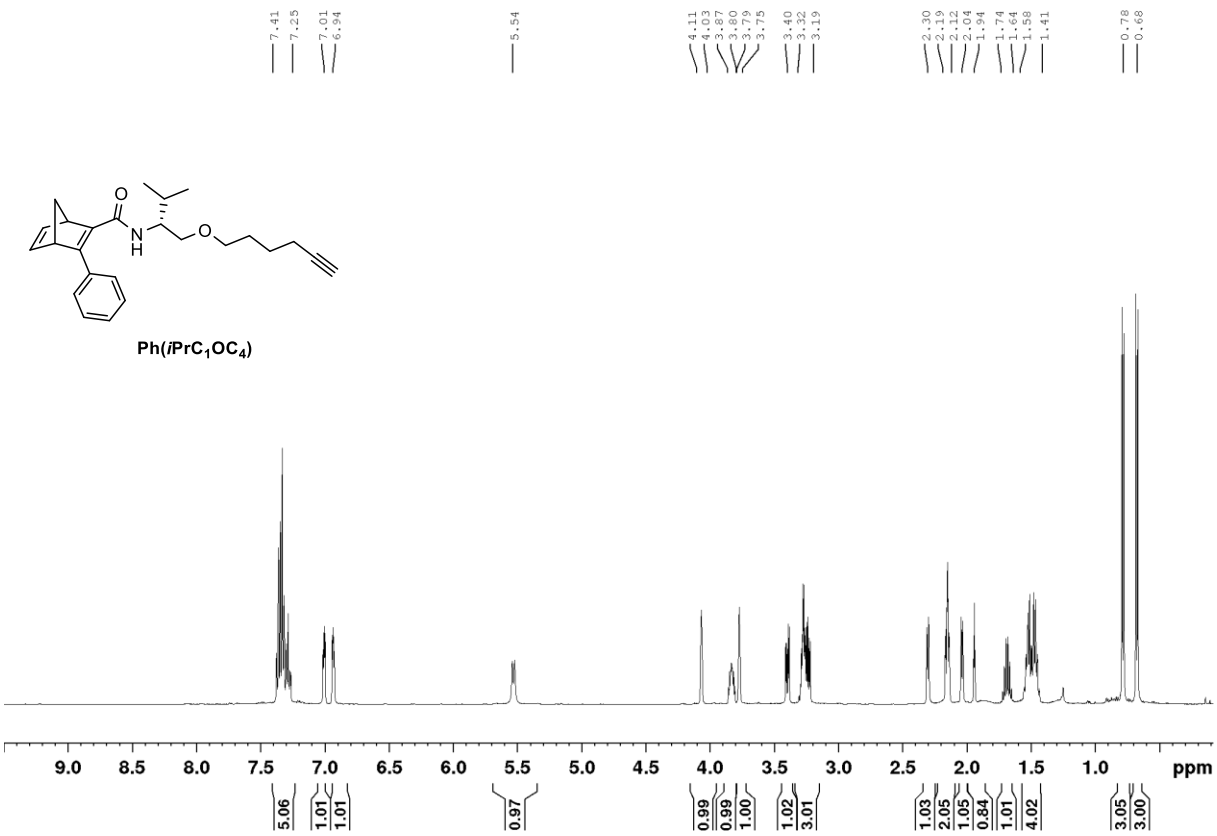

Figure S82. ^{1}H NMR spectrum (500 MHz, $CDCl_3$) of alkyne **Ph(*i*PrC$_1$OC$_4$)**.

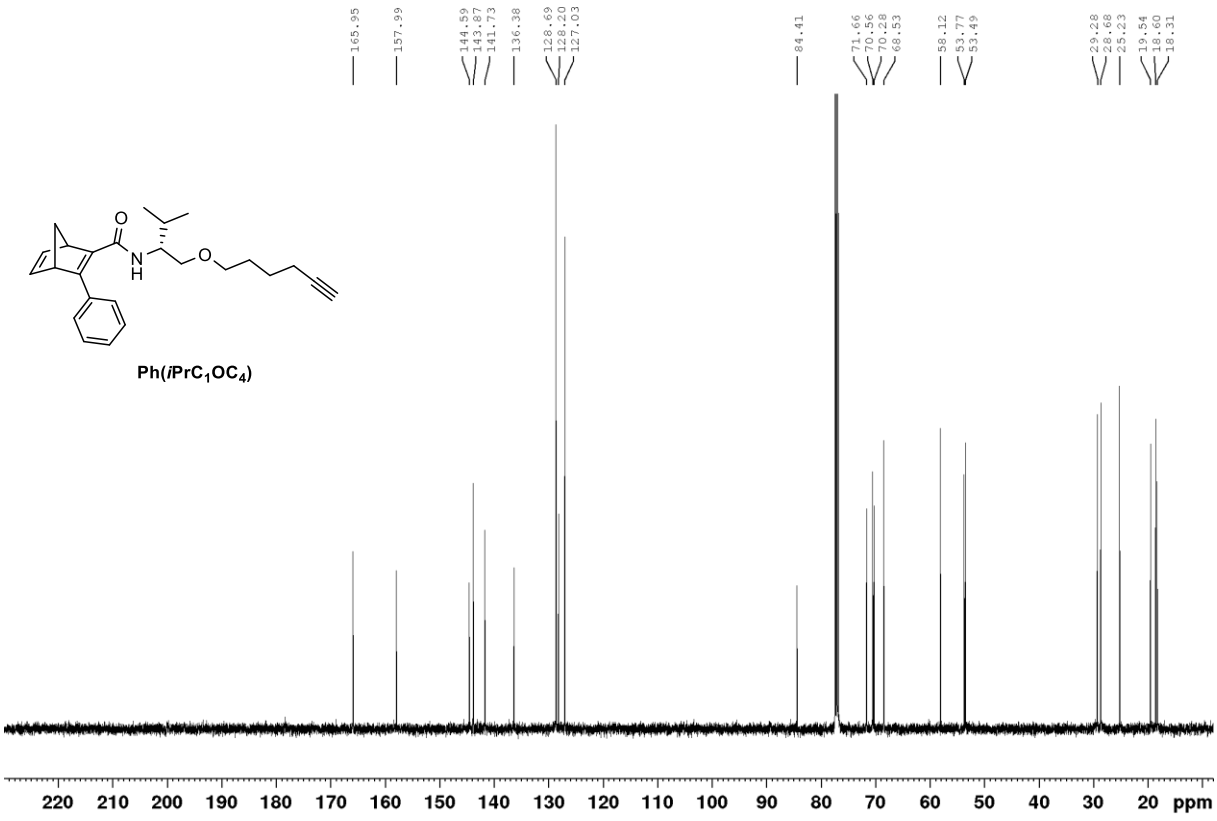

Figure S83. ^{13}C NMR spectrum (126 MHz, $CDCl_3$) of alkyne **Ph(*i*PrC$_1$OC$_4$)**.

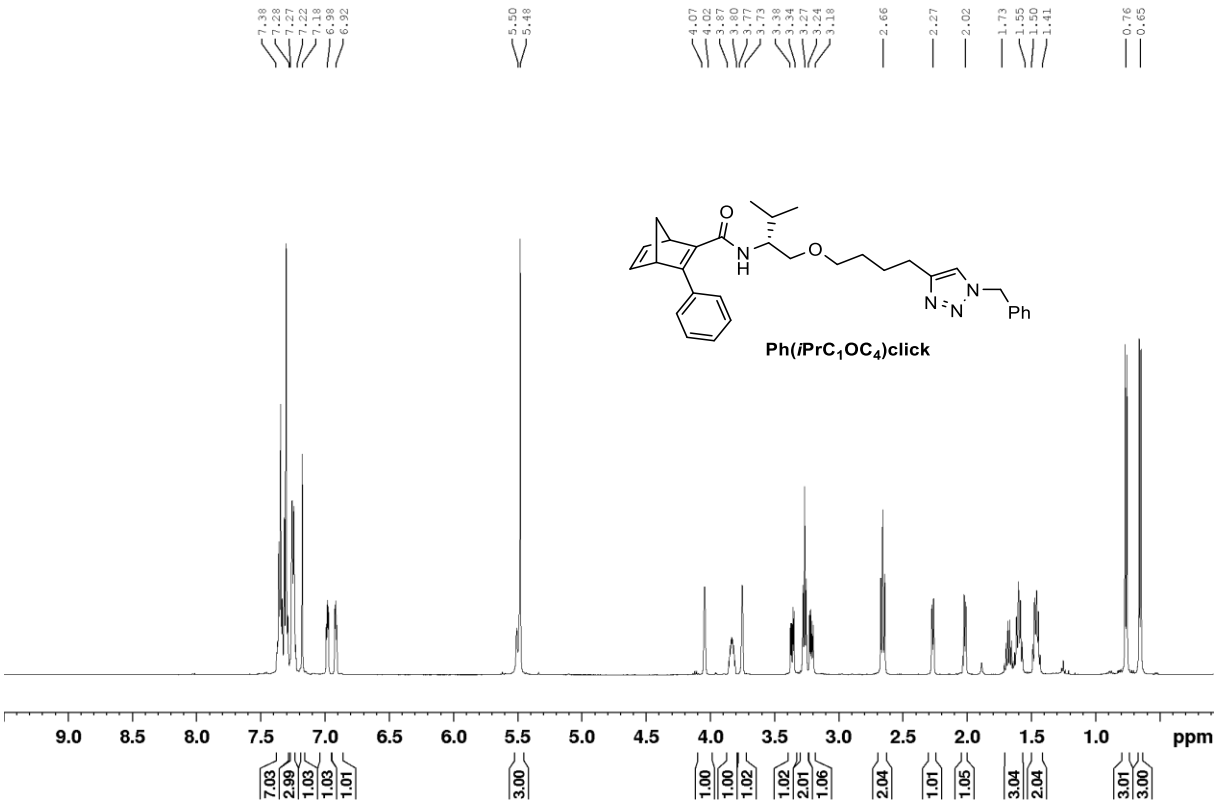

Figure S84. ^{1}H NMR spectrum (500 MHz, $CDCl_3$) of triazole **Ph(*i*PrC$_1$OC$_4$)click**.

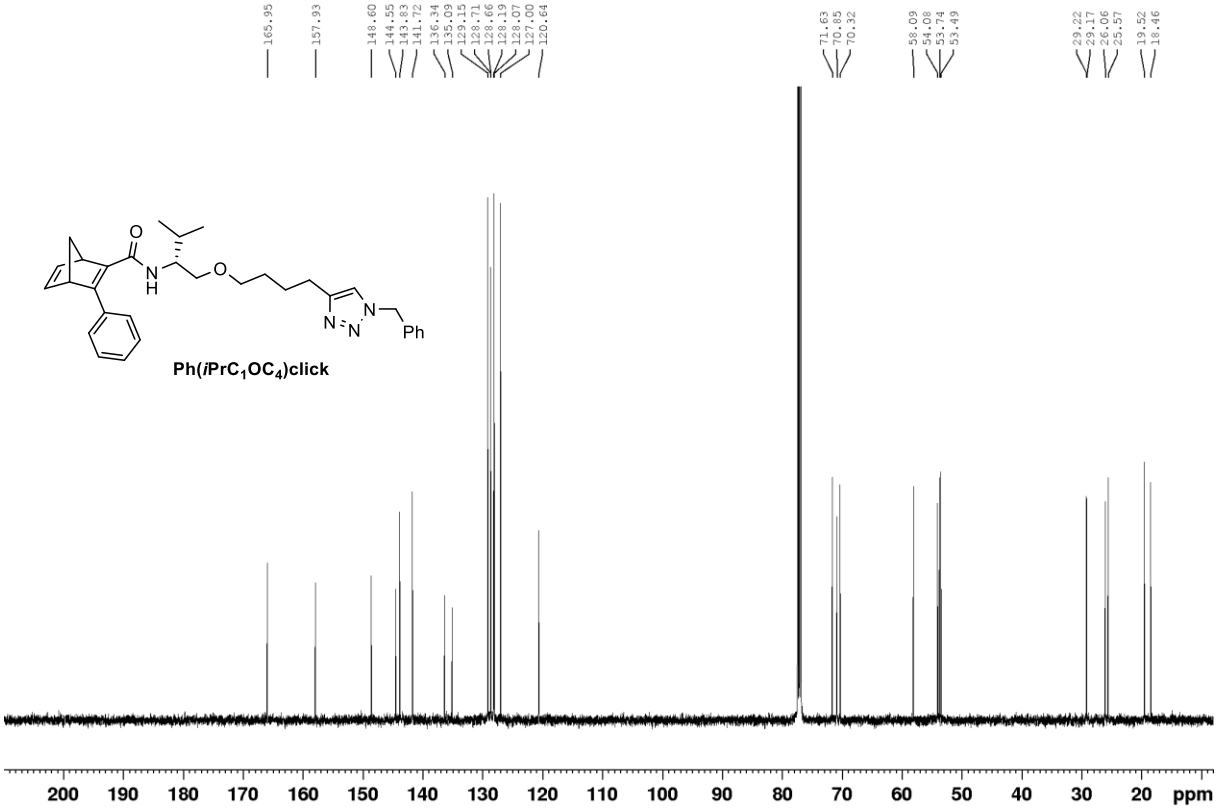

Figure S85. ^{13}C NMR spectrum (126 MHz, $CDCl_3$) of triazole **Ph(*i*PrC$_1$OC$_4$)click**.

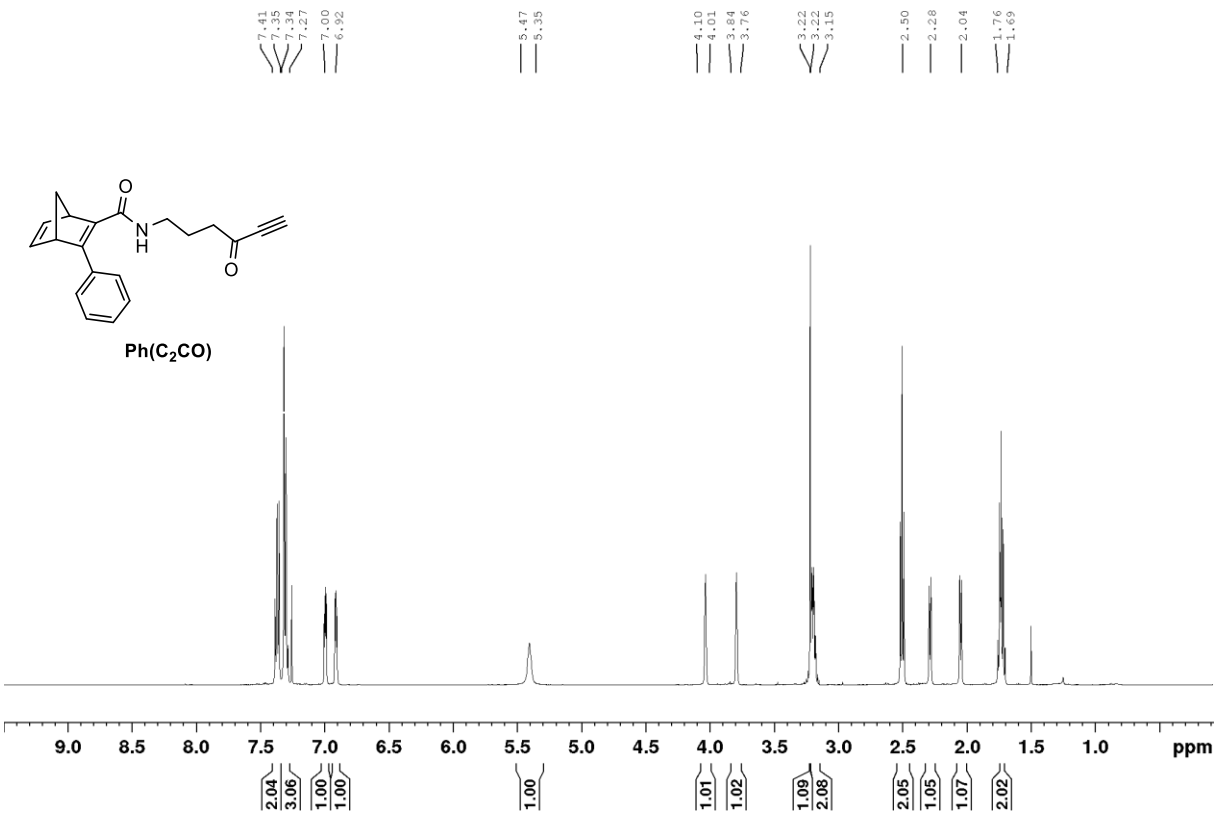

Figure S86. ^{1}H NMR spectrum (500 MHz, $CDCl_3$) of alkynone **Ph(C_2CO)**.

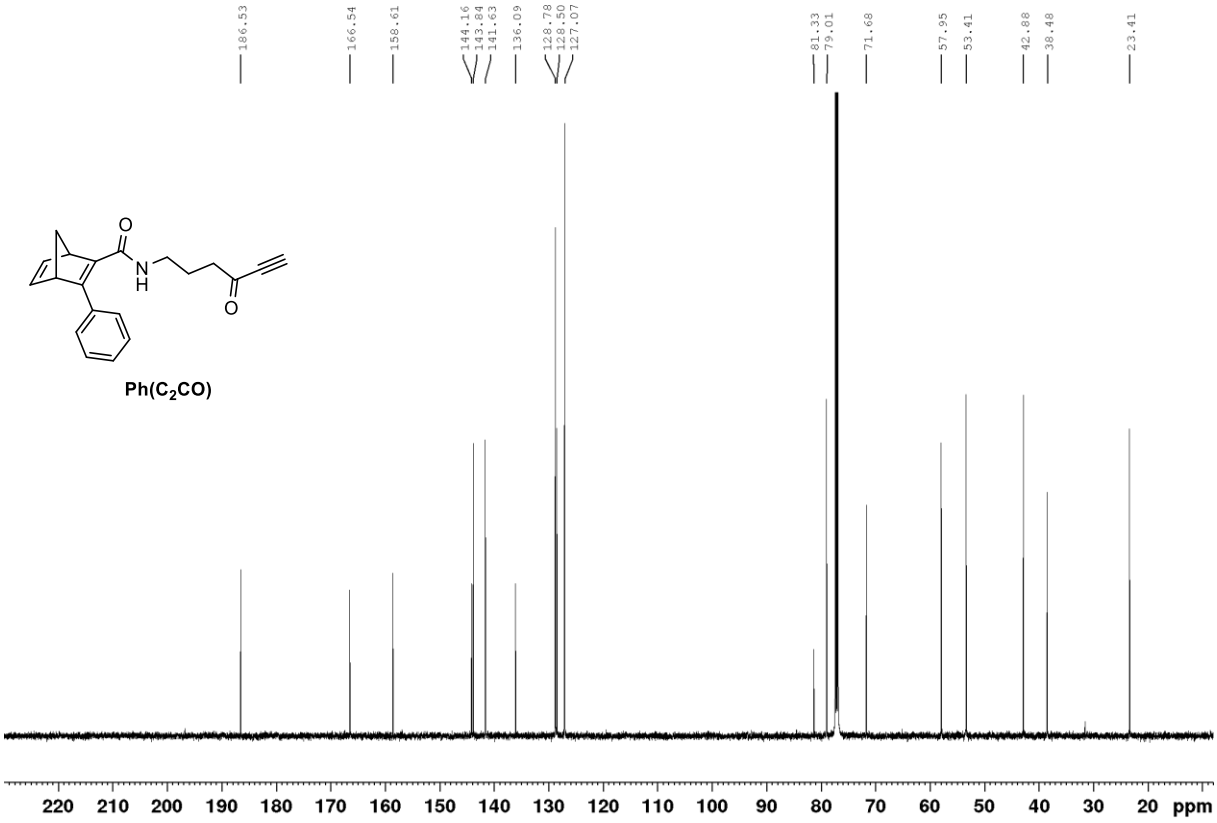

Figure S87. ^{13}C NMR spectrum (126 MHz, $CDCl_3$) of alkynone **Ph(C_2CO)**.

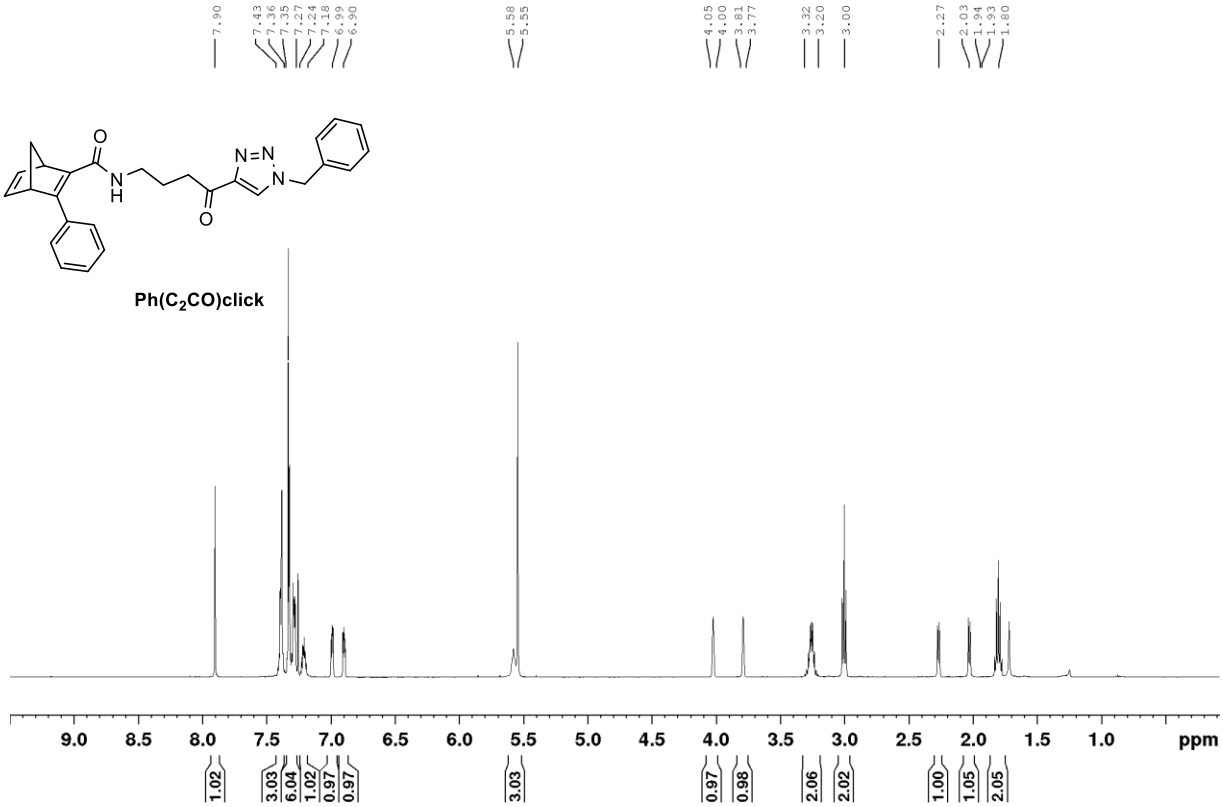

Figure S88. ^{1}H NMR spectrum (500 MHz, $CDCl_3$) of triazole **Ph(C_2CO)click**.

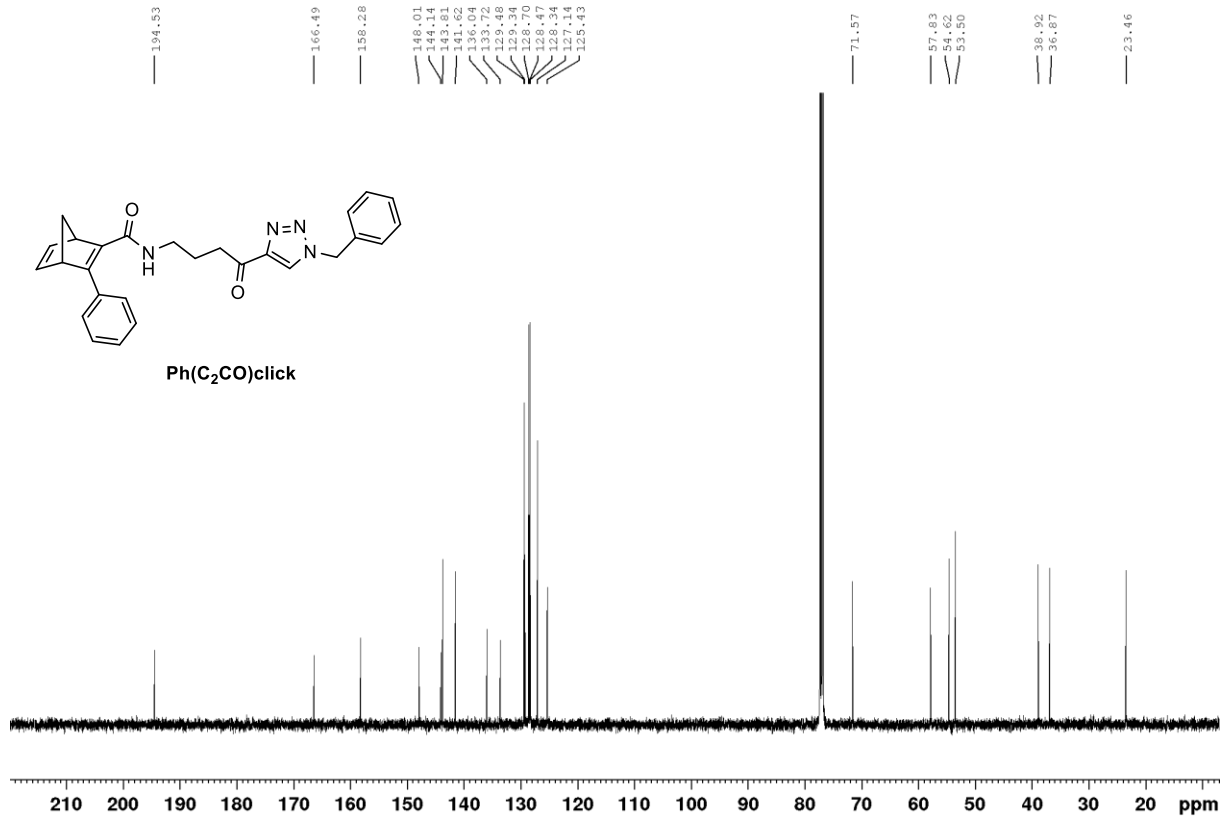

Figure S89. ^{13}C NMR spectrum (126 MHz, $CDCl_3$) of triazole **Ph(C_2CO)click**.

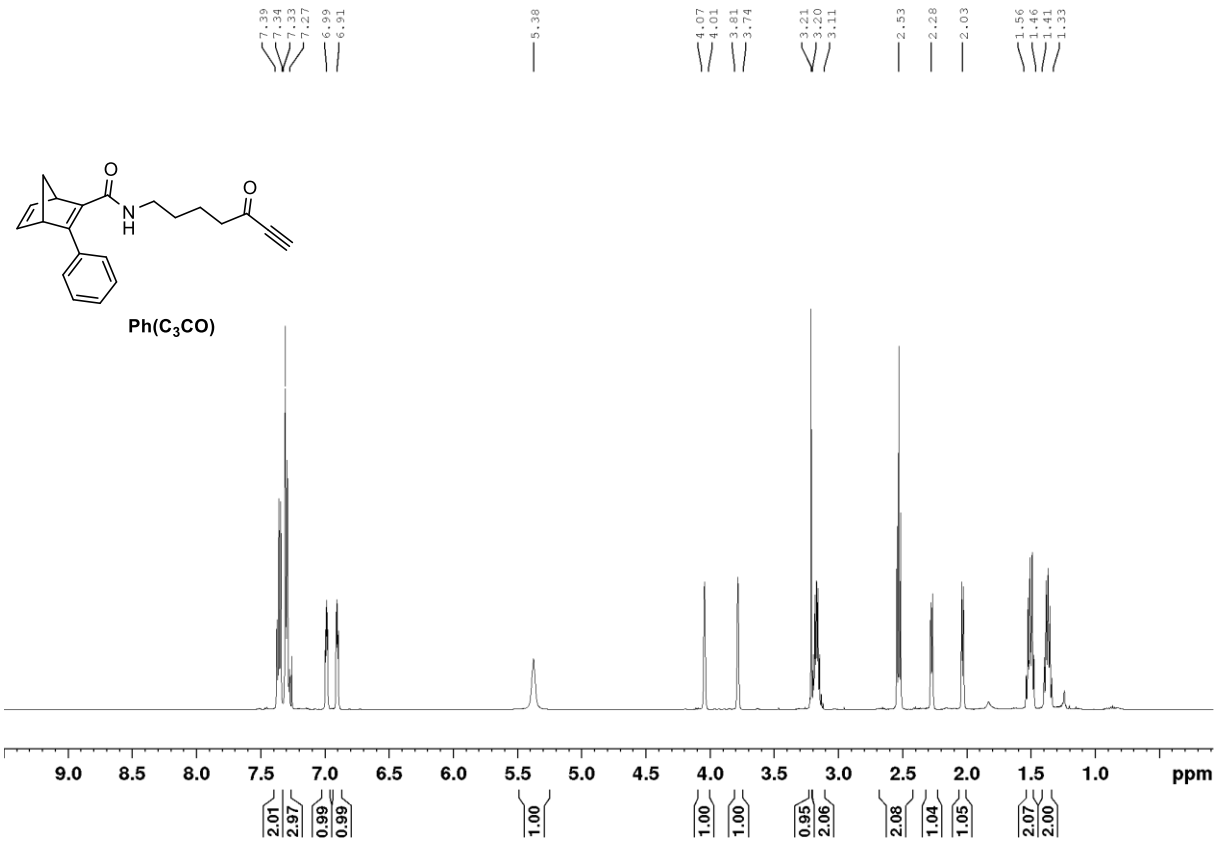

Figure S90. ^{1}H NMR spectrum (500 MHz, $CDCl_3$) of alkynone **Ph(C_3CO)**.

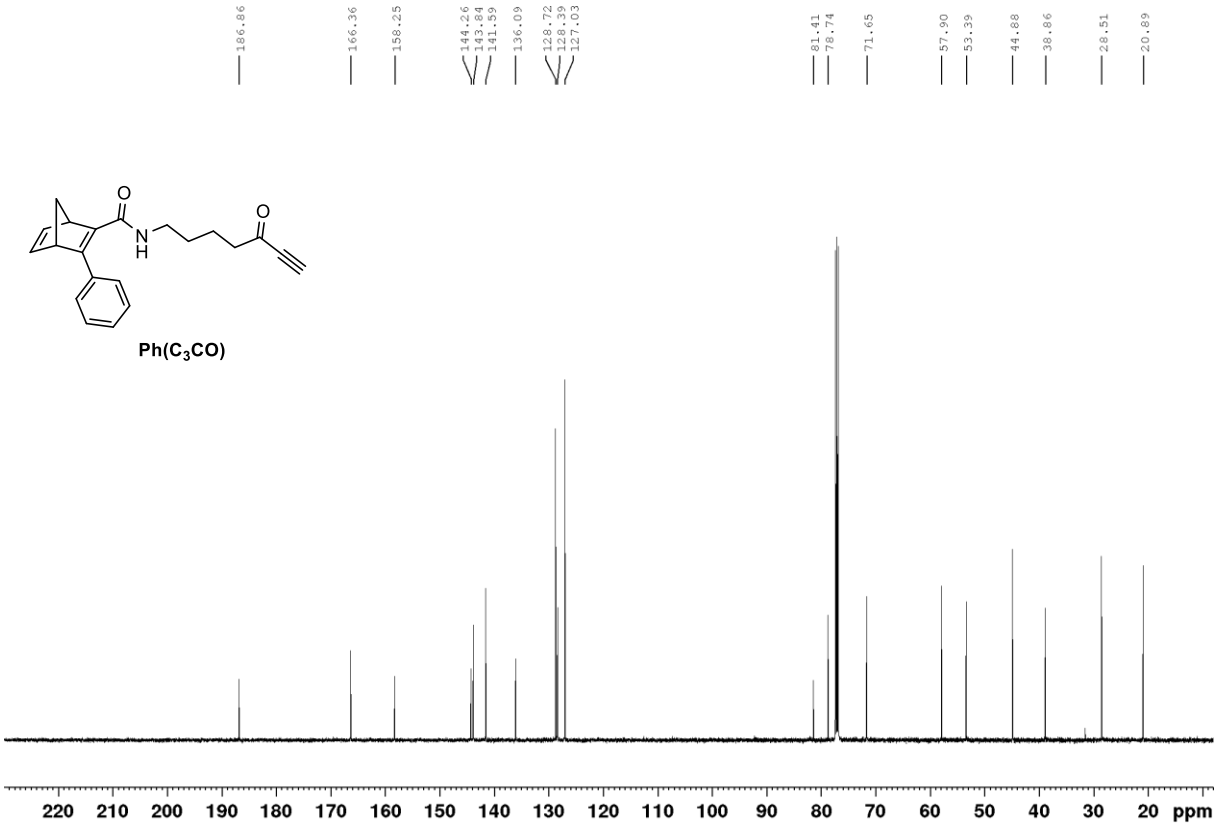

Figure S91. ^{13}C NMR spectrum (126 MHz, $CDCl_3$) of alkynone **Ph(C_3CO)**.

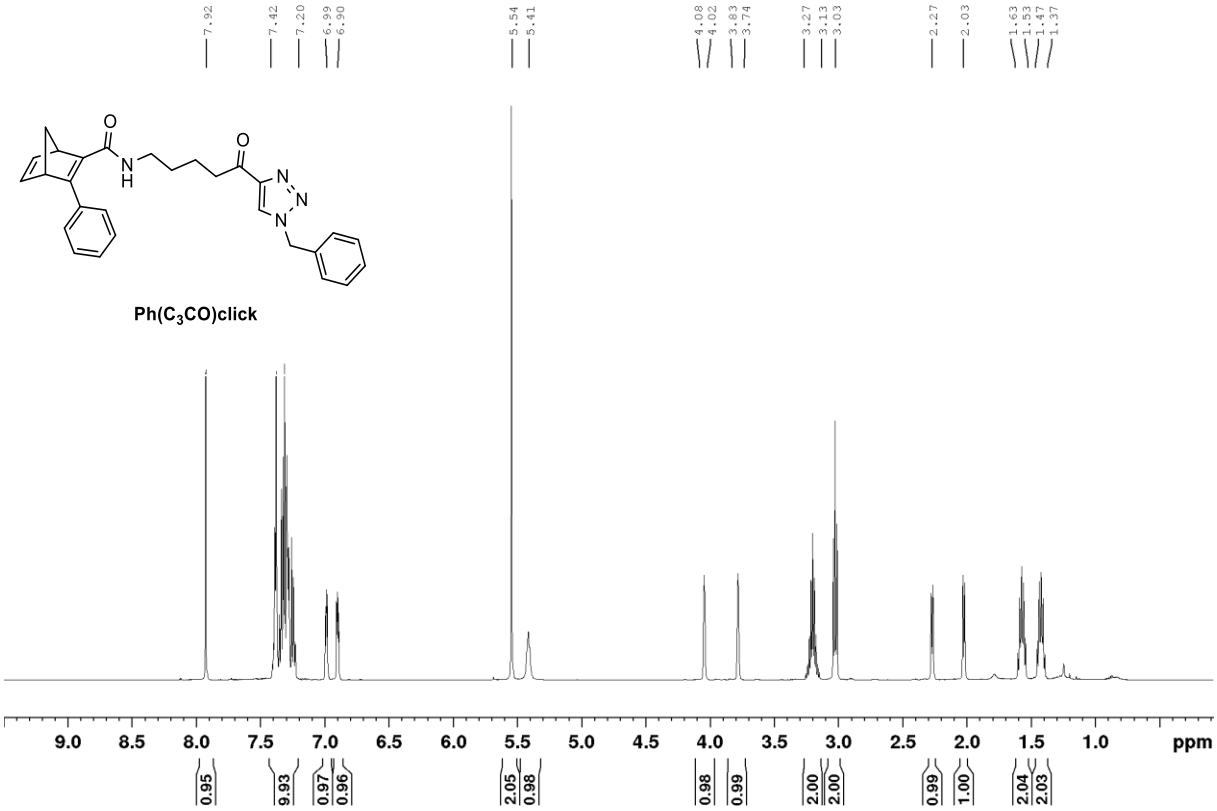

Figure S92. ^{1}H NMR spectrum (500 MHz, $CDCl_3$) of triazole **Ph(C_3CO)click**.

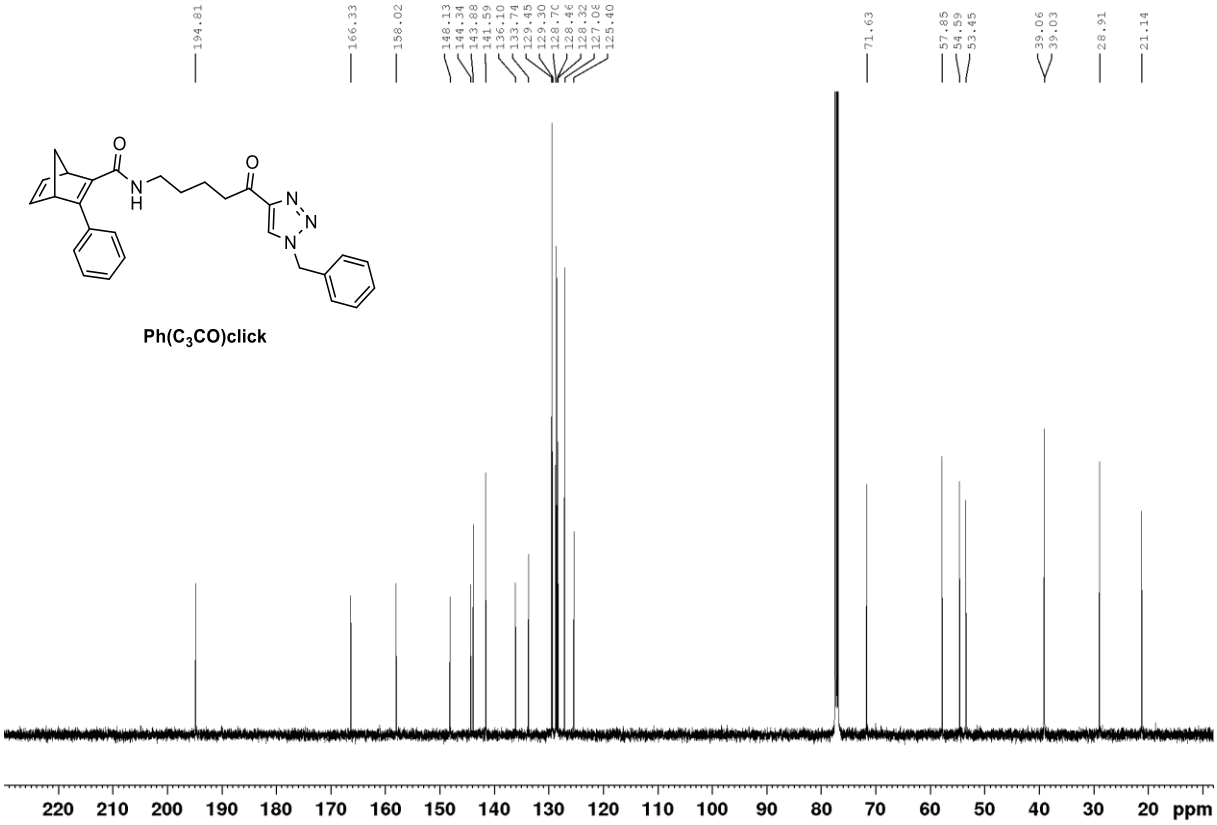

Figure S93. ^{13}C NMR spectrum (126 MHz, $CDCl_3$) of triazole **Ph(C_3CO)click**.

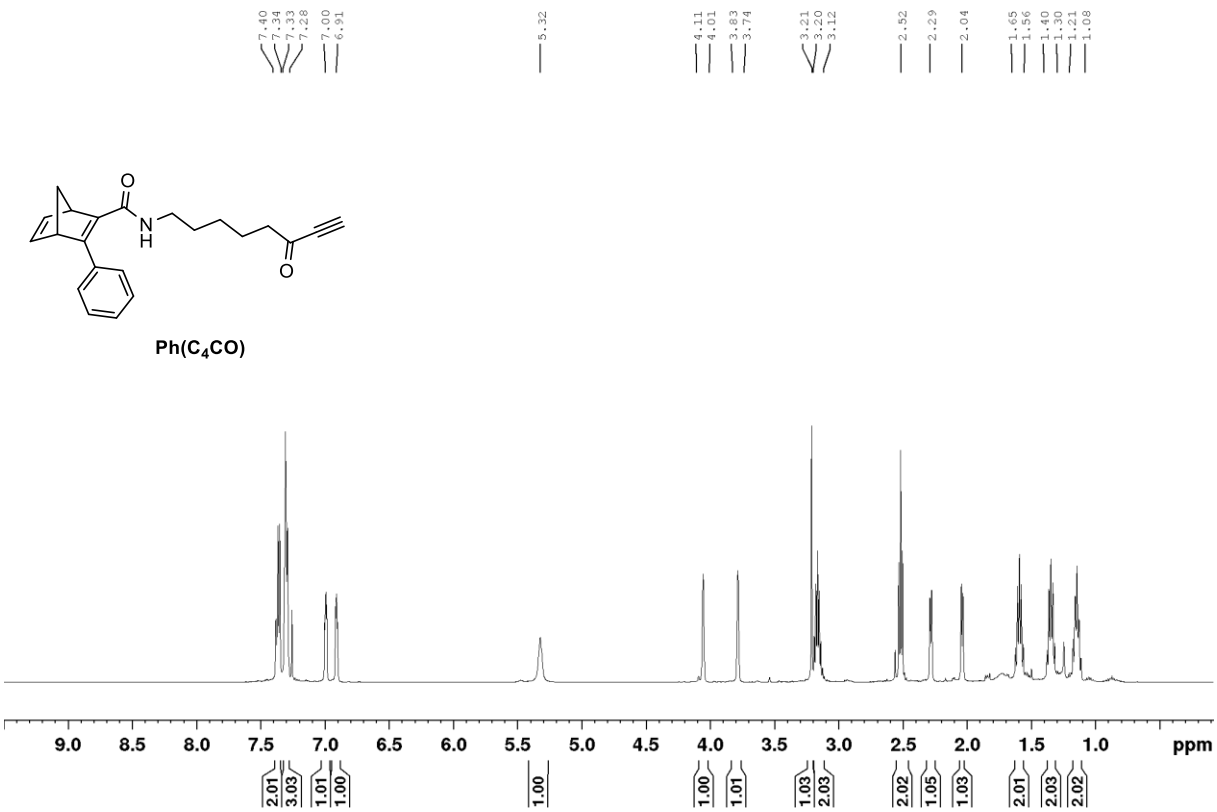

Figure S94. ^{1}H NMR spectrum (500 MHz, $CDCl_3$) of alkynone **Ph(C_4CO)**.

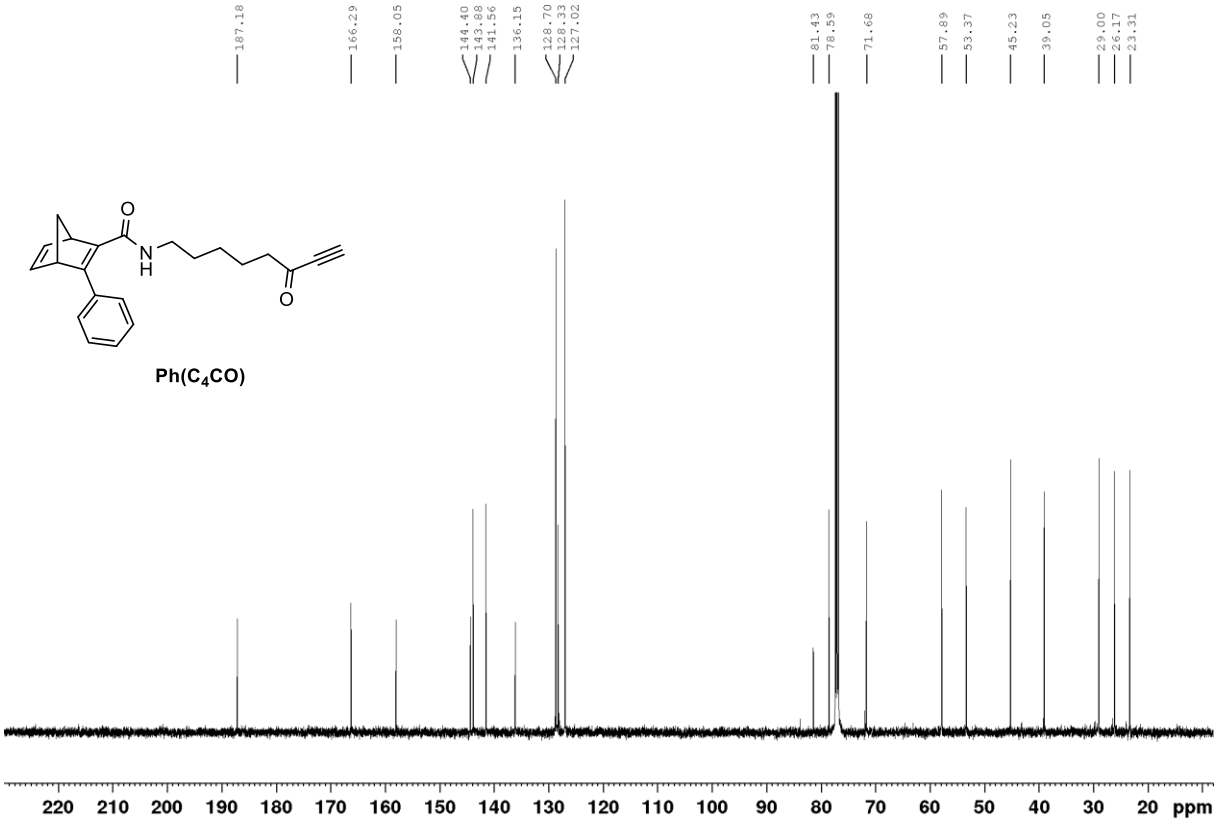

Figure S95. ^{13}C NMR spectrum (126 MHz, $CDCl_3$) of alkynone **Ph(C_4CO)**.

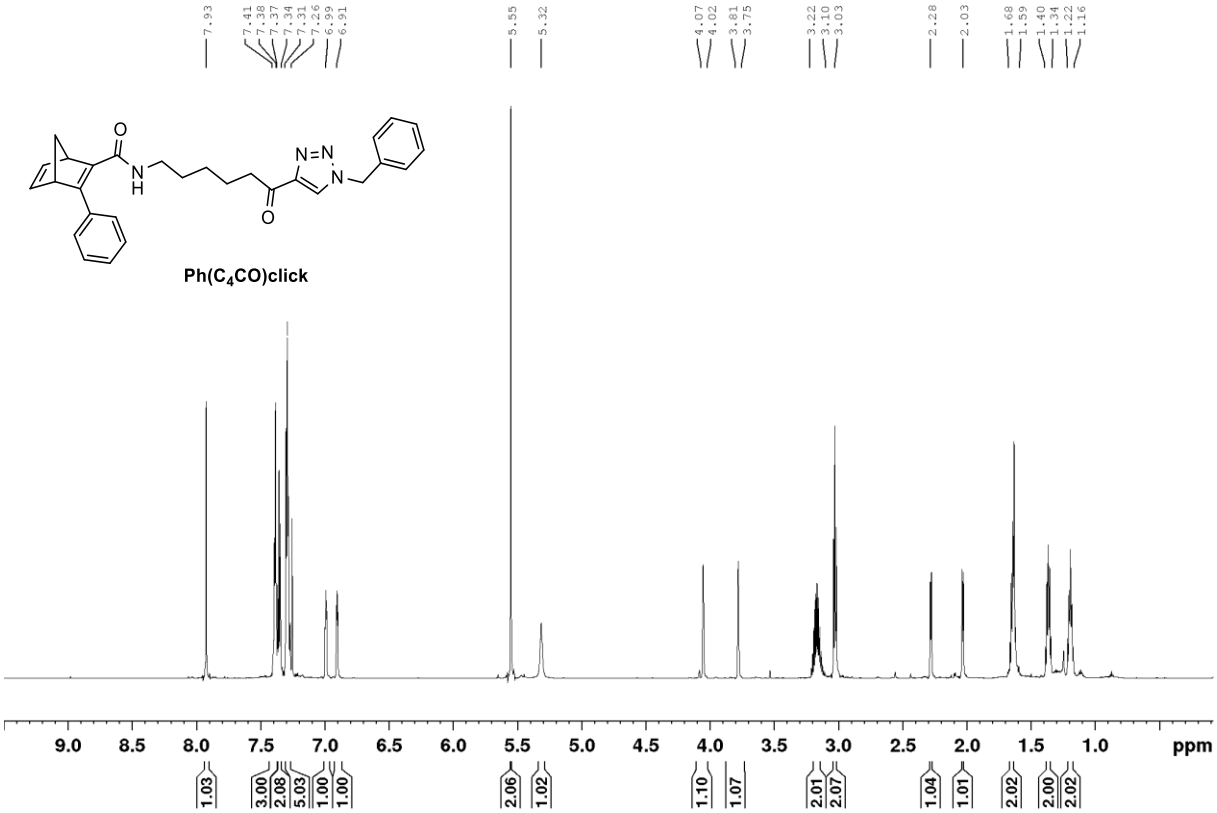

Figure S96. ^{1}H NMR spectrum (700 MHz, $CDCl_3$) of triazole **Ph(C_4CO)click**.

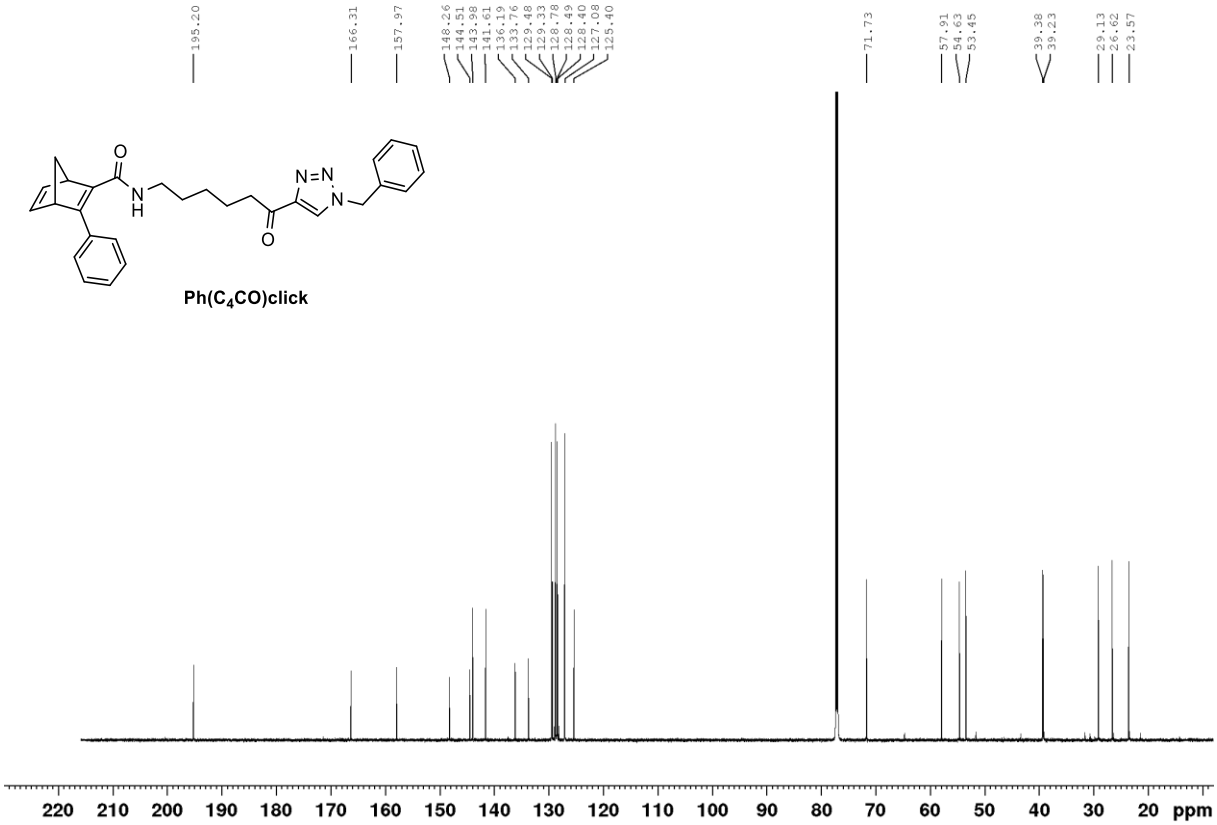

Figure S97. ^{13}C NMR spectrum (176 MHz, $CDCl_3$) of triazole **Ph(C_4CO)click**.

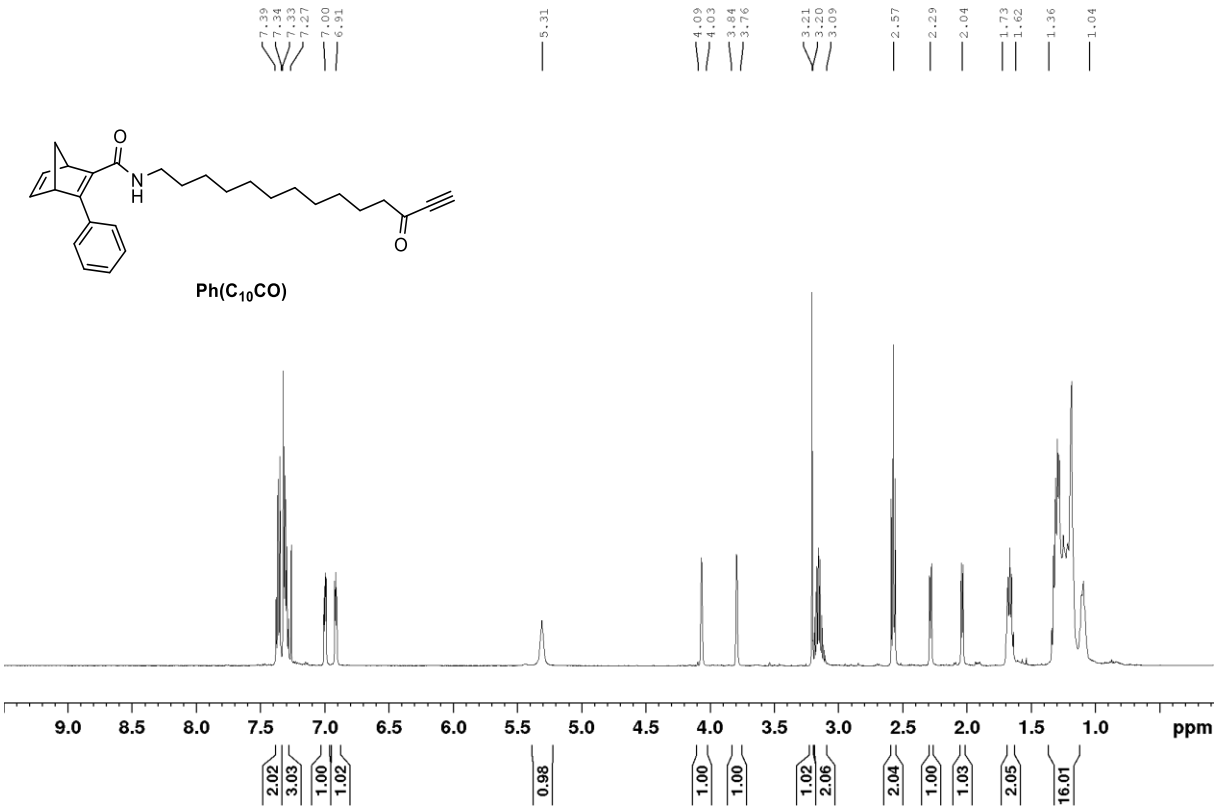

Figure S98. ^{1}H NMR spectrum (500 MHz, $CDCl_3$) of alkynone **Ph(C_{10}CO)**.

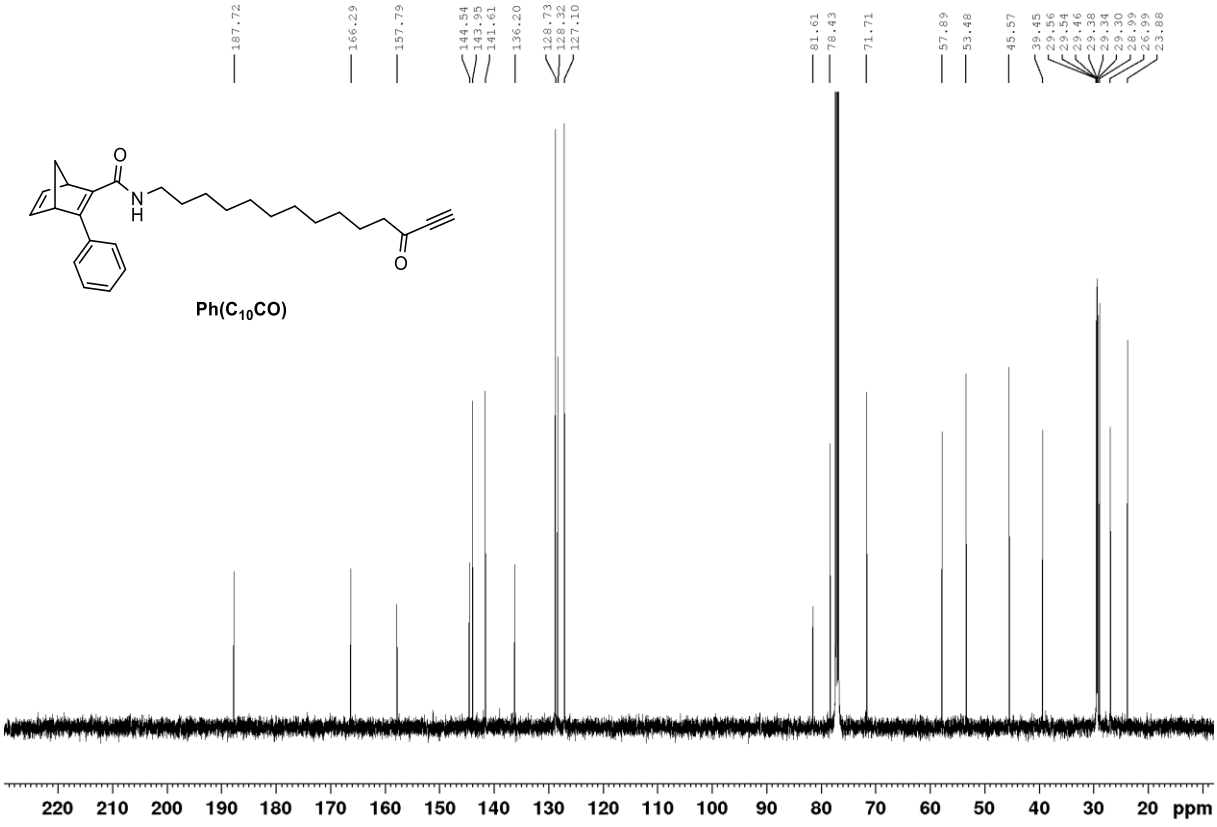

Figure S99. ^{13}C NMR spectrum (126 MHz, $CDCl_3$) of alkynone **Ph(C_{10}CO)**.

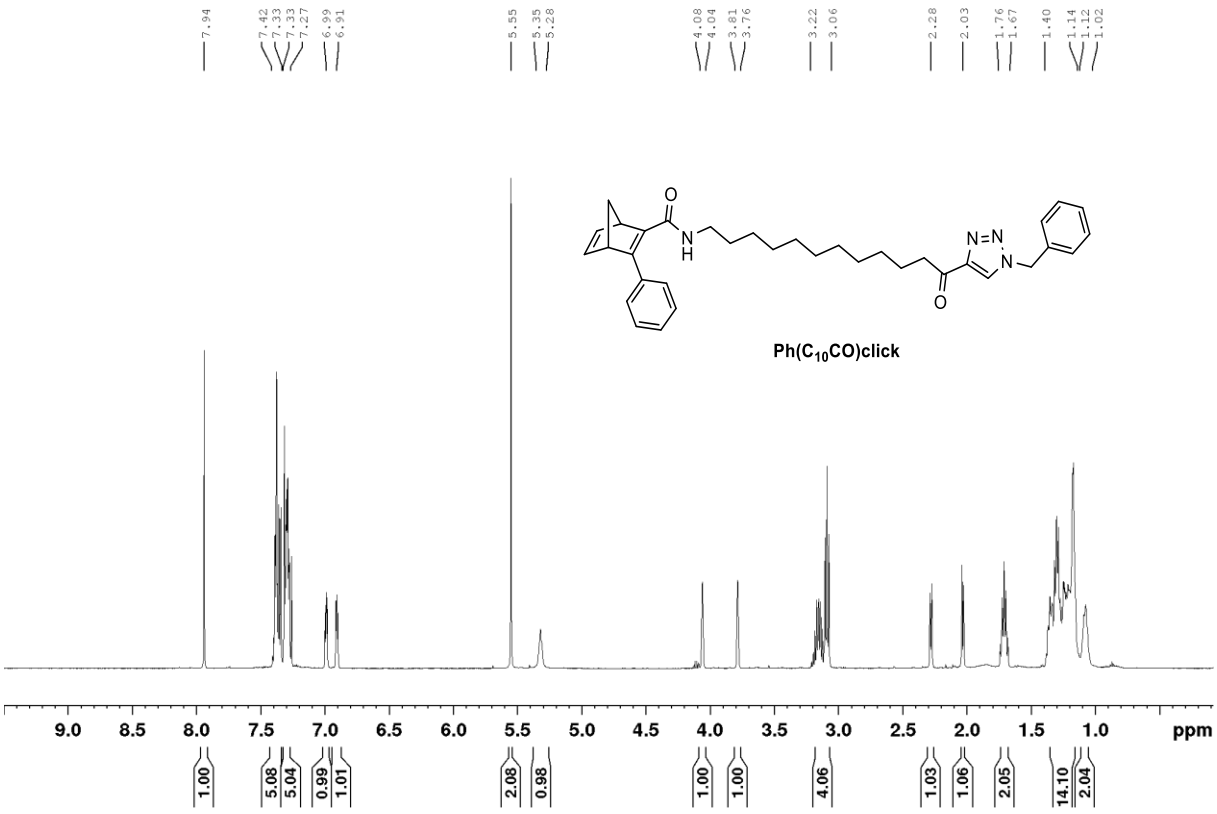

Figure S100. ^{1}H NMR spectrum (500 MHz, $CDCl_3$) of triazole **Ph(C_{10}CO)click**.

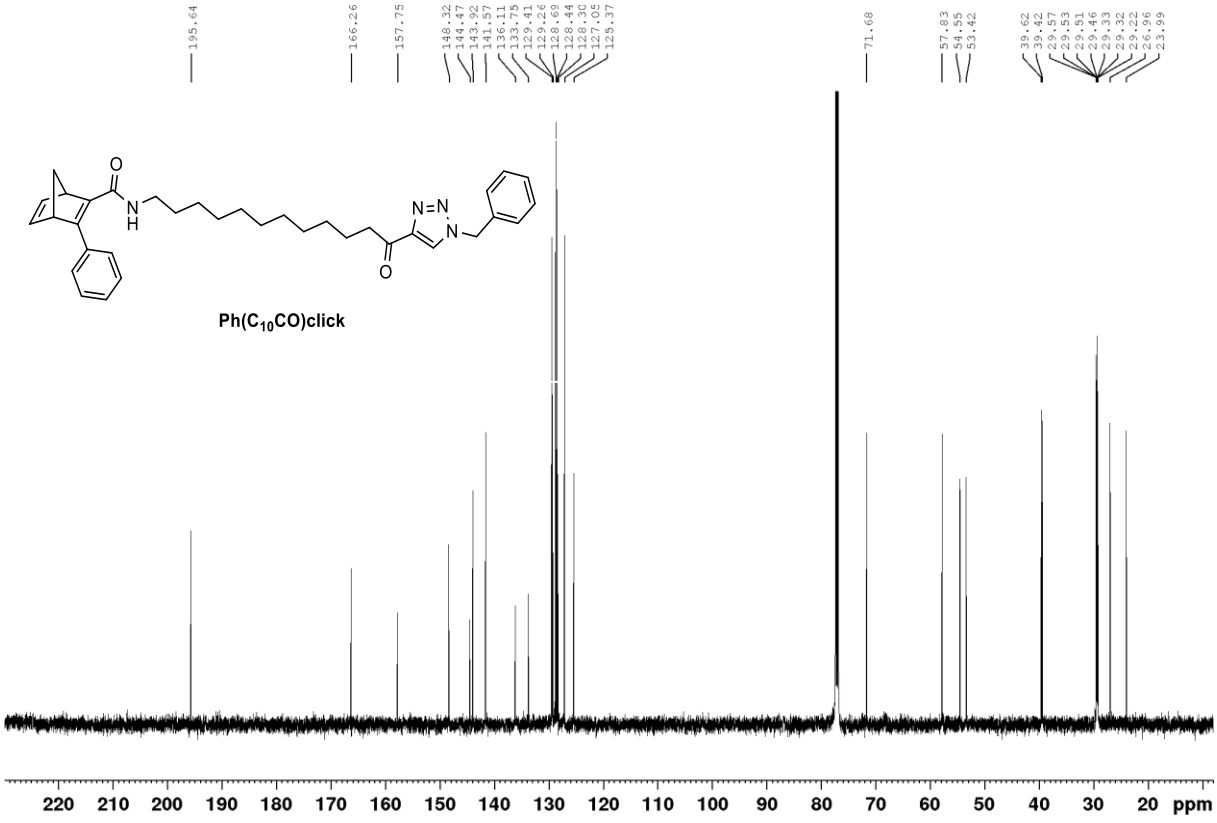

Figure S101. ^{13}C NMR spectrum (126 MHz, $CDCl_3$) of triazole **Ph(C_{10}CO)click**.

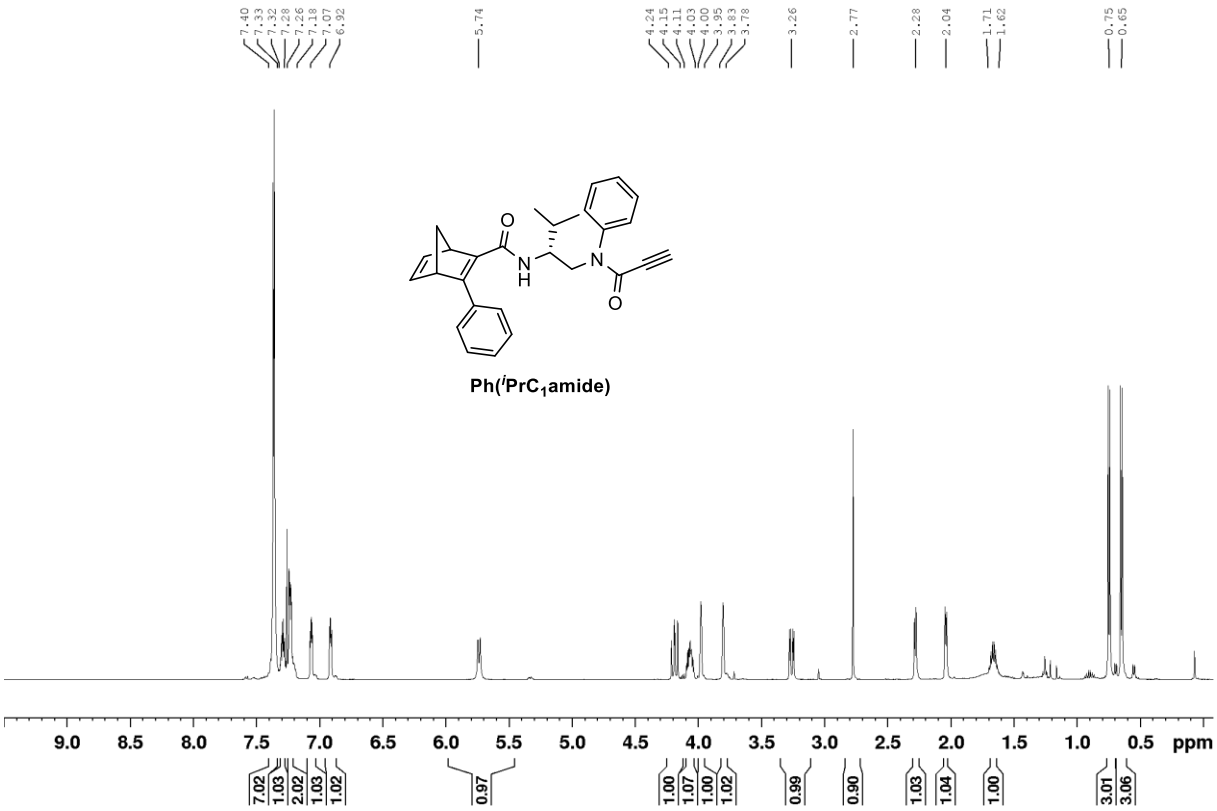

Figure S102. ^{1}H NMR spectrum (500 MHz, $CDCl_3$) of alkyne **Ph(*i*PrC$_1$amide)**.

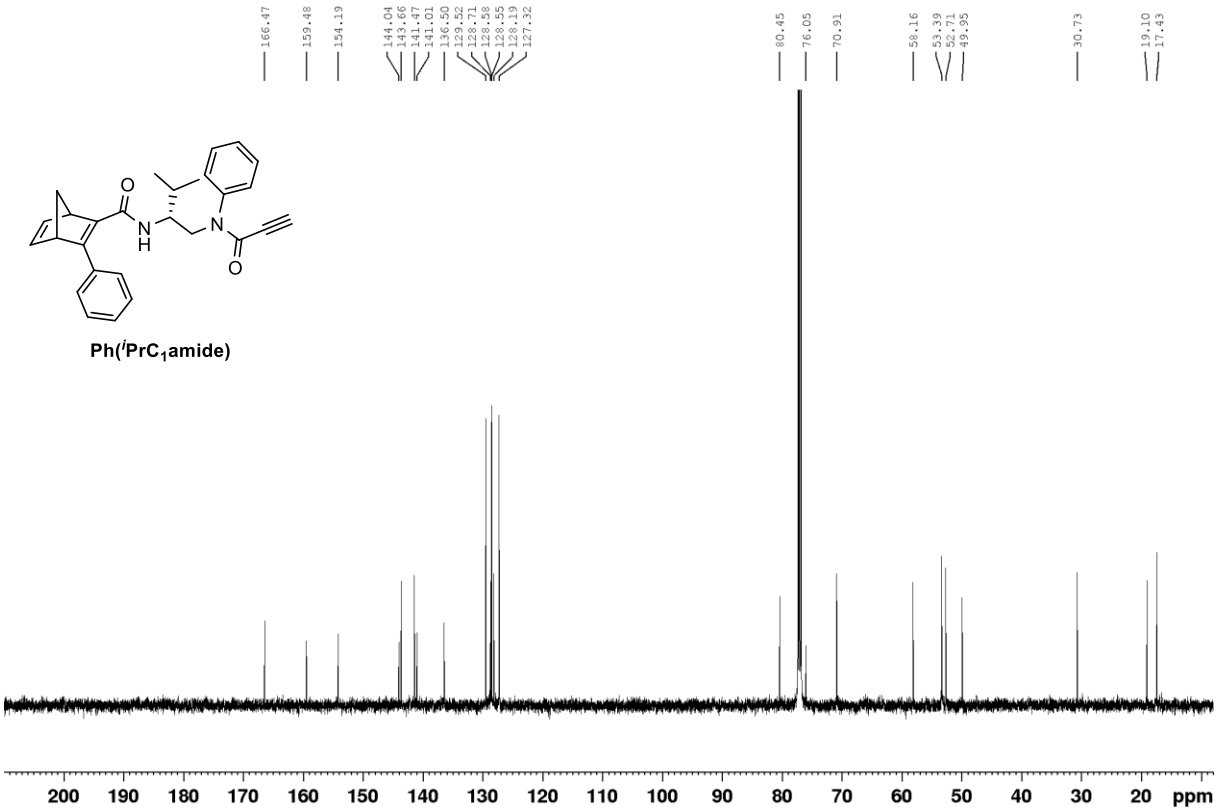

Figure S103. ^{13}C NMR spectrum (126 MHz, $CDCl_3$) of alkyne **Ph(*i*PrC$_1$amide)**.

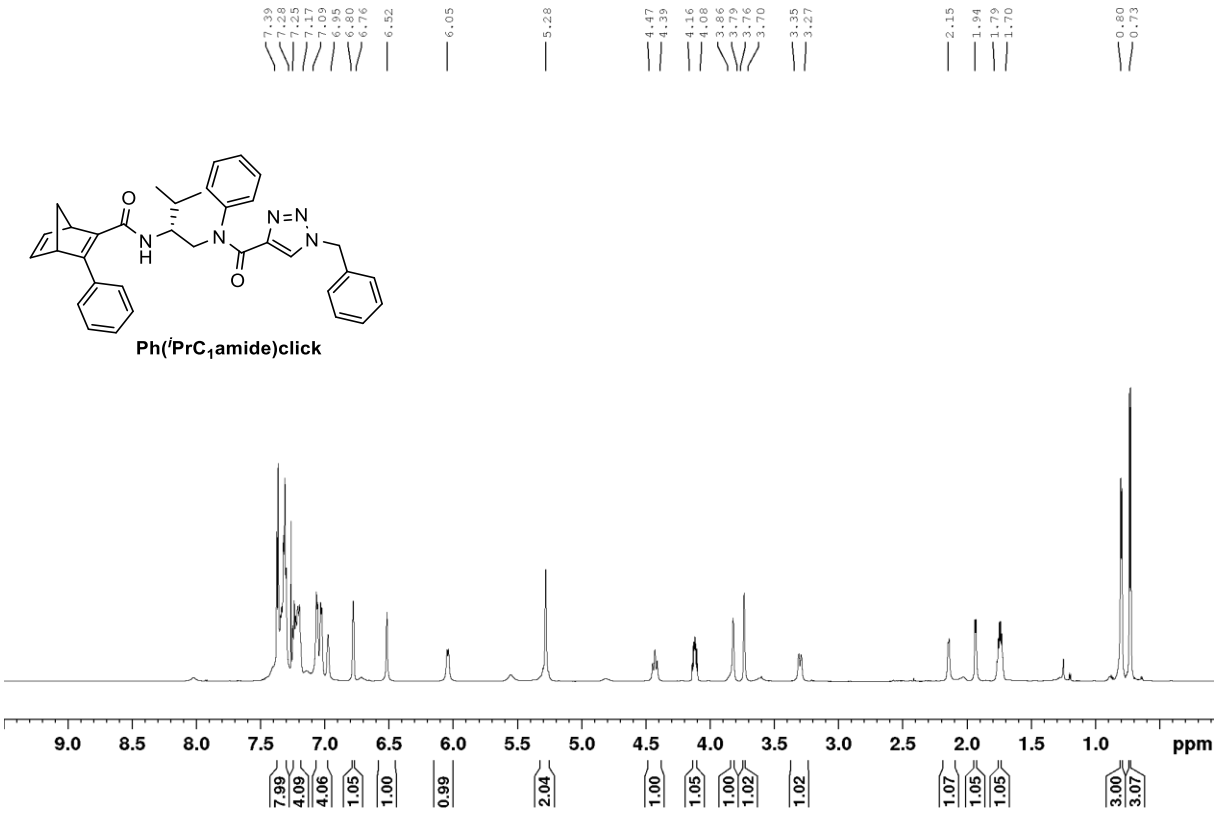

Figure S104. ^{1}H NMR spectrum (700 MHz, $CDCl_3$) of triazole **Ph(*i*PrC$_1$amide)click**.

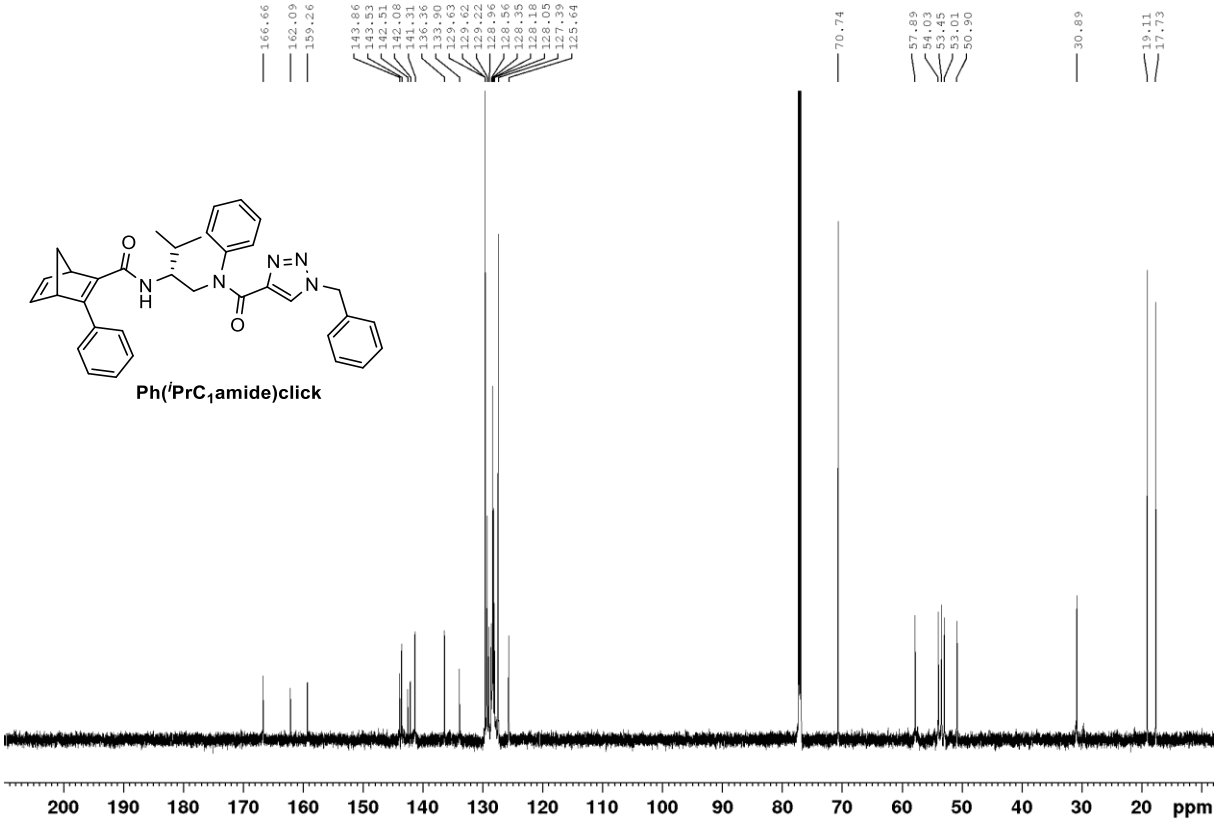

Figure S105. ^{13}C NMR spectrum (176 MHz, $CDCl_3$) of triazole **Ph(*i*PrC$_1$amide)click**.

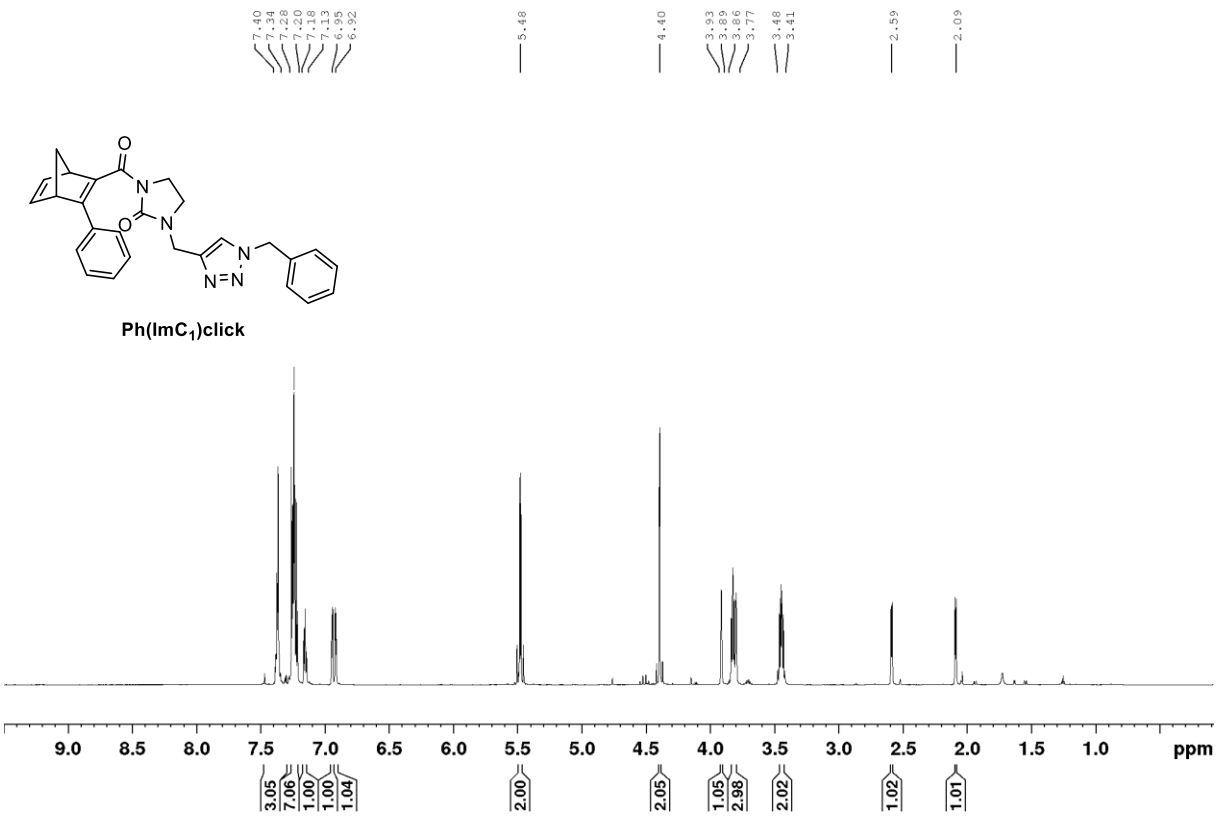

Figure S106. ^{1}H NMR spectrum (700 MHz, $CDCl_3$) of triazole **Ph(ImC$_1$)click**.

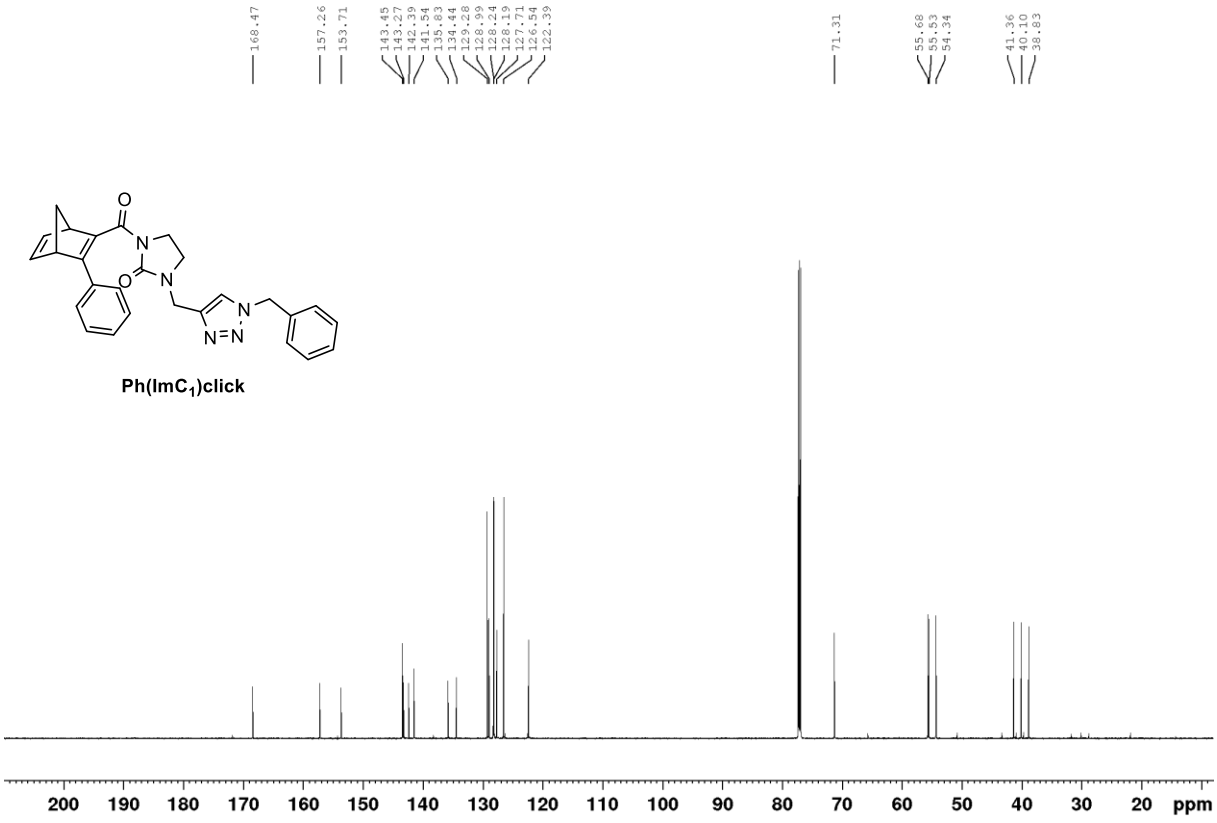

Figure S107. ^{13}C NMR spectrum (176 MHz, $CDCl_3$) of triazole **Ph(ImC$_1$)click**.

2.4 Rh-catalyzed 1,2-additions

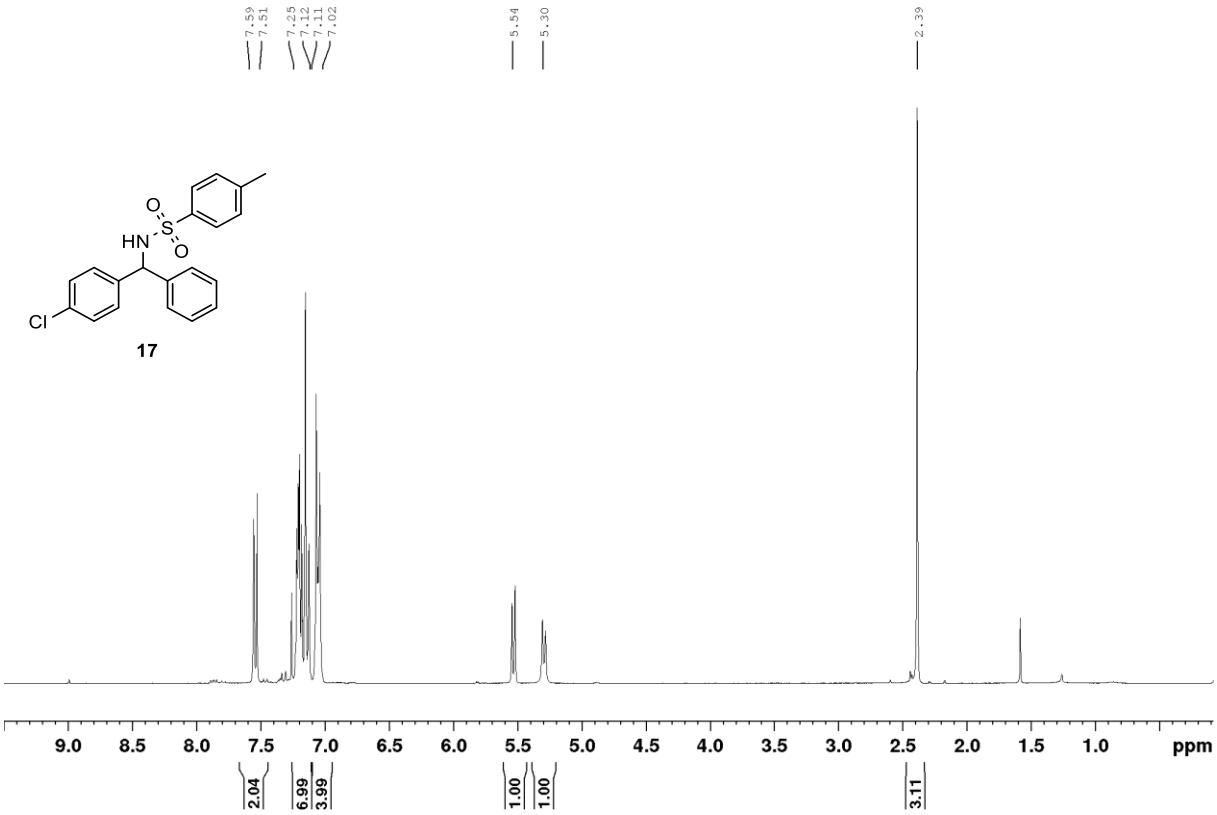

Figure S108. ^{1}H NMR spectrum (300 MHz, $CDCl_3$) of *N*-tosyl amine **17**.

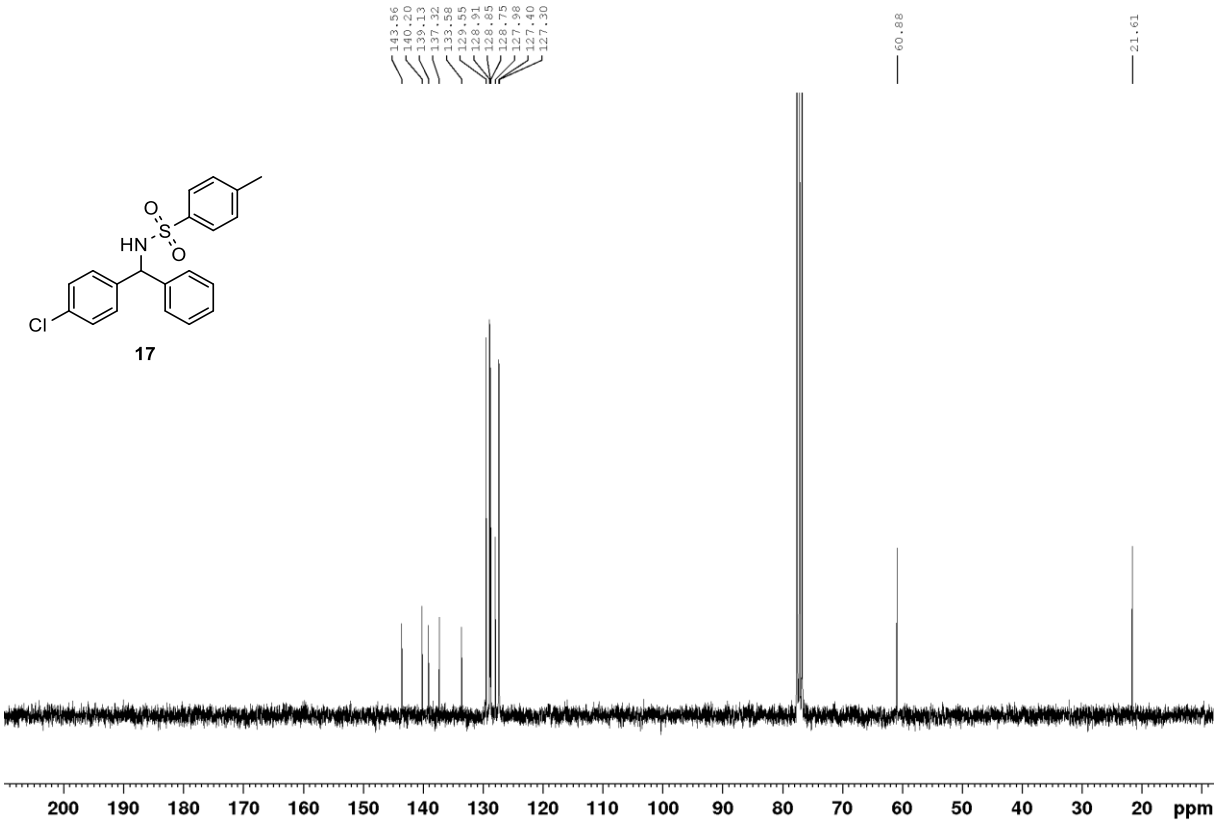

Figure S109. ^{13}C NMR spectrum (126 MHz, $CDCl_3$) of *N*-tosyl amine **17**.

3 Synthesis of the supports and immobilization of ligands

3.1 Synthesis of the mesoporous materials

OMS-2.6 (via true liquid crystal templating (TLCT))
The ordered mesoporous silica OMS-2.6nm was synthesized in accordance with a reported procedure.[20] 25.34 g of tetramethyl orthosilicate (TMOS, 98 %, Sigma Aldrich) were added to 18.00 g of 0.1 M hydrochloric acid in a polypropylene flask, which lead to the formation of silicic acid and methanol. The latter was removed at 40°C and 280 mbar for 15 min with the help of a rotary evaporator. 12.00 g of ethylhexadecyldimethylammonium bromide (CDEAB, for synthesis, Sigma Aldrich) were weighed into a polypropylene flask to which the silicic acid was added. The mixture was stirred with a KPG stirrer until homogeneous. The clear, viscous fluid was poured onto trays made of polytetrafluoroethylene and cured for 24 h at 80°C. The as-synthesized material was pulverized in a ball mill to result in a fine white powder.

OMS-4.9 (via TLCT)
The ordered mesoporous silica OMS-4.9nm was synthesized in accordance with a reported procedure.[21] 0.70 g of tetramethyl orthosilicate (TMOS, 98 %, Sigma Aldrich) were added to 20.55 g of 0.1 M hydrochloric acid in a polypropylene flask, which lead to the formation of silicic acid and methanol. The latter was removed from the mixture at 150 mbar and room temperature while stirring for 10 min. 20.33 g of Synperonic® PE/P84 (Sigma Aldrich) were weighed into a polypropylene flask to which the silicic acid was added. The mixture was stirred with a KPG stirrer until homogeneous. The clear, viscous fluid was poured onto trays made of polytetrafluoroethylene and cured for 96 h at 80°C. The as-synthesized material was pulverized in a ball mill to result in a fine white powder.

OMS-5.9 (via TLCT)
The ordered mesoporous silica OMS-5.9nm was synthesized in accordance with a reported procedure.[21] 15.23 g of tetramethyl orthosilicate (TMOS, 98 %, Sigma Aldrich) were added to 10.94 g of 0.1 M hydrochloric acid in a polypropylene flask, which lead to the formation of silicic acid and methanol. The latter was removed from the mixture at 150 mbar and room temperature while stirring for 10 min. 8.60 g of Pluronic® P-123 (average Mn ~5,800, Sigma Aldrich) were weighed into a polypropylene flask to which the silicic acid was added. The mixture was stirred with a KPG stirrer until homogeneous. The clear, viscous fluid was poured onto trays made of polytetrafluoroethylene and cured for 48 h at 80°C. The as-synthesized material was pulverized in a ball mill to result in a fine white powder.

OMS-6.8 (via cooperative sol-gel self-assembly mechanism)
The ordered mesoporous silica OMS-6.8nm (SBA-15) was synthesized in accordance with a reported procedure.[22] For the synthesis of SBA-15, 16 g of the triblock copolymer Pluronic® P-123 (average molar mass ~ 5800 g mol^{-1}, Sigma Aldrich) was dissolved in a mixture of 520 ml demineralized water and 80 ml 37 wt% hydrochloric acid at room temperature under stirring (100 rpm) in a 1l-teflonlined autoclave. Before adding 37 ml of tetraethyl orthosilicate (TEOS, 98 %, reagent grade, Sigma Aldrich) the solution was heated to 45°C. At this temperature, the mixture was stirred for 7.5 h under stirring (150 rpm). The hydrothermal treatment under static conditions at 80°C for 15 h followed. In the last step, the as-synthesized SBA-15 was separated under vacuum, washed with demineralized water and dried in an oven at 80 °C.

OMC-6.2nm and OMC-10.3 (Ordered Mesoporous Carbons)

For synthesis of the carbon materials 1 g of the the "Reverse Pluronic" SDA[23] (PPO_{55}-PEO_{181}-PPO_{55} for OMC_6.2nm and PPO_{95}-PEO_{454}-PPO_{95} for OMC_10.3nm), was dissolved in 20 g of EtOH and further mixed with an ethanolic precursor solution (phenolic oligomers). After stirring for 10 min the mixture was poured into a glass Petri dish for evaporation of the solvent (in the fume hood). For crosslinking, the polymer−precursor mixture was thermopolymerized at 100 °C for 24 h. The cross-linked film was finally removed from the Petri dish and the flakes then carbonized under a N_2 atmosphere (nitrogen flow rate of 4 L/min). The heating program encompassed a temperature ramp at 1 K/min from room temperature to 400 °C, followed by an increase with a rate of 10 K/min up to 700 °C, the sample was then held at this temperature for 2 h. The prepared OMC material was finally ball-milled to result in a fine black powder.

NT-mSiO_2-4.2 (non-templated SiO_2)

Non-templated mesoporous silica (NT-mSiO_2) was synthesized in accordance with a reported procedure.[24] 148 mg of L-lysine (Sigma Aldrich) was dissolved in 73.64 mL of Milli-Q H_2O. To this solution, 5.64 mL of tetraethyl orthosilicate (TEOS, 98 %, Sigma Aldrich) was added under stirring. The molar ratio of TEOS : L-lysine : H_2O was 1 : 0.04 : 162. The resultant mixture was stirred at 60°C for 24 h at a stirring rate of 550 rpm. The mixture was then aged without stirring under isothermal conditions at 100°C for 20 h. Excess solvent was evaporated by drying in an oven at 100°C for 24 h. Finally, the obtained powder was calcined at 400°C for 6 h (in air) at a heating rate of 1 K min^{-1}.

NT-mSiO_2-8.1 (non-templated SiO_2)

In a typical synthesis, 18.5 mg of L-lysine was dissolved in 18.41 mL of Milli-Q H_2O. To this solution, 1.41 mL of TEOS was added under stirring. The molar ratio of TEOS : L-lysine : H_2O was 1 : 0.02 : 162. The resultant mixture was stirred at 60°C for 24 h at a stirring rate of 550 rpm. The mixture was then aged without stirring under isothermal conditions at 100°C for 20 h. Excess solvent was evaporated by drying in an oven at 100°C for 24 h. The obtained powder was calcined at 400°C for 6 h (in air) at a heating rate of 1 K min^{-1}.

3.2 Selective functionalization of the materials

3.2.1 Ordered mesoporous silica[16]

Functionalization of the particle surface and the pore entrances
The functionalization of the particle surface and the pore entrances of as-synthesized material was done in 1,1,1-trimethyl-*N*-(trimethylsilyl)silanamine (≥98 % (for GC), Carl Roth GmbH + Co. KG). The suspension was stirred for 6 h at room temperature. Afterwards, the functionalized material was separated under vacuum, washed with demineralized water and dried in an oven at 80°C.

Template removal
The structure-directing template was removed from the pores of the functionalized material by Soxhlet extraction with ethanol over 112 h. The extracted material was dried in an oven at 80°C.

Thermal treatment in nitrogen
After the removal of the structure-directing template and before the functionalization of the pore walls, each material was heated with a heating rate of 2 K min^{-1} and a nitrogen flow of 58 l h^{-1} in an oven to 400 °C. At this temperature the material was treated for 6 h.

Functionalization of the pore walls with AzPTES
For the functionalization of the pore walls, a suspension of 15 ml toluene and $9.5 \cdot 10^{-4}$ mol 3-azidopropyltriethoxysilane (AzPTES, prepared according to ref.[25]) per gram sample was added and stirred at room temperature for 72 h. The functionalized material was separated by filtration, washed with ethanol and dried at 80 °C.

3.2.2 Ordered mesoporous carbon

Oxidation and Reduction of the carbon materials[26]
1 g of the carbon samples were treated for 1.5 h with a mixture of oxidative agents of 10 mL of concentrated HNO_3 and 3 mL of H_2O_2 at 60 °C ($1 \cdot 10^{-3}$ mbar) for surface oxidation. Afterwards, filtration was followed by washing with demineralized water. The filtered product was put into an oven at 100 °C for drying. The resulting surface carboxylic acid groups were reduced to hydroxyl groups by refluxing of 1 g of dried oxidized material in 50 mL $BH_3 \cdot THF$ solution for 24 h, followed by washing with water by Soxhlet extraction for 24 h.

Functionalization of the pore walls with AzPTES
For the functionalization with azide moieties, a suspension of 15 ml toluene and $9.5 \cdot 10^{-4}$ mol 3-azidopropyltriethoxysilane (AzPTES, prepared according to ref.[25]) per gram carbon material was prepared and stirred at 80 °C for 72 h. The functionalized material was separated under vacuum, washed with THF and dried at 100 °C.

Due to the low Rh loadings (cf. section 4.2) and the low yields in the heterogeneous molecular catalysis, a selective functionalization of the inner pore walls of the OMC materials was omitted.

3.2.3 Non-templated silica

Functionalization of the particle surface and the pore entrances
For the passivation of NT-$mSiO_2$, the following procedure was used:[24,27,28] 4 g of the triblock copolymer Pluronic® P-123 ($EO_{20}PO_{70}EO_{20}$, M_n = 5800 g mol^{-1}, Sigma Aldrich) were dissolved in 60 mL of EtOH. To this solution, 1 g of NT-$mSiO_2$ were added and the mixture was stirred

at room temperature for 24 h. The material was separated via filtration and dried under vacuum at 80 °C for 24 h. To the Pluronic® P-123 filled NT-mSiO_2, 4.02 mL of hexamethyldisilazane (HMDS, Sigma Aldrich) were added and allowed to react with the silica surface for 1 h under neat conditions. The unreacted HMDS was removed by washing the material with copious amounts of hexane. After passivation, the Pluronic® P-123 was removed via Soxhlet extraction in EtOH at 140 °C for 112 h and the resultant powder was dried.

Functionalization of the pore walls with AzPTES

For the functionalization of the internal pore surface with azide groups, a suspension of 15 mL toluene and 9.5 x 10^{-4} mol 3-azidopropyltriethoxysilane (AzPTES, FluoroChem, Derbyshire, UK) per gram material of NT-mSiO_2 was prepared and stirred at room temperature for 72 h. The functionalized material was separated by filtration, washed with EtOH and dried.

3.3 Immobilization of alkynes and alkynones

General procedure for the immobilization on supports via CuAAC [GP 14]

According to ref.[16] under a nitrogen atmosphere to a suspension of the respective support material (0.20 g, 1 eq. of azide groups) in a mixture of water (2 mL) and CH_2Cl_2 (4 mL) the respective alkyne or alkynone (1 eq.) was added. $CuSO_4 \cdot 5\ H_2O$ (1.5 eq.) and sodium ascorbate (3.0 eq.) were added and the reaction mixture was stirred for 3 d at room temperature in the dark. The reaction mixture was centrifuged (4000 rpm) and the supernatant was collected in a separatory funnel. The sediment was washed with CH_2Cl_2 (2 × 5 mL), a saturated EDTA solution (2 × 5 mL), water (2 × 5 mL) and acetone (2 × 5 mL). The sediment was dried under vacuum and then used for catalysis. The combined washing solutions were added into the separatory funnel, extracted with CH_2Cl_2 (3 × 30 mL) and the combined organic layers were dried over $MgSO_4$. The solvent was removed under reduced pressure and the residue was taken up in $CDCl_3$. Mesitylene was added and a ^{1}H NMR spectrum was recorded to determine the loading of the ligand on the support.

4 Characterization of the supports

Small-angle X-ray scattering

The mesopore arrangement was investigated by small-angle X-ray scattering (SAXS). For this, the pulverized, as-synthesized materials were filled into mark tubes made of quartz glass (Hilgenberg GmbH) with an outer diameter of 0.7 or 0.9 mm. Measurements were performed with a SAXSess mc^2 from Anton Paar. Samples were placed into a temperature controlled sample holder (TCS120) and kept at 25°C. Cu-K_α radiation (λ = 1.5418 Å) was generated by an ID3003 X-ray generator from Seifert (40 kV, 40 mA). For detection of the scattered intensity, the 1D CMOS detector Mythen 1K from Dectris was used. The sample to detector distance was calibrated with a reference sample of cholesteryl palmitate. The scattering data was background corrected and deconvolved with respect to the line collimated beam profile using the associated software SAXSquant.

The scattering maxima of the obtained scattering curves were fitted with Lorentzians to extract the according values of the scattering vector *q*. The space groups of the materials were determined from the characteristic ratios of these *q*-values. The calculated lattice parameters *a*, which equal the pore-to-pore distance in case of the space group *p*6*mm*, are listed in Table S1.

Table S1: Space groups and lattice parameters *a* as determined by SAXS for the as synthesized materials.

support	space group	*a* [nm]
OMS-2.6	*p*6*mm*	4.4
OMS-4.9	(*p*6*mm*)*	10.1
OMS-5.9	*p*6*mm*	11.2
OMS-6.8	*p*6*mm*	12.2
OMC-6.2	*p*6*mm*	12.7
OMC-10.3	*p*6*mm*	15.3

*An unambiguous determination of the space group was not possible due to a too small number of characteristic scattering peaks. For calculation of the lattice parameter *a* the space group given in parentheses was assumed.

Nitrogen physisorption measurements

The surface area as well as the pore size of the selectively functionalized materials were analyzed by nitrogen physisorption measurements. The adsorption and desorption isotherms were recorded using Autosorb iQ from Quantachrome Instruments. Before the measurements, the samples were heated up to 200 °C under vacuum with a heating rate of 2 K min^{-1} and were outgassed for 8 h. Afterwards, the nitrogen physisorption measurements were performed in a liquid nitrogen bath at -196 °C. From the adsorption isotherms, the surfaces were calculated using the BET method, whereas the pore sizes and pore size distributions were determined with the NLDFT method, taking into account the hexagonal pore structure. For the NT-mSiO_2 materials, adsorption and desorption isotherms were recorded using a Quantochrome Nova 800 Physisorption Analyzer. Prior to analysis, the samples were degassed at 200°C at a rate of 2 K min^{-1} under vacuum for a period of 8 h. The physisorption measurements were performed in a liquid nitrogen bath at -196°C. The surface areas were calculated using the BET method, and the pore sizes were determined from the NLDFT method using the cylindrical/spherical pore model. The pore sizes of the NT-mSiO_2 materials were additionally

determined by applying the Barett-Joyner-Halenda (BJH) model to the desorption branch of the isotherm. It should be noted that the pore size of non-templated mesoporous silica obtained via N_2 physisorption is a purely textural value, since the NLDFT does not take into account the tetrahedral and octahedral pore geometry. An overview of the BET results of all investigated materials is given in table S2.

Table S2: Total surface determined by the BET method (S_{BET}), total pore volume (V_{pore}) and pore diameters determined by the NLDFT method ($d_{pore,DFT}$).

support	S_{BET} [m^2g^{-1}]	V_{pore} [cm^3g^{-1}]	$d_{pore,DFT}$ [nm][b]
OMS-2.6	1282	0.58	2.6
OMS-4.9	694	0.66	4.9
OMS-5.9	629	0.66	5.9
OMS-6.8	739	0.94	6.8
OMC-6.2[a]	821	0.41	6.2
OMC-10.3[a]	794	0.46	10.3
NT-mSiO_2-4.2[a]	347	0.24	4.2
NT-mSiO_2-8.1[a]	294	0.28	8.1

[a] BET values were determined from the materials before AzPTES functionalization.
[b] mean pore diameter determined from the pore size distribution

The pore size distributions of the OMS, the NT-mSiO_2 and OMC materials that were determined with the NLDFT method are shown in Figure S110–S112.

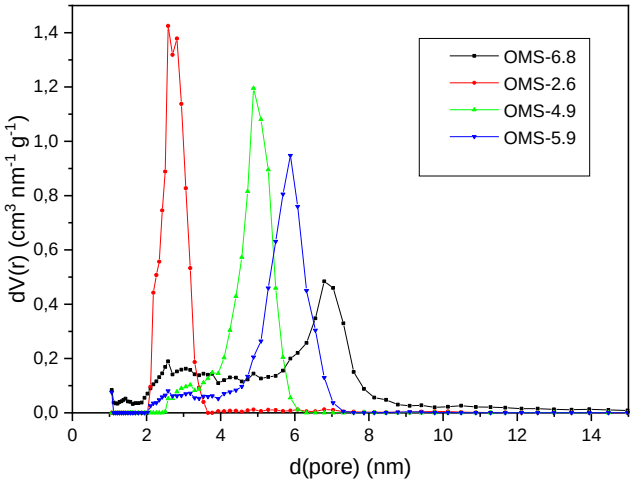

Figure S110. Pore size distribution of OMS materials determined with the NLDFT method.

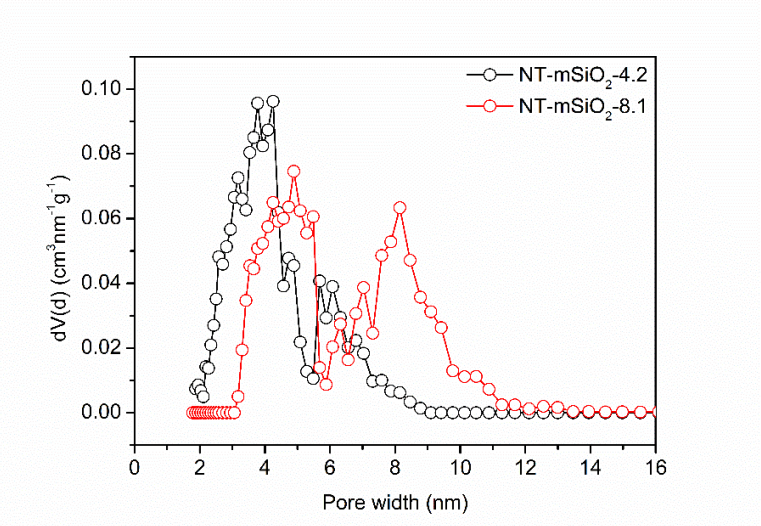

Figure S111. Pore size distribution of NT-mSiO$_2$-4.2 and NT-mSiO$_2$-8.1 determined with the NLDFT method.

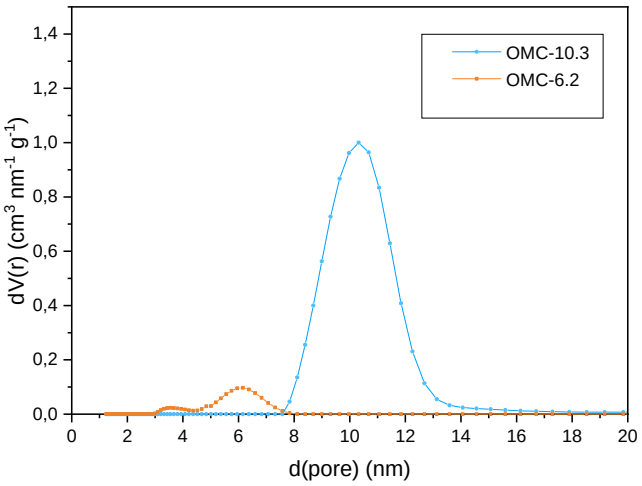

Figure S112. Pore size distribution of OMC materials determined with the NLDFT method.

Infrared spectroscopy (FTIR)

For the characterization of the surface, the materials were examined by IR spectroscopy. Before the measurements, tablets of potassium bromide (KBr for IR spectroscopy, Uvasol®, Sigma Aldrich) and the sample were prepared. The mass ratio of KBr to the sample was 200. For the measurements, the spectrometer Nicolet 6700 from Thermo Scientific was used. The spectra were examined in the range from 3800 cm^{-1} to 420 cm^{-1} with 16 scans and a resolution of 4 cm^{-1}.

Determination of the hydroxy surface concentrations[29,30]

For the determination of the silanol concentration the respective azide-functionalized support material was dried under vacuum for 24 h at 200 °C. The support material (0.10 g) was transferred into a nitrogen glovebox and a solution of ferrocene (10.0 mg, 53.7 µmol) and benzylmagnesium chloride (2.00 mL, 1.80 g, 2.00 mmol, 1 M in 2-methyltetrahydrofuran) in dry deuterated benzene (2.2 mL) was added. The reaction mixture was left to react for 30 min and a part of the supernatant (0.6 mL) was transferred into an NMR tube. A ^{1}H-NMR spectrum

was recorded and the toluene concentration was determined using ferrocene as the internal standard. The silanol concentration was determined from the toluene concentration and the weight of the support material.

Table S3. Concentration of surface hydroxy groups (silanol or C-OH) of different mesoporous materials determined by the hydrolysis of benzylmagnesium chloride.

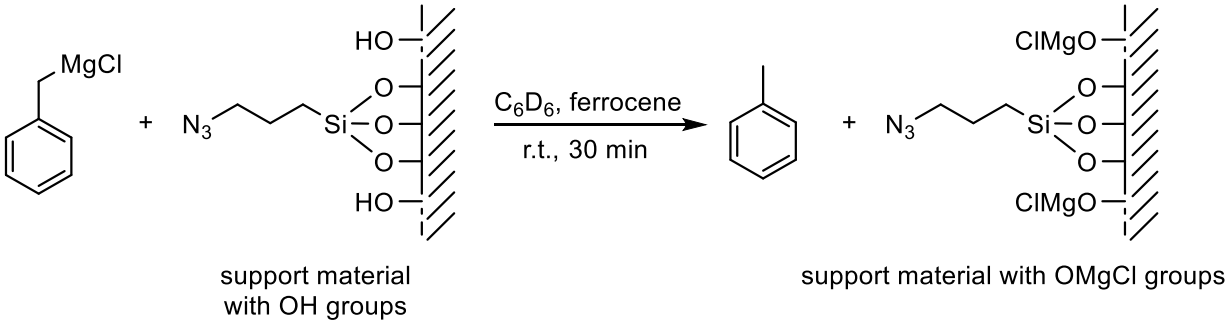

entry	support material	$c_{R\text{-}OH}$[a] [mmol/g]	S_{BET}[b] [m^2/g]	$c_{R\text{-}OH}$[c] [µmol/m^2]	OH groups per area[d] [nm^{-2}]
1	OMS-6.8	2.14	739	2.90	1.74
2	OMS-5.9	1.66	629	2.64	1.59
3	OMS-4.9	2.29	694	3.30	1.99
4	OMS-2.6	0.61	1282	0.47	0.29
5	OMS-2.6[e]	1.50	1282	1.17	0.70
6	OMS-2.6[f]	1.61	1282	1.25	0.75
7	OMC-6.2	1.00	821	1.22	0.73
8	NT-mSiO_2-4.2	1.78	347	5.13	3.09
9	NT-mSiO_2-8.1	2.05	294	6.97	4.20

[a] The concentration of surface hydroxy groups (silanol or C-OH) was determined from the ^{1}H NMR spectrum of the supernatant. Ferrocene was used as the internal standard. [b] Specific surface area determined by N_2 physisorption. [c] Surface concentration of the OH groups. These values were calculated dividing the concentration of surface hydroxy groups per gram support material by the specific surface area. [d] Calculated by multiplying the hydroxy surface concentration with the Avogadro constant. [e] Prolonged reaction time of 24 h. [f] Prolonged reaction time of 48 h.

4.1 FTIR spectra

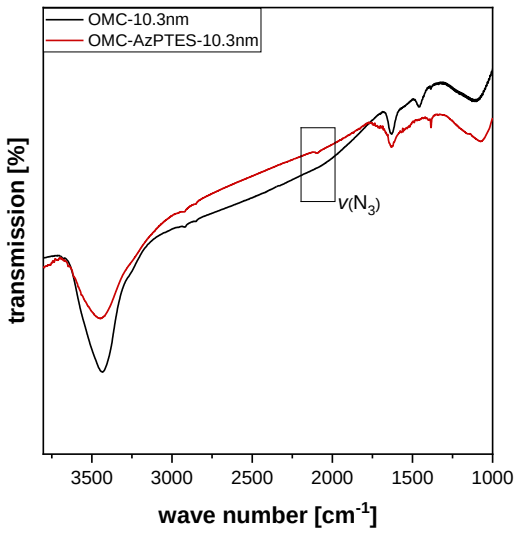

Figure S113: FT-IR spectra of one representative carbon material (OMC-10.3) before (black line) and after the functionalization step with AzPTES (red line). The signal at 2100 cm^{-1} (box) can be assigned to the azide vibrational band.

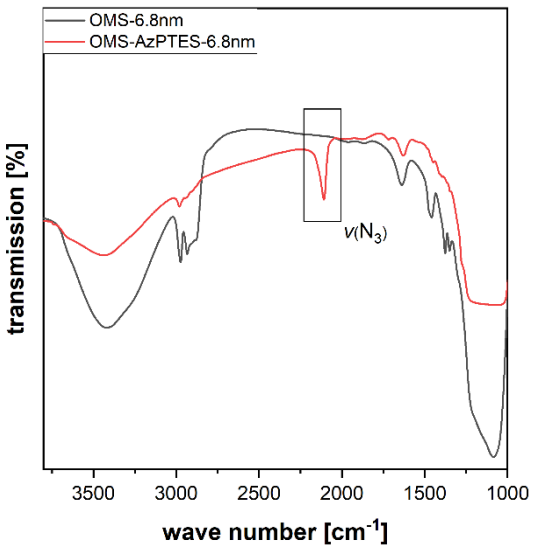

Figure S114: FT-IR spectra of one representative silica material (OMS-6.8) before (black line) and after the functionalization step with AzPTES (red line). The signal at 2100 cm^{-1} (box) can be assigned to the azide vibrational band.

4.2 ICP-OES Measurements

4.2.1 OMC materials

In our previous study[16] we could show that over 60 % of the initially used amount of Rh remained on silica materials after *in situ* complexation. Also, it was found that no leaching of the diene ligand occurred under the investigated 1,2-addition conditions. However, the low yields in catalysis with ligands immobilized on OMC materials indicated that the concentration of Rh diene catalyst was rather low. Thus, the Rh complex was formed with

OMC-6.2-**Ph(*i*PrC$_1$OC$_1$)click** and subsequent ICP-OES analysis was performed. In the following section the procedure is described.

Synthesis of OMC-6.2-Ph(*i*PrC$_1$OC$_1$)click-Rh

OMC-6.2-**Ph(*i*PrC$_1$OC$_1$)click** (25.0 mg, c_{diene} = 0.108 mmol/g, 2.70 µmol diene, 1 eq.) was suspended in degassed dioxane (1 mL) and $[RhCl(C_2H_4)_2]_2$ (0.53 mg, 1.35 µmol, 0.5 eq.) was added. The reaction mixture was stirred for 30 min at room temperature and then centrifuged (4000 rpm). The sediment was washed with dioxane (3 × 2 mL) and dried under vacuum.

Determination of the Rh loading on OMC-6.2-Ph(*i*PrC$_1$OC$_1$)click-Rh via ICP-OES

The rhodium loading was determined by ICP-OES. Therefore, the carbon material OMC-6.2-**Ph(*i*PrC$_1$OC$_1$)click**-Rh was dissolved in aqua regia and analyzed by ICP-OES. Rh was measured at 249.077 nm, the background was measured from 248.950 nm - 248.995 nm and from 249.126 nm - 249.150 nm. Calibration was accomplished using Rh standards in 1M nitric acid containing 0.1 - 10 mg Rh/L. 0.0045 mmol/g Rh/Carbon were detected in the solution. This means that only 4 wt/wt % of the Rh that was used for complexation was found immobilized on OMC-6.2-**Ph(*i*PrC$_1$OC$_1$)click**-Rh.

4.2.2 NT-mSiO$_2$ materials

Synthesis of NT-mSiO$_2$-Ph(*i*PrC$_1$OC$_1$)click-Rh (d_{pore} = 4.2, 8.1 nm)

NT-mSiO$_2$-**Ph(*i*PrC$_1$OC$_1$)click** (d_{pore} = 4.2, 8.1 nm, 25 mg, 1 eq. immobilized diene) was suspended in degassed dioxane (1 mL) and $[RhCl(C_2H_4)_2]_2$ (0.5 eq.) was added. The reaction mixture was stirred for 30 min at room temperature and then centrifuged (4000 rpm). The sediment was washed with dioxane (3 × 2 mL) and dried under vacuum. NT-mSiO$_2$-**Ph(*i*PrC$_1$OC$_1$)click**-Rh (d_{pore} = 4.2, 8.1 nm) was obtained as a yellow powder.

Determination of the Rh loading on NT-mSiO$_2$-Ph(*i*PrC$_1$OC$_1$)click-Rh (d_{pore} = 4.2, 8.1 nm) via ICP-OES

ICP-OES measurements were carried out similar as described for the OMC material above. The concentrations of Rh that were detected on NT-mSiO$_2$-**Ph(*i*PrC$_1$OC$_1$)click**-Rh (d_{pore} = 4.2, 8.1 nm) are listed in Table S4.

Table S4. ICP-OES results for the immobilized Rh complex NT-mSiO$_2$-**Ph(*i*PrC$_1$OC$_1$)click**-Rh (d_{pore} = 4.2, 8.1 nm).

entry	sample	*c*(Rh,in[a]) [mg g^{-1}]	*c*(Rh,out[b]) [mg g^{-1}]	Rh on support [wt/wt %]
1	NT-mSiO$_2$-8.1-**Ph(*i*PrC$_1$OC$_1$)click**-Rh	24.70	23.19	94
2	NT-mSiO$_2$-4.2-**Ph(*i*PrC$_1$OC$_1$)click**-Rh	26.76	21.46	80

[a] The abbreviation "in" describes the amount of Rh used for the complexation of the supported diene. [b] The abbreviation "out" describes the amount of Rh determined from the ICP-OES measurements of the final catalyst.

4.2.3 OMS materials

For the latter EXAFS experiments the immobilized dienes OMS-**Ph(C_{10}CO)click** were complexed with Rh as follows:

Synthesis of OMS-Ph(C_{10}CO)click-Rh (d_{pore} = 4.9, 5.9, 6.8 nm)
OMS-**Ph(C_{10}CO)click** (d_{pore} = 4.9, 5.9 or 6.8 nm, 0.20 g, 1 eq. immobilized diene) was suspended in degassed dioxane (4 mL) and $[Rh(C_2H_4)_2Cl]_2$ (0.5 eq.) was added. The reaction mixture was stirred for 30 min at room temperature and then centrifuged (4000 rpm). The sediment was washed with dioxane (3 × 2 mL) and dried under vacuum. OMS-**Ph(C_{10}CO)click**-Rh (d_{pore} = 4.9, 5.9, 6.8 nm) was obtained as a yellow powder.

Determination of the Rh loading on OMS-Ph(C_{10}CO)click-Rh (d_{pore} = 4.9, 5.9, 6.8 nm) via ICP-OES
ICP-OES measurements were carried out similar as described for the OMC material above. The concentrations of Rh that were detected on OMS-**Ph(C_{10}CO)click**-Rh (d_{pore} = 4.9, 5.9, 6.8 nm) are listed in Table S5.

Table S5. ICP-OES results for the immobilized Rh complex OMS-**Ph(C_{10}CO)click**-Rh (d_{pore} = 4.9, 5.9, 6.8 nm).

entry	sample	*c*(Rh,in[a]) [mg g $^{-1}$]	*c*(Rh,out[b]) [mg g $^{-1}$]	Rh on support [wt/wt %]
1	OMS-4.9-**Ph(C_{10}CO)click-Rh**	32.54	27.59	85
2	OMS-5.9-**Ph(C_{10}CO)click-Rh**	35.62	24.65	69
3	OMS-6.8-**Ph(C_{10}CO)click-Rh**	36.49	21.64	59

[a] The abbreviation "in" describes the amount of Rh used for the complexation of the supported diene. [b] The abbreviation "out" describes the amount of Rh determined from the ICP-OES measurements of the final catalyst.

5 Data for the immobilization on OMS

For all pore sizes and most ligands, a high norbornadiene loading ranging between 0.19–0.45 mmol g^{-1} was obtained (Table S6).

Table S6. Results of the immobilization of selected alkynes and alkynones on OMS with different pore sizes.

entry	ligand	c_{azide}[a] [mmol/g]	d_{pore} [nm]	c_{NBD}[b] [mmol/g]	name
1	**Ph(HC_1OC_1)**	0.39	4.9	0.36	OMS-4.9-**Ph(HC_1OC_1)click**
2	**Ph(HC_1OC_1)**	0.46	5.9	0.41	OMS-5.9-**Ph(HC_1OC_1)click**
3	**Ph(HC_1OC_1)**	0.43	6.8	0.36	OMS-6.8-**Ph(HC_1OC_1)click**
4	**Ph(BnC_1OC_1)**	0.39	4.9	0.33	OMS-4.9-**Ph(BnC_1OC_1)click**
5	**Ph(BnC_1OC_1)**	0.46	5.9	0.33	OMS-5.9-**Ph(BnC_1OC_1)click**
6	**Ph(BnC_1OC_1)**	0.43	6.8	0.33	OMS-6.8-**Ph(BnC_1OC_1)click**
7	**1-Naph(*i*PrC_1OC_1)**	0.39	4.9	0.25	OMS-4.9-**1-Naph(*i*PrC_1OC_1)click**
8	**1-Naph(*i*PrC_1OC_1)**	0.46	5.9	0.31	OMS-5.9-**1-Naph(*i*PrC_1OC_1)click**
9	**1-Naph(*i*PrC_1OC_1)**	0.43	6.8	0.43	OMS-6.8-**1-Naph(*i*PrC_1OC_1)click**
10	**2-Naph(*i*PrC_1OC_1)**	0.39	4.9	0.39	OMS-4.9-**2-Naph(*i*PrC_1OC_1)click**
11	**2-Naph(*i*PrC_1OC_1)**	0.46	5.9	0.45	OMS-5.9-**2-Naph(*i*PrC_1OC_1)click**
12	**2-Naph(*i*PrC_1OC_1)**	0.43	6.8	0.30	OMS-6.8-**2-Naph(*i*PrC_1OC_1)click**
13	**Ph(C_2CO)**	0.39	4.9	0.33	OMS-4.9-**Ph(C_2CO)click**
14	**Ph(C_2CO)**	0.46	5.9	0.42	OMS-5.9-**Ph(C_2CO)click**
15	**Ph(C_2CO)**	0.43	6.8	0.42	OMS-6.8-**Ph(C_2CO)click**
16	**Ph(C_4CO)**	0.39	4.9	0.26	OMS-4.9-**Ph(C_4CO)click**
17	**Ph(C_4CO)**	0.46	5.9	0.29	OMS-5.9-**Ph(C_4CO)click**
18	**Ph(C_4CO)**	0.43	6.8	0.19	OMS-6.8-**Ph(C_4CO)click**
19	**Ph($C_{10}CO$)**	0.39	4.9	0.32	OMS-4.9-**Ph($C_{10}CO$)click**
20	**Ph($C_{10}CO$)**	0.46	5.9	0.35	OMS-5.9-**Ph($C_{10}CO$)click**
21	**Ph($C_{10}CO$)**	0.43	6.8	0.36	OMS-6.8-**Ph($C_{10}CO$)click**

[a] Determined via elemental analysis. [b] Determined by extraction of the combined supernatants and washing solutions with CH_2Cl_2 and subsequent measurement of a ^1H NMR spectrum with mesitylene as the external standard.

6 Additional Experiments

6.1 Hot filtration test

To check whether catalysis only takes place with immobilized Rh species and no background catalysis in solution is present a hot filtration experiment was carried out as follows:[31]

Under a nitrogen atmosphere the immobilized ligand OMS-4.9-**Ph(*i*PrC$_1$OC$_1$)click** (57.1 mg, 20.0 µmol, c_{Ligand} = 0.35 mmol/g) was suspended in degassed dioxane (3.2 mL) and $[Rh(C_2H_4)_2Cl]_2$ (3.88 mg, 10.0 µmol) was added. The reaction mixture was stirred for 30 min at room temperature, 3.1 M KOH solution (25.8 µL, 29.2 mg, 80.0 µmol) was added and the reaction mixture was stirred for 20 min at room temperature. The reaction mixture was heated to 60 °C and triphenylboroxine **16** (0.15 g, 0.48 mmol) and the *N*-tosyl imine **15** (0.12 g, 0.40 mmol) were added. After *t* = 1, 2, 4, 8, 16, 32, 64, 128 min samples (0.1 mL) were taken with a syringe, filtrated over a short pad of silica (EtOAc) and the solvent of the filtrate was removed under reduced pressure. After taking the sample at *t* = 128 min half of the reaction mixture was filtered over a short pad of pre-heated Celite® into a second Schlenk tube. Both the unfiltered and the filtered reaction mixture were stirred at 60 °C and samples (0.1 mL) were taken with a syringe after *t* = 240, 360, 480, 600, 1440 min. The samples were filtered over a short pad of silica (EtOAc) and the solvent was removed under reduced pressure. The NMR yield of each sample was determined from the ^{1}H NMR spectrum of the residues and plotted against the reaction time (Figure S115).

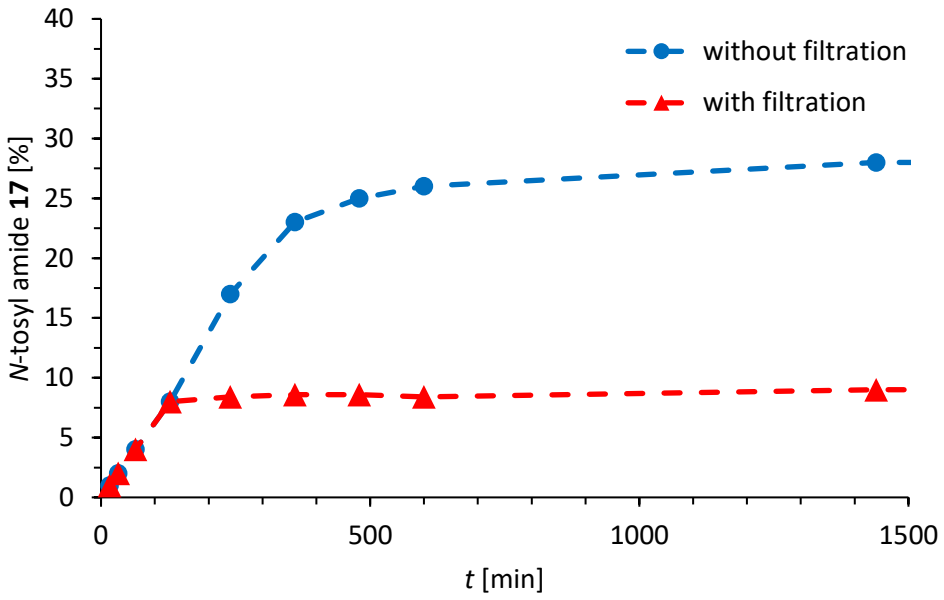

Figure S115. Kinetic curve for the Rh-catalyzed 1,2-addition using OMS-4.9-**Ph(*i*PrC$_1$OC$_1$)click** as ligand without hot filtration (blue dots) and after filtration at *t* = 128 min (red triangles).

Figure S115 indicates that background catalysis in solution does not take place.

6.2 Stability tests

6.2.1 OMS materials

Synthesis of OMS-in-Ph(C_4CO)click-Rh

OMS-**Ph(C_4CO)click** (d_{pore} = 4.9, 5.9 or 6.8 nm, 0.20 g, 1 eq. immobilized diene) was suspended in degassed dioxane (4 mL) and $[RhCl(C_2H_4)_2]_2$ (0.5 eq.) was added. The reaction mixture was stirred for 30 min at room temperature and then centrifuged (4000 rpm). The sediment was washed with dioxane (3 × 2 mL) and dried under vacuum. OMS-**Ph(C_4CO)click**-Rh (d_{pore} = 4.9, 5.9, 6.8 nm) was obtained as a yellow powder.

Physisorption measurements

To test for the stability of the OMS materials OMS-**Ph(C_4CO)click**-Rh was used in the 1,2-addition as described in GP 14 and the immobilized catalyst was separated from the reaction mixture after catalysis by centrifugation. Subsequently, the immobilized catalyst was washed with dioxane, water and acetone and dried under vacuum. Finally, nitrogen physisorption measurements were carried out with the native catalyst and the catalyst after catalysis (Table S7).

Table S7. Total surface area determined by the BET method (S_{BET}), total pore volume (V_{pore}) and pore diameters determined by the NLDFT method ($d_{pore,DFT}$) of native OMS-in-**Ph(C_4CO)click**-Rh and after catalysis.

immobilized catalyst	parameter	native	after catalysis
OMS-4.9-**Ph(C_4CO)click**-Rh	S_{BET} [m^2/g]	294	281
	V_{pore} [cm^3/g]	0.38	0.36
	$d_{pore,DFT}$ [nm]	4.9	4.9
OMS-5.9-**Ph(C_4CO)click**-Rh	S_{BET} [m^2/g]	303	244
	V_{pore} [cm^3/g]	0.42	0.36
	$d_{pore,DFT}$ [nm]	5.3	5.5
OMS-6.8-**Ph(C_4CO)click**-Rh	S_{BET} [m^2/g]	344	219
	V_{pore} [cm^3/g]	0.61	0.45
	$d_{pore,DFT}$ [nm]	6.6	6.6

For all immobilized Rh complexes OMS-in-**Ph(C_4CO)click**-Rh lower surface areas as well as pore volumes and in some cases even smaller pore diameters were observed as compared to the materials before the clicking of the ligand and the complexation with Rh (Table S2 and Table S7). This is due to the pore filling with the Rh diene catalyst. After catalysis the surface areas and pore volumes further decreased. The pore diameters stayed almost constant, which indicates that even though further pore blocking occurs during the course of the synthesis, the structure of the support material is stable.

Transmission electron microscopy (TEM)

To check if the hexagonally arranged cylindric pores are stable under the catalytic conditions OMS-in-**Ph(C_4CO)click**-Rh samples (d_{pore} = 4.9, 5.9, 6.8 nm) before and after catalysis was investigated by TEM. The measurements were performed with a Zeiss EM10C/CT TEM at 60 kV, the set up was further equipped with a water-cooled 1k slow-scan CCD Camera (7888-IV) from TRS for taking pictures with the attached software Image eSP. For sample preparation, the OMS materials were grinded, dispersed in ethanol by ultra-sound treatment and dropped onto a pioloform-coated copper grid (400 mesh) from Plano. Figure S116 displays the TEM images of the OMS-in-**Ph(C_4CO)click**-samples before and after the catalysis. No visible differences in the pore structures occur between the two states, suggesting they are stable against the catalysis conditions of the 1,2-addition.

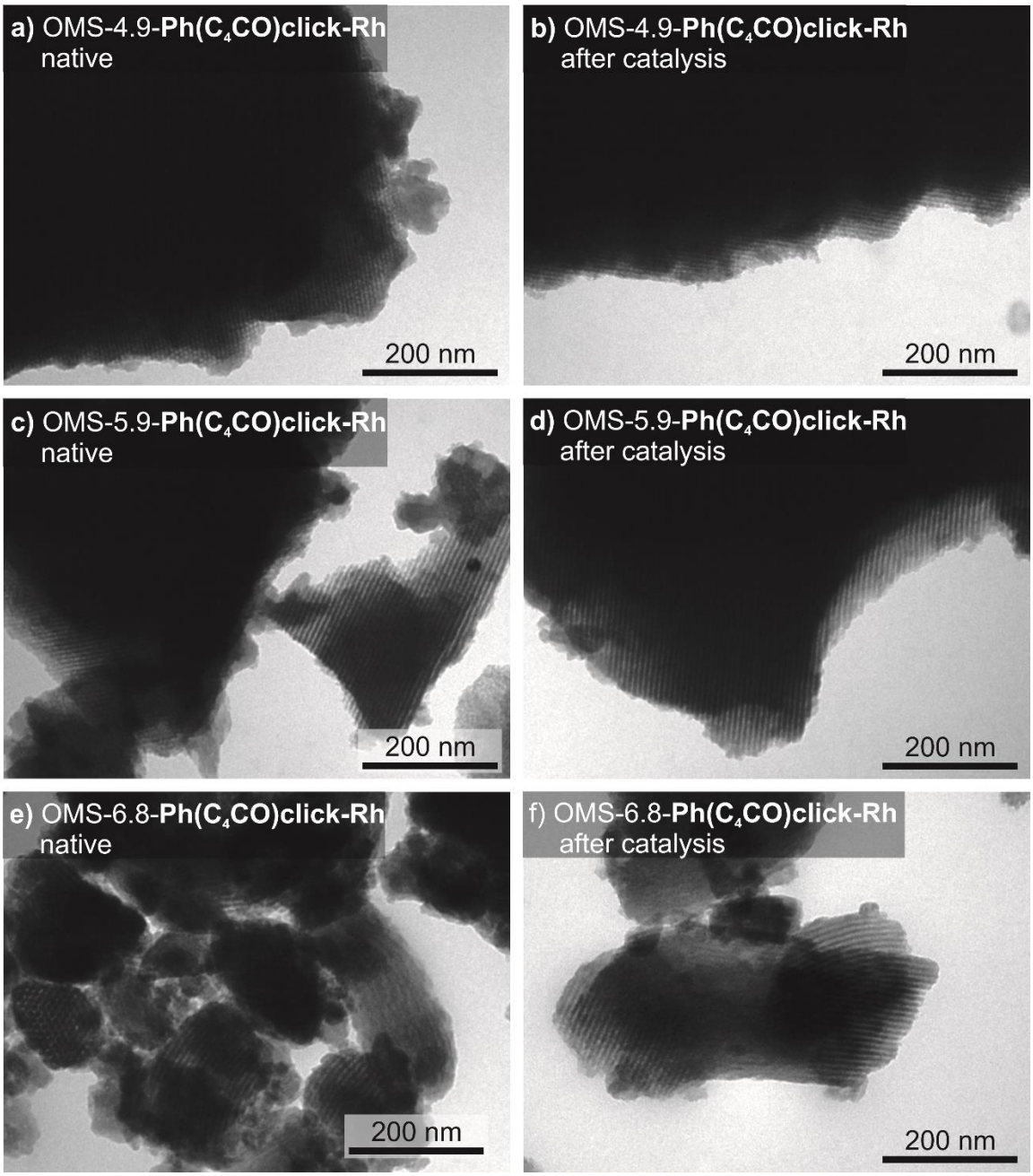

Figure S116. TEM pictures of native OMS-in-**Ph(C_4CO)click**-Rh (a, c, e) and after catalysis (b, d, f).

TEM pictures showed that the pores are stable under the catalysis conditions of the 1,2-addition. The hexagonally arranged cylindric pores were still abundant.

SAXS measurements

To verify that the mesopores structure of the OMS-in-**Ph(C$_4$CO)click**-Rh samples (d_{pore} = 4.9, 5.9, 6.8 nm) did not only seem stable in individual particles as can be observed by TEM, SAXS measurements of the samples before and after the catalysis were performed, which probe macroscopic sample volumes and therefore provide statistically meaningful information about the structural integrity. Figure S117 shows the scattering curves of the OMS-in-**Ph(C$_4$CO)click**-Rh samples in the native state as well after being applied in the 1,2-addition. In all three cases, the scattering curves before and after the catalysis look almost identically, especially in the region of the sharp peak, which is caused by the ordered mesopores structure. Only in case of OMS-4.9-in-**Ph(C$_4$CO)click**-Rh (Figure S117a) a decrease of the scattering intensity *I* at small scattering angles *q* occurs for the sample after catalysis compared to the native state. Considering that the scattering intensity *I* at small *q*-values mainly originates from the scattering on the surface of the silica particles and that it is proportional to the surface area of the average particle in the sample,[32] his indicates that the average particle size of OMS-4.9-in-**Ph(C$_4$CO)click**-Rh decreased during the catalysis, which can easily be explained by the mechanical stress exerted on the silica particles by the mechanical stirring. Nonetheless, the mesopores structure seems to be unharmed by this, as indicated by the resemblance of the scattering curve at higher *q*-values.

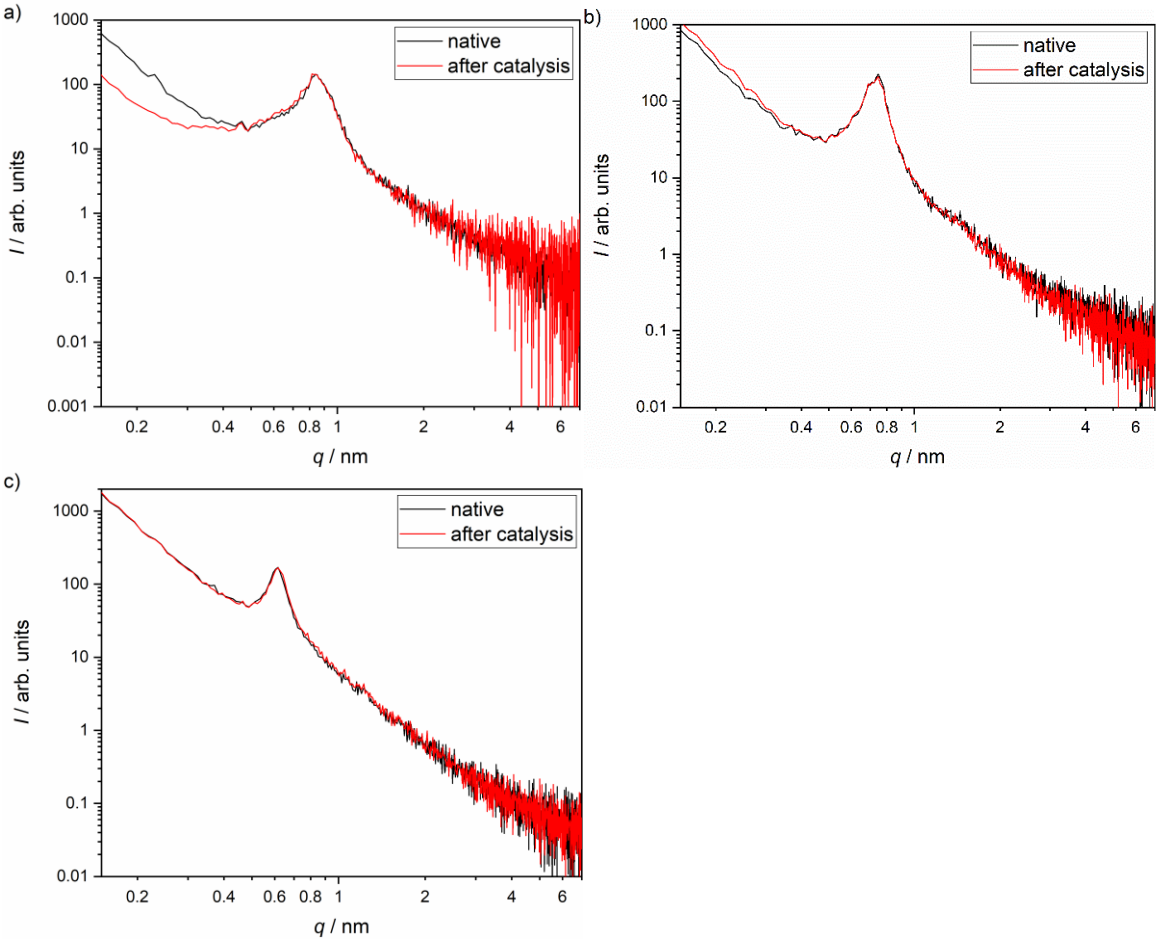

Figure S117. SAXS curves of a) OMS-4.9-in-**Ph(C$_4$CO)click**-Rh, b) OMS-5.9-in-**Ph(C$_4$CO)click**-Rh and c) OMS-6.8-in-**Ph(C$_4$CO)click**-Rh before (black) and after (red) the catalysis.

6.2.2 NT-mSiO$_2$ materials

Physisorption measurements

As described above for OMS materials the NT-mSiO$_2$ materials NT-mSiO$_2$-**Ph(C$_4$CO)click**-Rh were subjected to catalysis, purified and nitrogen physisorption measurement of the native catalyst and the catalyst after catalysis were carried out (Table S8).

Table S8. Total surface area determined by the BET method (S_{BET}), total pore volume (V_{pore}) and pore diameters determined by the NLDFT method ($d_{pore,DFT}$) of native NT-mSiO$_2$-**Ph(C$_4$CO)click**-Rh and after catalysis.

immobilized catalyst	parameter	native	after catalysis
NT-mSiO$_2$-4.2-**Ph(*i*PrC$_1$OC$_1$)click**-Rh	S_{BET} [m^2/g]	234	198
	V_{pore} [cm^3/g]	0.17	0.14
	$d_{pore,DFT}$ [nm]	3.2	3.8
	$d_{pore,BJH}$ [nm]	3.4	3.4
NT-mSiO$_2$-8.1-**Ph(*i*PrC$_1$OC$_1$)click**-Rh	S_{BET} [m^2/g]	324	186
	V_{pore} [cm^3/g]	0.31	0.18
	$d_{pore,DFT}$ [nm]	3.8	3.8
	$d_{pore,BJH}$ [nm]	3.7	3.6

Scanning Electron Microscopy (SEM) analysis

To evaluate the structural stability of the NT-mSiO$_2$ materials after catalysis, SEM images of the pure NT-mSiO$_2$ material and NT-mSiO$_2$ obtained after catalytic experiments were recorded. The SEM images were obtained on a Zeiss Merlin SEM (Carl Zeiss, Germany). Prior to analysis, the samples were sputtered with 5 nm of Ir to render the surface conductive.

A comparison of the SEM images of the as-prepared NT-mSiO$_2$ materials (Figure S118a, S119a) and the NT-mSiO$_2$ materials obtained after catalyst immobilization and catalytic tests (Figure S118c, S119 c) clearly shows that the structural integrity of the NT-mSiO$_2$ materials is preserved under the catalytic conditions.

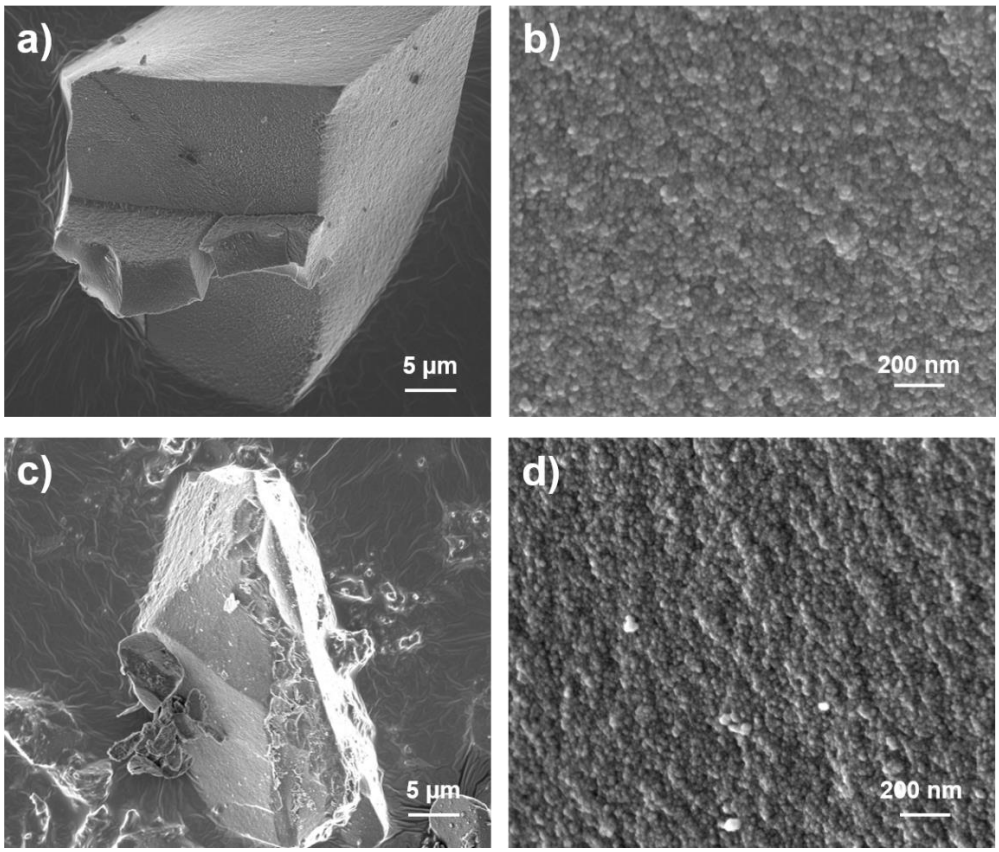

Figure S118. SEM images of a) as-prepared NT-mSiO_2-4.2 and c) NT-mSiO_2-4.2-**Ph(*i*PrC_1OC_1)click**-Rh after catalysis. Higher magnification SEM images of a) and c) are shown in b) and d), respectively.

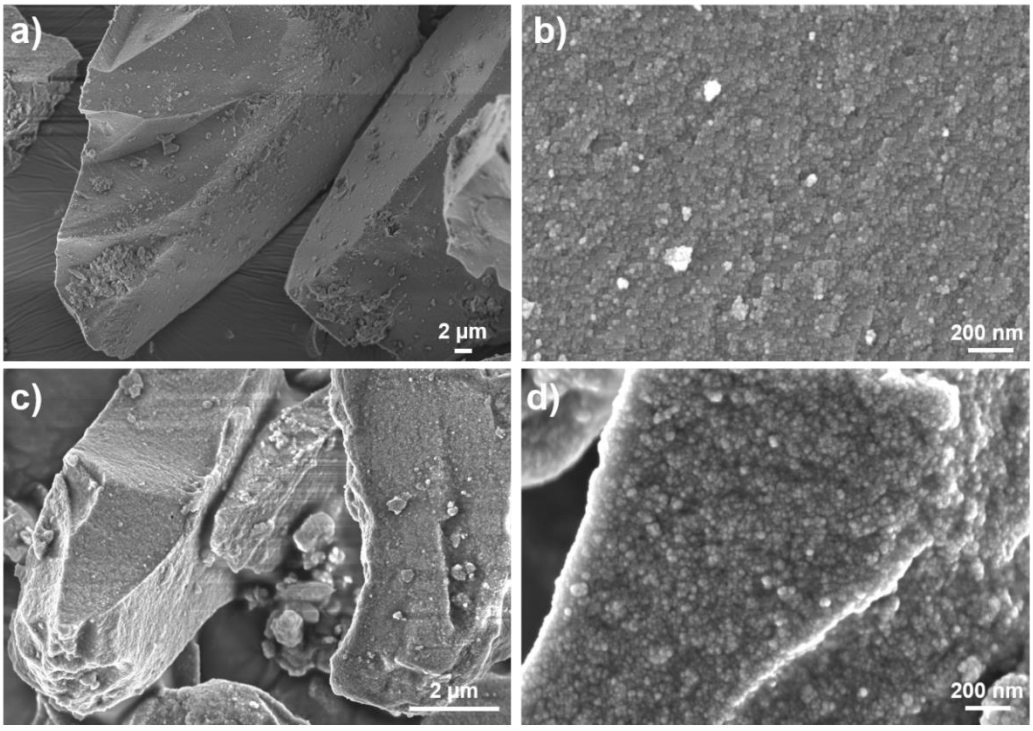

Figure S119. SEM images of a) as-prepared NT-mSiO_2-8.1 and c) NT-mSiO_2-8.1-**Ph(*i*PrC_1OC_1)click**-Rh after catalysis. Higher magnification SEM images of a) and c) are shown in b) and d), respectively.

6.3 Recycling and leaching test

Since it could be shown that the pore structure of OMS materials is not damaged during catalysis, recycling experiments with OMS-5.9-**Ph(C_4CO)click** were carried out as follows:

Under a nitrogen atmosphere the immobilized ligand OMS-5.9-**Ph(C_4CO)click** (0.12 g, 33.4 µmol, c_{NBD} = 0.29 mmol/g) was suspended in degassed dioxane (5.3 mL) and $[Rh(C_2H_4)_2Cl]_2$ (6.46 mg, 16.7 µmol) was added. The reaction mixture was stirred for 30 min at room temperature, 3.1 M KOH solution (42.3 µL, 47.9 mg, 0.13 mmol) was added and the reaction mixture was stirred for 20 min at room temperature. The suspension was heated to 60 °C, triphenylboroxine **16** (0.25 g, 0.80 mmol) and the *N*-tosyl imine **15** (0.20 g, 0.67 mmol) were added and the reaction mixture was stirred for 24 h at 60 °C. The reaction mixture was centrifuged (4000 rpm), the supernatant was removed, and the sediment was washed with dioxane (5 mL), water (5 mL) and acetone (5 mL). The washing solutions and the supernatant were filtered through a short pad of silica (EtOAc), the solvent was removed under reduced pressure and the NMR yield was determined from the crude product using mesitylene as the internal standard. The crude product was purified by column chromatography (hexanes / EtOAc = 10 : 1). Subsequently, the sediment was dried and a small fraction of the recycled catalyst was subjected to ICP-OES analysis to check for the Rh concentration. The rest of the recycled catalyst was used in catalysis as described before. This was repeated until the catalytic activity significantly decreased. The moles of substrates and 3.1 M KOH as well as the amount of solvent was adjusted to the amount of the reused catalyst for each cycle (Scheme S2).

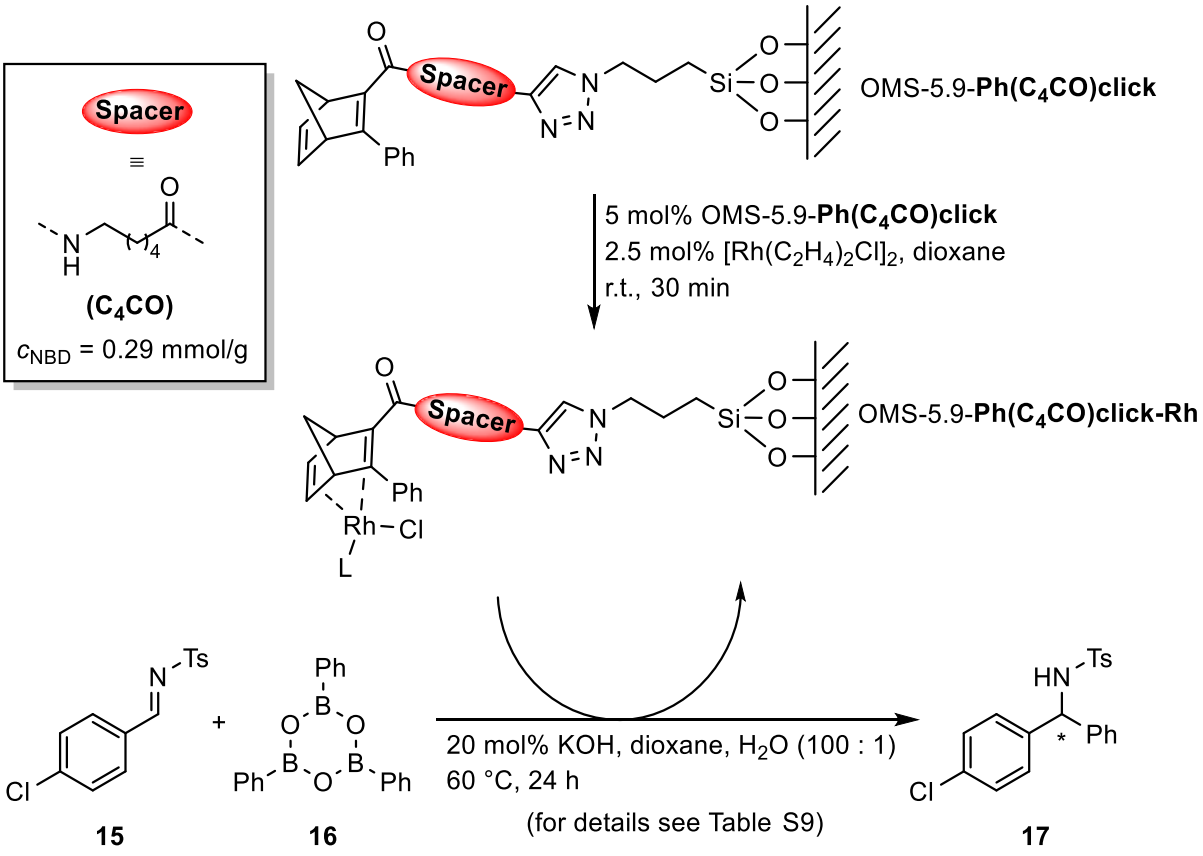

Scheme S2

The results are summarized in Table S9.

Table S9. Recycling experiments using OMS-5.9-**Ph(C_4CO)click** as ligand in the Rh-catalyzed 1,2-addition of triphenylboroxine **16** and *N*-tosyl imine **15**.

entry	cycle	yield [%]		e.r.[b] (*R*) : (*S*)	c_{Rh}[c] [mmol/g]
		NMR[a]	isol.		
1	1	79	70	18 : 82	0.24
2	2	83	79	17 : 83	0.24
3	3	86	80	12 : 88	0.24
4	4	45	35	17 : 83	0.22
5	5	51	48	17 : 83	0.18

[a] determined from the ^{1}H NMR spectrum of the crude product using mesitylene as the external standard. [b] determined by chiral HPLC (OD-H). [c] Rh concentration on the support material after the respective catalysis determined by ICP-OES.

After the first cycle 79 % *N*-tosyl amine **17** with an enantiomeric ratio of e.r. 18 : 82 were obtained (entry 1). For the second and the third cycle the yield and the enantioselectivity slightly increased (entries 2,3). After the fourth and fifth cycle only 45–51 % of *N*-tosyl amine **17** were observed (entry 4). However, the enantioselectivity was retained. The ICP-OES measurements agreed well with the observed catalysis results. No Rh leaching was observed until after the third cycle (entries 1–3). Subsequently, the Rh concentration on the OMS material started to slowly decrease after each cycle (entries 4,5). However, since the enantioselectivity was not influenced, it can be concluded that leached Rh species do not contribute to catalysis. The leached Rh species result in decreased amount of active catalyst.

6.4 Catalyst loading experiments

The catalyst loading experiments were performed with OMS-5.9-**Ph(C_4CO)click** according to GP 14 with 1.0 mol%, 2.5 mol% and 5.0 mol% Rh (Scheme S3).

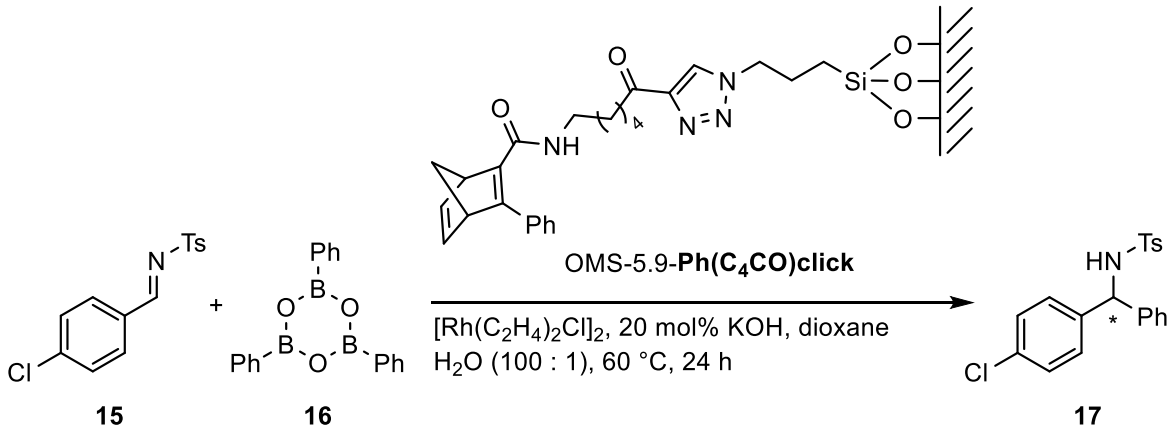

mol% [Rh]	NMR yield[a] [%]	isol. yield [%]	e.r.[b] (*R*) : (*S*)
5.0	79	70	18 : 82
2.5	19	14	15 : 85
1.0	20	14	18 : 82

[a] determined from the ^{1}H NMR spectrum of the crude product using mesitylene as the external standard. [b] determined by chiral HPLC (OD-H).

Scheme S3

7 Computational Studies

All DFT calculations were performed in Turbomole V7.4.1[33] in ChemShell[34,35] via DL-FIND.[34,35] The initial complex structures were created in Avogadro.[36,37] Subsequent use of the Conformer Rotamer Ensemble Sampling Tool (CREST)[38] resulted in several conformers at the GFN2-xTB level. The relevant conformers were extracted based on a visual inspection to maximize structural variety in combination with a comparably low energy. For the selected conformers, geometry optimizations were performed at the B3LYP-D3(BJ)/def2-SVP level followed by a single-point energy calculation of the optimized geometry at the B2PLYP-D3(BJ)/def2-TZVP level.

Table S10: Lowest relative electronic energy of each coordination mode relative to the total lowest coordination mode. All energies are given in kJ mol^{-1}. -

		relative electronic energy of the conformers/ kJ mol^{-1}					
entry	structure	triazole	oxygen	benzyl phenyl	naphthyl	no coord.	elongated
1	**Ph(*i*PrC$_1$amide)click**	0.0	27.0	-	-	-	138.0
2	**Ph(ImC$_1$)click**	89.6	0.0	-	-	-	133.8
3	**Ph(HC$_1$OC$_1$)click**	0.0	31.4	62.0	-	77.2	146.2
4	**Ph(BnC$_1$OC$_1$)click**	0.0	-	-	-	-	149.4
5	**Ph(*i*PrC$_1$OC$_1$)click**	0.0	54.0	50.3	-	76.0	157.7
6	**Ph(*i*PrC$_1$OC$_4$)click**	0.0	-	-	-	-	163.7
7	**1-Naph(^{i}PrC$_1$OC$_1$)click**	0.0	60.9	45.5	104.8	64.2	163.8
8	**Ph(C$_2$CO)click**	0.0	20.1	23.2	-	47.2	122.9
9	**Ph(C$_3$CO)click**	0.0	16.8	16.2	-	43.5	118.8
10	**Ph(C$_4$CO)click**	0.0	10.1	-	-	-	116.9
11	**Ph(C$_{10}$CO)click**	0.0	47.5	51.1	-	-	143.6

8 XAS measurements

8.1 Experimental details

The immobilized Rh complexes (immobilized in mesoporous OMS) were measured in pure powder form, since the concentration of Rh was low enough to avoid self-absorption effects. All XAS experiments were carried out at PETRA III beamline P64 at Deutsches Elektronensynchrotron (DESY) in Hamburg, Germany. The measurements at the Rhodium K-edge (23220 eV) were performed using a Si(311) double-crystal monochromator and a maximum synchrotron beam current of 100 mA. Spectra were recorded in fluorescence mode using a hyperpure Ge detector. For energy calibration, a Rhodium foil was used, which was measured prior to the sample measurements. Monochromator-energy calibration was performed using the first inflection point in Rh foil XANES spectrum. The data acquisition was performed in continuous scan mode and for further analysis rebinning was applied using the Athena software, which is part of the Demeter package.[39] All measurements were carried out at room temperature. No indications of radiation damage were observed.

8.2 Data analysis

In the first step of data analysis the background of the spectrum was removed by subtracting a Victoreen-type polynomial.[39–42] Due to the very differing shapes of the absorption edges of the samples and the used references, the first inflection point of the first derivative of the corresponding spectrum was defined as energy E_0. Afterwards a piecewise polynomial was used to determine the smooth part of the spectrum and was adjusted in a way that the low-R components of the resulting Fourier transform were minimal. The background subtracted spectrum was divided by its smoothed part and the photon energy was converted to photoelectron wave number *k*. For evaluation of the EXAFS spectra the resulting functions were weighted with k^2 and calculated with *ARTEMIS* program. Curve fitting was performed using ab-initio-calculated phases and amplitudes from the FEFF8 program from the University of Washington. *ARTEMIS* works based on the EXAFS function and according to a formulation in terms of radial distribution functions[43,44]:

$$\chi(k) = \sum_j S_0^2(k) F_j(k) \int P_j(r_j) \frac{e^{\frac{-2r_j}{\lambda}}}{kr_j^2} \sin\left[2kr_j + \delta_j(k)\right] dr_j$$

The number of independent points N_{ind} was calculated according to information theory to determine the degree of overdeterminacy[44]:

$$N_{ind} = \frac{2\Delta k \Delta R}{\pi}$$

Here, *Δk* describes the range in *k*-space used for data analysis and *ΔR* corresponds to the distance range in the Fourier filtering process. For the analysis a *Δk*-range of 8 and a *ΔR*-range of 4 was used, which yielded a number of independent points of 20. The quality of a fit was determined using two methods. The reduced χ^2_{red} considers the degree of overdeterminacy of the system and the number of fitted parameters *p*. It therefore allows a direct comparison of different models[45]:

$$\chi^2_{red} = \frac{(N_{ind}/N)}{N_{ind} - p} \sum_i \left(\frac{k_i^n}{\sum_j k_j^n \left| \chi_j^{exp}(k_j) \right|} \right)^2 (\chi^{exp}(k_i) - \chi^{theo}(k_i))^2$$

The R-factor, which represents the percental disagreement between experiment and adjusted function and takes into account both systematic and random errors according to the equation[45]:

$$R = \sum_i \frac{k_i^n}{\sum_j k_j^n \left| \chi_j^{exp}(k_j) \right|} \left| \chi^{exp}(k_i) - \chi^{theo}(k_i) \right| \cdot 100\%$$

The accuracy of the determined distances is 1 %, of the Debye-Waller-like factor 10 %[46] and of the coordination numbers depending of the distance 5–15 %. Initial values for coordination numbers and distances were adopted from the corresponding geometry optimization mentioned in the main part of this publication and afterwards iterated free in every fit as well as the Debye-Waller-like factors. The amplitude reducing factor was set to 1.

8.3 XANES analysis details

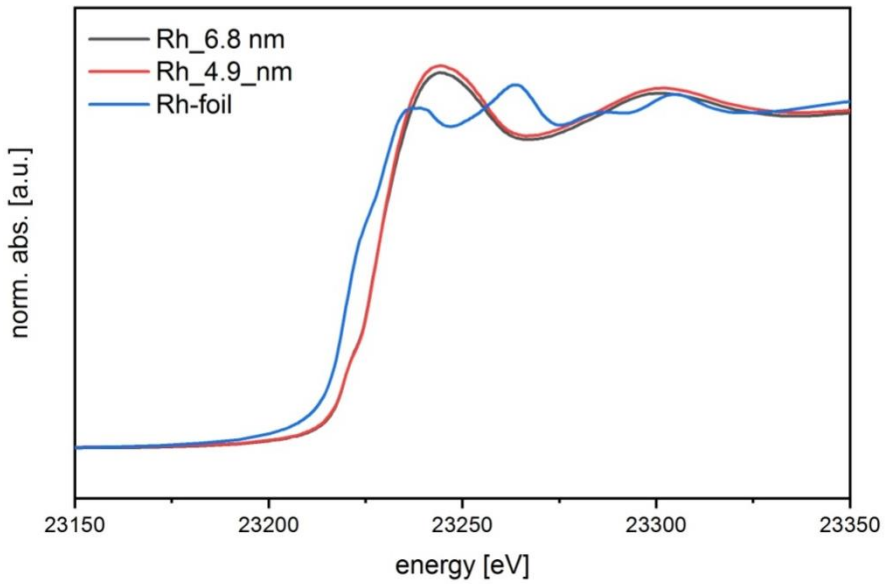

Figure S120. XANES spectra of the two immobilized Rh complexes as well as of the Rh(0) foil used for calibration (blue).

Table S11. Edge energies of the two immobilized Rh samples.

sample	edge energy E_0 [eV]
OMS-4.9-**Ph(C_{10}CO)click**-Rh	23228.0
OMS-6.8-**Ph(C_{10}CO)click**-Rh	23228.0
Rh(0) foil	23220.0

8.4 EXAFS analysis details

The *k*- and *R*-ranges of the analysis of the Rh complexes together with the corresponding fit parameters are collected in Table S12 and S14. Figure S121 and S122 illustrate the fitted function, experimental data, residual plot as well as first shell contributions for the Rh samples in *k*-space. The corresponding first shell scattering paths including coordination numbers, bond distances and Debye-Waller factors are collected in Table S13 and S15.

8.4.1 Parameters based on geometry optimization for triazole coordination

Table S12. *k*- and *R* ranges as well as corresponding fit parameters of the analysis of the two immobilized Rh samples.

sample	*k*-range [Å^{-1}]	*R*-range [Å]	*R*-factor	reduced Chi-square	S_0^2 value
OMS-4.9-**Ph(C_{10}CO)click**-Rh	3.03 - 13.50	1.15 - 4.00	0.0077	11	1.0
OMS-6.8-**Ph(C_{10}CO)click**-Rh	3.10 - 12.70	1.15 - 4.00	0.0107	15	1.0

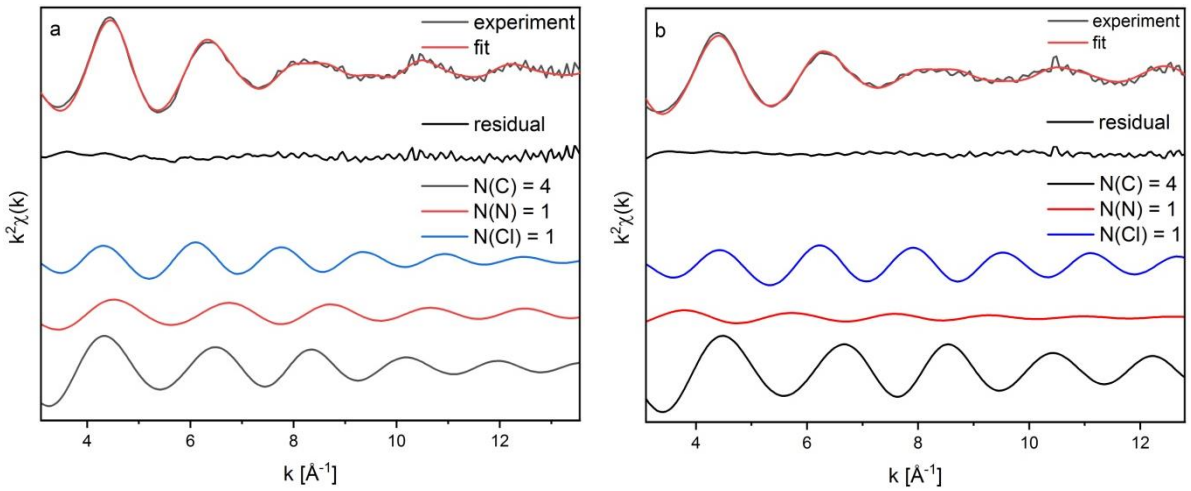

Figure S121. Fitted function compared with experimental data, residual plot and first coordination shell paths for the two immobilized Rh samples in *k*-space. Immobilized Rh complex in 4.9 nm pores (a) and immobilized Rh complex in 6.8 nm pores (b).

Table S13. First shell coordination Numbers (*N*), bond lengths (*R* + Δ*R*) and Debye-Waller factors of the two immobilized Rh complexes.

Scattering paths	4.9 nm pores			6.8 nm pores		
	N	*R* + Δ*R* [Å]	σ^2 [Å^2]	*N*	*R* + Δ*R* [Å]	σ^2 [Å^2]
immobilized Rh-samples						
Rh-C	4.0(2)	2.113(11)	0.0041(13)	3.9(2)	2.074(9)	0.0011 (6)
Rh-N	1.1(1)	2.014(23)	0.0016(9)	0.9(3)	2.252(76)	0.0054(31)
Rh-Cl	1.2(1)	2.373(12)	0.0052(17)	1.0(1)	2.339(11)	0.0017(15)

8.4.2 Parameters based on geometry optimization for carbonyl coordination

Table S14. *k*- and *R* ranges as well as corresponding fit parameters of the analysis of the two immobilized Rh samples.

sample	*k*-range [Å^{-1}]	*R*-range [Å]	*R*-factor	reduced Chi-square	S_0^2 value
OMS-4.9-**Ph(C_{10}CO)click**-Rh	3.08 - 13.55	1.15 - 4.00	0.0084	12	1.0
OMS-6.8-**Ph(C_{10}CO)click**-Rh	3.10 - 12.70	1.15 - 4.00	0.0109	16	1.0

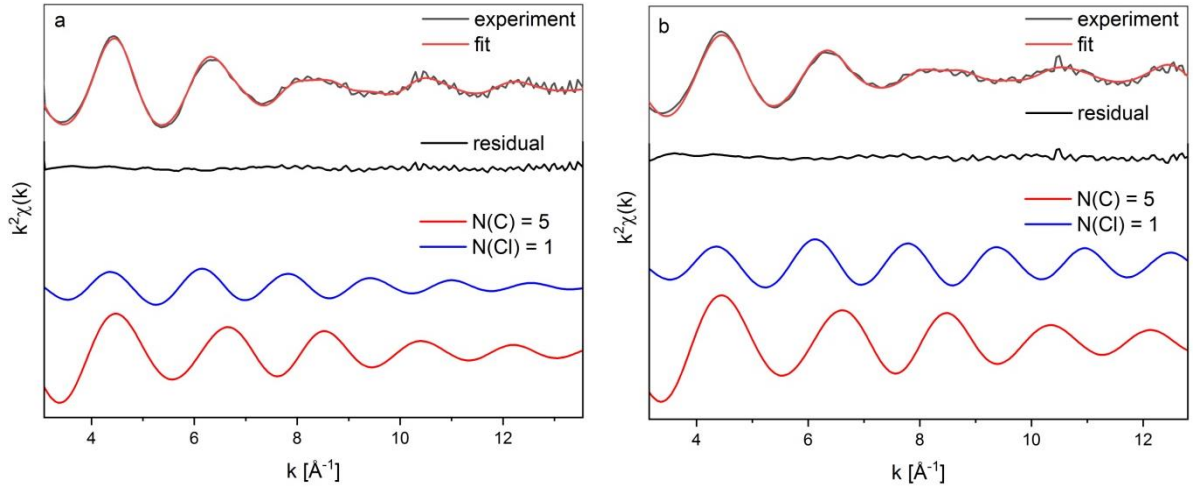

Figure S122. Fitted function compared with experimental data, residual plot and first coordination shell paths for the two immobilized Rh samples in *k*-space. Immobilized Rh complex in 4.9 nm pores (a) and immobilized Rh complex in 6.8 nm pores (b).

Table S15. First shell coordination Numbers (*N*), bond lengths (*R* + Δ*R*) and Debye-Waller factors of the two immobilized Rh complexes.

scattering paths	4.9 nm pores			6.8 nm pores		
	N	*R* + Δ*R* [Å]	σ^2 [Å^2]	*N*	*R* + Δ*R* [Å]	σ^2 [Å^2]
immobilized Rh-samples						
Rh-C	5.2(2)	2.079(19)	0.0042(7)	5.0(2)	2.089(9)	0.0030 (5)
Rh-Cl	1.2(2)	2.360(49)	0.0049(42)	1.0(1)	2.368(41)	0.0013(9)

9 HPLC Chromatograms

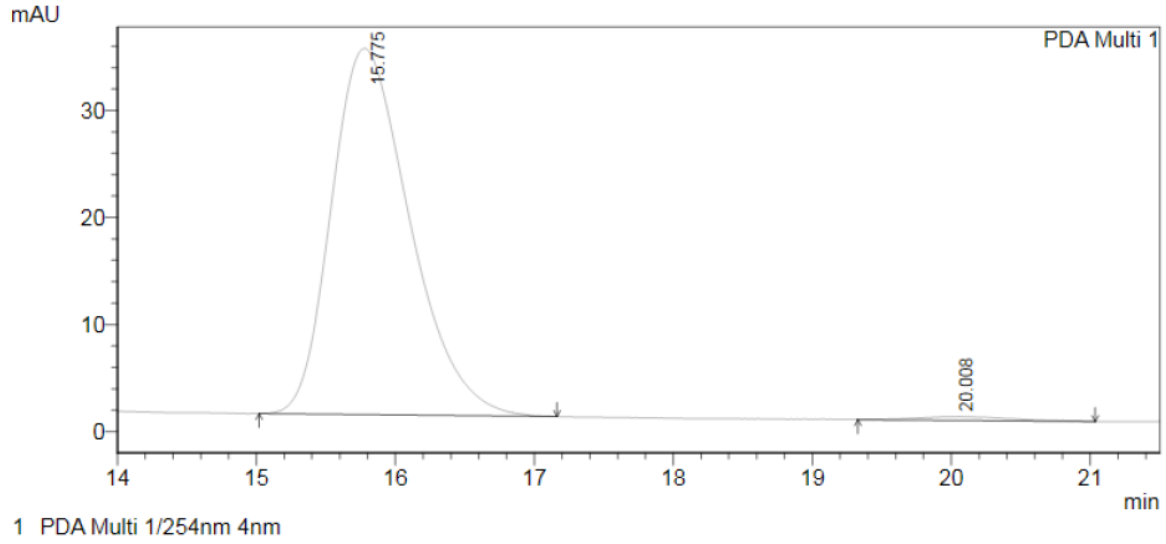

1 PDA Multi 1/254nm 4nm

PeakTable

PDA Ch1 254nm 4nm

Peak#	Ret. Time	Area	Height	Area %	Height %
1	15.775	1344429	34214	98.844	98.992
2	20.008	15723	348	1.156	1.008
Total		1360153	34563	100.000	100.000

Figure S123. HPLC chromatogram of 1,2-addition product **17** obtained with OMS-6.8-**1-Naph(*i*PrC$_1$OC$_1$)click** according to GP 14.

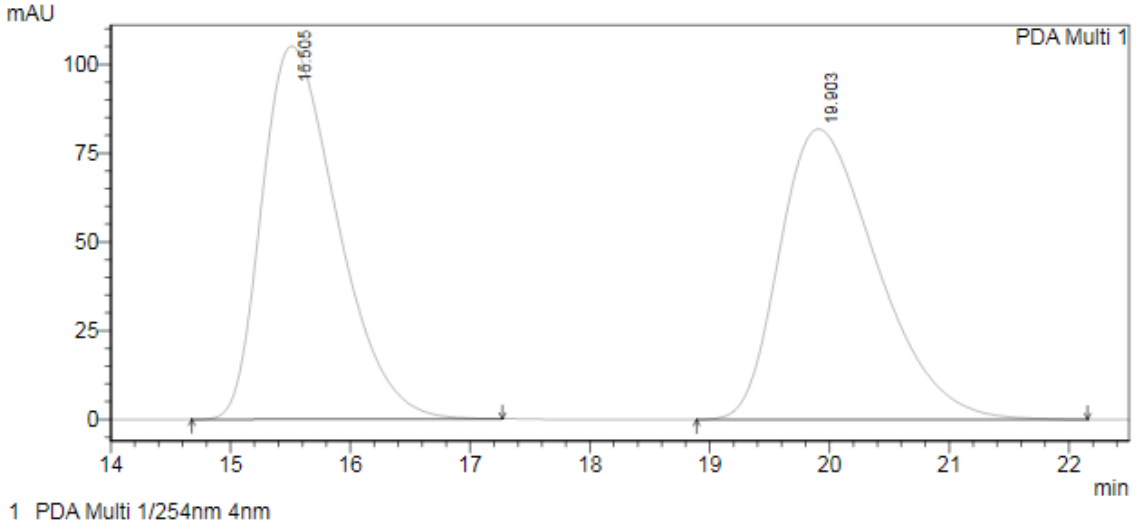

1 PDA Multi 1/254nm 4nm

PeakTable

PDA Ch1 254nm 4nm

Peak#	Ret. Time	Area	Height	Area %	Height %
1	15.505	4617359	105171	49.938	56.224
2	19.903	4628737	81887	50.062	43.776
Total		9246096	187058	100.000	100.000

Figure S124. HPLC chromatogram of 1,2-addition product **17** obtained with [Rh(COD)OH]$_2$ according to GP 13.

10 References

1 M. Deimling, M. Kirchhof, B. Schwager, Y. Qawasmi, A. Savin, T. Mühlhäuser, W. Frey, B. Claasen, A. Baro, T. Sottmann and S. Laschat, *Chem. – Eur. J.*, 2019, **25**, 9464–9476.

2 T. Yamamoto, A. Ishibashi and M. Suginome, *Chem. Lett.*, 2017, **46**, 1169–1172.

3 N. J. Line, B. P. Witherspoon, E. N. Hancock and M. K. Brown, *J. Am. Chem. Soc.*, 2017, **139**, 14392–14395.

4 N. F. O'Rourke and J. E. Wulff, *Org Biomol Chem*, 2014, **12**, 1292–1308.

5 D. H. Wadsworth, S. M. Geer and M. R. Detty, *J. Org. Chem.*, 1987, **52**, 3662–3668.

6 M.-X. He, Z.-Y. Mo, Z.-Q. Wang, S.-Y. Cheng, R.-R. Xie, H.-T. Tang and Y.-M. Pan, *Org. Lett.*, 2020, **22**, 724–728.

7 I. Hatial, R. Mukherjee, K. Senapati and A. Basak, *Tetrahedron Lett.*, 2015, **56**, 4275–4279.

8 K. Kasten, A. M. Z. Slawin and A. D. Smith, *Org. Lett.*, 2017, **19**, 5182–5185.

9 A. C. Götzinger, C. S. Michaelis and T. J. J. Müller, *Dyes Pigments*, 2017, **143**, 308–316.

10 M. Zhou, M. Chen, Y. Zhou, K. Yang, J. Su, J. Du and Q. Song, *Org. Lett.*, 2015, **17**, 1786–1789.

11 J.-H. Chen, C.-H. Deng, S. Fang, J.-G. Ma and P. Cheng, *Green Chem.*, 2018, **20**, 989–996.

12 M. Tanasova and B. Borhan, *Eur. J. Org. Chem.*, 2012, **2012**, 3261–3269.

13 H. Zheng and D. G. Hall, *Tetrahedron Lett.*, 2010, **51**, 3561–3564.

14 G. L. Khatik, V. Kumar and V. A. Nair, *Org. Lett.*, 2012, **14**, 2442–2445.

15 B. M. Nilsson, H. M. Vargas and U. Hacksell, *J. Med. Chem.*, 1992, **35**, 3270–3279.

16 A. Beurer, M. Kirchhof, J. R. Bruckner, W. Frey, A. Baro, M. Dyballa, F. Giesselmann, S. Laschat and Y. Traa, *ChemCatChem*, 2021, **13**, 2407–2419.

17 G. Broggini, G. Poli, E. M. Beccalli, F. Brusa, S. Gazzola and J. Oble, *Adv. Synth. Catal.*, 2015, **357**, 677–682.

18 F. Himo, T. Lovell, R. Hilgraf, V. V. Rostovtsev, L. Noodleman, K. B. Sharpless and V. V. Fokin, *J. Am. Chem. Soc.*, 2005, **127**, 210–216.

19 N. Tokunaga, Y. Otomaru, K. Okamoto, K. Ueyama, R. Shintani and T. Hayashi, *J. Am. Chem. Soc.*, 2004, **126**, 13584–13585.

20 F. Ziegler, H. Kraus, M. J. Benedikter, D. Wang, J. R. Bruckner, M. Nowakowski, K. Weißer, H. Solodenko, G. Schmitz, M. Bauer, N. Hansen and M. R. Buchmeiser, *ACS Catal.*, 2021, **11**, 11570–11578.

21 J. R. Bruckner, J. Bauhof, J. Gebhardt, A.-K. Beurer, Y. Traa and F. Giesselmann, *J. Phys. Chem. B*, 2021, **125**, 3197–3207.

22 V. Meynen, P. Cool and E. F. Vansant, *Microporous Mesoporous Mater.*, 2009, **125**, 170–223.

23 F. Markus, C. Vogler, J. R. Bruckner and S. Naumann, *ACS Appl. Nano Mater.*, 2021, **4**, 3486–3492.

24 S. R. Kousik, F. Ziegler, D. Sipp, A. Rodríguez-Camargo, H. Solodenko, W. Gassner, G. Schmitz, B. V. Lotsch, M. R. Buchmeiser, K. Koynov and P. Atanasova, *ACS Appl. Nano Mater.*, 2022, **5**, 14733–14745.

25 J. Nakazawa, B. J. Smith and T. D. P. Stack, *J. Am. Chem. Soc.*, 2012, **134**, 2750–2759.

26 D. Yu, Z. Wang, N. S. Ergang and A. Stein, in *Studies in Surface Science and Catalysis*, Elsevier, 2007, vol. 165, pp. 365–368.

27 J. D. Webb, T. Seki, J. F. Goldston, M. Pruski and C. M. Crudden, *Microporous Mesoporous Mater.*, 2015, **203**, 123–131.
28 F. Ziegler, J. Teske, I. Elser, M. Dyballa, W. Frey, H. Kraus, N. Hansen, J. Rybka, U. Tallarek and M. R. Buchmeiser, *J. Am. Chem. Soc.*, 2019, **141**, 19014–19022.
29 F. O. Guenther, *Anal. Chem.*, 1958, **30**, 1118–1120.
30 A. Meier and H. Gamsjäger, *React. Polym.*, 1989, **11**, 155–163.
31 H. Min, H. Miyamura, T. Yasukawa and S. Kobayashi, *Chem. Sci.*, 2019, **10**, 7619–7626.
32 G. Porod, O. Glatter and O. Kratky (Eds.), *Small Angle X-ray Scattering, first ed., Academic Press (London) LTC., London,* 15–51.
33 Turbomole V7.2.1 2017, a development of University of Karlsruhe and Forschungszentrum Karlsruhe GmbH, 1989–2007, TURBOMOLE GmbH, since 2007; available from http://www.turbomole.com.
34 P. Sherwood, A. H. de Vries, M. F. Guest, G. Schreckenbach, C. R. A. Catlow, S. A. French, A. A. Sokol, S. T. Bromley, W. Thiel and A. J. Turner, *J. Mol. Struct. THEOCHEM*, 2003, **632**, 1–28.
35 S. Metz, J. Kästner, A. A. Sokol, T. W. Keal and P. Sherwood, *Wiley Interdiscip. Rev. Comput. Mol. Sci.*, 2014, **4**, 101–110.
36 M. D. Hanwell, D. E. Curtis, D. C. Lonie, T. Vandermeersch, E. Zurek and G. R. Hutchison, *J. Cheminformatics*, 2012, **4**, 1–17.
37 Avogadro: an open-source molecular builder and visualization tool. Version 1.2.0. http://avogadro.cc/.
38 P. Pracht, F. Bohle and S. Grimme, *Phys. Chem. Chem. Phys.*, 2020, **22**, 7169–7192.
39 B. Ravel and M. Newville, *J. Synchrotron Radiat.*, 2005, **12**, 537–541.
40 M. Newville, P. Līviņš, Y. Yacoby, J. J. Rehr and E. A. Stern, *Phys. Rev. B*, 1993, **47**, 14126–14131.
41 M. Newville, *J. Synchrotron Radiat.*, 2001, **8**, 322–324.
42 T. S. Ertel, H. Bertagnolli, S. Hückmann, U. Kolb and D. Peter, *Appl. Spectrosc.*, 1992, **46**, 690–698.
43 N. Binsted and S. S. Hasnain, *J. Synchrotron Radiat.*, 1996, **3**, 185–196.
44 N. Binsted and F. Mosselmans, *EXCURV98 Manual, Daresbury, UK.*
45 M. Bauer and H. Bertagnolli, *J. Phys. Chem. B*, 2007, **111**, 13756–13764.
46 D. C. Koningsberger, B. L. Mojet, G. E. van Dorssen and D. E. Ramaker, *Top. Catal.*, 2000, **10**, 143–155.